



The University of  
**Nottingham**

UNITED KINGDOM • CHINA • MALAYSIA

**Factors Influencing Cycle-by-Cycle Combustion  
Characteristics of a Diesel Engine under Cold Idling  
Conditions**

**Michael James McGhee, M.Eng. (Hons)**

**Thesis submitted to the University of Nottingham for the degree of Doctor of  
Philosophy, September 2012**

**Dedicated to my Mother, Father and Sister who have given me continuous support, love and belief in me at all times.**

---

# Abstract

---

## **Factors Influencing Cycle-by-Cycle Combustion Characteristics of a Diesel Engine under Cold Idling Conditions**

**Michael James McGhee, 2012**

An experimental investigation of post-start cold idling behaviour has been carried out on a modern single-cylinder HPCR DI light duty diesel engine with a low compression ratio of 15.5:1 at temperatures between 10 and -20°C. The trend toward lower compression ratios from more common values of around 22:1 a few years ago has resulted in lower compression pressures and temperatures, which negatively affects cold idle operation. Improvements in cycle-by-cycle stability of indicated work output through fuel injection strategy and glow plug temperature changes have been explored. This is important to improve NVH and the consumer's perception of vehicle quality. The key effects on heat release characteristics have been identified and the associated impact on stability discussed. High speed imaging of ignition in a combustion bomb has been used to aid interpretation of engine results.

Up to four pilot injections placed in advance of the main have been used. Shorter separation between pilots and pilot-to-main improves stability independent of the number of pilot injections and extends the range of main injection timings to meet target stability of 10% or lower at -20°C. Increasing the number of pilot injections was effective in stabilising combustion at all investigated soak temperatures at fuelling levels producing indicated work required to match friction and ancillary demands. Stability can be susceptible to deterioration at moderate soak temperatures because fuelling demand is relatively low. If a high number of pilot injections are to be avoided to reduce potential wear, then increasing main injection quantity is an effective method to stabilise combustion for a lower pilot number strategy but any increase above target load has to be harnessed by additional ancillary devices.

Very high glow plug temperatures of up to 1200°C were examined using a smaller diameter tip ceramic type design. Stable combustion cannot be achieved through

higher glow plug temperatures alone. A temperature of 1000°C, which can be achieved using a low voltage metallic type, is adequate to stabilise combustion when combined with a triple-pilot strategy at sub-zero temperatures. The best stability is achieved using 1200°C, which can only be achieved using a more expensive ceramic type, in combination with a triple-pilot strategy producing the desirable target of ~5% or below; the effects are not mutually exclusive. At high glow plug temperatures and using three or four pilot injections, stability improved with warmer soak temperatures. At -5°C, stability was relatively poor when one or two pilots were used irrespective of glow plug temperature.

A high premixed contribution to main combustion is associated with improved stability. Minimum threshold values are necessary to stabilise combustion: ~25 J/° at -20°C, ~20 J/° at -5°C and only ~10 J/° at 10°C. A higher number of pilot injections raises pilot induced combustion and improves mixture distribution. These effects subsequently increase the premixed combustion and help sustain a strong main development with less variability. This benefit is maximised when using hotter glow plug temperatures raising IMEPg magnitude and reducing variation.

# Contents

---

<b>Acknowledgements</b> .....	<b>vi</b>
<b>Abbreviations</b> .....	<b>vii</b>
<b>Nomenclature</b> .....	<b>ix</b>
<b>Chapter 1</b> .....	<b>1</b>
<b>Introduction</b> .....	<b>1</b>
1.1. The Need to Investigate Cold Post-Start Idling Stability .....	1
1.2. Overview of Diesel Engines .....	3
1.3. Emission Standards.....	4
1.4. Thesis Objectives .....	6
1.5. Thesis Layout .....	8
1.6. Contribution to Diesel Engine Cold Idling Behaviour .....	8
<b>Chapter 2</b> .....	<b>10</b>
<b>Literature Review</b> .....	<b>10</b>
2.1. Introduction.....	10
2.2. Driving Forces for Low Compression Ratio.....	10
2.3. Diesel Combustion Characteristics .....	12
2.4. Diesel Engine Technological Advancements and Cold Start Technology .	14
2.5. Combustion Imaging Studies .....	16
2.6. Cold Start Performance .....	20

## Contents

---

2.7. Cold Idle Performance .....	23
2.8. Combustion Noise .....	25
2.9. Summary .....	26
<b>Chapter 3.....</b>	<b>27</b>
<b>Optical Study of Factors Influencing Combustion Initiation .....</b>	<b>27</b>
3.1. Introduction.....	27
3.2. Imaging Technique, Experimental Facilities and Data Acquisition .....	27
3.3. Image Post-Processing.....	29
3.4. Description of Initiation and Early Stages of Combustion .....	30
3.5. Injector Spray and Glow Plug Position.....	31
3.6. Influence of the Number of Pilot Injections.....	32
3.7. Influence of Pilot Injection Quantity.....	34
3.8. Influence of Injection Separation.....	35
3.9. Influence of Glow Plug and Vessel Temperature .....	36
3.10. Influence of Vessel Pressure.....	38
3.11. Discussion and Conclusions .....	39
<b>Chapter 4.....</b>	<b>42</b>
<b>Engine Test Facilities, Test Procedure and Data Processing.....</b>	<b>42</b>
4.1. Introduction.....	42
4.2. Experimental Facilities.....	42
4.2.1. Single Cylinder Test Engine .....	42
4.2.2. Rig Setup and Instrumentation .....	43

## Contents

---

4.2.3.	Data Acquisition and Fuel Injection Control .....	45
4.3.	Testing Procedure and Repeatability .....	46
4.4.	Data Processing .....	47
4.4.1.	Indicated Mean Effective Pressure (IMEP) .....	47
4.4.2.	Combustion Stability Indicator .....	48
4.4.3.	Cylinder Charge Heat Release Rate.....	49
4.4.4.	Cylinder Charge Heat Transfer.....	51
4.4.5.	Cylinder Charge Blowby .....	52
4.4.6.	Diesel Combustion Heat Release Characteristics.....	53
4.4.7.	Cycle Efficiencies .....	53
4.5.	Summary.....	54
<b>Chapter 5.....</b>	<b>56</b>	
<b>Analysis of Injection Parameters.....</b>	<b>56</b>	
5.1.	Introduction.....	56
5.2.	-20°C Soak Temperature .....	56
5.2.1.	Varying Separation and Main Injection Timing.....	56
5.2.2.	Number of Pilots and Pilot Quantity Optimisation.....	59
5.2.3.	Sensitivity of Stability to Total Fuelling Level .....	60
5.2.4.	The Effect of an Early Large Single Pilot .....	61
5.3.	-5°C Soak Temperature.....	62
5.3.1.	Number of Pilots and Pilot Quantity Optimisation.....	62
5.3.2.	Influence of Pilot Fuel Distribution for Single- and Twin-Pilot Strategies	63

## Contents

---

5.3.3. Influence of Pilot Fuel Distribution for Triple- and Quad-Pilot Strategies	65
5.3.4. Effect of Increasing Total Fuelling Level and Position .....	66
5.4. 10°C Soak Temperature .....	68
5.4.1. Number of Pilots and Pilot Quantity Optimisation.....	68
5.5. Soak Temperature Comparisons .....	69
5.6. Influences of Injection Strategies on Heat Release Characteristics and Associated Effects on Work Output and Stability .....	70
5.7. Discussion and Conclusions .....	73
<b>Chapter 6.....</b>	<b>75</b>
<b>Trade-Off between Injection Strategy and Glow Plug Temperature.....</b>	<b>75</b>
6.1. Introduction.....	75
6.2. Glow Plug Design and Control.....	75
6.3. Effect of Varying Glow Plug Temperature at -20°C .....	76
6.4. Effect of Varying Glow Plug Temperature at -5°C .....	76
6.5. Effect of Varying Glow Plug Temperature at 10°C .....	77
6.6. Soak Temperature and Heat Release Comparisons .....	78
6.7. Influence of Increased Fuelling Level.....	81
6.8. Discussion and Conclusions .....	83
<b>Chapter 7.....</b>	<b>86</b>
<b>Discussion, Further Work and Conclusions.....</b>	<b>86</b>
7.1. Introduction.....	86
7.2. Discussion .....	86



Contents

---

7.3. The Future for Low Compression Ratio Diesel Engines and Compatibility with Cold Idle Requirements .....	91
7.4. Further Work .....	94
7.5. Conclusions.....	96
7.5.1. Optical Vessel Study .....	96
7.5.2. Engine Study .....	96
<b>References .....</b>	<b>99</b>
<b>Tables .....</b>	<b>110</b>
<b>Figures .....</b>	<b>113</b>

# Acknowledgements

---

Firstly, I would like to offer my sincere gratitude to Professor Paul Shayler, Head of the Engines Research Group at the University of Nottingham for his continuous support and guidance throughout this research project. My thanks also go to the University of Nottingham allowing the use of the test facilities.

Secondly, my appreciation goes to Dave MacMillan for his persistent guidance and assistance offering a tremendous amount of his time during the early part of this project. I would like to thank Nino La Rocca for his continuous support in meetings and on the rig. My thanks go to Mike Murphy and Ian Pegg at Ford Motor Company for their assistance, advice and project funding. Thank you to David Hann and the CAMERA centre for their support and use of the high speed camera.

Thirdly, my unwavering thanks go to the technicians, Geoff Fryer, John Clark, Paul Johns and John McGhee (my Father) who have maintained and fixed the much needed engine rig.

Fourthly, my deepest gratitude go to the other members of the Engines Research Group, in particular JP and Greg who gave me a warm welcome and made this project more enjoyable and fun to do. Rich Gardiner often went out of his way to help setting up equipment on the rig, for which I'm very grateful of. My thanks also go to Sami Amin and Toby Bates who I have spent some time working with on this project.

Last but not least my sincerest gratitude and love to my beloved Father, John McGhee, my Mother, Janet McGhee and my Sister, Dawn McGhee, who have supported me and had belief in me at all times.

# Abbreviations

---

°ATDC	Degrees After Top Dead Centre
°CA	Degrees Crank Angle
BDC	Bottom Dead Centre
CAN	Control Area Network
CFD	Computational Fluid Dynamics
CO	Carbon Monoxide
CO <sub>2</sub>	Carbon Dioxide
CoV <sub>IMEPg</sub>	Coefficient of Variation in Gross Indicated Mean Effective Pressure [%]
DI	Direct Injection
EGR	Exhaust Gas Recirculation
ECU	Engine Control Unit
EOC	End of Combustion
FIE	Fuel Injection Equipment
FMEP	Friction Mean Effective Pressure [bar]
HC	Hydrocarbon
HCCI	Homogeneous Charge Compression Ignition
HPCR	High Pressure Common Rail
IMEPg	Gross Indicated Mean Effective Pressure [bar]
NEDC	New European Driving Cycle

## Abbreviations

---

NO <sub>x</sub>	Oxides of Nitrogen
NVH	Noise, Vibration and Harshness
PCCI	Partially-premixed Charge Compression Ignition
PLIF	Planar Laser Induced Fluorescence
PLRS	Planar Laser Rayleigh Scattering
PM	Particulate Matter
RTI	Real Time Interface
SOC	Start of Combustion
SOI	Start of Injection (electric energising start of the injector) [°ATDC]
StD <sub>IMEPg</sub>	Standard Deviation in Gross Indicated Mean Effective Pressure [bar]
TDC	Top Dead Centre
UIS	Unit Injector System
VVA	Variable Valve Actuation

# Nomenclature

---

$A$	Area [ $\text{m}^2$ ]
$A_{\text{ring}}$	Effective ring gap area [ $\text{m}^2$ ]
$C_p$	Specific heat at constant pressure [ $\text{kJ/kg K}$ ]
$C_v$	Specific heat at constant volume [ $\text{kJ/kg K}$ ]
$h_c$	Heat transfer coefficient [ $\text{W/m}^2 \text{K}$ ]
$\dot{m}$	Mass flow rate [ $\text{kg/s}$ ]
$m_{\text{trapped}}$	Trapped mass [ $\text{kg}$ ]
$n_c$	Indicated combustion efficiency [%]
$n_f$	Indicated fuel conversion efficiency [%]
$n_t$	Indicated thermal efficiency [%]
$N$	Engine speed [ $\text{rev/min}$ ]
$P$	Pressure [ $\text{Pa}$ ]
$Q_{\text{bby}}$	Blowby energy [ $\text{J}$ ]
$Q_{\text{gross}}$	Gross heat release [ $\text{J}$ ]
$Q_{\text{ht}}$	Heat transfer energy [ $\text{J}$ ]
$Q_{\text{LHV}}$	Lower heating value [ $\text{MJ/kg}$ ]
$Q_{\text{net}}$	Net heat release [ $\text{J}$ ]
$r_c$	Compression ratio [-]
$R$	Specific gas constant [ $\text{J/kg K}$ ]

## Nomenclature

---

$\bar{S}_p$	Mean piston speed [m/s]
T	Temperature [K]
U	Internal energy [J]
V	Volume [m <sup>3</sup> ]
$V_s$	Swept volume [m <sup>3</sup> ]
W	Work [J]
$\theta$	Crank angle [°CA]
$\gamma$	Ratio of specific heats ( $C_p/C_v$ )
$\rho$	Charge density [kg/m <sup>3</sup> ]

# Chapter 1

## Introduction

---

### 1.1. The Need to Investigate Cold Post-Start Idling Stability

Diesel engine design has advanced dramatically in recent years, as evidenced by improved fuel economy, and lower emissions of pollutants and noise [1]. However, despite the technological advances and a better understanding of the combustion process, there remains areas of performance in need of further improvement, particularly at reduced ambient air temperatures during engine cold starting and warming up [2]. The area of investigation reported in this thesis is idle stability during the early seconds after cold start-up, which is prone to be poor at low ambient temperatures. This is demonstrated in Figure 1-1, where a twin-pilot injection strategy performs poorly until the engine warms up. Cycle variation is poor and work output low, but can be improved by using a higher number of pilot injections placed in advance of the main injection. This raises work output and produces less cyclic variation particularly during the early stages of the test.

The trend over recent years towards the use of lower compression ratios [3] has exacerbated the problem of idle stability [4]. Compression ratios used for light duty diesel engines have decreased over recent years as part of a strategy to improve the NO<sub>x</sub>/PM trade-off at part load and achieve higher specific torque and power at full load by using higher boost pressures [5, 6]. A few years ago, compression ratios of around 22:1 were common, with values now declining to around 16:1 or even slightly lower. Lower compression ratios also allow for engine downsizing which tend to operate at higher specific engine loads in order to achieve lower fuel consumption [7]. A fuel consumption reduction of 9% is possible with a displacement reduction from 2.0 l to 1.6 l has been reported [8]. Gains are made by reducing pumping losses, heat transfer due to lower surface area and smaller construction which leads to improvements in mechanical friction [9]. The downside of reducing compression ratio is lower compression temperatures and pressures and higher propensity for poor cycle-by-cycle stability during cold, post-start idling [4]. At typical idle speeds under fully warm conditions, values for a commonly used indicator to assess

combustion stability,  $\text{CoV}_{\text{IMEPg}}$ , are expected to be  $<3\%$ . At cold idle, however,  $<5\%$  is difficult to achieve and values can be higher, giving rise to the perception of poor idling quality and 'rough' running [10].

Recent investigations [4] have found that start-up times for low compression ratio engines are generally not extended so long as an appropriate injection strategy is employed. Idling stability, however, is an area receiving greater attention because cycle-by-cycle variations in combustion and indicated work can be unacceptably large at low ambient temperatures. A higher fuelling level is generally required at cold temperatures to overcome the increased friction load due to higher oil viscosity. Cold starting aids are widely used in an attempt to improve fuel vaporisation and promote reliable ignition. Glow plugs are the most common aid and are essential for reliable starting and to improve idling combustion stability [4]. There is a trend to reduce tip diameter and raise temperature to reduce the surface area protruding into the cylinder that is a potential hindrance to fuel air mixing at fully warm operating conditions and to improve emissions. Low voltage metallic steel tip glow plugs can reach temperatures of around  $1050^{\circ}\text{C}$ , but higher temperatures require ceramic tips incurring a much higher cost. The trade-off between injection strategy and glow plug temperature is an area explored within this thesis to assess the level of improvement to combustion stability.

Mazda's recent attempt to improve emissions and fuel economy comes in the form of their Skyactiv-D diesel engine. The goal is to lower the fuel consumption of their global fleet by 30% by 2015 compared to 2008 figures. This small capacity engine offers a low compression ratio of 14:1 and a 20% reduction in fuel consumption [11]. Whilst the emissions benefits are apparent, complying with Euro 6 in Europe without the aid of an expensive  $\text{NO}_x$  aftertreatment system, ensuring cold-start capability remained a challenge. The adoption of ceramic glow plugs coupled with different injection patterns provided by multi-hole piezo injectors ensured reliable starting at cold temperatures. To prevent misfiring during the warm-up phase, the in-cylinder air temperature was increased through the adoption of a variable valve lift system for the exhaust valves. The exhaust valves are slightly opened during the intake stroke to recover a proportion of the hot exhaust gas and introduce it back into the cylinder [9].



This investigation has focused on determining the influences on cycle-by-cycle combustion stability at cold idling engine speeds following start-up and find possible solutions to make improvements.

## **1.2. Overview of Diesel Engines**

Diesel engines have a higher brake thermal efficiency than gasoline engines because they operate at higher compression ratios and can produce the same power output at lower engine speeds due to the use of higher boost pressures. Despite higher BMEP and downsizing of gasoline engines, power output at lower engine speeds remains inferior owing to the knock limitation of the fuel. Diesel engines also generally operate with quality governing of work output which allows part-load operation without high throttling losses [10, 12, 13]. Diesel engines have better torque characteristics which means when used with an optimised transmission system, vehicles can operate in higher gears for a longer period of time over the same drive cycle. These merits make diesel engines very desirable, but drawbacks are apparent compared to gasoline engines. Historically, their noise, vibration and harshness (NVH) is much worse compared to equivalent spark-ignition engines. There are higher costs associated with diesel engines, primarily due to expensive fuel injection hardware and exhaust aftertreatment systems. Achieving low emissions whilst retaining good fuel economy and acceptable NVH remains a challenge. Consumer perception has changed in recent years due to much improvement in NVH and their superior fuel economy is making diesel powered vehicles very desirable.

The efficiency of diesel engines have improved through measures such as direct injection systems, common rail injection, engine management systems, downsizing of engine capacity, increase in turbocharger boost and stop-start technology. Although these trends are mainly driven by meeting exhaust-out emissions, some technological advances assist cold starting and idling operation. The trend in fuel injectors has seen a higher number of smaller sized holes to aid fuel atomisation and spatial distribution, which is likely to favour vaporisation during cold temperature operation. The introduction of piezo-electric injectors is part of the improved fuel injection systems allowing good control and metering of fuel spray. Traditionally, injectors use electro-magnetic solenoids to control the injector needle and adjust the flow of fuel. Piezo-electric injectors use a stack of piezo-crystal plates. When an electrical current is supplied the crystals expand causing the needle to move either

directly or indirectly, offering good flow metering and repeatability. The capability of rate shaping and short dwell periods offers potential improvements in emissions [14, 15].

Implementing novel turbocharger systems maximises the efficiency of downsized engines. Some car manufacturers, such as VW and Mazda, are using twin-stage turbocharging. This way, the selection of the turbocharger to operate depending on speed and load conditions can enhance fuel efficiency and vehicle drivability [9]. Another enabler for fuel efficiency gains is variable valve timing (VVT). Using VVT in conjunction with downsizing maximises efficiency for a wider range of engine operating conditions through adjustment to the effective compression ratio. Varying compression ratio to optimise for minimum BSFC has been assessed by Sood et al. [16] and found that 16.4:1 was best at 1900 rev/min but should increase at higher speeds. One implication of this technology is that the effective compression ratio can be increased during cold starting and idling operation offering potential improvements in combustion stability. Rather than just changing the valve phasing and lift, the valves can be closed thus deactivating cylinders. Typically, half of the cylinders are deactivated, whilst the remaining active cylinders operate at twice the load that the engine would normally operate at if all the cylinders were firing. This can enable improvements in the soot-NO<sub>x</sub> trade-off and offer potential gains in fuel consumption.

In 2000, diesel vehicles accounted for 14.1% of the total new car registrations in the UK [17]. Through the help of improvements to diesel engines, diesel cars took a record 50.6% market share in 2011. The increasing popularity of diesel vehicles is illustrated in Figure 1-2. Market share grew between 2000 and 2011, with a reduction in 2009 due to the recession suppressing demand. The diesel share of the new car market by segment in 2000, 2010 and 2011 is shown in Figure 1-3. The inclusion of a new segment, specialist sports, is indicative of the change in consumer sentiment in favour of diesel engines, with around 23% diesel share of the UK new car market in 2011.

### **1.3. Emission Standards**

New cars and light duty vehicles since 1992 have been required to meet emission standards known as 'Euro' standards [18]. The current European exhaust emission requirements regulate four groups of compounds: nitrogen oxides (NO<sub>x</sub>),

hydrocarbons (HC), carbon monoxide (CO) and particulate matter (PM) tested through the standardised New European Drive Cycle (NEDC). An additional emission limit, solid particle number (PN), also became effective in 2011 for all categories of diesel vehicles. The emission standards are summarised in Table 1-1. Legislation is imposing stringent levels particularly on particulates and NO<sub>x</sub>. Euro 5 standards introduced in 2009 reduced PM by 80% and NO<sub>x</sub> by 28% from Euro 4, 2005. Euro 6 that comes into effect in 2013/2014 reduces NO<sub>x</sub> by a further 55%. Manufacturers have to minimise these emissions to reduce their polluting effect whilst needing to contend with any adverse effects during cold starting and idling.

Concerns over the impact of global warming have prioritised improving fuel economy and CO<sub>2</sub> levels. Car manufacturers in Europe voluntarily agreed to reduce average new car CO<sub>2</sub> emissions to 140 g/km by 2008-09 [17]. Although this target was not met, progress was made in reducing CO<sub>2</sub> emissions and the introduction of new technologies such as hybrid and electric vehicles. The marketplace remains dominated by gasoline and diesel vehicles contributing to over 98% of new car registrations in the UK. Potentially the main driver to emissions reduction is the EU new car CO<sub>2</sub> regulation together with taxation incentives from the government. The regulation covers new passenger cars and sets a sales-weighted CO<sub>2</sub> target of 130 g/km by 2015. The UK has set legally binding targets on greenhouse gas (GHG) emissions reductions of 34% by 2020 and 80% by 2050 from figures based in 1990 [19]. These targets are more stringent than EU targets, to make a 20% reduction by 2020 from a 1990 base. The shift into lower CO<sub>2</sub> emitting cars across the UK market is illustrated in Figure 1-4, with almost half the market (46.8%) now emitting 130 g/km or lower. This is compared to 10.6% in 2007 [17]. In 2002, EU emission regulations imposed a requirement for low temperature (-7°C) tests for gasoline engines. No such legislation has yet been implemented for diesel engines, but manufacturers are now monitoring emissions at -7°C and these are very likely to be legislated for in a few years time.

To comply with legislation manufacturers are pursuing improvements to aftertreatment systems such as diesel particulate filters (DPF), selective catalyst reduction (SCR) and lean NO<sub>x</sub> traps (LNT). Implementing such systems are expensive and reduce fuel economy benefits. To reduce costs of these systems manufacturers are seeking new ways to minimise engine-out emissions. Combustion processes such as Partially-premixed Charge Compression Ignition (PCCI) and Homogenous Charge Compression Ignition (HCCI) offer benefits in improving soot

and  $\text{NO}_x$  but at the expense of HC, CO and higher combustion noise with potential difficulties in controlling the combustion due to the ignition timing not being under control [12]. Due to continued development advanced diesel technology offers better fuel economy over conventional gasoline technology [17].

Although exhaust-out emissions haven't been the focus of this research, the work being undertaken is a direct result of engine design changes to meet imposed emission legislation. The work carried out within this thesis has focused primarily on the factors influencing combustion and the cold idling stability and therefore the effects on exhaust emissions have not been examined in this study.

#### **1.4. Thesis Objectives**

In a strategy to meet target emissions whilst improving fuel consumption, performance and consumer perception, cold idling stability has become an area that's receiving much attention. The aim of the work presented in this thesis is to investigate cycle-by-cycle stability of a 0.55 l single-cylinder DI diesel engine with a compression ratio of 15.5:1 at cold post-start idling conditions. The test engine is equipped with a HPCR fuel injection system with piezo-electric injectors. The influence of glow plug temperature and injection parameters has been examined and suggestions made on how to make improvements to meet desired targets determined from proposed performance indicators.

The single-cylinder engine coupled to a motor/regenerator dynamometer allows analysis of the combustion process at desired engine speeds. For modern engine designs, idle speed is governed electronically through changes to the injection strategy or ancillary loads. The use of a dynamometer to maintain a fixed speed therefore decouples the effects of control strategy and combustion characteristics on stability. Measuring in-cylinder pressure evolution has permitted the assessment of performance in terms of work output, cycle-by-cycle stability and heat release rates. A variety of soak temperatures have been investigated;  $-20^\circ\text{C}$  to  $10^\circ\text{C}$ . Tests have been conducted at indicated loads equal to friction mean effective pressure (FMEP) and ancillary demands at the various temperatures. This engine load target to overcome friction and driving ancillaries is deemed suitable since no power to propel the vehicle is required at idle speed. Achieving target load whilst maintaining the lowest cycle-by-cycle variation is paramount in achieving smooth idle operation.

To further understand the influences of injection strategies and charge conditions, high speed camera imaging has been utilised to observe the effects on the early stages of combustion initiation. Although modelling would have been appropriate, none was conducted due to the large amount of time that would need to be invested in setting up a robust working model. Less time would have, therefore, been spent on the experimental test engine and optical vessel. The test engine facility was also already in place. The model would also have to be validated against engine results, since it is this that ultimately provides the trends and guiding conclusions. Some modelling has been recommended to accompany this current work, which has been briefly discussed in the further work section.

The main objectives of this work are as follows:

- Assess the impact of cold temperatures on idle stability of a low compression ratio diesel engine.
- Examine the effect of injection separation on cold idle performance and fuelling strategy robustness to main injection timing.
- Explore the influence of number of pilots and pilot fuel distribution and identify the most suitable strategies for different fuelling levels.
- Investigate the injection strategy and glow plug temperature trade-off at various fuelling levels and soak temperatures.
- Explore the influence on heat release characteristics and associated impact on work output and stability.
- Identify the most dominant factors influencing stability levels.
- Use combustion imaging in a quiescent constant volume optical pressure vessel to explore the most influential parameters on initiation and the early stages of combustion to aid interpretation of the test engine results.
- Determine whether low compression ratio is compatible with cold idle requirements.

## **1.5. Thesis Layout**

This thesis is split into seven main chapters. Following this introduction to the area of research and highlighting the need to further investigate cold post-start idling behaviour, is a literature review highlighting previous work within the area and further work that requires investigation. Chapter 3 discusses findings from the visualisation of combustion using a high speed camera in a quiescent constant volume pressure vessel. A detailed overview of the engine test facilities, testing procedure and data acquisition has been provided in Chapter 4. A standard test point has also been discussed to observe repeatability and identify potential errors. The chapter derives and highlights important variables that have been extensively used in the post-processing of data to quantify performance. Heat release characteristics have then been discussed.

Chapter 5 reports on the influence of changing injection strategy parameters on work output and cycle-by-cycle stability. Parameters studied include separation, injection timing, number of pilots and fuel distribution between pilots and main injections. The effects of these on heat release characteristics are highlighted, detailing any links between early combustion initiation and main development, and corresponding association with poor stability. The effect of fuelling level variation has been assessed to examine injection strategy robustness. Investigating the dependence on injection strategy has been extended to cover a range of soak temperatures.

In Chapter 6, a ceramic glow plug capable of very high temperatures has been studied and the trade-off between injection strategy and glow plug temperature assessed at different soak temperatures and fuelling levels.

Finally in Chapter 7, discussions and conclusions have been presented together with proposed further work.

## **1.6. Contribution to Diesel Engine Cold Idling Behaviour**

This thesis contributes to the knowledge and understanding of cold idling behaviour for a low compression ratio DI diesel engine. The results provided in this thesis are considered to be broadly applicable to diesel engines for light duty vehicles given their similarities in combustion chamber design, and injector and glow plug position. The main contributions to knowledge have been made in the following areas:

- Determining fuel injection strategies that best achieve target load and stability at cold idling conditions. Target stability can be achieved across a wide range of injection timings through reducing separation and using multiple pilot injection strategies.
- Identifying how total pilot quantity and number of pilots affect cycle-by-cycle stability and associated interactions, and demonstrating that the performance of an injection strategy is dependent on fuelling level, with the need to have a minimum total pilot quantity and number of pilots to meet target load and stability.
- Addressing the impact of changing soak temperature and fuelling levels on injection strategies required to meet target work output and stability levels.
- Identifying the key effects of fuel injection strategies on heat release characteristics. Through the examination of heat release data it has been possible to determine the influence on combustion initiation and subsequent development of the main. The associated impact on work output and cycle-by-cycle stability has been quantified.
- Understanding the relative importance of injection strategy and glow plug temperature on combustion stability at various soak temperatures and fuelling levels. Target stability cannot be achieved through high glow plug temperatures alone; multiple pilot injections or higher fuelling levels are also necessary. The best stability is achieved when using multiple pilots in combination with very high glow plug temperatures but the necessary ceramic glow plug type are expensive.
- High speed photographic studies have been used to support interpretation of engine results, particularly during the initiation process and early stages of combustion.

Some of the research contributions have been published and presented at the IMechE Fuel Systems conference [20] and SAE world congress in 2012 [21].

# Chapter 2

## Literature Review

---

### 2.1. Introduction

This literature review is split into six sections, the first of which covers publications concerned with the driving forces for low compression ratio diesel engines with emphasis on areas where potential benefits are gained and lost. The second is a review of typical diesel combustion characteristics. The third is a brief overview of diesel engine technological advancements and cold start technology. The fourth is a review of imaging diagnostics used to visualise combustion and a discussion of parametric studies carried out to date detailing the effects on combustion ignition. The fifth and sixth sections review the impact of low compression ratio on start and idle behaviour, particularly at cold temperatures. The influence of injection strategies and other techniques used to make improvements have been highlighted, and the conclusions are then presented.

### 2.2. Driving Forces for Low Compression Ratio

Imposed legislation is targeting automotive manufacturers to reduce engine-out emissions, particularly soot and NO<sub>x</sub>. The adoption of lower compression ratios is an effective way to improve the soot-NO<sub>x</sub> trade-off [22]. Under normal operating temperature conditions, in-cylinder temperature and pressure are usually sufficient to ignite a prepared fuel air mixture. For diesel fuel to combust, in-cylinder temperature must be sufficiently high to crack the hydrocarbon chains and produce enough volatile species to promote further chemical processes and highly exothermic reactions [4]. A self-sustaining regime is reached when a critical rate is achieved resulting in autoignition and a corresponding rise in in-cylinder temperature and pressure. This relies on a temperature rise due to compression, which can be approximated by the following polytropic compression process

$$T_2 = T_1 r_c^{n-1}$$

2-1



Where  $T_1$  is the temperature of charge gas at bottom dead centre (BDC),  $T_2$  is the temperature at the end of compression,  $r_c$  is the compression ratio and  $n$  is the polytropic exponent. A lower intake temperature and compression ratio both result in a lower temperature end of compression.

One of the key reasons for lower compression ratios is to reduce  $\text{NO}_x$  emissions. According to Musculus [23] chemical pathways for in-cylinder NO formation include the Zeldovich thermal mechanism (high temperatures), prompt NO chemistry (generally fuel-rich), the nitrous oxide ( $\text{N}_2\text{O}$ ) pathway (generally fuel-lean) and nitrogen conversion contained in the fuel. All four mechanisms may contribute to NO formation, however, experimental data has shown that the thermal NO mechanism is the dominant NO formation pathway. A reduction in compression ratio to lower maximum in-cylinder temperatures can therefore be advantageous in reducing  $\text{NO}_x$ . From optical diesel engine studies [24-26], NO has been observed shortly after the premixed burn, primarily occurring on the lean side of the jet periphery during the hot diffusion flame. For the NO formation mechanism, the reaction rates increase significantly as the combustion temperature increases, thus increasing NO formation [27]. Studzinski et al. [28] states that small increases in bulk gas temperatures above 2000 K cause large increases in NO formation, for example, 2000 K to 2050 K increases NO formation by over 44%.

The effect of reducing compression ratio on fuel economy and emissions focusing on where benefits are gained and lost has been widely explored. MacMillan et al. [22] found that reducing compression ratio from 17.9:1 to 13.7:1 gave large soot benefits at both high and low load conditions. This was due to an increase in ignition delay allowing for a greater degree of premixing. The implication of this is the reduced dependency on expensive diesel particulate filters (DPF). At high load, reducing compression ratio improved the soot- $\text{NO}_x$  trade-off but at the expense of increased CO, HC and fuel consumption. Reducing compression ratio at light load gave rise to poor combustion efficiency evidenced by a large increase in CO and HC. This was attributed to combustion temperatures being too low for complete oxidation, which generally requires around 1500 K and 1200 K for CO and HC respectively. Higher levels of CO and HC were also attributed to larger spray penetration and greater wall wetting which can be partially alleviated by reducing rail pressure. This however reduced the soot benefit.

Similar observations have been reported by Beatrice et al. [6] when reducing compression ratio from 16.5:1 to 14.5:1. Hountalas et al. [29] performed a computational investigation and indicated a  $\text{NO}_x$  reduction of between 5 and 20% when reducing compression ratio from 18:1 to 14:1 depending on load, but there was an associated 4% increase in fuel consumption. Some recent studies have focused on the resultant low compression temperatures and pressures of reducing compression ratio to increase ignition delay times and subsequently raise the degree of premixing. In combination with high levels of EGR, very advanced injections can be used allowing low temperature combustion of a premixed charge. Ogawa et al. [30] indicated that EGR above 58% produced very low soot and  $\text{NO}_x$  at the expense of higher CO. Reducing compression ratio from 18:1 to 14:1 extended the load limit of low soot and  $\text{NO}_x$  operation from 4.5 bar to 5.8 bar. Operating at the highest EGR rates was, however, susceptible to misfire and thermal efficiency reduced even at optimum injection timings. Lower temperatures due to reduced compression ratio may also open up avenues to explore lower EGR rates to improve soot when  $\text{NO}_x$  is sufficiently low [4]. Further works by [16, 31-33] have helped understand how low compression ratio can be exploited to change the operating region on the  $\phi$ -T map. Extended mixing and lower temperatures associated with low compression ratio enables combustion to avoid or minimise the soot and  $\text{NO}_x$  peninsula but as mentioned this is often at the expense of higher CO, HC and fuel consumption.

Relying on compression heating to increase in-cylinder temperatures can be insufficient at cold temperatures, even with the aid of a glow plug, to achieve stable combustion of the fuel air charge. These conditions cause cold idle operation to go into an unstable region or total failure to idle. The aim of idle straight after start-up is to maintain a constant engine speed at a sufficient load to overcome friction and ancillary load demands. Cycle-by-cycle variation must therefore be minimised, thus avoiding poor work output cycles and misfires is paramount to improve unstable engine speed and audible deviation.

### **2.3. Diesel Combustion Characteristics**

The ignition process in a diesel engine can be characterised as follows: the fuel is injected into a compression heated air charge under high pressure producing a spray of liquid droplets which become entrained with the air and evaporate. This then forms a fuel/air mixture which under the right equivalence ratio and temperature, begins to form ignition sites. Further mixture preparation and

---

combustion is accelerated by heat release from the first mixture to combust [2]. The time between fuel introduction and the detection of heat release due to combustion is known as the ignition delay period. The physical processes contributing to ignition delay are spray formation, penetration, evaporation and mixing. The chemical processes include the formation of radicals and further chain reactions. The chemical process is highly dominated by temperature, but is also pressure dependent, as illustrated by Pischinger [34] in a combustion bomb. The ignition delay increases exponentially with reducing charge temperature. Crua et al. [35] investigated the effect of pressure on ignition delay for a temperature of 700 K. For a pressure reduction from 65 to 42 bar ignition delay increased from 2 to 3 ms. Shock tube experiments and kinetic rate computations have also shown similar effects of pressure on ignition delay [36, 37].

Under warm operating conditions, long ignition delays are associated with high premixed combustion due to a longer time for the fuel and air to mix. A shorter ignition delay therefore reduces peak heat release and hence rates of pressure rise. Combustion noise is mainly influenced by the rate of pressure rise, reducing ignition delay can reduce the noise emitted [38-40]. Typically, ignition delays can be reduced by the addition of a pilot injection. Pilot injections are small quantities of fuel introduced prior to the main injection. The reduction in ignition delay is caused by the fuel vaporisation and combustion of the pilot injection providing a favourable higher temperature and pressure environment for the main injection. The use of a pilot injection has been found to provide more control over the heat release profile [41, 42]. Park [43] suggests that multiple injections reduce the ignition delay of the main injection and contribute to a higher power output by controlling the premixed combustion. Keeler [12] states that a shorter ignition delay of the main injection increases the ratio of diffusion-to-premixed burning and subsequently results in higher soot output. According to Lindl and Schmitz [2], during a long ignition delay period fuel may leave the zone of favourable ignition conditions and/or adhere to the walls and consequently fail to retain a mixture within flammability limits. Under cold conditions, it is therefore likely that long ignition delays result in poor combustion and an increase in misfiring cycles, as demonstrated by MacMillan [4]. This typically leads to a reduction in engine speed and poor idle control.

Various methods are used to identify the ignition delay period. Start of injection is usually determined by sensors that detect needle lift or a current clamp that picks up signals sent from the ECU. The start of injection is assumed to coincide with the

---

current clamp signals; but there will be a time lag associated with this method. Two methods of identifying the beginning of combustion are typically employed. The first, which is used in the work undertaken for this thesis, is the detection of a change in apparent heat release or pressure. This technique has been used extensively and provides a robust and reliable means of locating the start of combustion. The second method involves optical techniques requiring expensive equipment and optical access to the cylinder [44-46]. Dec and Espey [47] found that the pressure-indicated heat release rate occurs about 0.5 °CA (at 1200 rev/min) before the first substantial soot spots appear, so the onset of soot luminosity is a fairly consistent marker, albeit delayed, to the start of combustion.

### **2.4. Diesel Engine Technological Advancements and Cold Start Technology**

Many of the advances in technology over the last decade have been driven by more stringent emission standards for PM and NO<sub>x</sub>, NVH, and market competition to achieve better fuel economy and performance [13]. Fuel injection equipment (FIE) has been an important part and an area of interest in improving emissions and engine performance. Technological advancements have allowed much greater flexibility of fuelling injection strategies and thus engine operating characteristics. The reduction of combustion noise is also closely linked to the continued development of the fuel injection system [48]. In recent years, the move from mechanically to electronically controlled systems has improved the delivery of fuel in terms of quantity and timing. The combination of electronic control systems with piezo-electric injectors provide the capability of injecting around six or more injections per cylinder per engine cycle. The adjustment of timing, quantity and the number of injections that subsequently determines the combustion process can facilitate the improvement of work output, cycle-by-cycle stability and combustion noise.

One of the early types of fuel injection systems was Pump-Line-Nozzle, where the fuel is pressurised in a pump and then distributed to each injector in turn to start the injection process. Fuel is injected into the cylinder when fuel pressure at the injector is above a particular threshold. The injection quantity and timing is therefore controlled by pump dynamics [49]. An alternative system is the Unit Injector System (UIS), where the fuel injection pump and nozzle form a single unit. There is one unit injector per cylinder fitted in the cylinder head. It is actuated either directly by a tappet or indirectly by a rocker arm driven by the camshaft. The latest generation of

High Pressure Common Rail (HPCR) systems are particularly common for light duty. With HPCR systems, the functions of pressure generation and fuel injection are separated. HPCR systems consist of a number of components, namely a high pressure fuel pump, common rail, a pressure regulator, solenoid or piezo-electric injectors and an ECU for system control. Stumpp and Ricco [50] highlight that the HPCR system is able to adapt injection pressure independent of engine speed and fuel quantity. The injection pressure is controlled by a high pressure pump, which feeds fuel to a pressure accumulator, the fuel rail. Fuel lines then direct the fuel from the rail to the injectors. Bosch [51] states that this system offers the greatest degree of flexibility in the choice of fuel injection parameters. HPCR systems are able to deliver pilot and post injections that precede or come after the main injection respectively. HPCR systems have been an important part in facilitating with this process, providing the opportunity for higher injection pressures. This technology has led to the movement within the diesel engine sector to use smaller and more injector holes. This setup allows for better fuel vaporisation and mixing of air and fuel for the same fuel delivery rate, resulting in smaller fuel droplets [10]. Multiple pilot injections and the ability to accurately control small quantities of fuel have improved performance in cold conditions [4]. Schommers et al. [48] have highlighted the advantages and disadvantages of various injection systems, including distributor pump, unit injection and HPCR systems.

To mitigate the adverse effects on combustion stability and perceived quality imposed by cold ambient temperatures, starting aids have been implemented in many diesel engines of various sizes. Starting aids for diesel engines come in many forms: air intake heating (either electric heaters or manifold burners), heated fuel injectors, block heaters and glow plugs. Each attempts to promote ignition of the fuel air mixture. Heat storage systems are also being explored to aid cold starting and warm-up. Work by Schatz [52] demonstrated the use of a heat battery to store exhaust heat in an insulated container and applied it to heating the coolant, assisting cold start of different vehicles. The limit of startability for diesel engines improved from  $-16^{\circ}\text{C}$  to  $-28^{\circ}\text{C}$  whilst improving noise characteristics. A reduction of CO and HC emissions of up to 80% were also reported at  $-7^{\circ}\text{C}$  cold start. Up to 13% savings in fuel economy were found during the early warm-up phase.

Glow plugs are fitted as a cold start aid to nearly all diesel engines for passenger and light duty vehicles. Beru [53] provides a wide range of diesel cold-start technology. They offer small tip 2-coil glow plugs incorporating three-phase glow

technology. This means the glow plug heats up in a very short time period, between 2 and 7 seconds, heats during starting, and remains on for a post-heat period to increase the amount of fuel burnt and reduce emissions. Tip temperatures of up to 1050°C are achievable. One coil maintains the heating temperature whilst the other regulates the temperature to prevent overheating. Beru claim up to 40% less pollutant emissions during the warm-up phase and reliable starting at temperatures down to -30°C [53]. Small tip ceramic glow plugs are also available, with tip temperatures of up to 1250°C, but are much more expensive and require additional controllers. The latest system of glow plugs offer instrumented pressure transducers, known as Pressure Sensor Glow Plugs (PSG). The sensor measures in-cylinder pressure and feeds this to the engine control electronics for optimum performance. Adjustments to fuelling strategy and glow plug temperature can be made accordingly to minimise cylinder imbalance.

A summary of cold starting aids is provided by Lindl and Schmitz [2]. They concluded that intake manifold burners were more suited to large displacement engines, above a piston displacement of 1 litre, and at arctic temperatures due to the high volume air flow. The use of glow plugs did not guarantee a successful cold start in combustion cylinders greater than 1.5 litres because of the comparable small initial heat release. They showed that electric air intake heaters can be used to reduce noise, emissions and improve cold starting and warm-up, suitable for small (0.2 litre) to medium (1 litre) sized cylinder displacement. Their investigation found that 30 W per 0.1 litre displacement was necessary.

### **2.5. Combustion Imaging Studies**

Various optical techniques are used to study combustion characteristics. Particle Image Velocimetry (PIV) provides instantaneous velocity vector measurements in a cross-section of a flow and Rayleigh scattering and Schlieren techniques are used to observe fuel vapour air mixture regions [54-57]. Another more widely used technique for the study of combustion processes is Planar Laser Induced Fluorescence (PLIF).

The natural light emission of diesel combustion consists of two components; chemiluminescence and soot luminosity, both providing a convenient, nonintrusive measure of transient combustion phenomena. In hydrocarbon combustion, the main contributors to visible and ultraviolet chemiluminescence are formaldehyde ( $\text{CH}_2\text{O}^*$ ),  $\text{CH}^*$ ,  $\text{C}_2^*$  and the hydroxyl  $\text{OH}^*$  radical (where \* denotes an electronically excited

state) [58, 59]. Since exothermic chemical reactions are required to produce this chemiluminescence, it closely represents the occurrence of combustion heat release both temporally and spatially. The onset of chemiluminescent emission relative to the start of heat release is of the order of a few microseconds.  $\text{OH}^*$  has a major role in the soot formation and oxidation process [60], being the main oxidant for soot. With the use of a narrow band pass interference filter (centred at a wavelength of 307 nm)  $\text{OH}^*$  chemiluminescence technique can be applied to view reaction regions.

Soot luminosity is produced from the thermal or 'grey body' emission from soot particles that are heated to near flame temperatures by the combustion process [58]. Soot formation requires combustion heating to pyrolyse the fuel and initiate the multi-step formation process. This usually occurs at temperatures ranging from 1300 K to 2800 K [61]. Soot formation is therefore delayed from the initial cool flame reactions, which mainly result from  $\text{CH}_2\text{O}^*$  and  $\text{CH}^*$  [47]. Chemiluminescence is a relatively weak signal so it is generally not detectable by conventional imaging systems and requires an image intensifier and a spectral filter. Soot is the insoluble fraction of PM [62] and forms from pyrolysis early in the combustion process in local fuel rich areas. Soot oxidation occurs later facilitated by air entrainment into the fuel spray [63]. Carbon molecules typically react with oxygen forming carbon monoxide and subsequently carbon dioxide. Soot formation begins with very small condensation nuclei that undergo surface growth and the coalescence of nuclei lead to primary particles known as spherules. These have a diameter of approximately 30 nm. These spherules can undergo one of two processes; agglomeration into larger particles, or oxidation, which is a surface burning process which provides gas phase products [63].

Autoignition is the beginning of the thermal explosion that follows a physical delay (fuel vaporisation and fuel air mixing) and a chemical delay (chemical reactions leading to the onset of a flame) [57]. Work conducted by Dec and Espey [47] investigated the effects of TDC in-cylinder temperature and density independently on diesel autoignition using chemiluminescence imaging. They observed that the cool-combustion (chemiluminescence) reactions must proceed to a certain point before transitioning to more rapid hot-combustion reactions. The way in which this process proceeds was found to be dependent on temperature and pressure. Increasing the air temperature by 200 K resulted in a reduced ignition delay and reduced the initial premixed combustion spike. With reducing temperature, the first detectable cool-combustion occurs later and the period of this emission is considerably longer. This

subsequently delays the onset of sooting combustion (hot-combustion). They concluded that the larger ignition delay was predominantly caused by the transition from cool-combustion to sooting combustion and only moderately affected by the onset of the initial cool-flame reactions. Similar observations were seen when varying density; increasing pressure showed a consistent trend of a shorter ignition delay and a reduction in the maximum premixed heat release. For the range of conditions investigated, the magnitude of the effect of density on the heat release rate was greater than that of temperature. With changing density, only a small difference in first detectable chemiluminescence was seen, but the time required for the initial cool-combustion reactions to proceed to hot-combustion reactions increases dramatically. For changes in either temperature or density, the changes in ignition delay were predominately a result of the chemical delay and to a smaller extent the physical delay. The variations in ignition delay from density changes were dominated by chemical effects to an even greater degree than they were for changes in temperature. This is important because it suggests that higher Cetane number fuels could potentially offer benefits during cold idling conditions and higher glow plug temperatures may promote chemical reactions to achieve a reliable ignition and sustained burn.

French and Scott [64] state that the function of the glow plug, unlike other forms of starting aids, is to act as a hot spot to initiate combustion rather than to increase the bulk gas temperature. The position relative to the spray fringe was therefore highlighted to be important, as supported by [65] and [2]. High speed photography tests undertaken by Austen and Lyn [66] using an IDI engine observed that combustion originated from the hottest point near to the glow plug and spread downstream. Work by Lindl and Schmitz [2] suggested that glow plugs are ideally suited to low displacement engines, achieving positive starts at  $-20^{\circ}\text{C}$  provided that the glow plug tip temperature was above  $1100^{\circ}\text{C}$  and the tip contacted the rim zone of the fuel spray. Studies by Walter et al. [65] have shown their large influence on stable combustion during cold idling, in particular tip temperature and position relative to the spray plume. Reducing tip temperature and rotating the spray away from the glow plug tip had adverse effects on achieving adequate pilot combustion and then sustained main fuel combustion development. The study of the effects of glow plug temperature was limited to a single-pilot injection strategy whereas the work presented in this thesis examines the injection strategy and glow plug temperature trade-off.



Perrin et al. [67] studied the different stages leading to fuel combustion and main combustion development during cold start and idle using a 13.7:1 4 cylinder diesel engine with optical access. In combination with numerical modelling, they observed the air heated by the glow plug is carried downstream by the rotational swirl motion. The temperature of this hot wake in the downstream portion can remain insufficient to induce combustion. However, the close proximity of the spray to the glow plug was adequate to provide a point of initiation near to the tip where favourable temperature conditions are likely to be found. The temperature of the hot area downstream of the glow plug was found to assist vaporisation in the spray's downstream portion and therefore in combustion development. The pilot combustion was reported to only take place in a few of the sprays, leaving many of the sprays un-ignited. When introducing the main spray, combustion initiated near to the glow plug tip, but also in the hot gases induced by the pilot injection. This resulted in the main spray having a reduced delay. Combustion was observed to expand and propagate from this region and ignite the other sprays producing an almost 'stair shape' heat release profile. It is therefore not surprising that poor pilot combustion can hinder the main combustion. They highlighted that poor pilot injection combustion is usually associated with an inefficient main combustion development. It is, therefore, important to know how best to utilise pilot injections; when to introduce them and the fuel quantity that should be used. Idle performance was further investigated at -5°C. Engine performance and combustion stability criteria such as speed and IMEP variation were demonstrated to be poorly correlated. A better relationship was found between engine speed variation and combustion duration; a reduced duration was desirable to minimise engine speed fluctuations. The correlation still remained poor however and was highlighted that further investigation was needed to identify contributing factors toward poor idling stability.

MacMillan [4] conducted an investigation using computational fluid dynamics (CFD) to determine the effects of pilot injections on mixture distribution. It was reported that single pilot injections were poor since they produced a spoke of rich fuel from each injector nozzle at the time of combustion initiation which left areas of poorly utilised oxygen. Increasing the number of pilot injections was found to create a more homogenous fuel distribution by the time of the main injection. Using a larger single pilot injected far in advance did not have the same benefit compared to a triple-pilot strategy. The fuel was reported to enter the squish region that is distant from the glow plug tip with increased time for liquid fuel to condense on the cold cylinder

surfaces. Having small well separated pilots allowed the fuel to distribute around the bowl facilitated by air motion with minimum time for fuel to adhere to the cold surfaces and consequently always having vapour near to the hot glow plug tip. The main is therefore introduced into an already reacting environment releasing energy to promote further chain reactions of the main fuel.

### **2.6. Cold Start Performance**

The viscosity of the lubricating oil is strongly dependent on temperature. During cold starting, frictional loads increase due to higher oil viscosity. Studies by Burrows [68] and Tindle [69] have shown reducing ambient temperatures cause a progressive fall in cranking speed, due in part to reduced starter motor output, which is primarily a consequence of poor battery performance, and increasing friction due to rising oil viscosity. This leads to an extended time delay before firing commences as a result of increased heat transfer and blowby losses which lower maximum in-cylinder temperatures and pressures. These findings are in agreement with [70] and [71]. To explain reduced cranking speeds, work by Shayler et al. [72] examined the effect of oil temperature on FMEP by performing teardown tests. They found a disproportionate increase in FMEP with reducing oil temperature, with friction significantly increasing when below 0°C.

There are three main phases of an engine start [68, 69]: from key on to first-fire, the phase of firing-assisted cranking and lastly the phase from this through the run-up to idle. Throughout all three phases achieving a large work output and avoiding misfires is important in successfully reducing the time to idle. Since the starter motor is limited to low engine speeds, a successful start requires IMEP to exceed FMEP. For the IDI engine studied, the engine rapidly accelerates to idle speed by combustion work at temperatures above -10°C. At temperatures below this, the corresponding increase in frictional losses is initially greater than the available work produced by combustion resulting in extended start times. When firing is accomplished, IMEP turns the engine against friction but the input from the starter motor is still necessary. The period that follows is the firing-assisted cranking defined by speeds that are considerably higher than those during normal cranking but the engine will stall if the starter motor is turned off. Continued cranking typically raises the temperature and lowers friction by reducing oil viscosity at critical bearing surfaces. A successful start is achieved when friction reduces enough and speed

increases to idle. A glow plug tip temperature of at least 850°C was required for best performance, which is reached in under 10 s at -20°C. Longer pre-heat times gave no further improvement due to the majority of the heat being lost to the coolant and the rest during the gas exchange part of the first cycle. They concluded from this that the glow plug doesn't function to raise the bulk temperature but rather act as an ignition source. Interestingly, reducing the tip protrusion was found to improve starting by increasing IMEP in firing cycles. This was attributed to the adverse effect on swirl in the pre-chamber and subsequently improved mixing. Re-optimising the injection strategy was found to improve IMEP and start times and deemed necessary for reliable starting at cold temperatures.

In addition to poor cranking performance due to higher friction, cold in-cylinder temperatures can hinder work output necessary to reach idle away from cranking speeds. Work by MacMillan et al. [4] investigated the effects of cold starting at two compression ratios, 18.4:1 and 15.4:1. The compression ratio was reduced by increasing the size of the piston bowl. At low engine speeds, less than 600 rev/min, there were significant reduced losses at the low compression ratio case. The lower in-cylinder pressure resulted in reduced losses to heat transfer and blowby. Reducing engine speed to around 300 rev/min saw significant increases in heat transfer losses and blowby due to extending the time under high pressure conditions. At 300 rev/min pilot injection was utilised at both compression ratios to extend the region of high work output, making the strategy more robust to changes in timing and speed. Faster deterioration in work output was seen for the low compression case as timing was retarded. Despite this, at 300 rev/min cold start conditions, the lower compression ratio was capable of higher IMEPg. This was attributed to reduced losses and reduced peak rates of heat release and longer combustion durations allowing more mixing and subsequently larger cumulative heat release.

Another recent study in 2008 examining the effects of reducing compression ratio (from 17:1 to 13.7:1) on cold starting has been conducted by Pacaud et al. [73] using a common rail 4 cylinder DI diesel engine with optical access at temperatures down to -25°C. Their study was also supported by CFD simulation. At 17:1 using the standard calibration, the start delay increased from 1.1 to 5.7 s when reducing temperature from 20 to -25°C. Reducing compression ratio using the same calibration set points extended the start delay to 17.5 s at 20°C with further

deterioration with lower temperature, until starting wasn't achieved at 0°C. This was attributed to two reasons; insufficient quantity of vaporised fuel due to the lower temperature and pressure, and the quantity of vaporised fuel near to the glow plug was inadequate for autoignition. Optimising the injection strategy for low compression ratio at -20°C resulted in comparable start delays to that achieved at high compression ratio. The benefits were established from an early injection timing to increase the time for vaporisation, increasing total fuel quantity, a close coupled pilot to the main injection and an optimum pilot quantity. The work presented in this thesis has indicated that similar fuelling strategies have provided benefits in improving work output and stability during cold idling.

Variations specific to injector spray and glow plug interactions were also studied [73]. The pre-glowing duration was found to be important and had a larger impact at colder temperatures. Beyond about 8 s pre-glow resulted in no further improvement in start delay. They found that by either changing the injector protrusion into the cylinder or rotating the injector spray and subsequently varying the proximity of the spray edge to the glow plug resulted in large changes in time to start. Time to idle reduces by around 3 s when varying spray orientation and as much as 10 s when changing injector tip protrusion. Tests were also conducted investigating the influence of cranking speed; an increase in cranking speed reduced time to idle due to the increase in temperature and pressure caused by a reduction in time for losses to heat transfer and blowby. Results from the CFD computations concluded that only around 15% of the injected fuel vaporised with the majority adhering to the piston bowl walls. Combustion initiation was found not to take place after the spray initially travels close to the glow plug, but after the fuel had vaporised in the spray periphery and re-circulated back toward the glow plug from the bowl. It is therefore apparent that reducing spray impingement is beneficial as to not devoid the fuel from vaporising and consequently reduce the likelihood of autoignition from the glow plug [74-76]. Areas of rich fuel however tended to be the coolest regions caused by the heat transfer from the surrounding air reducing the possibility for autoignition. An increase in total fuelling is therefore prone to over cooling the charge and having a negative impact on ignition [77]. An increase in fuelling level has been shown to promote the early stages of main combustion and subsequently improve idle stability in this study as detailed in Chapter 5 and 6.

Whilst starting deteriorates with colder temperatures, the above literature suggests that start-up times are not generally extended by reducing the compression ratio so

---

long as an appropriate injection strategy is employed. The deterioration in cold idling quality is, however, an area of greater concern as indicated by [4] and [73], but understanding the influences during cold start will almost certainly lend themselves well to help improve cold idling.

### 2.7. Cold Idle Performance

The idle phase commences immediately after start-up where maintaining a fixed speed is required with minimal deviation. Mitigating misfires is therefore important during this phase and can be problematic particularly at cold temperatures and even more so at low compression ratio [4].

Recent investigations of idle stability under cold conditions include those of MacMillan et al. [78, 79], Payri et al. [80], and Perrin et al. [67] who signal the importance of cool flame and hot premixed combustion in promoting rapid and reliable combustion of fuel delivered in the main injection. Work conducted by MacMillan et al. [4] found that at high compression ratio during typical idle speeds, a pilot injection was necessary to obtain significant positive work output at all temperatures investigated between  $-20^{\circ}\text{C}$  to  $10^{\circ}\text{C}$ . It was reported that stability becomes worse as temperature is reduced, and at  $-20^{\circ}\text{C}$ , it was not possible to achieve  $\text{CoV}_{\text{IMEPg}}$  of less than 10%. Increasing the number of pilots to two saw work output increase by around 25% for the same fuelling and achieve better than 10% stability over a range of timings. The improvement was attributed to a greater heat release half way through the main combustion. It was found that a triple-pilot injection strategy maximised this benefit, resulting in low  $\text{CoV}_{\text{IMEPg}}$  over a broad range of injection timings and engine speeds at  $-20^{\circ}\text{C}$ . Four pilots led to the re-introduction of poor cycles.

Deterioration in stability was reported at  $-20^{\circ}\text{C}$  idle speeds when lowering compression ratio with  $10\text{ mm}^3/\text{cycle}$  more fuel required to achieve similar IMEPg. The best stability attainable was around 20%, twice the level defined as acceptable under the test conditions. MacMillan et al. [79, 81] concluded that although target stability at high compression ratio could be achieved through the optimisation of the injection strategy and modest glow plug temperatures, at low compression ratio, injection strategy optimisation alone was not sufficient to achieve target stability. At low compression ratio, the most effective strategy to improve stability combined pilot injection and the use of glow plugs operating at higher temperatures. Significant

improvements were observed by raising glow plug temperature from typically standard values around 900-950°C to 1100°C. Beyond this the improvement was relatively small. The increase in glow plug temperature produced a reduced and less variable ignition delay, with an increase in peak rate of heat release.

Under cold conditions, multiple pilot injections to enhance heat release and ignition characteristics has been explored by [82] and [83] and shown to offset the effect of lower in-cylinder temperatures on ignition delay, as noted by Pischinger [34]. Okude et al. [84] point out that dividing the pilots is necessary when an increase in total pilot quantity is required to avoid liner impingement and to improve combustion. Reducing cylinder liner attack by pilot spray was also shown to reduce HC and CO emissions. Tomoda et al. [82] demonstrated the importance of injector design and multiple pilots. For an increase in number of injector holes for an equal nozzle flow rate, they observed a reduction in the amount of latent heat of vaporisation per nozzle hole and consequently reduced the temperature drop inside the fuel spray. Air entrainment was also said to increase assisting with fuel air mixing. Whilst the multiple holes distributed the spray spatially, multiple injections were found to improve combustion attributed to the control over the fuel temporally within the cylinder. They concluded pilot combustion and hence total heat release can be greatly enhanced with the use of multiple injections.

Han et al. [85] studied the effect of injection timing on combustion stability. Their experimental and analytical studies were aimed at developing a new diesel engine cold start strategy to improve or eliminate poor combustion stability. They concluded that long ignition delays are associated with very early main injection timings. This was attributed to low in-cylinder temperature and pressure causing liquid fuel to deposit on the cold walls and hindering fuel evaporation and mixing with the air. Retarding main injection timing was found to reduce ignition delay due to higher temperatures and pressures. A minimum ignition delay was reported just before TDC, with any further retardation in injection timing leading to an increase in ignition delay. Higher engine speeds were found to be more prone to deterioration at retarded timings due to less time available for the mixture to react at high temperature and pressure around TDC. Reducing ambient temperature was found to produce a smaller range of injection timings before the onset of misfiring. Misfiring tended to worsen for advanced main injection timings. Injection timing has been investigated as part of this work under -20°C conditions with similar findings.

Reducing separation between pilots and pilot-to-main and using a high number of pilot injections produced stable combustion over a wider range of timings.

Payri et al. [80] conducted an investigation into the combustion characteristics in a low compression ratio DI diesel engine at idle under low temperature conditions. The work undertaken was to better understand the effect of multiple injection strategies on IMEP and combustion stability. They found that the timing of the pilot closest to the main injection was the most influential parameter on the rate of heat release irrespective of the multiple injection strategy applied. A dwell angle of 6 °CA produced the highest IMEP and was associated with the largest pilot contribution leading to a strong main combustion development with a short ignition delay. Larger dwell angles between injections were associated with lower IMEP and longer ignition delays similar to findings in this study. Larger dwell angles delayed the main combustion toward the expansion stroke. This was attributed to the warming effect of the energy released by the pilot combustion reduced by the cooling effect of the cold walls. Splitting the pilot injection in two enhanced pilot combustion further and hence cumulative heat release resulting in higher IMEP. Stability was found to be well correlated to combustion phasing. If combustion is delayed then stability deteriorates sharply whilst marginally worsening when combustion is advanced. Combustion stability was poor when earlier and smaller pilot injections were used for a multiple injection strategy.

### **2.8. Combustion Noise**

The perception of idle quality is not only defined by combustion stability but also the noise deviation and absolute level emitted. This is particularly important during the idling phase for the consumer [86] and is often monitored and mitigated as much as possible by manufacturers during the calibration stage despite there being no direct regulation of combustion noise. The three primary sources of noise production in a diesel engine come from gas-flow, mechanical processes and combustion. Gas-flow noise is generated during the intake and exhaust phase and mechanical noise stems from inertia forces causing piston slap, from the valve train, gears, fuel injection system and bearings. The combustion noise originates from a steep rise of cylinder pressure after ignition [12, 86, 87]. These gas forces act on the structure and cause the engine block to vibrate resulting in combustion noise radiation.

It is unlikely that a combustion noise level in excess of 85 dB(A) will be tolerated by manufacturers and passengers [12] and this level will potentially be considerably lower during idling conditions. If excessive noise cannot be mitigated at source then noise dampening is generally required to improve both passenger and pedestrian comfort which has been a long time concern for diesel engines compared to gasoline.

### **2.9. Summary**

In this chapter, current knowledge base on the effects of reduced in-cylinder temperatures on cycle-by-cycle stability at start-up and idling conditions has been reviewed. Even though lowering the compression ratio deteriorated start time to idle particularly at cold temperatures, it appears that the adverse effects can be cancelled out by re-optimising injection strategy. An area of greater concern voiced by several authors was the poor cycle-by-cycle stability at cold idling. Only a few recent investigations have solely analysed the effect of injection strategy on heat release characteristics and associated connection with combustion cycle-by-cycle stability under cold idling conditions. In these investigations, high glow plug temperatures coupled with multiple injection strategies have been used to achieve stable combustion. If these do not yield acceptable levels of stability then additional aids such as air intake heaters may need to be considered to assist cold idling.

Photographic studies have been reviewed to further elucidate the effects on the combustion process, where typical test engines are restricted in providing spatial information. The role of the glow plug has been shown to function as an igniter and contributes little to heating the charge. Having fuel vapour near to the glow plug tip was shown to be important to achieve ignition since the glow plug is the only place in the cylinder creating adequate conditions. Poor pilot combustion had a direct impact on the main spray and led to a poor main combustion development. A high speed photographic study presented in Chapter 3 aims to build upon these current findings, and examine how glow plug temperature, injection strategies and other factors influence the initiation and early stages of combustion as a guide to help interpretation of results from the test engine.



# Chapter 3

## Optical Study of Factors Influencing Combustion Initiation

---

### 3.1. Introduction

In previous studies [4, 81-83], the use of high temperature glow plugs and multiple pilot injection strategies were shown to influence cycle-by-cycle stability under idling conditions, particularly at low ambient temperatures, but how these and other factors influence combustion initiation and early heat release is largely unexplored. This is due in part to what is usually limited access to the combustion system at the start of combustion. In this chapter, the results of high speed photographic studies of combustion initiation in a combustion bomb are described and interpreted. The aim of the study has been to investigate how factors influence the initiation and early stages of combustion as a guide to what influences these in the test engine. The factors investigated are glow plug temperature, vessel temperature and pressure, number of pilot injections, pilot quantity and separation (time between the start of two injections). The range and reasons chosen for each parameter are outlined in Table 3-1. These have been matched to engine settings as far as possible. Vessel temperature remains lower, vessel pressure rise due to combustion is reduced due to the larger volume, and initial conditions in the chamber are quiescent. Because of these differences, the bomb study has not been used to describe the later stages of combustion development.

### 3.2. Imaging Technique, Experimental Facilities and Data Acquisition

Natural light emissions during diesel combustion results from chemiluminescence and soot luminosity. These are frequently used diagnostics in combustion research, both providing a convenient, nonintrusive measure of transient combustion phenomena. The soot imaging technique has been used in this investigation, and the luminosity is produced from the thermal or 'grey body' emission from soot

particles that are heated to near flame temperatures by the combustion process [58]. These emissions have been used to provide an indication of reaction sites.

A schematic of the setup of the bomb facility used in the study reported here is given in Figure 3-1. A fuel pump provided the piezo-electric 8 hole injector with standard Shell V-Power pump fuel at 200 bar with the engine rig experimental facility providing the injector signal (the details of the engine rig setup are presented in Chapter 4). A 5V TTL signal was also sent to the camera from the engine rig to provide a rising edge to trigger the camera. A ceramic glow plug with a 3.3 mm diameter tip was used throughout. The temperature was monitored by an R-type thermocouple embedded in the tip and therefore gave an internal tip temperature. Compressed air was used to pressurise the optical vessel and three Watlow cartridge heaters, each providing approximately 350 W, were used to increase the bulk temperature of the air. The bulk temperature was monitored using K-type thermocouples. As a precautionary measure, a pressure safety valve was fitted to release pressure exceeding 75 bar. The pressure was measured using a piezo-resistive Kulite pressure transducer rated to 75 bar maximum pressure.

A National Instruments CompactDAQ modular hardware data acquisition system was used to measure signals. A cDAQ-9172 chassis housed two modules:

- NI9219 24 bit analog input used for thermocouple measurements (including cold junction compensation).
- NI 9201 12 bit analog used for pressure transducer measurements.

A model was created using LabView software to monitor the signals in real time. For the image acquisition system, a Phantom V12.1 CMOS high speed camera was used, capable of 6,242 frames per second at maximum resolution 1280×800 pixels and up to 1,000,000 frames per second at reduced resolution. The best compromise between image resolution and rate of data capture was found using 10,000 frames per second. This gave a resolution of 800×600 pixels. The images were saved at 8 bits per pixel, providing a grey level of 256. This number represents how many shades of grey makes up an image, so every pixel of a grey scale image has a brightness value ranging from 0 (black) to 255 (white). A fixed focal length, 105 mm lens with an aperture of f/22 and exposure time of 4  $\mu$ s were chosen. This aperture provided a good depth of field whilst the exposure time allowed sufficient luminosity of the combustion event. For the majority of data collected during this study, no

backlights were used to illuminate the area of interest since the combustion was easily detectable.

### **3.3. Image Post-Processing**

Two ways of analysing the images were adopted; visual inspection of the images at various points during the initiation process, and post-processing the images to identify the number of pixels representing the projected area of luminous emissions, or enflamed area of combustion, taken to be an indication of the vigour of combustion. The former gives an insight into local effects of the initiation process, whilst the latter provides quantitative data that is used to make test-to-test comparisons. The two methods have been used together to describe the initiation process.

The post-processing of the images recorded from the camera was achieved using MatLab. A script was written to read in the images and identify areas of combustion. This identification of areas representing combustion was subjectively chosen by recording the grey level of the background from an image containing no combustion. This was done for a variety of images, but since the quality of the images remained similar during a test run and didn't change from test-to-test, this value didn't significantly change. Therefore, any grey scale value above this threshold represents combustion. From this, a high contrast black and white version of the grey scale image was created. The white regions represent the enflamed area in the original image, and subsequently gave the number of pixels for each image providing an indication of the amount of sooting combustion. Although the combustion region has been referred to as enflamed area, it is the number of pixels that provides this indicator, and has not been converted to an actual area.

To help describe the effect of parameters on initiation and the early stages of combustion, six indicators have been proposed to characterise the progression of combustion:

- The time period from the start of the first injection to the first detectable luminous soot.
- Average enflamed area growth rate of the pilots from the first detectable soot to when the main injection begins. This provides an indication of the rate at which the enflamed area is growing before the main is injected.

- Enflamed area at the time of the main injection, which [88] reported to be important in influencing the course of the main combustion.
- Main initiation delay, defined as the time period between the start of the main injection and the point where the enflamed area reaches 1,000 pixels and continues to increase.
- Average enflamed area growth rate of the main, which is between the point of main initiation to either maximum enflamed area or up to 5 ms after the start of the main, whichever one comes first.
- Maximum enflamed area, which should be as high as possible to mark a successful ignition and a vigorous combustion.

In determining the main initiation delay, a threshold of 1,000 pixels represents between 1-5% of the maximum enflamed area for all the tests, and indicates a sufficient amount to mark the onset of initiation of the main injection. In the case of tests where the enflamed area from the pilots is much higher than 1,000 pixels, then the point of initiation is taken as the location where there is a rapid increase in enflamed area. For all tests, enflamed area up until 5 ms after the start of the main injection has been assessed, as this is deemed to be a sufficient amount of time to examine the early stages of combustion.

### **3.4. Description of Initiation and Early Stages of Combustion**

In this section, the typical features of initiation and the early stages of combustion are described. Figure 3-5 shows the temporal sequence of two fuelling strategies, single- and triple-pilot. The single-pilot has a 2 mg pilot, 18 mg main injection and a separation of 1.7 ms. The first detectable soot particles appear very close to the tip 1.4 ms after the start of the pilot injection, or around 1.1 ms after the sprays begin to pass the tip. More spots begin to appear forming several clusters up to the start of  $SOI_{Main}$  and 0.5 ms after. At this point, these particles are drawn away from the tip surface and mix in the main spray in the region closest to the tip up to 2.3 ms after  $SOI_{Main}$ . During this time, a small amount of particles travel a short distance on the periphery of the spray toward the nozzle. All of the generated particles appear to move in a swirl motion which is most probably caused by the shearing effect between the spray edge and the stagnant air. The point of initiation stems from this

location, and 2.3 ms after  $SOI_{Main}$ , this soot region begins to propagate downstream in the direction of the spray. This occurs around 0.3 ms after the end of injection.

For the triple-pilot case, each pilot is 2 mg, placed in advance of the main injection with a separation of 1.7 ms. The main quantity is reduced to 14 mg to keep total fuelling constant. The images begin at the start of the second pilot injection. The first detectable soot particles appear near the surface at 1.3 ms after the start of the first pilot injection. Soot particles from multiple locations near the tip surface then begin to emerge up until the start of the second pilot injection. 0.3 ms after the start of the second pilot, the soot particles begin to migrate away from the tip surface and mix in the spray near to the tip. For a further 0.5 ms several soot clusters form, which then begin to propagate downstream in the direction of spray. Generally, 500-1,500 pixels are formed before combustion proceeds to propagate. By the time of the start of the third pilot injection, a relatively large enflamed area, particularly on the right hand side, is formed stemming from the tip. The right spray directly penetrates the reaction region, whilst the edge of the left spray mixes with the soot particles. 0.8 ms after the start of the pilot, reactions quickly spread downstream from the location of the large sooting combustion region. Both main sprays penetrate this sooting region. The point of initiation of the main spray is not confined to the region near the tip, but also takes place throughout large regions of the cross section of the downstream portion. A more vigorous combustion ensues as shown in the images between 1 and 3 ms after  $SOI_{Main}$ . These findings are consistent with those reported by Desantes et al. [88], where they identified that a higher presence of pilot combustion improved combustion of the main injection.

### 3.5. Injector Spray and Glow Plug Position

The majority of tests were conducted at the same injector and glow plug position. A CAD drawing was created to show these dimensions, as illustrated in Figure 3-2. A 3.3 mm diameter ceramic glow plug tip is offset 3.3 mm from the injector. A plate was designed and manufactured to allow the injector to rotate around its longitudinal axis, incorporating graduation marks to measure angular rotation, as illustrated in Figure 3-3. Tests were conducted to decide the optimum angular position of the injector. To do this, backlighting was used to increase the luminosity of the fuel sprays so that they could be easily observed. This procedure involved running several tests until the edge of each spray plume either side of the glow plug were similar distances from the tip and the enflamed area progression was similar. When

these criteria were met, the injector position was set. This resulted in the injector spray rotated approximately  $4^\circ$  counter clockwise from the vertical axis. In this setup, only the two sprays either side of the glow plug tend to initiate since the remaining six sprays are too far away from the hot source. In extreme circumstances where one spray directly impinges the glow plug tip, the combustion region initiated by the glow plug is deflected and spreads to the surrounding sprays causing them to ignite.

Whilst determining the optimum angular position of the injector, it became apparent there was a high sensitivity of ignition to the distance between the spray plume edge and the glow plug tip. Rotating the injector so that the top spray was vertical i.e.  $4^\circ$  clockwise from the optimum position, it was found that the spray to the right of the glow plug tip failed to ignite. This is illustrated in Figure 3-4. Rotating the injector resulted in an increase of around 0.5 mm between the plume edge and the glow plug tip, so small changes do appear to have a significant impact on combustion initiation, which is consistent with findings from [65]. The most likely explanation is the amount of fuel vapour present near to the right hand side of the glow plug tip is insufficient and the local temperature is too low for initiation. The other noticeable change is the difference in enflamed area produced by the left spray. Reducing the distance between the plume edge and glow plug tip shows a large benefit. The first detectable soot is advanced by 0.6 ms, and 3 ms after  $SOI_{Main}$  a much larger enflamed area is observed. Although this was identified as an important parameter on combustion initiation, time constraints and availability of the camera restricted the amount of data that was captured and for these reasons a more detailed sweep was not assessed. These limitations also restricted a full investigation of interactions and a systematic design of experiment was not conducted. Nevertheless, this investigation has focused on six parameters, described above, that have been identified as principal factors in influencing combustion and cold idling cycle-by-cycle stability.

### 3.6. Influence of the Number of Pilot Injections

The evolution of combustion for different fuelling strategies where the number of pilot injections is varied from one to four, and one case where there is just a single main injection with no pilot, is illustrated in Figure 3-6 and Figure 3-7. Each pilot is 2 mg and total fuelling kept at 20 mg. A fixed separation of 1.7 ms is used between each of the pilots and pilot-to-main. In the single main injection case, the first soot luminosity is detectable 1.3 ms after  $SOI_{Main}$ , located very close to the glow plug tip

surface. Up to 1.7 ms, the number of soot particles increases, present in small clusters very near the tip surface. These pockets of soot particles begin to migrate away from the tip surface at 1.7 ms and mix in the part of the spray that's near to the tip. This occurs up until 2.7 ms, and from this location, the soot slowly propagates downstream in the direction of spray. By adding more pilot injections, a larger proportion of fuel is exposed to the tip before the main injection, with both triple- and quad-pilot strategies achieving a large pilot combustion at the time of the main injection.

One other benefit of using multiple pilots is that combustion induced by early pilots promotes the ignition of later pilots. This is illustrated in Figure 3-8 and Figure 3-9 for twin- and triple-pilot strategies respectively. In the twin-pilot case, pilot 1 and 2 were injected during different tests so no interactions took place, and compared with results when the two pilots were injected during the same test. In the second case, the enflamed area is much higher, suggesting that the soot generated from the first pilot contributes to an increase in enflamed area produced by the later pilot. A similar trend exists for the triple-pilot case, and by using three pilots instead of only two raises the enflamed area at  $SOI_{Main}$  by ten times.

Enflamed area is illustrated in Figure 3-10 for no pilot, single- and twin-pilot strategies. Two tests have been ensemble averaged; the individual test results are indicated by the range bars for each condition. The rate of pilot combustion is raised and main initiation delay reduced by increasing number of pilot injections, from 3.1 ms when no pilot is used, to 2.2 ms with a twin-pilot strategy. After the main initiation delay, the enflamed area increases more quickly when using more pilot injections, and a more vigorous combustion ensues generating a larger maximum enflamed area. The same effects are increased when three or four pilot injections are used, as illustrated in Figure 3-11.

To investigate the influence of the number of pilot injections used to deliver the same total mass, experiments were carried out using a fixed total of 6 mg in single-, twin- and triple-pilot strategies. The separation was held constant at 1.7 ms. In Figure 3-12, it can be seen that distributing the 6 mg over more pilot injections results in a larger enflamed area at  $SOI_{Main}$  and the enflamed area after  $SOI_{Main}$  increases more quickly. The improved combustion as a result of increasing the number of pilot injections is, therefore, not solely due to an increase in total pilot quantity. The mean

initiation delay for the single-pilot case is 2.2 ms, reducing to 1.6 ms for both twin- and triple-pilot strategies.

With increasing the number of pilots and maintaining equal separation, however, the time of first fuel introduction is advanced, which provides more time for the pilots to react. This has been addressed, but the conditions are different to those tests compared above. The tests compared are single- and twin-pilot strategies with a total pilot quantity of 4 mg. In the twin-pilot case, the separation is 0.83 ms. The pilot from the single-pilot strategy is introduced at the same time as the first pilot in the twin-pilot case, which is 1.7 ms before  $SOI_{Main}$ . The images are illustrated in Figure 3-13, with the enflamed area in Figure 3-14, which show an improvement in the twin-pilot case. The time of first detectable soot and enflamed area around  $SOI_{Main}$  is similar. There is no discernible change in main initiation delay, but there is an increase in the enflamed area which is particularly noticeable at 4 ms after  $SOI_{Main}$ , with both spray plumes exhibiting a larger combustion region. Since the main injection is the same, this suggests that there is a direct improvement in pilot combustion which is modifying the main combustion. The increased pilot combustion may not be apparent before the main injection because of the short amount of time from using small separations. The benefit of distributing the same total pilot fuel quantity over more injections and the same time period may stem from combustion from the first injection promoting a more vigorous combustion of the second injection. This is only comparing one set of conditions but it serves to show that more pilot injections remain advantageous when the total pilot quantity and the time of the first injection are the same. There is some uncertainty whether this same trend is followed when using different pilot quantities and separations, but further testing would be needed to explore their interactions.

### **3.7. Influence of Pilot Injection Quantity**

The effect of changing pilot quantity on enflamed area for a single-pilot strategy is illustrated in Figure 3-15. The first detection of soot occurs at a similar time and enflamed area at  $SOI_{Main}$  is similar across the range of total pilot quantities. The initiation delay reduces with increasing pilot quantity, from 2.5 ms when using 2 mg, to 1.8 ms when using 8 mg. The largest enflamed area following the main injection is achieved by using larger pilot quantities.



Similar but more pronounced trends arise when a twin-pilot strategy is used, as illustrated in Figure 3-16. The time of first detectable soot is similar for changes in pilot quantity, and there is no discernible difference in enflamed area at the start of the second pilot injection. A short time after the second pilot is introduced, the soot particles generated from the first pilot around the surface of the tip begin to mix, but in the higher total pilot quantity cases, the soot particles increase more quickly in the direction of spray. This results in an increase in enflamed area at  $SOI_{Main}$ , with greater gains achieved with higher pilot quantities. Increasing pilot quantity reduces initiation delay. The mean initiation delay is 2.4 ms when using 2 mg total pilot quantity, reducing to 1.5 ms when using 8 mg. The enflamed area of the main injection generally increases more quickly for both 6 and 8 mg total pilot quantities compared to 2 and 4 mg, with an associated increase in the maximum enflamed area. In the 8 mg case, there is a relatively large variation between the two tests. The test with the highest enflamed area before 3 ms is due to a very strong left hand side spray caused by a large pilot combustion. This then diminishes whilst the right spray produces a relatively large enflamed area, causing the total enflamed area to level off. With the other test, however, the left hand side spray is similar to the right, starting off less vigorous but produces a relatively large enflamed area at the same time causing a higher total enflamed area after 3 ms.

### 3.8. Influence of Injection Separation

Tests were performed using single- and twin-pilot strategies to investigate the influence of injection separation. The separations studied were 0.83, 1.7, 2.5 and 3.3 ms, which closely represent 5, 10, 15, and 20 °CA when running at 1000 rev/min. The separation between each pilot and pilot-to-main remained constant. Each pilot was maintained at 2 mg, so the single-pilot was [2,18] mg and the twin-pilot was [2,2,16] mg. The influence of separation on enflamed area for the single-pilot strategy is illustrated in Figure 3-17. The enflamed area around  $SOI_{Main}$  remains small for all separations, but increasing separation up to 2.5 ms produces a small rise, where it then marginally reduces. Initiation delay is similar for all separations, ranging from 2.4 to 2.5 ms. The enflamed area after main initiation for 3.3 ms separation is not very repeatable, but the mean is similar to all the other cases, apart from 2.5 ms separation which produces a larger enflamed area.

The dependency on separation is similar for the twin-pilot strategy, as illustrated in Figure 3-18. The enflamed area at the start of the second pilot injection rises when

increasing separation up until the 2.5 ms case, where it then slightly reduces. An increase in separation progressively raises the enflamed area at  $SOI_{Main}$ . Increasing separation from 0.83 to 2.5 ms does not affect initiation delay, each producing 2.2 ms, but further increasing separation to 3.3 ms produces a larger reduction, resulting in 1.6 ms. Enflamed area after main initiation increases much more quickly for 2.5 and 3.3 ms, and the maximum is raised. In these two large separation cases, the large region of soot particles at  $SOI_{Main}$  is penetrated by the main injection. Soot is quickly produced in large regions of the cross section of the downstream portion of the spray plumes. The direct improvement in pilot combustion is due to the increase in residence time that the pilot fuel is present near to the glow plug. A longer time period allows the glow plug to ignite more of the fuel vapour in its proximity and generate a larger region of sooting combustion to assist the burn of the main spray.

### 3.9. Influence of Glow Plug and Vessel Temperature

The effect of changing glow plug and vessel temperature on combustion initiation has been investigated. In the single-pilot case, the results are presented in Figure 3-19, and Figure 3-20 for different glow plug temperatures at a vessel temperature of 100°C. Increasing glow plug temperature from 900 to 1300°C advances the time of first detectable soot by around 0.6 ms for all vessel temperatures. The main initiation delay is marginally reduced and the enflamed area increases more quickly, resulting in a higher maximum enflamed area. The increase in the maximum enflamed area with increasing glow plug temperature is greater at higher vessel temperatures.

The combustion evolution for different vessel temperatures at a glow plug temperature of 900°C is shown in Figure 3-21. The influence of vessel temperature on the time of first detectable soot is generally very small. Enflamed area at  $SOI_{Main}$  is relatively low and insensitive to vessel temperature apart from at the highest glow plug temperature, where the highest is produced by 100°C vessel temperature. From the images, very little enflamed area is apparent around main injection timing and up to 2 ms after for all vessel temperatures. It is only when time reaches around 3 ms after  $SOI_{Main}$  that there is a distinguishable difference in enflamed area from varying the vessel temperature, with the highest temperature exhibiting the largest enflamed area. Increasing vessel temperature does not influence main initiation delay at any glow plug temperature, but the enflamed area increases more quickly and the maximum enflamed area is raised. The largest maximum enflamed area is established at the highest glow plug and vessel temperature, suggesting that high

glow plug temperatures cannot greatly alleviate poor combustion due to low vessel temperatures. The most likely explanation is that chemical reactions and vaporisation remain low. Work conducted in [47] explored the effect of changing bulk temperature from 627 to 827°C for diesel combustion initiated by compression heating rather than a glow plug. Their findings revealed that higher bulk temperatures predominately promote chemical reactions leading to a reduced ignition delay. The physical delay was also shortened but to a lesser extent, indicating that vaporisation is also promoted. The latter is supported by Lacoste [89], who studied the effect of air intake temperature on droplet behaviour at constant pressure, and found that smaller droplets were produced by raising temperature as a result of increased evaporation.

The twin-pilot results are presented in Figure 3-22, together with the combustion evolution in Figure 3-23 showing glow plug temperature changes at 100°C vessel temperature. The trend in time of first detectable soot is similar to the single-pilot case relative to the first injection, but since the extra pilot is placed in advance, sooting combustion does begin earlier relative to the main injection. The enflamed area at the time of the second pilot injection remains small, but the enflamed area at  $SOI_{Main}$  generally increases with rising glow plug temperature, which is most apparent at 200°C vessel temperature. Increasing glow plug temperature produces a small reduction in main initiation delay, and the growth rate of the main combustion is at its highest at the hotter glow plug temperatures. The maximum enflamed area is also raised when using hotter tip temperatures. The images show that the combustion of the right hand side spray for the highest glow plug temperature of 1300°C is not particularly strong, but the overall contribution to enflamed area is higher due to a strong left spray. One explanation for this variation may stem from the larger enflamed area on the left hand side of the glow plug tip around main injection timing. The left main spray penetrates this larger enflamed area, and advances the onset of sooting combustion in the downstream portion of the spray, as is evident 2 ms after  $SOI_{Main}$ . The result is a larger enflamed area throughout the entire spray plume, which is further evidence of the need to achieve a strong pilot combustion to help promote a vigorous burn of the main spray. Similar to the single-pilot case, the maximum enflamed area is more sensitive to glow plug temperature at 100 and 200°C vessel temperatures compared to 40°C.

The combustion evolution for different vessel temperatures at a glow plug temperature of 900°C is illustrated in Figure 3-24. Growth rate of the pilot

combustion and enflamed area at  $SOI_{Main}$  is generally raised with increasing vessel temperature, particularly at higher glow plug temperatures. Main initiation delay generally reduces, and is followed by an increase in growth rate and maximum enflamed area. This is shown in the images, where 200°C vessel temperature offers the largest enflamed area at the time of the main injection. This enflamed area is mostly to the right of the glow plug tip, and when the main spray is introduced, the right hand side spray burns more vigorously, engulfing the spray plume much more quickly. The largest maximum enflamed area is achieved at the highest glow plug and vessel temperature. Comparing these results to the single-pilot tests, the best combination from the twin-pilot tests remain better, which shows that multiple pilots are still advantageous even when using very high glow plug temperatures.

Ignition characteristics are not largely different to changes in glow plug and vessel temperature. Changes in glow plug temperature has a larger influence on the first detectable soot luminosity and on pilot combustion before the main injection, but an increase in either generally generates a larger enflamed area at the time of the main injection. A more vigorous combustion of the main injection is produced. The influence of these parameters on vaporisation and chemical reaction rates are not so clear, with further work needed to better understand their contribution to generating a larger enflamed area.

### 3.10. Influence of Vessel Pressure

The effects of varying vessel pressure between 20 and 50 bar on the early stages of combustion have been studied using single- and twin-pilot strategies. The enflamed area for the single-pilot case is shown in Figure 3-25. The variation in time of first detectable soot from changes in vessel pressure is small. The enflamed area at  $SOI_{Main}$  is small for all vessel pressures, but there is a trend of decreasing enflamed area as pressure is increased. Main initiation delay is not strongly influenced, with 50 bar producing the shortest at 2.2 ms, down from 2.5 ms for the lower pressures. Raising vessel pressure increases the growth rate of main combustion and the enflamed area. One explanation for this trend is attributed to the reduced spray velocity and greater dispersion at higher pressures due to the larger shear forces. Lacoste reported [89] that the velocities of the droplets are lower at higher pressures, and are lower on the spray periphery compared to those measured on the spray axis. This was due to the shear force having a greater effect on the droplets travelling on the edge, which in turn increases breakup generating smaller

droplets. These droplets will be present in the proximity of the glow plug for a longer period of time allowing for greater heat input.

The enflamed area profiles are presented in Figure 3-26 for the twin-pilot case. Similar to the single-pilot case, there is no large variation in first detectable soot, and the enflamed area at  $SOI_{Main}$  is smaller with increasing pressure. The most likely explanation for the higher pilot combustion growth rate at lower pressures is that more soot particles are being drawn away from the tip by the faster spray jets. The main initiation delay is around 2.1 ms and does not greatly vary with pressure. The enflamed area profiles show there is good repeatability at both 35 and 50 bar, where the enflamed area is consistently larger at 50 bar compared to 35 bar. However, there is a large variation in the 20 bar case starting shortly after the main initiation. One test is similar to the 50 bar case, whilst the other behaves like the 35 bar case. The variation between the 20 bar tests mainly stems from the right hand side spray combustion. In the best test at the time of main initiation, some of the soot particles generated by the pilots are located further downstream in the main spray, causing a quicker growth of soot particles in the downstream portion. The maximum enflamed area in the 20 bar cases are not the worst, unlike in the single-pilot strategy, because of the sufficient enflamed area around main timing that helps promote the main combustion. Generally though, higher vessel pressures appear to more consistently produce a larger enflamed area following the main injection.

### 3.11. Discussion and Conclusions

The effect of enflamed area around  $SOI_{Main}$  and the combustion growth rate of the pilots on the maximum enflamed area is illustrated in Figure 3-27. Both plots incorporate data sets from all the parameters examined. Some large scatter is produced when pilot combustion is low, but the maximum enflamed area is generally raised when increasing the pilot combustion growth rate or enflamed area at  $SOI_{Main}$  and reduces the number of tests achieving very low maximum enflamed areas.

To determine the level of influence of each parameter, the response on each of the indicators has been explored and the most important parameters identified. A summary of the ranking order is presented in Table 3-2. Lower numbers denote a larger response, and the ranking order is defined within each parameter, and not across parameters. Note that the range has been reduced for some of the parameters to more closely match the range used inside the test engine providing a

common base for comparison. The baseline conditions are two pilot injections, each 2 mg, a total fuelling of 20 mg, and 1.7 ms separation between pilots and pilot-to-main. The glow plug temperature is 900°C, with a vessel temperature and pressure of 100°C and 35 bar respectively. Each factor is changed independently, but the response to glow plug temperature has been assessed at a vessel temperature of 200°C and not at the baseline 100°C. The reason for this is to provide a closer match to the operating conditions to that inside the engine. The range and the response on the six indicators from each of the parameters are presented in Figure 3-28.

The growth rate of pilot combustion and enflamed area around  $SOI_{Main}$  is most sensitive to the number of pilot injections and glow plug temperature. The remaining parameters are substantially, and equally less important on these indicators. The most influential parameters on growth rate of main combustion are number of pilots, vessel temperature and glow plug temperature. Quantity per pilot, vessel pressure and separation all have an equally lower influence. There is more of a distinction between the parameters for the maximum enflamed area. Number of pilots and vessel temperature remain the most influential, but glow plug temperature has a smaller influence similar to the quantity per pilot. Both vessel pressure and separation have the least effect.

The advantage of increasing the number of pilot injections stems from later pilots mixing with the sooting combustion generated from previous pilot/s. These soot particles promote a more vigorous combustion. The largest pilot sooting combustion around the time of the main injection is produced by triple- or quad-pilot strategies and is substantially higher compared to a lower pilot number strategy. The initiation of the main injection takes place both in the vicinity of the glow plug tip and in the generated hot gases, resulting in a shortened main initiation delay and a larger maximum enflamed area. These findings are consistent with those reported by Perrin et al. [67].

There remains a benefit in using multiple pilot injections even at the highest glow plug temperature. The best combination to promote a larger enflamed area is therefore multiple pilot injections and a high glow plug temperature. At low vessel temperatures, pilot and main combustion is poor irrespective of glow plug temperature, reflecting the relatively strong dependence on vessel temperature. The role of the glow plug is not so well understood, with some uncertainty whether it is promoting vaporisation and chemical reactions, or just chemical reactions, and how

much of this is shared between the air charge. The glow plug generally produces the largest response at the highest vessel temperatures, so the air charge is important for the successful operation of the glow plug. Although the results were found to be sensitive to spray position relative to the glow plug tip, given the similar location of injector sprays and glow plug tip position with the engine, the results presented should largely be applicable to the early stages of initiation to that inside of the engine. Further discussion of the optical vessel results and comparisons to the engine study is presented in Chapter 7.

# Chapter 4

## Engine Test Facilities, Test Procedure and Data Processing

---

### 4.1. Introduction

This chapter details the experimental facilities used with emphasis on the test engine, rig setup, instrumentation, data acquisition and fuel injection control system. The testing procedure employed has been outlined and repeatability tests presented. The post-processing of data has been explained detailing the performance indicators used throughout this investigation and key parameters derived from the heat release data.

### 4.2. Experimental Facilities

#### 4.2.1. Single Cylinder Test Engine

The experimental studies were carried out on a single cylinder DI diesel engine with a compression ratio of 15.5:1, as shown in Figure 4-1. A single cylinder engine eliminates effects from other cylinders and offers ease of maintenance and accessibility. The engine is a Ricardo Hydra, with the cylinder head, piston assembly and crankshaft from a production Ford 2.2 Puma Upgrade DI diesel engine. The specification is given in Table 4-1.

The engine was installed on a test bed incorporating instrumentation, data acquisition and ECU control system, and connected to a David McClure swinging frame DC dynamometer with a rated capacity of 60 kW at 4500 rev/min. The dynamometer was controlled by a Control Techniques Mentor II DC drive unit capable of motoring and absorbing operation to maintain a steady speed against varying engine torque throughout the cycle.

The engine was equipped with HPCR fuel injection equipment (FIE), including an 8 hole centrally mounted piezo-electric injector, offering up to 6 injections per cycle at



a pressure of up to 2000 bar. The nozzle holes had a diameter of 120  $\mu\text{m}$ . The diesel fuel used was a cold winter fuel with a  $-25^{\circ}\text{C}$  cold filter plugging point temperature to avoid waxing and a Cetane number of 54.

#### **4.2.2. Rig Setup and Instrumentation**

A 12 V battery connected to a trickle charger is the main source of power to the ECU, current clamp and the standard self-regulating glow plug. To enable the investigation of cold conditions, the coolant, 50/50 mixture of water and BS6580 ethylene antifreeze, was chilled by a F+R VP45WC 5.8 kW chiller, capable of chilling down to  $-30^{\circ}\text{C}$ . The coolant was circulated around the engine to mimic cold conditions ( $-20^{\circ}\text{C}$  coolant was the lowest temperature investigated in this study). An 80 litre plenum upstream of the intake manifold was used as a reservoir to store air, which was chilled using an atmospheric cooling radiator. Chilled coolant was circulated through a water jacket around the intake manifold to ensure the intake air was kept at a low temperature. The fuel was also directly chilled using a radiator with coolant circulating through it which also flowed around the fuel rail. Oil was continuously pumped around the engine, and therefore being chilled indirectly. Insulating jackets were placed over the engine to maintain the low temperatures. Three soak temperatures were investigated which were  $-20^{\circ}\text{C}$ ,  $-5^{\circ}\text{C}$  and  $10^{\circ}\text{C}$  defined by the engine out coolant temperature. It is acknowledged that despite measures being taken, at  $-5^{\circ}\text{C}$ , the intake air temperature increased by  $\sim 5^{\circ}\text{C}$  during the test. At  $-20^{\circ}\text{C}$ , the intake air temperature was around  $-16^{\circ}\text{C}$  at the beginning and increased by  $\sim 5^{\circ}\text{C}$  during the test. At  $10^{\circ}\text{C}$ , the temperature remained constant throughout the test.

For the purpose of conditioning the engine after a day of testing, heaters were used to directly increase the coolant and oil temperature. A Watlow Industries 3 kW immersion heater was used for the coolant fluid, and two Eltron Chromalox sump mounted heaters for the oil. The additional heat input from these heaters were necessary since the single cylinder engine doesn't produce sufficient heat to achieve typical warm operating conditions, whilst a Carter M3 series cooling tower was used rather than a radiator for heat rejection. A schematic of the coolant system layout is presented in Figure 4-2.

A series of sensors were used to record pressure and temperature at various positions around the engine. The most important of which is possibly capturing the

in-cylinder pressure at a high accuracy. For this, a Kistler 6125B quartz pressure transducer was used rated at 250 bar peak pressure. This was connected to a Kistler 5011 charge amplifier, consisting of a high-gain inverting voltage amplifier with a MOSFET as its input to achieve high insulation resistance. This transducer was also chosen for its high resistance to thermal shock. Since the transducer is piezo-electric, the signal drifts with little or no change in pressure. The transducer was therefore referenced to a pressure recorded in the intake manifold by a Kulite sensor at BDC of the intake stroke every cycle. The Kistler transducer was calibrated using a Budenberg hydraulic deadweight calibration bench to 0.05% accuracy. Fuel rail pressure was measured with a Kulite pressure transducer capable of up to 2200 bar. This was connected to a Kulite amplifier to produce a 0-10 V signal required for the input to the dSpace data acquisition system. Other engine pressures, intake manifold, exhaust and oil were captured using Kulite pressure transducers. These transducers output signals to in-house amplifiers (0-10 V) and then input to the dSpace system. All pressure transducers were calibrated using the Budenberg hydraulic deadweight calibration bench under steady state conditions.

An AVL 450 combustion noise meter was placed after the in-cylinder pressure signal amplifier to determine the combustion noise level. This allows the contribution of the combustion process to total engine noise to be assessed. Its operating principle is based on the analysis of the cylinder pressure in the frequency domain which includes passing the signal through a series of filters to provide an output dB with an A-scale weighting. This is applied because the human ear doesn't respond equally to all frequencies and therefore not all sound pressures are equally loud. Applying the filter accounts for this dependency. The noise level in dB is a logarithmic scale and is output relative to the reference sound pressure level of  $20\mu$  Pascal. A 10 dB increase in sound level corresponds approximately to a perceived doubling of loudness [90]. Noise levels presented in this thesis are given in dB(A).

Engine temperatures, such as air intake, exhaust, coolant, fuel and oil were recorded using sheathed TC Limited K-type Chomel-Alumel thermocouples. They were calibrated in a crushed ice water bath at  $0^{\circ}\text{C}$  and in a thermostatic oil bath at  $10^{\circ}\text{C}$  intervals up to  $100^{\circ}\text{C}$  to ensure sufficient accuracy and operating range. The exhaust thermocouple was calibrated up to  $300^{\circ}\text{C}$  suitable for the purpose of this investigation.

### 4.2.3. Data Acquisition and Fuel Injection Control

To monitor crankshaft position and to trigger the data acquisition (crank angle time domain), a Hohner Automation optical shaft encoder capable of 0.5 °CA resolution was used. This meant that it output one DC pulse every 0.5 °CA; 720 pulses per revolution and 1440 per cycle. The encoder TDC marker was set to coincide with piston TDC in the cylinder. To ensure accurate TDC position, an AVL 402 dynamic probe was used. Accurate measurement was required since small errors in TDC measurement can result in large calculation errors in IMEP [91]. The shaft encoder was set to within 0.2 °CA compared to TDC measured using the capacitance probe. This was deemed suitable since this investigation focuses on trends in IMEP rather than absolute values. Other measurements such as air, coolant, exhaust, fuel and oil temperatures were recorded on the time based board in dSpace at 100 Hz.

A dSpace modular hardware system was used for data acquisition from the engine sensors and for engine control. The unit consists of three A/D boards, a Control Area Network (CAN) board and a single processor that runs the uploaded Simulink model. This system allows data to be sampled at specified intervals using the time-triggered boards, at crank angle resolution using the hardware-triggered boards and converts analogue data signals into digital signals using the A/D converter boards. Electrical signals are also output for use in controlling engine hardware systems using the output boards. The Simulink model controlled the real-time data processing and hardware boards. The block diagrams contained in the model represented the data flow to calculate engine variable such as IMEP<sub>g</sub>, in-cylinder pressure and injection events. The data calculated is presented in real time using the Real Time Interface (RTI) which is subsequently displayed using Control Desk software. This enabled the author to monitor various data using virtual instruments and record the information for post-processing using MatLab.

ATI Vision software was used to communicate with the engine's ECU. The software provided control of various injection parameters such as injection quantity, injection timing (and therefore separation), number of injections and rail pressure. Up to six injections per cycle were possible on this system but five were the maximum used in this study (four pilot injections followed by a main injection). A form of injection strategy used in this study is illustrated in Figure 4-3. The pilot injections are always placed in advance of the main. ATI denotes the injection quantity in mg/stroke, or more specifically (mg/cylinder)/stroke. Since there is only one firing stroke per cycle

in a single cylinder engine, the notation used here for the injection quantity is mg/cycle which indicates the fuel injected from one injector over one cycle. The principal data signals between the computer, ATI, dSpace and the test engine are illustrated in Figure 4-4.

Fuelling tests were carried out to examine the fuel delivered compared to the fuel demanded from ATI. The results are shown in Figure 4-5. Fuelling levels down to 0.5 mg/cycle and up to 20 mg/cycle were assessed. Each data point is averaged from 40 cycles and the results show a good delivered to demanded quantity. In the range investigated the delivered fuelling level is within 10% of demanded and there does not appear to be a large dependence on soak temperature.

### 4.3. Testing Procedure and Repeatability

The test plan was organised around a common daily procedure. The engine was soaked for two to three hours at the start of the day to achieve the target temperature. The engine-out coolant temperature was the reading that monitored engine temperature and subsequently defined the test temperature. For each test the engine was started from stationary. The glow plug was turned on for a pre-glow period of 7.5 s and remained on during the test. The engine was motored for 15 cycles, allowing the desired engine speed and rail pressure to be met and maintained. Injections would then commence on cycle 16 and remained for 40 consecutive cycles which allows a sufficient number of cycles to be analysed to study idle performance behaviour and heat release characteristics. This marked the end of the test, after which fuel injection stopped and the engine motored for two minutes to draw air through the cylinder. Inter-conditioning tests were run to maintain repeatable cylinder conditions for subsequent tests. A time period of 15 minutes is employed in between tests to allow the engine to return to a cold state condition. A few inter-conditioning tests were also run before testing commenced to draw fuel through the injection system and condition ready for testing.

The inter-conditioning tests were also used to monitor test-to-test variation throughout the day. Figure 4-6 shows some key response variables that have been extensively used in this study such as cumulative heat release, IMEP<sub>g</sub> and CoV<sub>IMEP<sub>g</sub></sub> for fourteen inter-conditioning tests over four separate days. These response variables are discussed in detail later in this chapter. Previous research by MacMillan [4] conducted with this engine rig found that 20 tests per day are possible

with the conditioning technique employed, after which stability decreases in the value of peak compression pressure before injection. This experimental approach allowed for a sufficient amount of data collection without sacrificing accuracy of the results. In this study around 15 tests per day are more common and the results show good repeatability throughout the day and day-to-day variation is small. For the key parameters defined in section 4.4, cumulative heat release is typically  $\pm 7\%$  and IMEPg  $\pm 0.5$  bar. Combustion stability defined by  $\text{CoV}_{\text{IMEPg}}$  is typically  $\pm 3\%$  absolute.

Tests conducted at the start and end of the day over nearly a two month period were also monitored to assess long term drift. These tests were the same as the inter-conditioning tests. The results presented in Figure 4-7 show no long term drift but an increase of  $\sim 0.5$  bar in IMEPg from the start to the end of the day.  $\text{CoV}_{\text{IMEPg}}$  values remain unaffected with values generally in the region of 4-10%. Tests were randomised throughout the day to minimise variations but the results presented here are deemed adequate for cold conditions.

At the end of a testing day, coolant and oil heaters are switched on and the engine run under fully warm operating conditions for around 45 minutes. This cleaned the engine of any potential soot build-up, fuel impinged on the cylinder walls and potential water and ice build-up. Due to the cold conditions and poor combustion efficiencies at cold temperatures, the oil and oil filter were changed on a weekly basis to avoid significant build-up of fuel that could potentially negatively affect the lubricating properties.

### **4.4. Data Processing**

#### **4.4.1. Indicated Mean Effective Pressure (IMEP)**

The in-cylinder pressure is measured using a piezo-electric 6125 Kistler pressure transducer. The pressure data are used to determine the IMEP. IMEP is used as a performance measure and allows the direct comparison of engines with different displacements. IMEP is defined as the work per cycle per unit of swept cylinder volume [10]. This parameter has units of pressure (force per unit area) and expressed in bar ( $10^5 \text{ N/m}^2$ ). According to Heywood [10], two definitions of indicated work output per cycle  $W_{c,i}$  (per cylinder) are in common use; gross indicated work per cycle  $W_{c,ig}$ , which is the work delivered to the piston over the compression and expansion strokes only (closed part of the cycle), and net indicated work per cycle

$W_{c,in}$ , which is the work delivered to the piston over the entire four-stroke cycle. The gross indicated work output per cycle is obtained by integrating between  $BDC_{intake}$  and  $BDC_{expansion}$  and given by

$$W_{c,ig} = \int_{BDC_{intake}}^{BDC_{expansion}} p dV \quad 4-1$$

Similar to indicated work output, IMEP has two definitions; gross IMEP which is the work delivered to the piston by the working gases over the compression and expansion strokes only per unit of cylinder swept volume, and net IMEP which is the work delivered to the piston over the entire four-stroke cycle per unit of cylinder swept volume.

Assuming that the swept volume remains constant, dividing the gross indicated work per cycle by the cylinder swept volume results in the gross IMEP

$$IMEPg = \frac{W_{c,ig}}{V_s} = \frac{\int_{BDC_{intake}}^{BDC_{expansion}} p dV}{V_s} \quad 4-2$$

IMEPg rather than IMEPn is used as a measure of the work produced by charge combustion. This avoids the potential for cycle-by-cycle fluctuations in pumping work due to external conditions such as wave motion in the intake and exhaust ducting to confound the trends due to variations in combustion. In practice, the pumping work was small and trends in net and gross IMEP data were very similar.

#### 4.4.2. Combustion Stability Indicator

The Coefficient of Variation in IMEPg ( $CoV_{IMEPg}$ ) is used to define the cycle-by-cycle variability in indicated work. It is quantified using the mean IMEPg (over 40 cycles as used in this investigation to study post-start idle stability), which can be expressed as  $\overline{IMEPg}_{g40}$ , and standard deviation  $StD_{IMEPg}$ , which is given by

$$\sigma_{IMEPg_{g40}} = \sqrt{\frac{1}{n-1} \sum_{i=1}^n (IMEPg_i - \overline{IMEPg}_{g40})^2} \quad 4-3$$

Since 40 cycles are studied in this investigation, the standard deviation is determined from 40 IMEPg values. One characteristic of cold conditions and lowering the compression ratio is the large variation in increasing IMEPg throughout a test from improvements in combustion efficiency as a consequence of warming up. To decouple this warming up effect from misfired cycles,  $StD_{IMEPg}$  has been defined

---

as a deviation from a trend line of best fit as illustrated in Figure 4-8. Low IMEPg cycles deviating from the moving mean in IMEPg could therefore be accounted for.

CoV<sub>IMEPg</sub> is expressed as the standard deviation of IMEPg as a percentage of the mean IMEPg, and is given by

$$CoV_{IMEPg} = \frac{\sigma_{IMEPg}}{\overline{IMEPg}} \times 100 \quad 4-4$$

The mean IMEPg is taken to be  $\overline{IMEPg}_{40}$  for the purpose of this investigation. Heywood [10] states that vehicle driveability problems usually result when CoV<sub>IMEPg</sub> exceeds about 10%.

#### 4.4.3. Cylinder Charge Heat Release Rate

Heat release rate is defined as the rate at which the chemical energy of the fuel is released by the combustion process [10]. Heat release analysis provides information on the magnitude, phasing, and variation of heat release.

To derive the gross heat release rate from cylinder pressure data, the Traditional First Law (TFL) method has been applied and mostly taken from Heywood [10]. A diesel engine can be modelled as an open system which is quasi static. The first law for this system is

$$\frac{dQ}{d\theta} - p \frac{dV}{d\theta} + \sum_i \dot{m}_i h_i = \frac{dU}{d\theta} \quad 4-5$$

where  $dQ/d\theta$  is the heat transfer rate across the system boundary into the system,  $p(dV/d\theta)$  is the rate of work transfer done by the system due to system boundary displacement,  $\dot{m}_i$  is the mass flow rate into the system across the system boundary at location  $i$ ,  $h_i$  is the enthalpy of flux  $i$  entering or leaving the system and  $U$  is the energy of the material contained inside the system boundary.

According to Heywood [10], the only mass flows across the system boundary during the closed part of the cycle are the fuel and the crevice flow. Blowby has been included later on in section 4.4.5, so Equation 4-5 becomes

$$\frac{dQ}{d\theta} - p \frac{dV}{d\theta} + \dot{m}_f h_f = \frac{dU}{d\theta} \quad 4-6$$

If  $\dot{m}_f$  is taken to be the fuel mass flow rate into the system,  $h_f$  the sensible enthalpy of the injected fuel and  $U$  the sensible internal energy, then  $dQ/d\theta$  becomes the difference between the chemical energy or heat released by combustion of the fuel (a positive quantity) and the heat transfer from the system (a negative quantity). Compared to the cylinder volume, the volume occupied by the injected fuel quantity can be assumed to be negligible and can therefore be neglected. Equation 4-6 becomes

$$\frac{dQ_{net}}{d\theta} = \frac{dQ_{gross}}{d\theta} - \frac{dQ_{ht}}{d\theta} = p \frac{dV}{d\theta} + \frac{dU}{d\theta} \quad 4-7$$

This equation indicates the apparent (results are approximations to the real quantities which cannot be determined exactly) net heat release rate. The net heat release rate is the difference between apparent gross heat release rate and the heat transfer rate to the walls. This in turn is equal to the rate at which work is done on the piston plus the rate of change of sensible internal energy of the cylinder contents. Assuming the cylinder contents can be modelled as an ideal gas, Equation 4-7 becomes

$$\frac{dQ_{net}}{d\theta} = p \frac{dV}{d\theta} + mC_v \frac{dT}{d\theta} \quad 4-8$$

The ideal gas law equation

$$pV = mRT \quad 4-9$$

can be used in its differential form

$$\frac{d(pV)}{d\theta} = mR \frac{dT}{d\theta} \quad 4-10$$

and substituted into Equation 4-8 to eliminate the temperature term (T) to become

$$\frac{dQ_{net}}{d\theta} = p \frac{dV}{d\theta} + \frac{C_v}{R} \frac{d(pV)}{d\theta} \quad 4-11$$

Expanding Equation 4-11 gives

$$\frac{dQ_{net}}{d\theta} = \left(1 + \frac{C_v}{R}\right) p \frac{dV}{d\theta} + \frac{C_v}{R} V \frac{dp}{d\theta} \quad 4-12$$

Rearranging this equation and replacing  $C_v/R$  in terms of gamma; the ratio of specific heats, yields the net heat release rate



$$\frac{dQ_{net}}{d\theta} = \frac{\gamma}{\gamma-1} p \frac{dV}{d\theta} + \frac{1}{\gamma-1} V \frac{dp}{d\theta} \quad 4-13$$

The net heat release rate equation relies on instantaneous cylinder pressure, cylinder volume and gamma ( $\gamma$ ). The data capture resolution allows  $dQ_{net}/d\theta$  values to be evaluated at 0.5 °CA increments. Typically, an appropriate range of  $\gamma$  for diesel heat release analysis is 1.3 to 1.35 [10]. However, since  $\gamma$  is influenced by charge temperature and composition, it is calculated from the charge temperature at 0.5 °CA resolution using the following correlation by Brunt and Platts [92, 93]. This was developed from previous work by authors such as Gatowski et al. [94] and was found to reliably offer good results for various charge compositions inherent to diesel engine operation.

$$\gamma = 1.44 - (1.2 \times 10^{-4}T) + (1 \times 10^{-8}T^2) \quad 4-14$$

In this investigation, the gross heat release rate is used and can be obtained by accounting for the energy exchange of heat transfer to the cylinder walls and to blowby past the piston rings. The gross heat release rate equation can be written as

$$\frac{dQ_{gross}}{d\theta} = \frac{\gamma}{\gamma-1} p \frac{dV}{d\theta} + \frac{1}{\gamma-1} V \frac{dp}{d\theta} + \frac{dQ_{ht}}{d\theta} + \frac{dQ_{bby}}{d\theta} \quad 4-15$$

The calculations of the heat transfer and blowby energy are discussed in the following sections.

#### 4.4.4. Cylinder Charge Heat Transfer

According to Heywood [10], heat transfer accounts for typically 15 to 20% of the gross cumulative heat release. Three heat transfer mechanisms are involved: radiation, conduction and convection. The heat transfer of the cylinder charge is mostly dominated by convection occurring near the cooled walls. Convective heat transfer has been modelled using

$$Q_{ht} = h_c A \Delta T \quad 4-16$$

where  $h_c$  is the heat transfer coefficient,  $A$  is the cylinder surface area and  $\Delta T$  is the temperature difference between the cylinder charge and the cylinder wall. The mean bulk temperature is calculated at each 0.5 °CA using the ideal gas law whilst the cylinder wall temperature remains constant. Pugh [49] reported many correlations that can be used to determine approximate values of  $h_c$ . The Hohenberg correlation

[95] was the preferred choice since the coefficients used are readily available from engine data. MacMillan [4] subsequently modified the correlation and adapted the coefficients for low temperature conditions so that the heat release was zero on a motored cycle with no fuel injection. The correlation is given by Equation 4-17.

$$h_c = 67.7V^{-0.06}p^{0.8}T^{-0.4}(1.49 + \bar{S}_p)^{0.8} \quad 4-17$$

Where  $\bar{S}_p$  is the mean piston speed in metres per second.

#### 4.4.5. Cylinder Charge Blowby

According to Heywood [10], under fully warm conditions during high speed operation, total energy transfer to blowby accounts for 1 to 2% of the total energy release. Blowby gases pass from the cylinder through the piston rings into the crankcase, predominantly during the compression and expansion strokes. This subsequently causes a reduction in cylinder pressure. The loss of charge mass is a function of ring gap area, charge density and instantaneous cylinder pressure. As detailed in [96] the simplest model of blowby flow is a flow through an orifice with an upstream pressure equal to the cylinder pressure and a downstream pressure equal to the crankcase pressure. This method has been adopted in this study giving an instantaneous blowby mass flow rate of

$$\dot{m} = A_{ring}\gamma^{0.5} \left(\frac{2}{\gamma+1}\right)^{\frac{\gamma+1}{2(\gamma-1)}} (\rho p)^{0.5} \quad 4-18$$

Where  $\rho$  is the density of the blowby gases and  $A_{ring}$  is the effective ring gap area. This area is usually determined by measuring blowby gases from the crankcase and adjustments made to  $A_{ring}$  so that the calculated value equals experimental data. According to MacMillan [4] however, the large pulsating pressurisation of the crankcase makes direct measurements difficult. Previous experiments [4, 49] made adjustments to the value for a similar DI diesel multi-cylinder engine under fired conditions at -20°C. A value of  $4.5 \times 10^{-8} \text{ m}^2$  was therefore used in this investigation. The rate of energy transfer due to blowby is modelled as

$$\frac{dQ_{bby}}{d\theta} = \frac{60\dot{m}}{360N} \frac{pV}{m_{trapped}} \frac{\gamma+1}{\gamma-1} \quad 4-19$$

Where  $N$  is the engine speed in rev/min and  $m_{trapped}$  is the total mass of air trapped in the cylinder at BDC.

---

#### **4.4.6. Diesel Combustion Heat Release Characteristics**

A typical heat release profile for cold idle combustion is given in Figure 4-9. This figure illustrates the main phases of combustion and other important aspects during the combustion event for a quad-pilot injection strategy. The cumulative heat release has been used to determine the total amount of fuel burned per cycle by integrating the gross heat release rate between the start of the first injection and end of combustion (EOC). EOC is defined when a mean 5 point moving average falls to a mean 9 point average located at 65 °ATDC where no heat release occurs, plus 2. This method ensures the majority of the heat release is captured providing an approximate cumulative heat release value. Just before the main injection is a small amount of heat release from the pilot injections. It is sometimes apparent, although not always, that pilot combustion exists; it's highly dependent on in-cylinder conditions, the pilot quantity and number of pilot injections. After the main injection a depression in heat release rate is apparent caused by the fuel vaporising converting sensible internal energy into latent heat. Ignition delay is the period between the start of main injection and the start of combustion (SOC). In this study SOC is defined as the first point where 2.5 J/° is reached and the next two consecutive points increase. The ignition delay period is where air and fuel mixes prior to the premixed combustion phase. The fuel air mixture that has been produced during the ignition delay period burns in this phase. The mixing controlled combustion or diffusion burning phase follows this after the fuel air mixture during the premixed phase has been burnt. The proceeding rate of combustion and heat release is dictated by fuel vaporisation and mixing of the fuel air mixture. Following this is the late combustion phase where low rates of heat release are detected.

#### **4.4.7. Cycle Efficiencies**

The cumulative heat release value can be used in engine efficiency calculations to give an indication of how well the fuel is being utilised and transferred to useful work. Indicated combustion efficiency is a measure of how much fuel has been burnt. How effective this burnt fuel has been transferred to IMEPg is represented by indicated thermal efficiency. The product of these two efficiencies gives an indication of how well the fuel injected is converted to IMEPg. Using the definitions given by Heywood [10], combustion efficiency is calculated using the following formula

$$n_c = 100 \frac{RoHR_{Cum}}{q_{fuel} \times Q_{LHV}}$$

Where  $RoHR_{Cum}$  is the cumulative gross heat release in Joules,  $q_{fuel}$  is the fuel quantity injected per cycle in mg and  $Q_{LHV}$  is the lower heating value of the fuel in MJ/kg. The lower heating value used in this investigation is 42.5 MJ/kg [97]. The indicated thermal efficiency is given by the following formula

$$n_t = 100 \frac{IMEP_g \times V_s}{RoHR_{Cum}}$$

Where  $IMEP_g$  is in Pascals and  $V_s$  is the swept volume in  $m^3$ , 0.00055. The indicated fuel conversion efficiency is given by

$$n_f = \frac{n_c \times n_t}{100}$$

#### 4.5. Summary

The single cylinder test engine used in this investigation has been described with an overview of the modifications made to allow for low temperature tests to be conducted. The rig setup is capable of chilling the coolant and intake air to mimic cold temperature conditions, with  $-20^\circ\text{C}$  coolant being the lowest temperature investigated. An overview of the instrumentation used has been discussed to monitor temperature and pressure at various locations around the engine. In-cylinder pressure was captured using a Kistler 6125B quartz transducer rated at 250 bar peak pressure. To account for the drift the transducer was referenced to the pressure recorded in the intake manifold by a Kulite sensor at BDC of the intake stroke. All pressure transducers and thermocouples were calibrated prior to being installed on the rig to ensure a good accuracy of captured data. Details of the data acquisition and fuel injection system have been provided. The engine testing has been discussed, highlighting the day-to-day running procedure in order to reliably study the post-start idling combustion behaviour. Good repeatability in terms of  $IMEP_g$ ,  $CoV_{IMEP_g}$  and heat release response indicators has been demonstrated providing confidence in achieving results with a small error contribution.

Important parameters have been highlighted with details of their derivation that have been extensively used in the post-processing of data. The gross indicated mean effective pressure ( $IMEP_g$ ) is used to quantify the work done over a cycle or an

average over forty cycles from ensemble averaged data. A high IMEP<sub>g</sub> is desirable to maximise the usage of fuel introduced and to minimise cycle-by-cycle variation to avoid poor stability. Calculations to determine heat release have been explained and key parameters introduced that uses heat release data to determine cycle efficiencies and engine performance.

# Chapter 5

## Analysis of Injection Parameters

---

### 5.1. Introduction

In this chapter, the effects of injection parameters on heat release characteristics and IMEP<sub>g</sub> magnitude and variation at cold idling conditions from -20 to 10°C are reported. The influence of injection separation over a range of main injection timings has been assessed together with the dependency on number of pilot injections at various timings. The uncertainty of what has the most influence, number of pilots or total pilot quantity, or a combination of the two, on work output and cycle-by-cycle stability has been addressed. Different fuelling levels have been examined to assess injection strategy robustness and ability to achieve stability demands. Finally, the influence of heat release characteristics on combustion stability has been described and trends highlighted.

### 5.2. -20°C Soak Temperature

#### 5.2.1. Varying Separation and Main Injection Timing

The data presented in Figure 5-1 and Figure 5-2 provides an overview of how the number of pilot injections affects IMEP<sub>g</sub>, StD<sub>IMEP<sub>g</sub></sub> and CoV<sub>IMEP<sub>g</sub></sub> over a range of injection timings and values of injection separations. The total fuel quantity was kept constant at 20 mg/cycle, and each pilot quantity 2 mg/cycle. Highest IMEP<sub>g</sub> and lowest CoV<sub>IMEP<sub>g</sub></sub> were achieved around -8 °ATDC for all strategies. At advanced timings, increasing number of pilots is detrimental to IMEP<sub>g</sub> and CoV<sub>IMEP<sub>g</sub></sub> because the early pilots deliver fuel into adverse cylinder conditions. The benefit of increasing number of pilots to three or four is limited to retarded timings since the pilots are introduced into relatively warmer in-cylinder temperatures favouring vaporisation. Even though improvements can be made by increasing number of pilots at retarded timings, they fail to achieve comparable IMEP<sub>g</sub> and CoV<sub>IMEP<sub>g</sub></sub> obtained at optimum and advanced timings.

Reducing separation from 10 to 6 °CA (degrees between the starts of successive injections) improves  $CoV_{IMEPg}$  by raising IMEPg and reducing  $StD_{IMEPg}$ . This extends the range of timings which can be used without performance deteriorating greatly, particularly at advanced timings. As illustrated in Figure 5-3, ignition delay generally reduces with increasing number of pilot injections and marginally reduces with smaller separation. Further reductions are observed with retarding main injection timing. The benefit of reducing ignition delay at retarded timings is offset by poor combustion phasing late into the power stroke, as supported by combustion and thermal efficiencies presented in Figure 5-4 and Figure 5-5 respectively. Both combustion and thermal efficiencies increase around optimum timings and worsen at advanced and retarded timings. As illustrated in Figure 5-6, fuel conversion efficiency can be improved for all main injection timings and injection strategies by reducing separation, with an improvement of up to 8% at a main injection timing of -8 °ATDC.

The heat release characteristics, shown in Figure 5-7, indicate the benefit of reducing separation comes from an improvement in combustion efficiency. This is at least partly due to the improvement in pilot combustion which is evident in Figure 5-8, illustrating the heat release achieved by the pilots without a main injection. The stronger pilot combustion contributes directly to an increase in the total heat release and also by promoting improved heat release in the second half of the main combustion as can be seen in Figure 5-7. Close pilot separation appears to be particularly advantageous for the quad-pilot case, giving a relatively high rate of heat release at the time of main injection. The closer separation delays the injection of the first pilot by 16 °CA, reducing spray outside the bowl and improving phasing. The reduced time available for fuel dispersal promotes higher local rates of heat release when the pilot fuel ignites, and may also contribute to higher rates of main combustion. The single-pilot strategy in both separation cases exhibits a relatively long ignition delay and offers a poor premixed contribution. This leads to a late combustion of the main injection resulting in the poor thermal efficiency as presented in Figure 5-5. A single main injection of 20 mg/cycle without any pilot injections has been compared to the single- and twin-pilot strategies at 6 °CA separation. The heat release and IMEPg data, as presented in Figure 5-9, shows a further deterioration when using no pilot injections. The ignition delay is increased with a similar phasing to the single-pilot case. The premixed contribution is extremely poor with no improvement in heat release development. The IMEPg data shows a significantly

higher number of misfired cycles contributing to very little useful work output during those cycles. This results in a poor  $\text{CoV}_{\text{IMEPg}}$  of around 70% through the combination of a high  $\text{StD}_{\text{IMEPg}}$  and a relatively low IMEPg of 2.4 bar.

Results for the advanced timing,  $-16^\circ\text{ATDC}$ , are presented in Figure 5-10. This timing gives advanced combustion phasing, with the premixed combustion occurring before TDC. The injections are poorly phased and introduced into adverse in-cylinder temperatures and combustion efficiency is reduced. Reducing pilot separation gives some amelioration but combustion efficiency remains lower than for optimum timings. The most significant advantage of the reduced separation is a large improvement in  $\text{CoV}_{\text{IMEPg}}$ . The exploration of pilot combustion development without the influence of the main, as illustrated in Figure 5-11, showed more presence of pilot combustion around main timing and better development around TDC. This provides more ideal conditions for the main spray increasing both premixed and main development, with a reduced spread in total fuel burned compared to  $10^\circ\text{CA}$  separation. This stems from the fact that pilot fuel is spread over a shorter crank angle interval and sprayed into higher in-cylinder temperatures.

Results at the retarded timing,  $4^\circ\text{ATDC}$ , are given in Figure 5-12. Despite shorter ignition delays compared to optimum timings, combustion and thermal efficiencies are worse. The retarded timing places pilot combustion near to TDC and the heat release appears too early to promote the combustion of the main, which has a relatively low rate of heat release following the start of main injection. Whereas at the advanced timing, reduced separation improved stability near to optimum timings, this wasn't achieved at retarded timings. The result of poor combustion at retarded timings is supported by Lindl et al. [2], adding that the flame is likely to be quenched when pressure and temperature drop in the downward stroke and placing the mixture beyond the lean limits of combustion.

Further assessment of injection separation with a main timing of  $-8^\circ\text{ATDC}$  is illustrated in Figure 5-13. There appears to be no further improvement in work output or stability for separations smaller than around  $5$  or  $6^\circ\text{CA}$ . This is likely to be due to the injections being too closely coupled to allow a sufficient dwell period as to avoid any interactions between individual injections.



### 5.2.2. Number of Pilots and Pilot Quantity Optimisation

It is not clear from results presented earlier whether the number of pilots, or the total pilot quantity, or a combination of the two has most influence on work output and stability. A series of tests have been conducted to address this uncertainty, using total pilot quantities of 2, 4, 6 and 8 mg/cycle and maintaining the total pilot plus main quantity constant. The distribution between the pilot injections was kept equal i.e. for a quad-pilot case with a total pilot quantity of 4 mg/cycle, the fuelling demand is [1, 1, 1, 1, main] mg/cycle. Tests are conducted at the optimum main timing of -8 °ATDC and focused on 6 °CA separation.

The results for 20 mg/cycle total fuelling level are presented in Figure 5-14. IMEP<sub>g</sub> values of around 6 bar and 5% stability are achieved across a combination of pilot quantities and number of pilot injections provided a minimum of two pilots are used. A twin-pilot strategy with a total pilot quantity of 4 mg/cycle closely matches the best CoV<sub>IMEP<sub>g</sub></sub> achieved, with little advantage gained using triple- or quad-pilot or a higher pilot quantity. A single-pilot strategy offers 20% and 4.5 bar IMEP<sub>g</sub> at best, with stability levels worsening when increasing the pilot quantity. As illustrated in Figure 5-15, both IMEP<sub>g</sub> and StD<sub>IMEP<sub>g</sub></sub> dictate the level of stability; where stability worsens, IMEP<sub>g</sub> reduces and StD<sub>IMEP<sub>g</sub></sub> increases. The heat release profiles for single- and quad-pilot strategies are presented in Figure 5-16. In the single-pilot case, there is no indication of pilot combustion around main injection timing for either of the pilot quantities. Premixed combustion is relatively low for all pilot quantities, with lower amounts producing a small increase in combustion development. The extra fuel added in the pilot injection does not appear to promote any further mixing and more fuel is potentially residing on or near the bowl surface away from the glow plug at the time of the main injection initiation. Introducing the pilot fuel over four injections promotes some pilot combustion, as is evident in the 6-8 mg/cycle total pilot quantity cases. Independent of the pilot quantity, combustion duration is reduced for the quad-pilot strategy compared to single-pilot, but the fuel burns much more intensely. The premixed combustion is raised with a further increase in the mixing controlled phase. This follows a shorter ignition delay period, which indicates that the mixing rate is much improved as a consequence of smaller well-spaced injections. The combination of an increase in pilot combustion at the time of the main injection and potentially improved mixing with the larger pilot quantities appears to be sufficient to combat the reducing main quantity.

### 5.2.3. Sensitivity of Stability to Total Fuelling Level

The influence of the pilots and main total fuel injected is illustrated in Figure 5-17 and Figure 5-18, for 18 mg/cycle and 16 mg/cycle respectively. At 16 mg/cycle fuelling, stability deteriorates for all strategies and stable combustion is achieved by fewer combinations, with the need to use triple- or quad-pilot strategies with high total pilot quantities to achieve 11-12%. The use of two pilots is no longer sufficient to achieve the stability target, achieving at best 27% as the result of falling IMEP<sub>g</sub> and rising StD<sub>IMEP<sub>g</sub></sub>.

A total pilot quantity of 4 mg/cycle is required to achieve the best values of stability for total fuelling levels of 20 and 18 mg/cycle, and 6-8 mg/cycle in the 16 mg/cycle total fuelling case. Examining the pilot combustion for 2 and 4 mg/cycle in Figure 5-19, without a main injection, no heat release is observed until TDC for all injection strategies in the 2 mg/cycle case, and even then only a very small amount develops. This appears to be inadequate to encourage the vigorous combustion of the main, and a total pilot fuelling of at least 4 mg/cycle appears to be necessary. For 4 mg/cycle, pilot combustion is observable around the main injection timing for all but single-pilot, which begins at a more retarded timing of -5 °ATDC.

The heat release profiles presented in Figure 5-20 show that for either load, triple- and quad-pilot offers a higher initial rate of premixed combustion than twin-pilot, sustaining a strong combustion in the mixing controlled phase. At 20 mg/cycle, combustion efficiencies for twin-, triple- and quad-pilot strategies are similar; 74, 79 and 77% respectively. Single-pilot produces a considerably lower value of 51%. In the 16 mg/cycle case, however, combustion efficiencies are lower, particularly for the single- and twin-pilot strategies, which exhibit markedly weaker combustion at the early stages and further development. The twin-, triple- and quad-pilot strategy combustion efficiencies are 45, 61 and 60% respectively, and 19% for the single-pilot. It is apparent that not only are absolute levels of combustion efficiency reduced when lowering total fuelling levels, but single- and twin-pilot strategies are impacted the most. It's likely that in the lower load case, the pilot heat release and potentially poorer mixing produced by single- and twin-pilot strategies is insufficient to combat the reduced main quantity. This leads to a reduction in average premixed combustion, followed by a large deterioration in the mixing controlled phase. Triple- and quad-pilot on the other hand utilise the larger pilot quantities better and produce

sufficient improvements in heat release and mixing to combat the reducing main quantity.

#### **5.2.4. The Effect of an Early Large Single Pilot**

At fixed separation, an increase in number of pilot injections increases the crank angle interval over which the pilot fuel is introduced. To investigate whether an early large single pilot can achieve better stability than a close coupled pilot, a single 6 mg/cycle pilot was used in tests conducted using a total fuelling of 20 mg/cycle, and injected at 12 and 24 °CA in advance of the main injection at -8 °ATDC. The pilot timings correspond to the timings of the earliest pilots for a twin- and quad-pilot strategy respectively. A close coupled 6 mg/cycle pilot injection (6 °CA separation) produces around 3 bar IMEPg and 32% stability. Advancing the pilot to achieve 12 °CA separation results in around 2.8 bar and 40% stability. Advancing the pilot injection to achieve 24 °CA separation results in a large deterioration, 1.4 bar and 64%. The trend suggests that close coupled pilot injection to the main is advantageous. By introducing the pilot fuel far in advance and giving more time for mixture preparation does not achieve the same effect as a higher pilot number strategy.

The heat release profiles illustrated in Figure 5-21 show these are similar for both the 6 and 12 °CA separation. Increasing separation to 24 °CA produces a longer ignition delay, a relatively low premixed spike and poor main combustion development. IMEPg for 24 °CA separation is considerably lower and reflects the poor cumulative heat release. MacMillan [4] provides an explanation by analysing the effect of temporal fuel distribution on spatial distribution using a CFD model. Introducing a large single pilot injection far in advance of the main resulted in a large proportion being trapped in the squish region away from the glow plug. The fuel was poorly distributed around the time of expected start of main combustion. By splitting the pilot fuel into smaller well-spaced injections, turbulent mixing carries the fuel vapour around the entire bowl without being lost to the squish region. Smaller fuel quantities per injection reduce the speed of the spray giving more time for evaporation before the chance to adhere to cold walls. In addition to this, the direct increase in pilot combustion, as supported by the optical vessel study, may also contribute to better cycle-by-cycle stability. The benefit of increasing number of pilot

injections, therefore, appears to be twofold; increased pilot induced combustion and better mixture distribution.

### 5.3. -5°C Soak Temperature

#### 5.3.1. Number of Pilots and Pilot Quantity Optimisation

At -5°C, tests were carried out using a lower fuelling level, 12 mg/cycle, in line with meeting a lower FMEP target of 3.5 bar at a warmer soak temperature. At this lower fuelling level, the pilot fuelling is a higher proportion of the total. Nevertheless, the last injection of the set has been referred to as the main injection for consistency.

The results illustrated in Figure 5-22 reveal that improvements in stability are achieved by increasing number of pilot injections, but target stability can only be achieved through a small number of combinations. IMEPg values of around 3.5 bar are achieved using a quad-pilot strategy with 4-6 mg/cycle total pilot fuelling. The corresponding stability values are around 6%. A lower total pilot quantity is inadequate to achieve 10%  $CoV_{IMEPg}$ , even for a quad-pilot case. Triple-pilot offers around 3.3 bar at best with stability around 12%. Further reducing number of pilot injections to one or two greatly deteriorates stability and stable combustion cannot be achieved. Twin-pilot offers no better than 25%, with single-pilot offering a very poor stability of 55%.

The heat release profiles along with the IMEPg for all fired cycles are illustrated in Figure 5-23 for the 4 mg/cycle total pilot quantity case. For a higher number of pilot injections, the level of IMEPg is higher with fewer poor burning cycles. The corresponding heat release profiles reveal a strong premixed combustion spike for a higher number of pilot injections. This appears to promote a strong and more consistent burn of the main fuel. Poor burning cycles are largely eliminated when using a quad-pilot strategy, but in the case of triple-pilot, there are one or two poor burning cycles. The heat release profiles for the best, average and worst IMEPg cycles are presented in Figure 5-24 for the triple-pilot strategy. For the poor burning cycle, combustion initiation is delayed and the early stages of main combustion are much worse with no significant heat release to promote further combustion. The best cycle appears to produce low level heat release around main injection timing which would help encourage a faster burn of the main fuel. The average and best profiles

exhibit much higher premixed combustion with a significant second combustion phase leading to improved cumulative totals.

Strategies with a lower number of pilot injections are much more susceptible to stability deterioration with varying total pilot quantities. To demonstrate this, Figure 5-25 compares the heat release profiles for single- and quad-pilot strategies for different total pilot quantities. In the single-pilot strategy case, no pilot induced combustion is observable around main injection timing for either of the pilot quantities. The 2 mg/cycle produces the highest combustion development suggesting an improvement in mixing. The larger pilot quantities are possibly poorly distributed inside the bowl with some fuel residing near the cold bowl walls and away from the glow plug. When a smaller main quantity is then introduced, combustion development is suppressed. A much larger pilot combustion contribution is evident for the quad-pilot strategy around main injection timing particularly for larger pilot quantities. It is for this reason coupled with potentially additional mixing that promotes a stronger premixed combustion of the main. The largest total pilot quantity, however, appears to be too high, which causes a low premixed combustion and a subdued development despite a large pilot combustion at main injection timing. This suggests that the main quantity is too small highlighting the importance that sacrificing too much fuel to the pilots is detrimental to achieving a successful early main combustion and development.

### **5.3.2. Influence of Pilot Fuel Distribution for Single- and Twin-Pilot Strategies**

Figure 5-26 presents results taken at  $-5^{\circ}\text{C}$  for a single pilot injection of varying quantity delivered at -32, -26, -20, -14  $^{\circ}\text{ATDC}$  with the main set at -8  $^{\circ}\text{ATDC}$ . The total fuelling quantity is 12 mg/cycle and therefore the main quantity has been reduced when increasing pilot quantity to maintain a constant total fuelling level. Independent of pilot quantity, stability is improved when the pilot is positioned close to the main, with the best achieved using lower pilot quantities. For any combination of pilot quantity and position, however, IMEP<sub>g</sub> and stability remains very poor and stable combustion cannot be achieved. The influence of the position of a 6 mg/cycle pilot injected on heat release is presented in Figure 5-27. Irrespective of the pilot position, no pilot induced combustion is observable around the main injection and in all cases the premixed spike is low followed by a subdued development. Ignition delay isn't very sensitive to pilot position and the combustion duration is similar. The cumulative total is particularly poor when the pilot injection is placed in the most

advanced position away from the main injection. Spraying the pilot injection far in advance is likely to suffer from over dispersal in the region outside of the piston bowl and result in a poor mixture distribution near the time of main injection initiation. Retarding the pilot injection leads to a small alleviation toward achieving a better pilot mixture distribution, but coupled with a low pilot induced combustion it is insufficient to promote a strong main combustion.

The effect of the position of a larger pilot has been further examined for a twin-pilot strategy case. The results presented in Figure 5-28 incorporate two total pilot quantities, 4 and 6 mg/cycle, placed in the first two positions closest to the main injection i.e. -20 and -14 °ATDC. There is a small indication that if pilot distribution is not equal between pilots, then the larger pilot should be positioned close to the main injection to maximise IMEP<sub>g</sub> and reduce CoV<sub>IMEP<sub>g</sub></sub> independent of the total pilot quantity. A total pilot quantity of 4 mg/cycle generally results in higher IMEP<sub>g</sub> and lower CoV<sub>IMEP<sub>g</sub></sub> values with StD<sub>IMEP<sub>g</sub></sub> values marginally higher compared to the 6 mg/cycle case. In either of the total pilot quantity cases, there is no advantage gained by introducing the pilot fuel unequally, with a small deterioration observed particularly for the total pilot quantity of 6 mg/cycle.

Placing a pilot injection far in advance and keeping one close coupled to the main injection has also been assessed. This configuration consists of a pilot placed at -32 °ATDC and -14 °ATDC positions with the main at -8 °ATDC. The results are presented in Figure 5-29. The 4 mg/cycle total pilot quantity cases produce higher IMEP<sub>g</sub> and marginally lower CoV<sub>IMEP<sub>g</sub></sub> compared to 6 mg/cycle. StD<sub>IMEP<sub>g</sub></sub> values are similar. However, in the unequal split cases, placing the larger pilot in the far advanced position offers better stability through higher IMEP<sub>g</sub> and slightly lower StD<sub>IMEP<sub>g</sub></sub>. This is opposite to the trend observed when the pilot injections are close coupled. This is likely to be due to the 1 mg/cycle pilot injection mixing beyond the lean limits of combustion and producing a small heat release that is likely to be extinguished by the time of the next pilot injection. The conditions are likened more to a close coupled single-pilot strategy. Ultimately, there is little to no benefit in splitting pilot quantity unequally irrespective of position, and no better than ~20% is achievable.

The effect of pilot fuel distribution on the heat release for the 6 mg/cycle total pilot quantity case with each pilot positioned close to the main injection i.e. -20 and -14 °ATDC, is illustrated in Figure 5-30. An equal distribution of the pilot fuel produces

the highest cumulative total which stems from a relatively high premixed spike and a higher mixing controlled combustion. Placing a larger pilot quantity in either of the two positions produces a similar or lower premixed spike, with a more subdued second phase which results in a low cumulative total. Placing a pilot far in advance does little to alleviate the low heat release rates as illustrated in Figure 5-31.

### 5.3.3. Influence of Pilot Fuel Distribution for Triple- and Quad-Pilot Strategies

The influence of pilot fuel distribution has also been examined for both triple- and quad-pilot strategies. To assess this, a total pilot quantity of 6 mg/cycle was used. The results presented in Figure 5-32 incorporate a 2 mg/cycle pilot placed in each position i.e. -26, -20 and -14 °ATDC with the main at -8 °ATDC. The -32 °ATDC position has not been used. The other pilot injection configurations also use these positions but alternate the allocation of a 4 mg/cycle pilot injection whilst the other two are 1 mg/cycle each. The stability sensitivity to the allocation of the 4 mg/cycle pilot injection is small.  $StD_{IMEPg}$  values are similar, but  $IMEPg$  is worst when the 4 mg/cycle pilot is positioned in the most advanced position examined, -26 °ATDC.  $IMEPg$  is similar up until this point for all the cases. There is no advantage gained to using other configurations away from an equal fuel quantity distribution of pilots.

Heat release profiles shown in Figure 5-33 reveal that ignition delay isn't sensitive to pilot fuel distribution. The highest cumulative totals are achieved when the pilot fuel distribution is equal and when the larger pilot quantity is placed in the two closest positions to the main injection. The lowest cumulative total is produced when the larger pilot quantity is placed in the most advanced position, potentially due to a large proportion of this pilot fuel being far away from the glow plug in the squish region outside of the bowl which produces a poor mixture distribution near the time of main ignition. This is reflected by a lower rate of heat release rate in the mixing controlled combustion phase.

Similar tests have been conducted for a quad-pilot strategy where the total pilot quantity is 6 mg/cycle. The results presented in Figure 5-34 consist of tests where 1.5 mg/cycle pilots have been placed at -32, -26, -20 and -14 °ATDC with the main at -8 °ATDC, and others where a 3 mg/cycle pilot injection has been moved to each of these locations whilst keeping all other pilots at 1 mg/cycle. Similar to the triple-pilot case stability sensitivity to the placement of the larger pilot injection, 3 mg/cycle, is small but there is a marginal increase in  $CoV_{IMEPg}$  when placed in the most

advanced timings away from the main injection; -32 and -26 °ATDC. This is mainly due to a reduction in IMEP<sub>g</sub>; StD<sub>IMEP<sub>g</sub></sub> values remain similar. There remains no advantage to using other configurations different from an equal pilot fuel quantity distribution. All of the configurations investigated can achieve around 10% or lower. Triple- and quad-pilot strategies also produce lower and generally more repeatable test-to-test CoV<sub>IMEP<sub>g</sub></sub> values compared to a twin-pilot strategy.

The heat release for the quad-pilot strategy tests are presented in Figure 5-35. Both the maximum premixed and mixing controlled rate of heat release are higher than in the triple-pilot cases leading to higher cumulative totals. The trend in the heat release profiles is similar to the triple-pilot strategy; the highest cumulative total is produced by an equal pilot fuel distribution and when the larger pilot quantity is placed in the two positions closely coupled to the main injection. Placing the larger pilot quantity any further in advance produces both a lower premixed spike and a mixing controlled combustion resulting in lower cumulative totals. This is again attributed to placing the larger pilot quantities outside of the piston bowl, which may hinder a successful main development and reduce the amount of fuel exposed to the glow plug.

### 5.3.4. Effect of Increasing Total Fuelling Level and Position

Utilising different pilot quantity distributions in various positions has not improved stability beyond those of equal fuel quantity distribution and closely separated injections. Increasing the total level of fuelling has been examined in an attempt to alleviate unstable operation at -5°C. Fuelling has been increased by 4 and 8 mg/cycle and placed in the main injection. Total fuelling levels have therefore been increased from 12 to 16 and 20 mg/cycle. For all of the pilot strategies, each pilot is 2 mg/cycle apart from the quad-pilot strategy, where it is 1.5 mg/cycle to limit the maximum total pilot quantity to 6 mg/cycle. The results are presented in Figure 5-36. Increasing the main fuelling quantity increases IMEP<sub>g</sub> independent of the pilot strategy and generally reduces StD<sub>IMEP<sub>g</sub></sub> apart from in the single-pilot case where it increases. This is because IMEP<sub>g</sub> increases but misfiring cycles remain frequent resulting in a larger effect on StD<sub>IMEP<sub>g</sub></sub> values. Stability improves for all pilot strategies with fewer pilot injections exhibiting a much larger difference between the fuelling levels. In the 16 mg/cycle case, a twin-pilot is adequate offering a CoV<sub>IMEP<sub>g</sub></sub> of 7% and 4.6 bar, with triple- and quad-pilot strategies offering around 3-5% and ~5 bar. A single-pilot strategy offers 3.7 bar which meets the target load but only manages



24% due to  $StD_{IMEPg}$  remaining high. Further increasing to 20 mg/cycle reduces  $CoV_{IMEPg}$  to 3% (6.6 bar) for a twin-pilot strategy and offers similar stability for triple- and quad-pilot strategies; 2-4% and ~6.7 bar. A single-pilot still only offers 14% (5.7 bar).

Although increasing the fuelling level improves stability for all pilot strategies and a twin-pilot strategy is adequate to stabilise combustion, the associated increase in load is above the target of 3.5 bar that is deemed necessary to overcome friction and ancillary load demands at idle. Any increase over this target will have to be harnessed to avoid over speeding through the use of additional ancillary loading devices. An example of which maybe heaters to assist warming up the oil and coolant that would help lower engine friction levels and achieve fully warm operating temperatures more quickly. There is also an associated increase in combustion noise level for some of the injection strategies which is another potential barrier to using higher fuelling levels. This increase is likely to contribute to passenger discomfort if sound proofing isn't implemented.

Heat release response to fuelling level variation for both twin- and quad-pilot strategies is illustrated in Figure 5-37 and Figure 5-38 respectively. In the twin-pilot case, an increase in main injection fuelling increases the premixed spike and produces a much more intense burn in the mixing controlled phase over a similar combustion duration suggesting that the additional fuel promotes better mixing. The cumulative totals suggest that not only is all of the additional fuel burned but extra fuel is too. In the quad-pilot case, no more than the extra fuel is burned but similar trends are observed; the largest difference occurs in the mixing controlled phase where the burn rate is considerably higher over a similar duration at higher fuelling levels.

To assess where the best place is to introduce the additional fuel, further tests have been conducted using twin- and quad-pilot strategies where the additional 4 mg/cycle for the 16 mg/cycle total fuelling case has been placed in the pilot positions. In the twin-pilot case, the configuration is [2, 2, 8] mg/cycle at [-20, -14, -8] °ATDC. The extra 4 mg/cycle is added to each of the pilot positions. In the quad-pilot case, the configuration is [1.5, 1.5, 1.5, 1.5, 6] mg/cycle at [-32, -26, -20, -14, -8] °ATDC. Likewise, the additional 4 mg/cycle is placed in each of the pilot positions. The results are presented in Figure 5-39, with the additional fuel also placed in the main for comparison purposes. In the quad-pilot case, stability is insensitive to the

placement of the additional fuel. IMEP<sub>g</sub> marginally reduces as the larger injection quantity is advanced, whilst  $StD_{IMEPg}$  values remain unchanged. In the twin-pilot case, IMEP<sub>g</sub> reduces and  $StD_{IMEPg}$  increases when the additional fuel is placed at -20 °ATDC leading to a small deterioration in  $CoV_{IMEPg}$ . There is therefore no advantage and sometimes a small deterioration when introducing the additional fuel anywhere else aside from the main injection highlighting the sacrificial role of the pilot injections.

Heat release response to changes in additional fuelling position for both twin- and quad-pilot strategies is presented in Figure 5-40 and Figure 5-41 respectively. In the twin-pilot case, the premixed spike magnitude is similar but the mixing controlled combustion is highest for the additional fuelling placed in either the main injection or the pilot placed closest to the main. A slightly lower magnitude is observed when the extra fuel is positioned in the advanced pilot timing. In the case of the quad-pilot strategy, there is a discernible level of pilot heat release when the extra fuel is placed in the pilot position closest to the main injection which produces the shortest ignition delay. This advances the main combustion relative to all the other configurations but overall cumulative levels are comparable apart from when the extra fuel is placed in the main where it is higher.

### 5.4. 10°C Soak Temperature

#### 5.4.1. Number of Pilots and Pilot Quantity Optimisation

Total fuelling level has been further reduced to 9 mg/cycle to meet the target IMEP<sub>g</sub> of 2.5 bar. The results for 10°C soak temperature are presented in Figure 5-42. Combustion stability is much improved compared to -5°C, and achieved through a larger number of combinations. IMEP<sub>g</sub> is highest when using 2-4 mg/cycle total pilot quantity, producing around 2.3 bar. A twin-pilot offers around 7% at best, with the need to use a triple-pilot strategy to achieve below 5%. Quad-pilot offers no further advantage, and a single-pilot strategy remains insufficient to meet target stability, offering 1.4 bar IMEP<sub>g</sub> and 17% stability at best.

The influence of varying the number of pilot injections for the 4 mg/cycle total pilot quantity case on heat release and IMEP<sub>g</sub> is presented in Figure 5-43. A large deterioration in IMEP<sub>g</sub> magnitude is observed using a single-pilot strategy, with strategies using a higher number of pilot injections offering a higher magnitude and

less cycle-by-cycle variation. The poor IMEP<sub>g</sub> reflects the low cumulative burn observed from the heat release profile. Combustion initiation is marginally delayed but the most noticeable difference is that the premixed spike is considerably worse and fails to achieve a substantial second phase around 5 °ATDC that is evident from the other strategies.

The effect of varying total pilot quantity for single- and quad-pilot strategies on heat release and IMEP<sub>g</sub> is illustrated in Figure 5-44. For the single-pilot strategy, 2 mg/cycle pilot quantity provides a marginally higher premixed with a relatively strong second phase of combustion that is not achieved using a higher pilot quantity. This is likely to be due to the reduction in main quantity without any significant improvement in pilot combustion from the additional pilot fuel. Instead, combustion in this phase is subdued reflecting a main quantity that is too low to promote a strong main development. The quad-pilot strategy produces significantly higher heat release around main injection timing. Combined with potentially better mixing of the pilot fuel, both of these are likely to contribute to a larger premixed spike and less variable main development. Despite having the largest pilot induced combustion, 8 mg/cycle total pilot quantity remains the poorest with the lowest cumulative burn. The small 1 mg/cycle main injection appear to be inadequate and the large pilot-to-main fuel ratio is averse to achieving a high premixed combustion with a sustained development.

Reducing the fuelling level by 2 mg/cycle so that the total is decreased to 7 mg/cycle mostly adversely affects the stability of single- and twin-pilot strategies. For a twin-pilot strategy with each pilot equal to 2 mg/cycle, stability worsens from 7% to 20%. Triple- or quad-pilot with a total pilot quantity of 4 mg/cycle is necessary to achieve around 9% and a higher total pilot quantity of 6 mg/cycle offers no better than 25% due to the small 1 mg/cycle main injection. Despite being able to achieve stable combustion the best IMEP<sub>g</sub> is no higher than 1.2 bar which is far below the target of 2.5 bar indicating a fuelling quantity lower than 9 mg/cycle is inadequate.

### **5.5. Soak Temperature Comparisons**

At fuelling levels required to meet FMEP targets, stability is particularly poor at -5°C soak temperature. Target stability was achieved through fewer combinations and a quad-pilot strategy was necessary to attain below 10% stability. To understand why stability is particularly adverse to -5°C soak temperature conditions, the results have

been compared at the three soak temperatures to assess whether IMEP<sub>g</sub> or StD<sub>IMEP<sub>g</sub></sub>, or a combination of the two, is the dominant factor contributing to the non-progressive trend. The total fuelling level chosen for -20°C is 18 mg/cycle, and 12 mg/cycle and 9 mg/cycle for -5°C and 10°C respectively. Figure 5-45 and Figure 5-46 present results for single- and quad-pilot strategies at the various total pilot quantities. Systematic improvements are observed in StD<sub>IMEP<sub>g</sub></sub> to increasing soak temperature. CoV<sub>IMEP<sub>g</sub></sub> on the other hand is less systematic, suggesting that IMEP<sub>g</sub> magnitude is falling at a faster rate than StD<sub>IMEP<sub>g</sub></sub> which contributes to the non-progressive trends.

The effect of number of pilots and total pilot quantity on combustion and thermal efficiency is shown in Figure 5-47, Figure 5-48 and Figure 5-49 for -20°C, -5°C and 10°C soak temperatures respectively. For all soak temperatures and irrespective of total pilot quantity, increasing the number of pilot injections up to three improves combustion efficiency; introducing a fourth can lead to a deterioration or improvement. For warmer soak temperatures, thermal efficiency is relatively poor when increasing total pilot quantity particularly when using a low number of pilot injections. This is attributed to the very small main injection quantity that is insufficient to promote a strong combustion after TDC. A small main injection quantity also leads to poor combustion efficiency, with the majority of the fuel introduced in the pilot injections during lower in-cylinder temperature and pressure conditions. Generally, improvements in IMEP<sub>g</sub> with increasing number of pilots are dominated by increasing combustion efficiencies with small improvements in thermal efficiencies due to higher maximum rates of heat release occurring closer to TDC with shorter durations.

### **5.6. Influences of Injection Strategies on Heat Release Characteristics and Associated Effects on Work Output and Stability**

This section reports on the influence of injection strategies on heat release initiation and subsequent development. Initial comparisons have been made using -20°C soak temperature results at 20 and 16 mg/cycle total fuelling levels. Indications of how pilot injection strategy influences the burn of fuel delivered in the pilots and the effect on premixed combustion can be seen in Figure 5-50. The values of gross rate of heat release at main injection timing are small and uncertainty large. The individual results should clearly be treated with caution, but the trend suggests

higher heat release at main injection timing promotes a large premixed combustion spike. This relationship holds for both fuelling levels. Changing the pilot quantity alone is insufficient and an increase in number of pilot injections is necessary to improve combustion for all total pilot quantities. These trends are supported by Perrin et al. [67]. They observed that a poor main combustion development is usually correlated with poor pilot injection combustion, and the main heat release behaves similar to that without a pilot injection. The corresponding influence of gross rate of heat release at main injection timing on stability is illustrated in Figure 5-51. For both fuelling cases, a higher rate of heat release improves stability.

The relationship between premixed combustion and rate of heat release at main injection timing at  $-5^{\circ}\text{C}$  and  $10^{\circ}\text{C}$  soak temperatures is presented in Figure 5-52. The results at these temperatures indicate that the maximum premixed combustion spike can remain low for an increase in gross rate of heat release at main injection timing. These relatively low tests occur when using a higher number of pilot injections with a large total pilot quantity. This combination results in higher rates of heat release at main injection timing. The reason for the low premixed combustion spike is attributed to the smaller main injection quantity at these warmer soak temperatures. It is therefore not only important to achieve a higher rate of heat release at main injection timing, but also a moderate main injection quantity to produce a larger premixed spike. This is important to sustain combustion development, shown as a high heat release rate in the mixing controlled phase which is illustrated in Figure 5-53 for the three soak temperatures for all combinations of pilot quantity and number of pilots. The maximum mixing controlled value strongly influences the cumulative heat release, as shown in Figure 5-54, where a higher magnitude produces a larger cumulative value. Generating a high cumulative gross heat release is important to increase IMEP<sub>g</sub>, as shown in Figure 5-55, where 100 J of heat release results in approximately 0.9 bar.

Typically, for single injection strategies under fully warm operating conditions, high levels of premixed combustion are associated with long ignition delays through the increase in residence time for the fuel and air to mix. One method of reducing the ignition delay period and therefore lower the amount of premixed burn is to use pilot injections. The effect of injection strategy on ignition delay and the relationship against maximum premixed combustion is illustrated in Figure 5-56. The results presented here, shown for two fuelling levels at  $-20^{\circ}\text{C}$ , reveal that the pilot strategies producing the highest premixed combustion contribution, those with a higher number

of pilot injections, also tend to give shorter ignition delays. The influence of ignition delay on premixed combustion isn't particularly strong, with relatively large changes in maximum premixed combustion for little or no change in ignition delay. Nevertheless, there is a weak trend indicating shorter ignition delays generally result in higher premixed combustion. These findings are opposite to those that are generally accepted when running at fully warm conditions. Lindl and Schmitz [2] provide an explanation to this trend; a long ignition delay under cold conditions is unlikely to maintain a mixture within flammability limits and therefore results in a poor early heat release and further development. For all pilot strategies, there is a general trend that higher total pilot quantities produce shorter ignition delays, but doesn't always lead to higher premixed combustion. The corresponding influence of ignition delay on stability at  $-20^{\circ}\text{C}$  is illustrated in Figure 5-57. The trend between ignition delay and cycle-by-cycle stability is not so well defined as that between heat release at the time of main injection and stability, which appears to be more significant. The dependence of stability on ignition delay at  $-5^{\circ}\text{C}$  and  $10^{\circ}\text{C}$  soak temperatures is shown in Figure 5-58. There isn't a well-defined trend for  $10^{\circ}\text{C}$  soak temperature, but the results at  $-5^{\circ}\text{C}$  indicate that shorter ignition delays are desirable to achieve better stability. Further assessment of ignition delay to changes in injection strategy and glow plug temperature has been examined in Chapter 6.

The sensitivity of stability to changes in premixed combustion is illustrated in Figure 5-59 for  $-20^{\circ}\text{C}$  soak temperature. A similar trend emerges for the two fuelling cases. Cycle-by-cycle stability improves as the maximum premixed value increases. For values of  $\text{CoV}_{\text{IMEPg}}$  around 10%, the value of the maximum premixed combustion spike needs to be at least  $25 \text{ J}/^{\circ}$ , with greater than  $30 \text{ J}/^{\circ}$  needed to achieve 5%. These minimum criteria are necessary and sufficient to achieve the stability targets. Further increases do not produce a further clear improvement in stability. The results for  $-5^{\circ}\text{C}$  and  $10^{\circ}\text{C}$  soak temperatures are presented in Figure 5-60. Similar to  $-20^{\circ}\text{C}$ , strong trends are observed for both temperatures. At  $-5^{\circ}\text{C}$ , the value of the maximum premixed combustion spike needs to be around  $20 \text{ J}/^{\circ}$  to achieve the 10% target, or about  $25 \text{ J}/^{\circ}$  to reach the desirable 5% stability. At  $10^{\circ}\text{C}$ ,  $10 \text{ J}/^{\circ}$  is necessary to achieve 10%, and  $15 \text{ J}/^{\circ}$  to achieve 5%. This reflects the poorer conditions for vaporisation at colder temperatures. This trend illustrates the importance of the early stages of combustion to achieve that more complete burn, high  $\text{IMEPg}$ , low  $\text{StD}_{\text{IMEPg}}$  and improved stability.

The importance of the maximum premixed combustion is apparent when looking at the influence it has on IMEP<sub>g</sub> and StD<sub>IMEP<sub>g</sub></sub>, as illustrated in Figure 5-61. In all soak temperature cases, increasing the premixed value is associated with a rise in IMEP<sub>g</sub>. Also, increasing the premixed value generally reduces StD<sub>IMEP<sub>g</sub></sub> and therefore leads to a stability improvement. At -5°C soak temperature and 16 mg/cycle total fuelling at -20°C, StD<sub>IMEP<sub>g</sub></sub> begins to reduce when the premixed value is small. This can be explained by looking at the corresponding IMEP<sub>g</sub> values which are very small. Any deviation in IMEP<sub>g</sub> therefore has a smaller effect on StD<sub>IMEP<sub>g</sub></sub> values. Despite these relatively lower StD<sub>IMEP<sub>g</sub></sub> values the small IMEP<sub>g</sub> magnitude produces very poor stability.

### 5.7. Discussion and Conclusions

The influence of fuel injection strategies on heat release characteristics and IMEP<sub>g</sub> magnitude and variation in cold idling conditions have been reported in this chapter. Smaller pilot-to-pilot and pilot-to-main separations improve stability independent of the number of pilot injections through increasing IMEP<sub>g</sub> and reducing StD<sub>IMEP<sub>g</sub></sub>. A separation of 6 °CA was found to give the highest IMEP<sub>g</sub> and lowest StD<sub>IMEP<sub>g</sub></sub> allowing CoV<sub>IMEP<sub>g</sub></sub> to be reduced to around 5% at -20°C soak temperature. A minimum of two pilot injections were necessary to achieve this level of stability, with each pilot equal to 2 mg/cycle. Reducing separation extends the range of main injection timings before stability greatly deteriorates. The benefit of smaller separation is attributed to lower residence times for fuel dispersal, introducing fuel into higher temperatures and pressures, and a smaller proportion of fuel spraying outside of the bowl. The rate of heat release induced by the pilot fuel increased and subsequently modified the combustion of the main injection; both the premixed and mixing controlled spike increased, which is associated with a higher total fuel burn and IMEP<sub>g</sub>.

The key to achieving stable combustion at sub-zero temperatures is producing a premixed combustion spike of at least 20J/°. If the heat released in the premixed spike is lower, then the following development of the burn is reduced and more variable, leading to a lower IMEP<sub>g</sub> and higher StD<sub>IMEP<sub>g</sub></sub>. A smaller premixed spike is necessary at 10°C, which reflects the improved conditions for vaporisation and the promotion of ongoing heat release at warmer temperatures. Generally, stability is improved by using triple- or quad-pilot strategies over single- and possible twin-

pilots. At -20°C soak temperature using 20 mg/cycle total fuelling, target stability was achieved through a combination of pilot quantities and number of pilot injections; a total pilot quantity of at least 4 mg/cycle is necessary coupled with two pilot injections. Little advantage is gained when using three or four pilot injections and a higher total pilot quantity. Target stability cannot be solely achieved by varying pilot quantity; an increase in the number of pilot injections is crucial to aid mixing and induce a sufficient pilot combustion.

Increasing soak temperature does not guarantee an improvement in stability. Reduced fuelling levels to meet lower friction and ancillary demands makes stability particularly poor at -5°C soak temperature. Combustion can only be stabilised through a small number of pilot injections and pilot quantity combinations. The best attainable stability, below 10%, was achieved using a quad-pilot strategy, with triple-pilot offering around 12% at best. Fewer pilot injections offered worse stability. An unequal pilot fuel distribution offered no additional benefit compared to an equal pilot fuelling distribution with all injections closely separated. Raising the fuel quantity in the main injection improved stability independent of the injection strategy; a twin-pilot was sufficient to stabilise combustion producing a  $CoV_{IMEPg}$  of 7%. Using three or four pilots gave little further improvement. Placing an additional 4 mg/cycle in the main injection raising the total to 20 mg/cycle produced only incremental improvements in stability but IMEPg levels were approximately 3 bar higher than required for idling, which would require restraint such as additional ancillary devices to avoid over speeding.

At 10°C soak temperature, target stability is achieved through a higher number of combinations. Twin-pilot strategy gives stability values around 7% with 2-4 mg/cycle total pilot quantity, with the need to use triple-pilot to reach 5% or better with 4 mg/cycle total pilot quantity. A single-pilot is still insufficient, giving no better than 17%.



# Chapter 6

## Trade-Off between Injection Strategy and Glow Plug Temperature

---

### 6.1. Introduction

Results presented in Chapter 5 were obtained using a standard steel glow plug with a tip diameter of 4.5 mm operating at a self regulating surface temperature of around 850°C. In the tests reported in this chapter, the standard glow plug was replaced with a ceramic glow plug with a tip diameter of 3.3 mm capable of internal tip temperatures of up to 1250°C. The aim was to examine the trade-off between fuel injection strategy and glow plug temperature. Sensitivity to total fuelling level has been explored and the optimum pilot quantities identified in the previous chapter have been used for each of the injection strategies.

### 6.2. Glow Plug Design and Control

Equal glow plug protrusion was maintained to that of the standard glow plug, and tip temperature was measured by an instrumented R-type thermocouple placed inside the tip. The signal was amplified using an S-Products amplifier and fed into dSpace to achieve the required 0-10 V range. The glow plug was operated by a dedicated controller allowing three voltages to be supplied to account for the effects of charge motion cooling the tip. A pre-heat period of ~10 seconds was used rather than 7.5 seconds used for the standard self-regulating glow plug and the plug remained on throughout the test. Ceramic glow plugs can typically reach maximum temperatures within 3 seconds, giving them an advantage over standard steel tip self-regulating designed plugs. The glow plug used in this investigation was not capable of reaching maximum temperatures as quickly, potentially due to the controller that was used. The temperature profiles are illustrated in Figure 6-1. The profiles provide representative temperatures for all conditions tested. Although a higher voltage is supplied to account for air charge motion cooling the tip through forced convection, it

cannot be entirely mitigated and consequently a reduction in internal tip temperature is observed.

### 6.3. Effect of Varying Glow Plug Temperature at -20°C

To investigate the impact of glow plug temperature on idle stability at -20°C soak temperature, a total fuelling level of 18 mg/cycle was chosen. The total pilot quantity was maintained at 4 mg/cycle for all strategies except single-pilot, where it was 2 mg/cycle. The glow plug temperatures examined were 850, 1000 and 1200°C. The influence of glow plug temperature and injection strategy on IMEP<sub>g</sub>, StD<sub>IMEP<sub>g</sub></sub> and CoV<sub>IMEP<sub>g</sub></sub> is illustrated in Figure 6-2. Independent of injection strategy, an increase in glow plug temperature produces improvements in CoV<sub>IMEP<sub>g</sub></sub>, which stem from higher IMEP<sub>g</sub> and generally lower StD<sub>IMEP<sub>g</sub></sub>. CoV<sub>IMEP<sub>g</sub></sub> also progressively improves up to three pilot injections, with four pilots offering either similar stability or a slight deterioration. For the optimum strategy, triple-pilot, stability is still improved using higher glow plug temperatures; the effects are not mutually exclusive. For a single-pilot injection strategy, stability is around 50% at 850°C offering around 2 bar IMEP<sub>g</sub>. Using a glow plug temperature of 1200°C increases IMEP<sub>g</sub> to around 4 bar but still only offers around 20% cycle-by-cycle stability. Target stability is, therefore, not achievable by solely changing glow plug temperature alone. To meet target stability, a twin-pilot strategy is necessary and sufficient but requires a very high temperature of 1200°C. Around 5 bar is achievable using this combination. An increase to three pilot injections lowers the glow plug temperature necessary to achieve target stability, requiring a more moderate 1000°C. A glow plug temperature of 1200°C in combination with triple-pilot can be used to achieve near to the desirable stability of 5% offering around 5.5 bar IMEP<sub>g</sub>. There is no need to use four pilot injections.

### 6.4. Effect of Varying Glow Plug Temperature at -5°C

The trade-off between injection strategy and glow plug temperature has been further explored at -5°C. The same pilot quantities have been used compared to those at -20°C, but the main quantity reduced to achieve a total fuelling of 12 mg/cycle.

The IMEP<sub>g</sub>, StD<sub>IMEP<sub>g</sub></sub> and CoV<sub>IMEP<sub>g</sub></sub> results are presented in Figure 6-3. An increase in glow plug temperature always improves IMEP<sub>g</sub> and generally StD<sub>IMEP<sub>g</sub></sub>. Improvements in CoV<sub>IMEP<sub>g</sub></sub> are therefore established. As can be seen, IMEP<sub>g</sub> is

considerably lower when using a glow plug temperature of 850°C for all injection strategies. An increase in glow plug temperature to 1000°C offers a significant improvement in IMEP<sub>g</sub>, with 1200°C offering a further improvement but to a lesser extent. Similar to -20°C soak temperature, a quad-pilot strategy offers little benefit compared to the triple-pilot strategy, but stability is progressively improved from using one pilot to three pilot injections. These improvements generally stem from higher IMEP<sub>g</sub> and lower StD<sub>IMEP<sub>g</sub></sub>. Exceptions to this are the low StD<sub>IMEP<sub>g</sub></sub> values for single- and twin-pilot strategies at 850°C glow plug temperature. This is due to the low IMEP<sub>g</sub> values of these tests and reflects the insensitivity of StD<sub>IMEP<sub>g</sub></sub> when the magnitude of IMEP<sub>g</sub> remains low. A single-pilot strategy offers no better than 30% despite using a glow plug temperature of 1200°C. A twin-pilot strategy in combination with 1200°C achieves near to the stability target, offering 13% and 3 bar IMEP<sub>g</sub>. The use of three pilot injections reduces the glow plug temperature necessary, with 1000°C sufficient to achieve stable combustion. A triple-pilot injection strategy coupled with the highest glow plug temperature of 1200°C achieves below 5%. The benefit of a triple-pilot injection strategy compared to a twin-pilot strategy is apparent when looking at the StD<sub>IMEP<sub>g</sub></sub>; the value reduces by more than 50% when using the hotter glow plug temperatures. An increase of at least 20% in IMEP<sub>g</sub> is also seen. Combustion stability at -5°C was identified in the previous chapter as being particularly poor. The results presented in this chapter also show this trend. Dependency of stability on soak temperature has been further investigated later in the chapter.

### 6.5. Effect of Varying Glow Plug Temperature at 10°C

Main fuelling level is further reduced to achieve a total fuelling of 9 mg/cycle. The IMEP<sub>g</sub>, StD<sub>IMEP<sub>g</sub></sub> and CoV<sub>IMEP<sub>g</sub></sub> results are presented in Figure 6-4. At a soak temperature of 10°C, target stability is achieved through a greater number of combinations of glow plug temperatures and number of pilot injections. Independent of the injection strategy, an increase in glow plug temperature invariably improves CoV<sub>IMEP<sub>g</sub></sub> through higher IMEP<sub>g</sub> and lower StD<sub>IMEP<sub>g</sub></sub>. Similar to below zero soak temperatures, quad-pilot strategy offers little or no benefit over triple-pilot. Improvements in stability can be achieved by using a greater number of pilot injections. These improvements are caused by higher IMEP<sub>g</sub> and lower StD<sub>IMEP<sub>g</sub></sub>. Large improvements in stability are achieved by using a twin-pilot strategy over a single-pilot strategy. The best stability achieved by a single-pilot strategy is around

12% when using the highest glow plug temperature. Using a twin-pilot strategy can achieve the target stability using a glow plug temperature of 1000°C, or attain the desired stability of 5% by using 1200°C. Around 2 bar IMEP<sub>g</sub> is possible when using a twin-pilot strategy. Triple-pilot offers further improvements but to a lesser extent. Using three pilot injections offers around 3% at best and 2.3 bar IMEP<sub>g</sub>. The desired stability can also be achieved when using 1000°C, with 850°C offering a relatively good 7%.

At 10°C, glow plug temperature and the number of pilots have a similar influence on stability levels. At sub-zero temperatures, glow plug temperature appears to have a higher influence on combustion stability than number of pilot injections, with stability greatly deteriorating below 1000°C. The level of sensitivity largely depends on the injection strategy, where a fewer number of pilots is most prone to greater swings in stability levels when changing tip temperature. This is not due to larger changes in StD<sub>IMEP<sub>g</sub></sub>, but is caused by operating at low IMEP<sub>g</sub> levels which can result in large stability percentage values. The level of influence to changes in the number of pilots also depends on the combination used; stability is more sensitive at lower glow plug temperatures. The most important point here, however, is that there is a limit to how much stability can be improved when either raising the glow plug temperature or the number of pilots. Target stability can only be achieved when using a combination of these at sub-zero temperatures. At 10°C, target stability or very near to is achieved by either raising glow plug temperature to 1200°C whilst using a single-pilot strategy, or using triple- or quad-pilot strategies and a low glow plug temperature of 850°C. These findings are similar to those presented by MacMillan [4], where stable combustion cannot be achieved without a sufficiently high glow plug temperature at cold operating temperatures. The glow plug is a necessity to achieve a successful cold idle operation, but multiple pilot strategies are also required to achieve target stability.

### 6.6. Soak Temperature and Heat Release Comparisons

To study the stability dependency on soak temperature, a compilation of results for IMEP<sub>g</sub>, StD<sub>IMEP<sub>g</sub></sub> and CoV<sub>IMEP<sub>g</sub></sub> are presented in Figure 6-5 and Figure 6-6 for single- and twin-pilot strategies respectively and in Figure 6-7 and Figure 6-8 for triple- and quad-pilot cases respectively. The values are represented by the diameter of the circles; the scale is different for each figure. Smaller diameter circles represent more

stable combustion. As previously mentioned, for a given fuelling strategy, raising the glow plug temperature invariably produces an improvement in stability. Also, increasing the number of pilot injections up to three progressively improves stability, with no significant advantage introducing a fourth pilot injection. Thus, generally the best stability values at any soak temperature are achieved using the highest glow plug temperature in combination with three pilots. Changes in stability with soak temperature are less systematic, with the worse stability results being recorded at the middle soak temperature,  $-5^{\circ}\text{C}$ . As stability is improved by increasing glow plug temperature and the number of pilot injections, a systematic improvement with rising soak temperature appears to be established. Despite this, values of  $\text{CoV}_{\text{IMEPg}}$  for  $-5^{\circ}\text{C}$  soak temperature are generally the worst. The  $\text{StD}_{\text{IMEPg}}$  results generally show a systematic improvement with rising soak temperature. The  $\text{StD}_{\text{IMEPg}}$  values at  $-5^{\circ}\text{C}$  do, however, remain relatively high, and the combination of low IMEPg values causes a non-progressive trend. Systematic trends are only realised when work output is sufficiently increased and cycle-by-cycle variation is reduced, achieved by increasing number of pilot injections in combination with moderate to high glow plug temperatures.

Sets of heat release and IMEPg characteristics for single- and twin-pilot strategies are presented in Figure 6-9 and Figure 6-10 respectively. In each case there are three glow plug temperatures. The single-pilot results show a marked sensitivity of IMEPg to glow plug temperature in both magnitude and cycle-by-cycle variation. The results for  $-5^{\circ}\text{C}$  are the worst and include a relatively high proportion of cycles which produce little work output at the lowest glow plug temperature. The average heat release results for this  $850^{\circ}\text{C}$  case show little or no evidence of a premixed combustion spike, and the heat release rate is subdued and slowly varying, although the combustion duration is similar to that for the other glow plug temperatures. The results for the highest glow plug temperature show a distinct hump in the heat release rate appearing 10-15  $^{\circ}\text{CA}$  after a discernible premixed spike. This appears to be critical for the development of a strong burn to subsequently achieve a higher IMEPg. The very high  $\text{CoV}_{\text{IMEPg}}$  values for  $-5^{\circ}\text{C}$  are associated with poor burning cycles and lack of work output. The results for the twin-pilot strategy indicate how increasing the number of pilot injections produces higher premixed combustion and stronger development. This effect is pronounced when more pilot injections are used, as shown by the results for triple- and quad-pilot strategies in Figure 6-11 and Figure 6-12 respectively. In all cases, there is a discernible premixed spike and at

the higher glow plug temperatures, a strong mixing controlled hump in the heat release. At  $-5^{\circ}\text{C}$ , the average work output is raised, and particularly at the lowest glow plug temperature, this improves  $\text{CoV}_{\text{IMEPg}}$ .

An overview of how glow plug temperature and number of pilot injections affects combustion and thermal efficiencies is presented in Figure 6-13 and Figure 6-14 respectively for the three soak temperatures. Thermal efficiency generally remains above 40% for all soak temperatures and isn't greatly sensitive to either glow plug temperature or number of pilot injections. A greater sensitivity in combustion efficiency is observed. There is a general trend of increasing combustion efficiency when increasing glow plug temperature. Combustion efficiency also increases when utilising up to three pilot injections with a fourth introducing a deterioration or little to no benefit. The highest combustion efficiency is achieved when using the highest glow plug temperature,  $1200^{\circ}\text{C}$ , in combination with a high number of pilot injections. For the lowest glow plug temperature,  $850^{\circ}\text{C}$ , and a low number of pilot injections, single- and twin-pilot strategies, combustion efficiency is particularly poor at the  $-5^{\circ}\text{C}$  soak temperature. Weak burning cycles and lack of work output is reflected in the low combustion efficiencies. Significant improvements are only realised when three or four pilots are used at glow plug temperatures of  $1000^{\circ}\text{C}$  and greater. This combination sufficiently raises work output and reduces cycle-by-cycle variation resulting in systematic changes in stability in response to soak temperature.

In Figure 6-15,  $\text{CoV}_{\text{IMEPg}}$  is plotted against IMEPg values normalised against target IMEPg. The compilation of data at each soak temperature incorporates four injection strategies and three glow plug temperatures. Stability improves for all soak temperatures as the normalised IMEPg approaches unity. This largely reflects improving combustion efficiency; the lowest  $\text{CoV}_{\text{IMEPg}}$  values are achieved when combustion is most complete. Target load, or at least very near to, can be achieved across the range of soak temperatures. The improvement in stability is also due in part to reducing  $\text{StD}_{\text{IMEPg}}$  as illustrated in Figure 6-16 for all soak temperatures. Sensitivity of  $\text{StD}_{\text{IMEPg}}$  is greater for sub-zero soak temperatures, with  $10^{\circ}\text{C}$  showing relatively low values across the range of tests. The improved ability for above zero soak temperature to maintain stability below the 10% region for a large number of tests is strongly influenced by low  $\text{StD}_{\text{IMEPg}}$  values.

In Figure 6-17, IMEPg and  $\text{StD}_{\text{IMEPg}}$  is plotted against the peak value of premixed combustion illustrating the importance of the early stages of the burn in achieving

---

that more complete combustion and lower cycle-by-cycle variation. As identified in the previous chapter, cycle-by-cycle stability is strongly dependent on the premixed combustion and a higher peak value increases further development in the mixing controlled combustion phase. The dependency of stability on these peak values is illustrated in Figure 6-18. The minimum premixed values necessary to achieve target stability can be matched or exceeded for all soak temperatures, with the highest premixed values achieved when using three and four pilot injections in combination with 1200°C glow plug temperature. In Chapter 5, it was reported that stability didn't appear to be greatly sensitive to ignition delay, but there was a small suggestion that shorter ignition delays increase the premixed value and subsequently improves stability. Clearer trends are defined here as illustrated in Figure 6-19, where shorter ignition delays are achieved when raising either the number of pilots or glow plug temperature, or a combination of these. Suggestions from Lindl and Schmitz [2] indicate that during long ignition delay periods the fuel may leave the zone of favourable ignition conditions near the glow plug and adhere to cold surfaces failing to retain a mixture within flammability limits. Ignition delays should, therefore, be kept as short as possible to achieve a high initial main burn, less variable development and a better cycle-by-cycle stability.

### **6.7. Influence of Increased Fuelling Level**

The dependence of stability on soak temperature reflects the influence of engine friction levels on the target IMEP<sub>g</sub> and the influence of cylinder conditions on how this target is met. These conditions therefore have some influence on the total fuelling level that is necessary to reach the target IMEP<sub>g</sub>. The results for -5°C show this combination can disturb systematic variations with soak temperature. The required level of total fuelling decreases with rising soak temperature, reducing the main injection for a given pilot fuelling strategy. On the other hand, rising compression temperature and fuel temperature improve mixture conditions around the time of combustion initiation and early development.

The fuelling level of the main injection has been increased by 2 mg/cycle at each soak temperature to examine the sensitivity of stability and whether it facilitates the use of a lower number of pilot injections or a lower glow plug temperature to meet target stability. This is a relatively small change, but Figure 6-20 illustrates the shift toward higher IMEP<sub>g</sub> levels and subsequently better stability for a larger combination of tests at each soak temperature. Sensitivity to the level of total fuelling

is illustrated in Figure 6-21 and Figure 6-22 for single- and twin-pilot strategies respectively. Increasing the fuelling level improves stability through invariably increasing IMEP<sub>g</sub> level and for the majority of cases, reducing StD<sub>IMEP<sub>g</sub></sub>, but values of CoV<sub>IMEP<sub>g</sub></sub> for the single-pilot case are the highest and increasing fuelling level makes little difference. Stability is improved more when using a twin-pilot strategy at the lower fuelling level, with further gains when increasing fuelling level. Of these various influences, sensitivity to the level of total fuelling does therefore not dominate levels of stability within the range investigated. The sensitivity of stability to the level of total fuelling level for triple- and quad-pilot strategies is shown in Figure 6-23 and Figure 6-24 respectively. A similar or lesser response is observed with only small changes in stability levels particularly at the higher glow plug temperatures. Even though the best stability is achieved when using high fuelling levels in combination with three pilots at 1200°C, the IMEP<sub>g</sub> can be up to 1 bar over target requiring a higher electrical loading to harness this extra load.

Since the change in fuelling is to the main injection, and the pilot injections are the same, this suggests the initiation and early progress of combustion is being modified. Extra fuel increases the premixed combustion spike and subsequently the maximum rate of heat release of the mixing-controlled phase which is consistent with the strong influence of glow plug temperature and number of pilot injections.

Despite relatively small variations in stability levels to changes in total fuelling, target stability can be achieved using a fewer number of pilot injections and a lower glow plug temperature. At lower fuelling levels, target stability can be met using 1000°C in combination with a triple-pilot strategy at sub-zero temperatures, and a twin-pilot at 10°C. Whilst maintaining a glow plug temperature of 1000°C, one less pilot is necessary to achieve ~10% CoV<sub>IMEP<sub>g</sub></sub> at the higher fuelling level. This means that a single-pilot is sufficient at 10°C and a twin-pilot at sub-zero temperatures. At the lower fuelling level, achieving stable combustion using this number of pilots was only achieved by using 1200°C, so using higher fuelling levels also manages to avoid having to use very high tip temperatures. At -20°C, a single-pilot can also be used, but 1200°C is necessary at the higher fuelling level. Stable combustion cannot be achieved at -5°C using a single-pilot strategy. Generally, using a higher fuelling level with a twin-pilot strategy produces near comparable stability compared to triple- and quad-pilot at the lower total fuelling level. This cannot be achieved with a single-pilot at the fuelling levels investigated.



## 6.8. Discussion and Conclusions

Achieving stable combustion is important in terms of improving NVH. Increasing the premixed combustion has been shown to be associated with improved stability, and a more intense burn in the mixing controlled phase is well correlated with a higher total fuel burned and IMEP<sub>g</sub>. The sensitivity of these to the parameters investigated in this study has been examined to identify the most influential.

The effects of the individual parameters are assessed at each soak temperature, and the ranking order is only defined within each temperature and not between temperatures. Each parameter is changed independently and the common test conditions are two pilot injections, each 2 mg/cycle, main injection timing of -8 °ATDC with 6 °CA separation and a standard glow plug with a surface temperature of ~850°C. At -20°C soak temperature, the total fuelling level for comparison is 20 mg/cycle. This has been used instead of the lower fuelling level, 18 mg/cycle, to provide a common basis for comparison since main injection timing and separation were examined at the higher level. Fuelling level reduces to 12 mg/cycle at -5°C and 9 mg/cycle at 10°C, which are considered to be the lower fuelling levels. The range chosen for each parameter is considered to provide realistic values that are within acceptable calibration limits and provides a good indication to the level of sensitivity. Investigating the sensitivity to glow plug temperature was conducted using the smaller diameter tip ceramic design, rather than the larger diameter tip standard glow plug. Two sets of results were used when investigating the sensitivity to the number of pilot injections. The first set uses 2 mg/cycle per pilot injection. The second set differs by using a total pilot quantity of 4 mg/cycle apart from a single-pilot, where it uses 2 mg/cycle pilot injection. This second data set also uses the ceramic glow plug set at 1000°C internal tip temperature. The second data set is marked with an asterisk (\*). Sensitivity to total fuelling was also conducted using the ceramic tip glow plug set at 1000°C.

The response of cycle-by-cycle stability to each parameter is presented in Figure 6-25 for each of the soak temperatures (note the extended stability response range at -5°C). At -20°C, there are more parameters under comparison since some of these were not investigated at warmer soak temperatures. Of these various parameters within the range specified, the greatest response occurs when varying glow plug temperature and the number of pilot injections. The remaining parameters have a lower and similar dependency. At -5°C, glow plug temperature has the

dominant effect on stability, followed by the number of pilot injections. The total fuelling level and quantity per pilot injection reveal a smaller influence. At 10°C, the parameters have a similar influence, apart from total fuelling with the lowest response. A summary of the ranking order is presented in Table 6-1 together with the range for each parameter. Lower numbers denote the most influential parameters.

The effect of each parameter on the maximum premixed combustion is shown in Figure 6-26, with a summary of the ranking order provided in Table 6-2. The results suggest that at sub-zero temperatures, the number of pilot injections and glow plug temperature have the most influence on the level of premixed combustion. At 10°C, there is a similar response for a change in each of the parameters. The response of the maximum mixing controlled combustion to the various parameters is illustrated in Figure 6-27, with a summary of the ranking order provided in Table 6-3. At sub-zero temperatures, both glow plug temperature and number of pilots have the greatest influence. At -20°C, main injection timing also produces a large response, which is attributed to phasing changes of the heat release profile; retarding the timing reduces the peak value due to combustion occurring in a lower in-cylinder pressure and larger volume. At 10°C, total fuelling level produces the largest response, with all other parameters having a smaller influence.

Changing one parameter at a time has shown that stability levels are generally most dominated by glow plug temperature and the number of pilot injections, but to fully realise the potential benefits of changing these parameters, they should be used in conjunction and are not fully interchangeable. Results indicate that stable combustion cannot be achieved using higher glow plug temperatures alone at sub-zero temperatures; a multiple pilot injection strategy or an increase in fuelling level is also necessary.

The best stability values at any soak temperature are achieved using the highest glow plug temperature, 1200°C, in combination with three pilots; the effects are not mutually exclusive. This combination produced the highest premixed combustion, which increased the heat release rate in the development stage with less variability, raising IMEP<sub>g</sub> and reducing StD<sub>IMEP<sub>g</sub></sub>. Changes in stability with soak temperature are less systematic, with the worst stability results being recorded at the middle soak temperature, -5°C, due to the lower fuelling level to meet reduced friction demands. As stability is improved through increasing the number of pilot injections and using

higher glow plug temperatures, a systematic improvement with rising soak temperature is established. At 1000°C glow plug temperature, three pilots are necessary at sub-zero temperatures, and two pilots at 10°C. Increasing glow plug temperature to 1200°C reduces the necessary number of pilots by one to achieve  $CoV_{IMEPg}$  of around 10%. At 10°C, a glow plug temperature of 850°C permits stable combustion through an increase in number of pilot injections, indicating a lower dependence on glow plug temperature at this warmest soak temperature. Increasing the fuelling level by just 2 mg/cycle avoids the need to use 1200°C, whilst also keeping the necessary number of pilots low; two pilots at sub-zero temperatures and one pilot at 10°C with a glow plug temperature of 1000°C.

# Chapter 7

## Discussion, Further Work and Conclusions

---

### 7.1. Introduction

The work presented in this thesis has been concerned with improving cycle-by-cycle combustion stability of a diesel engine under cold idling conditions, which has been made worse by the trend toward lower compression ratios due to lower compression temperatures and pressures. The problem has been tackled through injection strategies and raising glow plug temperature. Cycle-by-cycle stability has been examined during the early stages of the idle phase, over forty fired cycles. During this period the engine is near to its coldest temperature, and combustion is prone to be incomplete and variable in its characteristics. One limitation of the experimental work carried out on the test engine is the limited information it provides on the early stages of combustion where heat release is too low to be detectable by the in-cylinder pressure transducer. The location of reactions is also not well defined. These issues have been addressed by carrying out a second experimental investigation using a combustion bomb with optical access. These two streams of investigation complement each other in the information obtained but the bomb study is not a direct representation of the engine because of the quiescent conditions, lower temperature, and the smaller rise in pressure due to combustion because of the large volume. For these reasons, the focus of attention has been the initiation of combustion rather than the complete process.

### 7.2. Discussion

Smaller pilot-to-pilot and pilot-to-main separations were found to improve cycle-by-cycle combustion stability independent of the number of pilot injections by simultaneously raising IMEP<sub>g</sub> and lowering StD<sub>IMEP<sub>g</sub></sub>. These findings are consistent with those reported by Payri et al. [80]. The range of main timings where multiple pilots achieved stable combustion, CoV<sub>IMEP<sub>g</sub></sub> values of 10% or lower, was extended. It was demonstrated that reducing separation caused a direct improvement in pilot combustion. Although levels of heat release from pilot combustion tend to be low,

these strongly influence the course of main combustion; higher heat release from the pilots promotes a higher premixed contribution to main combustion and a strong and less variable development ensues. Spraying less fuel outside of the bowl and less time for fuel dispersal may also contribute to a strong main combustion event due to the potential increase in fuel present near to the glow plug which is readily available to allow the main combustion to continue. In the past, the factor limiting the minimum separation that can be used has been hardware. However, the latest generation of piezo-electric injectors allows smaller separations and the possibility of rate shaping which may be exploited to reduce emissions [14]. The optical vessel results did not support these findings, where it was showed that larger separations were advantageous in achieving a larger enflamed area from the pilots and main injection. The most likely explanation for this inconsistency is appointed to the exclusion of air motion which allows the fuel to remain near the glow plug region for a longer period of time, and the early phasing of the pilots are not subject to lower pressures and temperatures. In the engine, shorter separation also sprays less of the pilot fuel outside of the bowl, which the optical vessel does not account for, and reduces the time for fuel to disperse away from the glow plug when subjected to turbulence.

The ability to achieve stable combustion depends on the use of multiple pilot injections at all the test temperatures investigated. A higher number of pilot injections improve cycle-by-cycle stability through the combination of raising  $IMEP_g$  and reducing  $StD_{IMEP_g}$ . At  $-20^{\circ}C$ , triple- or quad-pilot strategies offered the best stability over single- and possible twin-pilot strategies. A total pilot fuelling of at least 4 mg/cycle was necessary. Single-pilot strategies always offered poor stability irrespective of pilot quantity and position. Heat release analysis revealed that operating a higher pilot number strategy raised pilot combustion, which promoted a higher premixed spike with an associated increase in main combustion development and cumulative total. The optical vessel results showed that distributing the pilot fuel over more injections increased the growth rate of pilot combustion and generated a larger sooting combustion region around the timing of the main injection. Luminous soot from early pilots were found to mix with later pilot sprays, promoting a larger enflamed area, with large gains offered by triple- and quad-pilot strategies. These strategies produced the largest sooting combustion region at main injection timing. The main spray directly penetrated these regions, providing a second location for initiation other than that close to the glow plug. The result was a more vigorous combustion with a larger maximum enflamed area.

Previous work conducted at The University of Nottingham [4, 98] demonstrated a second influence of multiple pilot operation in that, as CFD simulations reveal, small, frequent pilots allow fuel to be distributed around the bowl by air motion ensuring there is always vapour near to the glow plug during the important TDC period. This was not the case with a single-pilot injection, even when introducing a large pilot far in advance. Instead, fuel was poorly distributed in the squish area away from the glow plug thereby hindering a successful propagation from the point of ignition.

Reducing the main quantity led to poorer combustion efficiency for all pilot strategies and particularly for single- and twin-pilot strategies. This reflects a more general dependence of stability on the total fuel injected. The benefit of more pilot combustion and improved mixture distribution for larger pilot numbers is more apparent at a reduced fuelling level.

Reduced fuelling levels to meet lower friction and ancillary load demands mean cycle-by-cycle stability is prone to be poor at moderate temperatures. Stability was generally worse than at  $-20^{\circ}\text{C}$ , with a triple- or quad-pilot strategy necessary to achieve around 10% or below with a minimum of 4 mg/cycle total pilot quantity. Attempts were made to improve stability for lower number pilot strategies by examining changes to pilot fuel distribution and position. Ultimately there was no advantage to splitting the pilot fuel unequally or placed in advanced timing positions and a  $\text{CoV}_{\text{IMEPg}}$  of around 10% or lower could not be achieved by using fewer than three or four pilot injections. A solution was proposed where the total fuelling level was increased and placed in the main injection. Placing the additional fuel in the pilots provided no benefit to stability and produced a small deterioration when placed in advanced positions. Stability was improved for all pilot strategies by raising  $\text{IMEPg}$  and generally reducing  $\text{StD}_{\text{IMEPg}}$ . A twin-pilot strategy was sufficient to alleviate the poor stability producing an  $\text{IMEPg}$  of 4.6 bar and a  $\text{CoV}_{\text{IMEPg}}$  of 7%. At this higher fuelling level only small stability improvements were gained by using three or four pilots. The increased load above target, however, would need to be harnessed with additional ancillary devices, which may not always be possible. Using higher fuelling levels during warm-up is a common method for raising exhaust temperatures to enable the aftertreatment system to start working earlier, so this approach may be beneficial toward this. On the other hand, using a high number of pilot injections show a strong potential to improve stability whilst avoiding having to use higher fuelling levels.

At a test temperature of 10°C, stable combustion was achieved using a twin-pilot strategy, using either 2-4 mg/cycle total pilot quantity. Triple-pilot was required to reach 5% or better with 4 mg/cycle total pilot quantity. A single-pilot strategy remained insufficient.

The key to achieving stable combustion is to produce sufficient premixed combustion to ensure a viable transition to the mixing controlled phase is achieved. At sub-zero temperatures, if the heat released in the premixed spike is lower than around 20 J/°, the following development of the burn is subdued and variable, and may end early. Around 10 J/° at 10°C is adequate, due to the warmer temperature providing favourable conditions for vaporisation and promotion of further heat release. The combination of a moderate soak temperature, -5°C, and a relatively low fuelling level to meet target load leads to low premixed combustion values, particularly for single- and twin-pilot strategies, where the IMEP<sub>g</sub> is falling more quickly than the StD<sub>IMEP<sub>g</sub></sub> resulting in relatively poor stability.

Higher glow plug temperatures were not solely sufficient to stabilise combustion at sub-zero temperatures; a multiple pilot injection strategy or a higher fuelling level was also necessary. The best stability at any soak temperature is achieved using a triple-pilot strategy in combination with 1200°C glow plug temperature. Heat release analysis revealed that for this combination, average heat release rates during the early stages of the main burn were the highest and consequently translated through to higher rates with less variability during the main combustion development. The optical vessel results revealed that at higher glow plug temperatures, the onset of sooting combustion was generally advanced and the growth rate of the enflamed area from the pilots was increased. This resulted in more sooting combustion at the time of the main injection followed by a larger enflamed area. Both studies revealed that even at the highest glow plug temperature, there is still an advantage to using multiple pilot injection strategies.

Ceramic glow plugs are capable of temperatures up to around 1200-1250°C, but low voltage metallic plugs are a more feasible option, which are capable of temperatures up to around 1000-1050°C. Using a high glow plug temperature of 1200°C is an effective way to reduce the necessary number of pilots whilst achieving CoV<sub>IMEP<sub>g</sub></sub> of around 10%; two pilots are necessary at sub-zero temperatures and one pilot at 10°C. The incurred higher cost of ceramic plugs, however, is a potential barrier for using them in production due to manufacturers striving to minimise system costs. To

avoid having to use expensive ceramic plugs, stable combustion can be achieved with a glow plug temperature of 1000°C but at the expense of using more pilots; a triple-pilot strategy at sub-zero temperatures and a twin-pilot strategy at 10°C is necessary. By raising the fuelling level by just 2 mg/cycle, a low number of pilots in combination with 1000°C can be used to reach stable combustion. This means that at 10°C a single-pilot strategy is sufficient, and twin-pilot strategies are adequate at sub-zero temperatures. IMEP<sub>g</sub> either remains similar or increases by ~0.5 bar, but indicated load remains closely matched to friction and ancillary demands, so little or no additional ancillary load is required to harness this increase. However, despite an increase in total heat release for this configuration, more fuel is left un-burnt, contributing to extra fuel being expelled as products of incomplete combustion. A variety of pathways can achieve stable combustion, but reducing the necessary number of pilot injections comes at the expense of the need to increase fuelling level and sometimes the use of very high glow plug temperatures. Ceramic glow plugs are necessary for these high temperatures but are more expensive and more susceptible to tip breakage compared to steel tip designs.

As described above, there are common trends to both the optical vessel and engine study but discrepancies also exist. Using a quiescent constant volume optical pressure vessel provides a lower cost technique to studying the influence of injection strategy and charge conditions on the early stages of combustion, but is best used as a supplement to engine testing rather than as a substitute, as it is the engine results that give the guiding conclusions. Whilst the two streams of investigation employed and the set of tests that were conducted answered some important questions regarding the best way to improve stability and the associated influence on heat release characteristics and enflamed area, some uncertainties still remain. The first one is the mechanism responsible for higher combustion rates due to hotter glow plug temperatures. It is not clear whether it is promoting vaporisation and then igniting it, or whether chemical reactions are only being promoted. In what proportion these mechanisms are shared with air charge temperature is also not well defined. To help elucidate this, chemiluminescence imaging of OH\*, CH\* and CH<sub>2</sub>O\*, could be used which would reveal reactions occurring prior to sooting combustion. As identified in the literature, CH\* is an indicator of low temperature reactions occurring after the fuel is completely mixed and vaporised, and OH\* is often linked to exothermic chemical reactions. Visualising these species can be done with or without a laser, but an image intensifier is necessary due to their weak signal. Using



a Planar Laser Induced Fluorescence (PLIF) technique will, however, provide more detailed information due to the higher spatial and temporal resolution [99], and highlighted as the most appropriate method for determining fuel air ratio information by Crua [57]. Using these combustion diagnostic tools in combination with CFD programs such as KIVA, CHEMKIN and AVL FIRE would be useful.

A second uncertainty is the transition period between the initial stages of main combustion and further development. The optical study has not provided any information on flame development, and although the engine study has revealed the importance of achieving a high average initial premixed burn to help sustain a strong development, similar premixed spikes can result in subdued development resulting in a poor burning cycle. The volume in which the heat release occurs and the location of the remaining fuel is unknown, both of which are likely to strongly influence combustion development. Modification to the current optical vessel would be needed to explore this. To better replicate in-cylinder temperatures inside the optical vessel the air charge could be pre-heated inside a separate vessel and fed into it prior to injection. This was demonstrated by Sjoberg et al. [100] and achieved a pre-heated gas temperature of 660°C. This method also has advantages of being able to introduce turbulence during the filling process to more closely mimic real engine conditions and would need to be implemented with a reduction in volume. An alternative approach would be a rapid compression machine, which would better simulate engine conditions but at a higher cost.

### **7.3. The Future for Low Compression Ratio Diesel Engines and Compatibility with Cold Idle Requirements**

The work presented in this thesis was instigated because at low compression ratio, cold idling stability was noted to be poor. This effect on stability has been reported in several papers [4, 73, 80]. The work reported in this thesis shows that multiple injections and hotter glow plug temperatures can be used to ameliorate the problem. Multiple injection strategies in combination with glow plug operation have helped low compression ratio engines closely match the cold idle cycle-by-cycle stability performance of high compression ratio engines. This does, however, generally require a higher number of pilot injections. Reducing the necessary number of pilots comes at the expense of higher fuelling levels and sometimes higher glow plug temperatures.

In recent years, new ways to further reduce emissions and improve fuel consumption such as start-stop technology puts even greater emphasis on glow plug systems. The tip diameter has been reduced to fulfil quicker heat up times and meet packaging restrictions imposed by the valves. More frequent starts place a higher demand on the durability of plugs to make sure they operate reliably under these heavy load conditions. To achieve lower emissions during the warm-up phase has prompted the introduction of performance optimised glow strategies. A control unit manages tip temperatures and durations during the pre-glow, intermediate and post-glow phases. It was announced in 2010 that such a system is going to be installed in both BMW's new 1 and 3 Series diesel models. Containing newly developed ceramic glow plugs with fast heat up times of less than 2.5 s, the low voltage requirement enables high temperatures even under starting voltage drop conditions. Beru, the company responsible for this system, highlight that various glow strategies can be used to either reduce fuel consumption, emissions or to improve comfort (engine speed stability, engine noise and start time).

In relation to tests carried out by Beru over the standard NEDC cycle at engine temperatures of 30°C and above [101, 102], it is claimed that raising glow plug temperature from 1000°C (near to maximum metallic glow plug temperatures) to 1250°C (near to maximum ceramic glow plug temperatures) reduces CO and HC emissions at the expense of increasing NO<sub>x</sub>. An increase in fuel consumption and a corresponding small increase in CO<sub>2</sub> were also reported since a 40 to 50% higher glow plug power was required. Improvements in HC emissions and exhaust gas opacity achieved using extremely high ceramic glow temperatures have also been reported by [2] and [65]. Emissions at sub-zero temperatures are also typically much higher than those recorded during warmer temperatures due to poor fuel preparation and incomplete combustion. If emission limits are introduced for diesel engines at sub-zero temperatures, as they have been for gasoline engines since 2002 through tests at -7°C, the case for using ceramic plugs may become compelling and possibly essential. These merits need to be traded-off against the incurred higher costs and durability of ceramic plugs, but the associated benefits show promising improvements in key areas of engine development and may warrant more widespread future use.

The multiple injection strategies that can be employed to improve cold idle stability are also frequently used to directly reduce emissions emitted from the combustion

chamber. It is unlikely that any future design changes to fuel injection systems will negatively impact cold idling behaviour. Ultra-high pressure fuel injection of ~3000 bar will be possible in the near future. In conjunction with this, smaller nozzle holes are being investigated to improve atomisation [89] and facilitate very high rail pressures whilst reducing liner and bowl impingement [103]. Better atomisation and improved air entrainment should be favourable to promote vaporisation and combustion in cold temperatures at start-up and idling. Close attention will have to be paid to smaller holes, however, as injector fouling was identified as a problem during the early stages of this work, contributing to a large deterioration in stability. High zinc levels were found in the test fuel that was being used, which has been shown to increase the formation of deposits around the injector nozzle [104]. Running high sooting conditions is also likely to have exacerbated the problem. Replacing the fuel with one containing a lower zinc content, frequent cleaning of the injector nozzle and operating higher rail pressures during the end-of-day cleaning test provided a solution. This was confirmed by repeatability tests conducted at the start and end of the day together with inter-conditioning tests, which showed that good repeatability was achieved based on IMEPg and stability levels; generally within  $\pm 0.5$  bar and  $\pm 3\%$  (percentage point) respectively. No significant long term drift was apparent. This is compared to stability values of over 100% for an injector that had been affected by coking.

If any unforeseen changes in future diesel engine design or uptake in alternative fuels that are adverse to stable cold idle operation, additional aids may be required combined with multiple pilot injection operation and high glow plug temperatures. Utilising internal EGR as used on the Mazda Skyactiv-D engine, heated fuel injectors and manifold heaters may be necessary to alleviate poor stability in cold temperatures. These will inevitably add to the system cost and heaters may introduce further challenges of power management due to their high power requirements. Implementing air intake heaters will also lend themselves well to reducing HC and CO emissions [102, 105], serving an additional purpose other than producing potential improvements in combustion stability. Further research into the potential gains of these hardware modifications on cold idle operation would be worthwhile.

The consumer's perception of idle quality is not only dependent on smooth running operation defined by cycle-by-cycle stability, but is also characterised by the noise emitted directly from the combustion event. This is therefore a focus for engine

developers, but has not been studied as part of this work. Stable combustion at 10°C produces a combustion noise level of around 67 dB(A), rising to 70 and 72 dB(A) as temperature reduces to -5 and -20°C respectively due to a higher indicated load. These do not appear to be excessively high, but further analysis of the frequency components would be required to provide a more detailed insight into the perceived noise sound quality [106]. This is an avenue worth exploring to build upon this work. Defining an indicator that not only takes into account cycle-by-cycle stability, but also impulsive noise would be a useful tool at the calibration stage to help judge acceptable cold idling quality.

#### **7.4. Further Work**

This work has answered important questions regarding the compatibility of having a low compression ratio and meeting cold idle performance requirements, but has also highlighted additional questions which need to be investigated:

- Whilst high speed photography has provided a useful insight into the level of sensitivity of injection parameters on combustion initiation, the underlying mechanisms that are responsible for the changes that occur are not so well defined from this optical vessel work. Using PLRS and PLIF to observe fuel vapour regions and chemical intermediate species other than soot particles will provide additional information into both physical and chemical phenomena, mixture preparation and help clarify the role of the glow plug i.e. does it act to promote both chemical reactions and vaporisation or just act as an ignition source to the already formed vapour? CFD simulations will also further aid interpretation of the effects of injection strategies and glow plug operation on local temperatures and vapour distribution.
- There is some uncertainty in the conditions that need to be met for combustion to develop successfully after the initial stages i.e. is a well prepared mixture near to the glow plug necessary, or is it mostly dictated by the requirement to achieve a minimum intensity and volume of the burning gases during the early stages of main combustion? A rapid compression machine with optical access would facilitate answering this question.
- Whilst injection strategies have been identified to influence cycle-by-cycle stability, the effect on acoustic noise emissions hasn't been assessed. A

greater understanding of the stability and noise trade-off would be beneficial to determine whether stable combustion compromises idle noise. Subjective testing by a jury panel is a commonly used method [107] to assess sound irregularity and overall loudness level, both of which have been shown to be important in influencing how consumers perceive idle quality. Previous research [106, 108-110] has proposed indicators to assess combustion level and impulsiveness to support objective target thresholds. These can be used and further developed to examine idle combustion behaviour and to define targets for idle sound quality. Having the engine situated in an anechoic chamber would probably be necessary to ensure good quality recordings of the actual combustion event and will unavoidably add cost to the engine rig setup. In conjunction, accelerometers could also provide additional information into engine speed variations and ultimately vibrations that will be detected by the driver whilst idling.

- Exhaust out emissions haven't been studied in this investigation. It is therefore not known whether the injection strategies that lend themselves well to achieve stable combustion produce high levels of emissions. There is currently no legislation for emission targets at sub-zero temperatures for diesel engine vehicles, but with EURO 6 being introduced in 2014, this warrants an investigation to examine if there are conflicting requirements of the strategies to simultaneously reduce emission levels and improve idle quality.
- Other cold starting aids aside the glow plug such as heated fuel injectors and intake air heaters could potentially provide more flexibility to the required injection strategies necessary to stabilise combustion. Further research into the potential benefits that these additional aids may offer would be worth considering.
- It is important to address the impact of alternative fuels on cold idle stability that may be more widely used in the future. Sensitivity to different fuels such as biodiesel and different Cetane number fuels would be worth investigating to examine their combustion behaviour and whether they jeopardise cold idle stability. The optical vessel can be used as a useful tool to study the effects of different fuel blends on the early stages of ignition and the sensitivity to parameter changes [111].

## 7.5. Conclusions

Cold idle cycle-by-cycle stability of a low compression ratio, 15.5:1, DI diesel engine has been investigated at soak temperatures down to -20°C. An optical vessel study has helped interpretation of these results. The main findings from this work are:

### 7.5.1. Optical Vessel Study

- The factors that have the highest influence on enflamed area of the pilots are the number of pilot injections and glow plug temperature. Increasing either of these parameters raises enflamed area growth rate and enflamed area around main injection timing.
- Achieving a larger enflamed area at the time of the main injection is advantageous in producing a larger maximum enflamed area. This highlights the importance of the local conditions in which the main injection is introduced into.
- The growth rate of the enflamed area following the main injection is most sensitive to the number of pilot injections, glow plug temperature and vessel temperature. The maximum enflamed area is most sensitive to the number of pilots and vessel temperature, and less sensitive to glow plug temperature. Generally, quantity per pilot, vessel pressure and separation have a smaller influence.
- The growth rate of the enflamed area following the main injection and the maximum enflamed area are increased by using more pilot injections or using higher glow plug and vessel temperatures. These are largest when using multiple pilots in combination with high tip temperatures; the effects are not mutually exclusive.

### 7.5.2. Engine Study

- Stable combustion,  $CoV_{IMEPg}$  of around 10% or lower, has been achieved down to -20°C. Cold idle stability is similar to that offered by a higher compression ratio diesel engine.

- Smaller separation between pilot injections, and pilot-to-main, improves stability independent of the number of pilot injections through the combination of increasing IMEP<sub>g</sub> and reducing StD<sub>IMEP<sub>g</sub></sub>. At -20°C, reducing separation from 10 to 6 °CA widens the range of main injection timings that achieve stable combustion. Separation is limited by hardware, but the latest generation of directly actuating piezo-electric injectors may facilitate even closer separations potentially offering further improvements.
- The best stability at all soak temperatures examined is achieved when using triple- or quad-pilot strategies over single- and possible twin-pilot strategies. Although pilot quantity has been shown to have an influence, the number of pilot injections is more important. The best stability is achieved when using a minimum total pilot quantity of 4 mg/cycle.
- At -20°C using a total of 20 mg/cycle, a twin-pilot strategy with each pilot equal to 2 mg/cycle gives CoV<sub>IMEP<sub>g</sub></sub> values better than 10%, closely matching triple- and quad-pilot. At lower fuelling levels, stability worsens and achieved by fewer combinations, requiring three or four pilots to achieve the best attained stability of around 10%, in both cases using 2 mg/cycle per pilot injection.
- Reduced fuelling levels to meet lower friction and ancillary load demands mean cycle-by-cycle stability is prone to be poor at moderate temperatures. At -5°C, stable combustion is achieved using three or four pilots. A higher fuelling level also improves stability and reduces the necessary number of pilots to two, but an increase over the target load will have to be harnessed by additional ancillary devices.
- At 10°C, a twin-pilot strategy is sufficient and necessary for <10%, with triple-pilot required to reach 5% or better with 4 mg/cycle total pilot quantity.
- A higher level of premixed combustion improves stability; around 20J/° is necessary at sub-zero temperatures, below which main development is subdued and variable. The threshold value for stable combustion reduces as soak temperature increases.

From tests carried out after the standard 4.5 mm diameter steel tip glow plug was replaced with a ceramic glow plug with a 3.3 mm diameter tip:

---

- The best stability,  $CoV_{IMEPg}$  of around 5% or lower, at any soak temperature is achieved through the combination of three pilots and 1200°C glow plug temperature; the effects are not mutually exclusive.
- Higher glow plug temperatures raise the premixed spike and produce a strong second phase of combustion. The combination of high tip temperatures and a high number of pilot injections maximises this benefit and produces the highest heat release rates following a shorter ignition delay which is associated with low  $StD_{IMEPg}$  and high IMEPg.
- Target levels of combustion stability at sub-zero ambient temperatures cannot be achieved solely by raising glow plug temperature. This must be combined with the use of multiple pilots and possibly also an increase in total fuelling.
- At high glow plug temperatures and using three or four pilots, stability improved with warmer soak temperature. At -5°C, stability was relatively poor when one or two pilot injections were used irrespective of glow plug temperature.
- At 1000°C, three pilots are necessary to produce stable combustion at sub-zero temperatures, and two pilots are adequate at 10°C. This tip temperature is achievable using a low voltage metallic glow plug, which is a lower cost alternative to the ceramic type.
- Raising glow plug temperature to 1200°C reduces the necessary number of pilot injections; two pilots are adequate at sub-zero temperatures, and one pilot at 10°C, but the incurred higher cost and durability issues of ceramic plugs are a potential barrier to using this combination. Additional benefits such as reduced emissions of CO and HC may warrant a higher future usage of this type particularly if cold start emission legislations are imposed similar to the -7°C gasoline test introduced in 2002.
- Increasing the main quantity by just 2 mg/cycle achieves stable combustion with the benefit of requiring only two pilots at sub-zero temperatures and one pilot at 10°C, and a glow plug temperature of 1000°C. For this combination, indicated load matches friction and ancillary demands.



# References

---

1. Hikosaka, N., A View of the Future of Automotive Diesel Engines. SAE Paper 972682 1997.
2. Lindl, B., Schmitz, H.G., Cold Start Equipment for Diesel Direct Injection Engines. SAE Paper 1999-01-1244, 1999.
3. Petchers, N., Combined Heating, Cooling and Power Handbook: Technologies and Applications 2003: The Fairmont Press, Inc.
4. MacMillan, D., Influences on the Cold Start Behaviour of a Diesel Engine at Reduced Compression Ratio, PhD Thesis, 2009, University of Nottingham.
5. Cursente, V., Pacaud, P., Gatellier, B, Reduction of the Compression Ratio on a HSDI Diesel Engine: Combustion Design Evolution for Compliance the Future Emission Standards. SAE Paper 2008-01-0839, 2008.
6. Beatrice, C., Avolio, G., Giacomo, N.D., Guido, C, Compression Ratio Influence on the Performance of an Advanced Single-Cylinder Diesel Engine Operating in Conventional and Low Temperature Combustion Mode. SAE Paper 2008-01-1678, 2008.
7. Thirouard, M., Mendez, S., Pacaud, P., Chmielarczyk, V., Ambrazas, D., Garsi, C., Lavoisier, F., Barbeau, B., Potential to Improve Specific Power using Very High Injection Pressure in HSDI Diesel Engines. SAE Paper 2009-01-1524, 2009.
8. Korfer, T., Lamping, M., Rohs, H., Adolph, D., Pischinger, S., Wix, K., The Future Power Density of HSDI Diesel Engines with Lowest Engine out Emissions - A Key Element for Upcoming CO2 Demands. Fisita F2008-06-015, 2008.
9. <http://www.mazda.com/mazdaspirit/skyactiv/engine/skyactiv-d.html>. Accessed November 2011.

## References

---

10. Heywood, J.B., Internal Combustion Engine Fundamentals, 1988, McGraw-Hill: London.
11. [http://www.mazda.co.uk/aboutmazda/mazdanews/mazda\\_corporate/mazda-drives-into-the-future-with-skyactiv/](http://www.mazda.co.uk/aboutmazda/mazdanews/mazda_corporate/mazda-drives-into-the-future-with-skyactiv/). Accessed November 2011.
12. Keeler, B., Constraints on the Operation of a DI Diesel Engine in Partially-premixed Combustion Mode, PhD Thesis, 2009, The University of Nottingham.
13. Lippmann, M., Environmental Toxicants: Human Exposures and Their Health Effects. Third ed 2009: John Wiley & Sons.
14. Kastner, O., Atzler, F., Soriano, O., Weigand, A, Multiple Small vs Single Large Pilot Injections for Diesel Engines. IMechE Fuel Systems for IC Engines 2012.
15. Kastner, O., Atzler, F., Juvenelle, R., Rotondi, A., Weigand, A, Directly Actuated Piezo Injector for Advanced Injection Strategies Towards Cleaner Diesel Engines. 2009. Continental Automotive GmbH, Siemensstrasse 12, 93055 Regensburg, Germany.
16. Al-Sood, M.M.A., Ibrahim, A.M., Abdel-Latif, A.A, Optimum Compression Ratio Variation of a 4-Stroke, Direct -Injection Diesel Engine for Minimum BSFC. SAE Paper 1999-01-2519, 1999.
17. The Society of Motor Manufacturers and Traders. New Car CO2 report. 2012.
18. <http://www.dieselnet.com/standards/eu/ld.php#stds>. Accessed September 2011.
19. [http://www.direct.gov.uk/en/NI1/Newsroom/DG\\_179190](http://www.direct.gov.uk/en/NI1/Newsroom/DG_179190). Accessed June 2012.
20. McGhee, M.J., Shayler, P. J., La Rocca, A., Murphy, M., Pegg, I, Investigations of Injection Strategies for Stable Cold Idling of an HPCR Diesel Engine with a Compression Ratio of 15.5:1. IMechE Conference C1342 Fuel Systems for IC Engines, London, 2012.

## References

---

21. McGhee, M.J., Shayler, P. J., La Rocca, A., Murphy, M., Pegg, I, The Influence of Injection Strategy and Glow Plug Temperature on Cycle by Cycle Stability Under Cold Idling Conditions for a Low Compression Ratio, HPCR Diesel Engine. SAE International Journal of Engines, 2012. 5(3): p. 923-937.
22. MacMillan, D., Law, T., Shayler, P. J, The Influence of Compression Ratio on Indicated Emissions and Fuel Economy Responses to Input Variables for a DI Diesel Engine Combustion System. SAE Paper 2012-01-0697, 2012.
23. Musculus, M.P.B., Measurements of the Influence of Soot Radiation on In-Cylinder Temperatures and Exhaust NO<sub>x</sub> in a Heavy-Duty DI Diesel Engine. SAE Paper 2005-01-0925, 2005.
24. Dec, J.E., Canaan, R. E., PLIF Imaging of NO Formation in a DI Diesel Engine. SAE paper 980147, 1998. SAE Transactions, 107, No. 3: p. 176-204.
25. Martin, G.C., Mueller, C. J., Progress in NO Detection by Planar Laser Induced Fluorescence in a Direct Injection Diesel Engine. ILASS Americas, 16th Annual Conference on Liquid Atomization and Spray Systems, Monterey, CA, 2003.
26. Dec, J.E., Coy, E. B., OH Radical Imaging in a DI Diesel Engine and the Structure of the Early Diffusion Flame. SAE Paper 960831, 1996. SAE Transactions, 105, No. 3 (1127-1148).
27. Badami, M., Millo, F., D'Amata, D.D, Experimental Investigation on Soot and NO<sub>x</sub> Formation in a DI Common Rail Diesel Engine with Pilot Injection. SAE Paper 2001-01-0657, 2001.
28. Studzinski, W.M., Liiva, P.M., Choate, P.J., Acker, W.P., Litzinger, T., Bower, S., Smooke, M., Brezinsky, K., A Computational and Experimental Study of Combustion Chamber Deposit Effects on NO<sub>x</sub> Emissions. SAE Paper 932815, 1993.
29. Hountalas, D.T., Zannis, T.C., Mavropoulos, G.C, Potential Benefits in Heavy Duty Diesel Engine Performance and Emissions from the use of Variable Compression Ratio. SAE Paper 2006-01-0081, 2006.

## References

---

30. Ogawa, H., Li, T., Miyamoto, N., Kido, S., Shimizu, H, Dependence of Ultra-High EGR and Low Temperature Combustion on Fuel Injections Conditions and Compression Ratio. SAE Paper 2006-01-3386, 2006.
31. Parlak, A., Yasar, H., Sahin, B, Performance and Exhaust Emission Characteristics of a Lower Compression Ratio LHR Diesel Engine. Energy Conversion and Management, 44:163-175, 2003.
32. Li, T., Suzuki, M., Ogawa, H, Characteristics of Smokeless Low Temperature Diesel Combustion in Various Fuel-Air Mixing and Expansion of Operating Load Range. SAE Paper 2009-01-1449, 2009.
33. Murata, Y., Kusaka, J., Daisho, Y., Kawano, D., Suzuki, H., Ishii, H., Goto, Y, Miller-PCCI Combustion in an HSDI Diesel Engine with VVT. SAE Paper 2008-01-0644, 2008.
34. Pischinger, F., Verbrennungsmotoren, 1995. Vol. 2, Course paper, RWTH Aachen.
35. Crua, C., Kennaird, A.D., Sazhin, S.S., Heikal, M.R., Gold, M.R, Diesel Autoignition at Elevated In-Cylinder Pressures. International Journal of Energy Research, 2004. 5(4): 365-374.
36. Gaffuri, P., Curran, H.J., Pitz, W.J., Westbrook, C.K, Combustion of n-Heptane in a Shock Tube and in a Stirred Reactor: A Detailed Kinetic Modelling Study. Proceeding of the Joint Technical Meeting of the Central and Western States Sections of the International Combustion Institute, San Antonio, TX, April 23-26, 1995.
37. Ciezki, H.K., Adomeit, G., Combustion and Flame, 1993. 93: p. 421-433.
38. Zhang, L., A Study of Pilot Injection in a DI Diesel Engine. SAE Paper 1999-01-3493, 1993.
39. Alt, N.W., Wiehagen, N., Steffenc, C., Heuer, S., Comprehensive Combustion Noise Optimization. SAE Paper 2001-01-1510, 2001.
40. Corcione, F.E., Vaglieco, B.M., Corcione. G.E., Lavorgna, M., Potential of Multiple Injection Strategy for Low Emission Diesel Engines. SAE Paper 2002-01-1150, 2002.

## References

---

41. Augustin, U., Schwarz, V., Low-Noise Combustion with Pilot Injection. Truck Technology International, 1991.
42. Schulte, F., et al, The Influence of Pilot Injection on Combustion in DI Diesel Engines. FEV Technical Papers, 1989.
43. Park, C., Kook, S., Bae, C, Effects of Multiple Injections in a HSDI Diesel Engine Equipped with Common Rail Injection System. SAE Paper 2004-01-0127, 2004.
44. Bermudez, V., Garcia, J.M., Julia, E., Martinez, S, Engine with Optically Accessible Cylinder Head: A Research Tool for Injection and Combustion Processes. SAE Paper 2003-01-1110, 2003.
45. Lai, M.-C., Henein, N.A., Xie, X., Chue, Tsan-Hai., Itoh, Y., Bryzik, W, Diesel Cold-Starting Study Using Optically Accessible Engines. SAE Paper 952366, 1995.
46. Solbrig, C.E., Litzinger, T.A, The Effect of Intake Charge Temperature on Combustion and Emissions in an Optically Accessible DI Diesel Engine With and Without Swirl. SAE Paper 902060, 1990.
47. Dec, J.E., Espey, C, Chemiluminescence Imaging of Autoignition in a DI Diesel Engine. SAE Paper 982685, 1998.
48. Schommers. J., D.F., Stotz, M., Peters, A., Ellwanger, S., Koyanagi K., Gildein., H, Potential of Common Rail Injection System for Passenger Car DI Diesel Engines. SAE Paper 2000-01-0944, 2000.
49. Pugh, G.J., The Analysis of Heat Release in the Investigation of Split-Main Fuel Injection in a Diesel Engine, PhD Thesis, 2004, University of Nottingham.
50. Stumpp, G., Ricco. Mario, Common Rail - An Attractive Fuel Injection System for Passenger Car DI Diesel Engines. SAE Paper 960870, 1996.
51. Bosch, R., Diesel-Engine Management. Third ed 2004, GmbH: Professional Engineering Publishing Ltd.

## References

---

52. Schatz, O., Cold Start Improvement by use of Latent Heat Stores. SAE Paper 921605, 1992.
53. <http://www.beru.com/products/diesel-cold-start-technology/glow-plugs/high-tech-glow-plugs-ge-gn>. Accessed September 2011.
54. Zhao, F.Q., Hiroyasu, H, The Applications of Laser Rayleigh-Scattering to Combustion Diagnostics. Prog. Energy Combust. Sci, 1993. 19 (447-485).
55. Eckbreth, A.C., Laser Diagnostics for Combustion Temperature and Species. 2nd ed. Vol. 3. 1996, Amsterdam: Gordon and Breach Publishers.
56. Espey, C., Dec, J.E., Litzinger, T.A., Santavicca, D.A, Planar Laser Rayleigh Scattering for Quantitative Vapor-Fuel Imaging in a Diesel Jet. Combustion and Flame, 1997. 109(1-2): p. 65-78.
57. Crua, C., Combustion Processes in a Diesel Engine, PhD Thesis, 2002, University of Brighton.
58. Dec, J.E., Espey, C, Ignition and Early Soot Formation in a DI Diesel Engine Using Multiple 2-D Imaging Diagnostics. SAE Paper 950456, 1995.
59. Kosaka, H., Aizawa, T., Kamimoto, T, Two-Dimensional Imaging of Ignition and Soot Formation Processes in a Diesel Flame. International Journal of Engine Research, 2004. 6(1): p. 21-42.
60. Kosaka, H., Nishigaki, T., Kamimoto, T., Sano, T., Matsutani, A., Harada, S, Simultaneous 2-D Imaging of OH Radicals and Soot in a Diesel Flame by Laser Sheet Techniques. SAE Paper 960834, 1996.
61. Wagner, H.G., Soot Formation: An Overview in Particulate Carbon Formation During Combustion, D.C. Siegla, Smith, G.W1981, New York: Plenum Press.
62. Eastwood, P., Critical Topics in Exhaust Gas Aftertreatment 2000: Research Studies Press Ltd.
63. Li, X., Wallace, J, A Phenomenological Model for Soot Formation and Oxidation in Direct-Injection Diesel Engines. SAE Paper 952428, 1995.

## References

---

64. French, G.R., Scott W.M., Giving the IDI Diesel a Fresh Start. SAE Paper 850452, 1985.
65. Walter, B., Perrin, H., Dumas, J.P, Laget, O, Cold Operation with Optical and Numerical Investigations on a Low Compression Ratio Diesel Engine. SAE Paper 2009-01-2714, 2009.
66. Austen, A.E.W., Lyn, W.T., Some Investigations on the Cold Starting Phenomena in Diesel Engines. Proc. IMechE, Number 5, 1956-60.
67. Perrin, H.M., Dumas, J.P., Laget, O., Walter, B, Analysis of Combustion Process in Cold Operation with a Low Compression Ratio Diesel Engine. SAE Paper 2010-01-1267, 2010.
68. Burrows, J.A., An Investigation into the Cold Start Performance of Automotive Diesel Engines, PhD Thesis, 1998, The University of Nottingham.
69. Tindle, C.R., An Investigation of Factors which Influence the Cold Start Performance of Diesel Engines, PhD Thesis, 2000, The University of Nottingham.
70. Zahdeh, A., Henein, N., Bryzik, W, Diesel Cold Starting - Actual Cycle Analysis under Border-Line Conditions. SAE Paper 900441, 1990.
71. Gonzalez, M.A., Borman, G.L., Reitz, R.D, A Study of Diesel Cold Starting using both Cycle Analysis and Multidimensional Calculations. SAE Paper 910180, 1991.
72. Shayler, P.J., Leong, D. K. W., Murphy, M., Contributions to Engine Friction During Cold, Low-Speed Running and the Dependence on Oil Viscosity. SAE Paper 2005-01-1654, 2005.
73. Pacaud, P., Perrin, H., Laget, O, Cold Start on Diesel Engine: Is Low Compression Ratio Compatible with Cold Start Requirements. SAE Paper 2008-01-1310, 2008.
74. Tsunemoto, H., Yamada, T., Ishitani, H, Behaviour of Adhering Fuel on Cold Combustion Chamber Walls in Direct Injection Diesel Engines. SAE Paper 861235, 1986.

## References

---

75. Phatak, R., Nakamura, T, Cold Startability of Open-Chamber Direct-Injection Diesel Engines - Part 2: Combustion Chamber Design and Fuel Spray Geometry and Additional Air and Glow Plug as a Starting Aid. SAE Paper 831396, 1983.
76. Mina, T.I., A Detailed Study of the Start and Run-up Behaviour of a Multi-Cylinder Direct Injection Diesel Engine. IMechE Paper Number C372/011, 1989.
77. Lyn, W.T., Valdmanis, E, The Effects of Physical Factors on Ignition Delay. Proc. IMechE Vol. 181 Part 2A Number 1, 1966-67.
78. MacMillan, D., La Rocca, A., Shayler, P.J., The Effect of Reducing Compression Ratio on the Work Output and Heat Release Characteristics of a DI Diesel under Cold Start Conditions. SAE Paper 2008-01-1306, 2008.
79. MacMillan, D., La Rocca, A., Shayler, P.J., Murphy, M., Pegg, I., Morris, T, Comparison of the Indicated Work Outputs, Idle Stabilities, and Heat Release Characteristics of a Direct-Injection Diesel Engine Operating Cold at Two Compression Ratios. proc. IMechE Vol. 224 Part D: J. Automobile Engineering, 2010.
80. Payri, F., Broatch, A., Salavert, J.M., Martin, J, Investigation of Diesel Combustion Using Multiple Injection Strategies for Idling After Cold Start of Passenger-Car Engines. Experimental Thermal and Fluid Science 2010-857-865, 2010. 34.
81. MacMillan, D., La Rocca, A., Shayler, P.J., Investigating the Effects of Multiple Pilot Injections on Stability at Cold Idle for a DI Diesel Engine. SAE Paper 2009-01-0612, 2009.
82. Tomoda, T., Ohki, H., Koyama, T., Fujiwara, K, Study of Diesel Combustion Improvement for Ultra Low Compression Ratio. Aachener Kolloquium Fahrzeug-und Motorentchnik, 2010.
83. Ishida, M., Chen, Z-L., Luo, G-F., Ueki, H, The Effect of Pilot Injection on Combustion in a Turbocharged D.I. Diesel Engine. SAE Paper 941692, 1994.



## References

---

84. Okude, K., Mori, K., Shiino, S., Yamada, K., Matsumoto, Y, Effects of Multiple Injections on Diesel Emission and Combustion Characteristics. SAE Paper 2007-01-4178, 2007.
85. Han, Z., Henein, Naeim., Nitu, Bogdan, Diesel Engine Cold Start Combustion Instability and Control Strategy. SAE Paper 2001-01-1237, 2001.
86. Heinrichs, R., Groemping, U, Customer Driven Diesel Vehicle Sound Quality. Inter-Noise, 2004.
87. Russell, M.F., The Dependence of Diesel Combustion on Injection. Proceedings of the IMechE Seminar Future Engine and System Technologies - The EURO IV Challenge, 1997. (S490/005/97): p. 65-82.
88. Desantes, J.M., Garcia-Oliver, J.M., Pastor, J.M., Ramirez-Hernandez, J.G, Influence of Nozzle Geometry on Ignition and Combustion for High-Speed Direct Injection Diesel Engines under Cold Start Conditions. Fuel 90; 3359-3368, 2011.
89. Lacoste, J., Characteristics of Diesel Sprays at High Temperatures and Pressures, PhD Thesis, 2006, University of Brighton.
90. Matthews, C., IMechE Engineers' Data Book. 2nd ed 2000: Professional Engineering Publishing Ltd.
91. Brown, N., Gupta, V., Rocca, A. LA, Shayler, P.J., Murphy, M., Pegg, I, Watts, M, Effects of Injection Strategies on the Cold Start up of DI Diesel Engines. Proc. IMechE, 221 (Part D): 1415-1423, 2007.
92. Brunt, M., Harjit, R., Emtage, A, The Calculation of Heat Release Energy from Engine Cylinder Pressure Data. SAE Paper 981052, 1998.
93. Brunt, M., Platts, K., Calculation of Heat Release in Direct Injection Diesel Engines. SAE paper 1999-01-0187, 1999.
94. Gatowski, J.A., Balles, E.N., Nelson, F.E., Ekchian, J.A., Heywood, J.B, Heat Release Analysis of Engine Cylinder Pressure Data. SAE Paper 841359, 1984.

## References

---

95. Hohenberg, G., Advanced Approaches for Heat Transfer Calculations. SAE Paper 790825, 1979.
96. Cheng, K., Processes Influencing the Indicated Work Output of Direct Injection Diesel Engines During Cold Starting, PhD Thesis, 2002, The University of Nottingham.
97. Bosch Automotive Handbook. Sixth ed 2004: Robert Bosch GmbH.
98. La Rocca, A., MacMillan, D.J., Shayler, P.J, Multiple Pilot Injection Spray Evolutions Emerging from a Multi-Hole HPCR Injector. VTI, Changchun, China, 2012.
99. <http://www.dantecdynamics.com/Default.aspx?ID=18373&Purge=True>. Accessed September 2012.
100. Sjoberg, M., Angstrom, H-E., Bergman, M., Karlsson, H, Spray-Study Equipment: Hot-Gas Supply and Unit Injector Actuator for Bomb Studies. SAE Paper 1999-01-0198, 1999.
101. Toedter, O., Last, B., Rottner, M., Stockle, J., BorgWarner Beru Systems. Influence of Glow Temperature on Emissions and Fuel Consumption. [http://www.beru.com/download/produkte/whitepaper\\_iss\\_en.pdf](http://www.beru.com/download/produkte/whitepaper_iss_en.pdf). Accessed April 2012.
102. Last, B., Houben, H., Rottner, M., Stotz, I., Beru AG. Influence of Modern Diesel Cold Start Systems on the Cold Start, Warm Up and Emissions of Diesel Engines. [http://www.beru.com/download/produkte/fachvortrag\\_influence\\_en.pdf](http://www.beru.com/download/produkte/fachvortrag_influence_en.pdf). Accessed April 2012.
103. Zhang, W., Nishida, K., Gao, J., Miura, D, An Experimental Study on Flat-Wall-Impinging Spray of Microhole Nozzles under Ultra-High Injection Pressures. Proceedings of the IMechE Part D Journal of Automobile Engineering, 2008. 222 (9). : p. 1731-1741.
104. Birgel, A., Ladommatos, N., Aleiferis, P., Zulch, S., Milovanovic, N., Lafon, V., Orlovic, A., Lacey, P., Richards, P, Deposit Formation in the Holes of Diesel Injector Nozzles: A Critical Review. SAE Paper 2008-01-2383, 2008.

## References

---

105. Payri, F., Broatch, A., Serrano, J.R, Study of the Potential of Intake Air Heating in Automotive DI Diesel Engines. SAE Paper 2006-01-1233, 2006.
106. Sellerbeck, P., Nettelbeck, C., Heinrichs, R., Abels, T, Improving Diesel Sound Quality on Engine Level and Vehicle level - a Holistic Approach. SAE Paper 2007-01-2372, 2007.
107. Otto, N., Amman, S., Eaton, C., Lake, S, Guidelines for Jury Evaluations of Automotive Sounds. SAE Paper 1999-01-1922, 1999.
108. Payri, F., Broatch, A., Tormos, B., Marant, V, New Methodology for In-Cylinder Pressure Analysis in Direct Injection Diesel Engine - Application to Combustion Noise. Measurement Science and Technology, 2005.
109. Payri, F., Broatch, A., Margot, X., Monelletta, L., Sound Quality Assessment of Diesel Combustion Noise using In-Cylinder Pressure Components. Measurement Science and Technology, 2008.
110. Ghaffarpour, M.R., Noorpoor, A. R, A Numerical Study of the use of Pilot or Split Rate Injection to Reduce Diesel Engine Noise. Proc. IMechE Vol. 221 Part D:J. Automobile Engineering, 2006.
111. Suppes, G., J., Srinivasan, B., Natarajan, V.P, Autoignition of Biodiesel, Methanol, and a 50:50 Blend in a Simulated Diesel Engine Environment. SAE Paper 952758, 1995.

# Tables

## Chapter 1

**Table 1-1: EU emission standards for diesel passenger cars [18]**

Stage	CO	HC	HC+NO <sub>x</sub>	NO <sub>x</sub>	PM	PN
	g/km					#/km
Euro 1 (1992)	2.72	-	0.97	-	0.14	-
Euro 2, IDI (1996)	1.0	-	0.7	-	0.08	-
Euro 2, DI (1996)	1.0	-	0.9	-	0.1	-
Euro 3 (2000)	0.64	-	0.56	0.5	0.05	-
Euro 4 (2005)	0.5	-	0.3	0.25	0.025	-
Euro 5a (2009)	0.5	-	0.23	0.18	0.005	-
Euro 5b (2011)	0.5	-	0.23	0.18	0.005	6.0×10 <sup>11</sup>
Euro 6 (2014)	0.5	-	0.17	0.08	0.005	6.0×10 <sup>11</sup>

## Chapter 3

**Table 3-1. Range and reasons for each of the parameters investigated**

Parameter	Range	Reason
<b>Number of pilot injections [-]</b>	0-4	Representative of the number of pilot injections used during cold idling operation
<b>Vessel temperature [°C]</b>	40-200	Restricted by cartridge heaters and safe operating conditions
<b>Glow plug temperature [°C]</b>	900-1300	Ceramic glow plugs offer a good operating range where high temperatures tend to alleviate poor cycle-by-cycle stability
<b>Quantity per pilot [mg]</b>	1-8	Offers a wide range to investigate split fuelling strategies
<b>Vessel pressure [bar]</b>	20-50	Offers a wide range to replicate variations in compression ratio and crank angle pressure evolution. Motored peak compression pressure in the engine is no higher than around 40 bar
<b>Separation [ms]</b>	0.8-3.3	Representative of 5-20 °CA at 1000 rev/min, shorter separations limited by hardware

**Table 3-2. Ranking order of the indicators response to a change in each of the parameters at a time. The baseline conditions are two pilot injections, each 2 mg, total fuelling of 20 mg, 1.7 ms separation, 900°C glow plug temperature, and vessel temperature and pressure of 100°C and 35 bar respectively**

Parameter	First detectable soot [ms]	Pilot combustion growth rate [Pixels/ms]	Enflamed area at SOI <sub>Main</sub> [Pixels]	Main initiation delay [ms]	Main combustion growth rate [Pixels/ms]	Maximum enflamed area [Pixels]
Number of pilot injections (1-3) [-]	1	1	1	1	1	1
Vessel temperature (40-200) [°C]	1	2	2	1	1	1
Glow plug temperature (900-1300) [°C]	1	1	1	2	1	2
Quantity per pilot (1-3) [mg]	1	2	2	1	2	2
Vessel pressure (20-35) [bar]	1	2	2	2	2	3
Separation (0.8-1.7) [ms]	1	2	2	2	2	3

## Chapter 4

**Table 4-1: Single cylinder DI diesel test engine specification**

Bore [mm]	86
Stroke [mm]	94.6
Displacement [litre/cm <sup>3</sup> ]	0.55/550
Compression ratio	15.5:1
Injection system	2000 bar Bosch high pressure pump, common rail, 8 hole (120 µm diameter) centrally mounted piezo-electric injector
Valves	4/cylinder – 2 intake, 2 exhaust
Swirl ratio	1.5

# Chapter 6

Table 6-1. Ranking order of cycle-by-cycle stability response to various parameters at three soak temperatures

Parameter	-20°C	-5°C	10°C
Glow plug temperature (850-1200) [°C]	1	1	1
Number of pilot injections (1-3) [-]	1/2*	2/2*	1/1*
Total fuelling level (18-20, 12-14, 9-11) [mg]	2	3	2
Quantity per pilot (1-3) [mg]	2	3	1
Separation (6-10) [°CA]	2	No data	No data
Main injection timing (-12 - -4) [°ATDC]	2	No data	No data

Table 6-2. Ranking order of maximum premixed combustion response to various parameters at three soak temperatures

Parameter	-20°C	-5°C	10°C
Glow plug temperature (850-1200) [°C]	1	1	1
Number of pilot injections (1-3) [-]	1/1*	1/1*	1/1*
Total fuelling level (18-20, 12-14, 9-11) [mg]	2	2	1
Quantity per pilot (1-3) [mg]	2	2	1
Separation (6-10) [°CA]	2	No data	No data
Main injection timing (-12 - -4) [°ATDC]	2	No data	No data

Table 6-3. Ranking order of maximum mixing controlled combustion response to various parameters at three soak temperatures

Parameter	-20°C	-5°C	10°C
Glow plug temperature (850-1200) [°C]	2	1	2
Number of pilot injections (1-3) [-]	1/2*	1/1*	2/2*
Total fuelling level (18-20, 12-14, 9-11) [mg]	3	2	1
Quantity per pilot (1-3) [mg]	3	2	2
Separation (6-10) [°CA]	3	No data	No data
Main injection timing (-12 - -4) [°ATDC]	2	No data	No data

# Figures

## Chapter 1

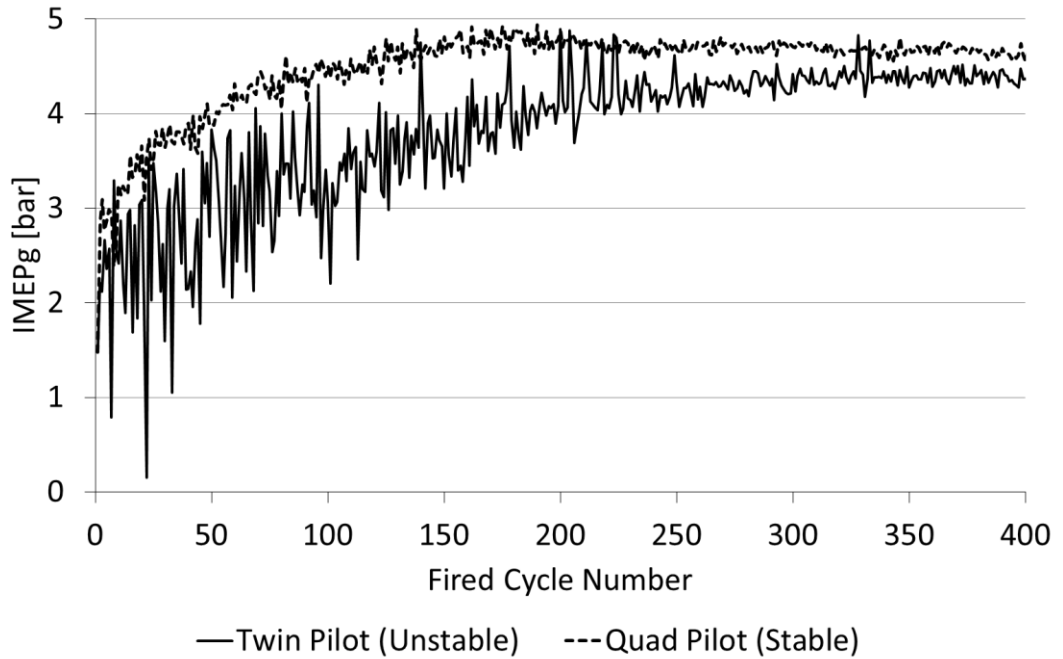


Figure 1-1. Stable and unstable operation

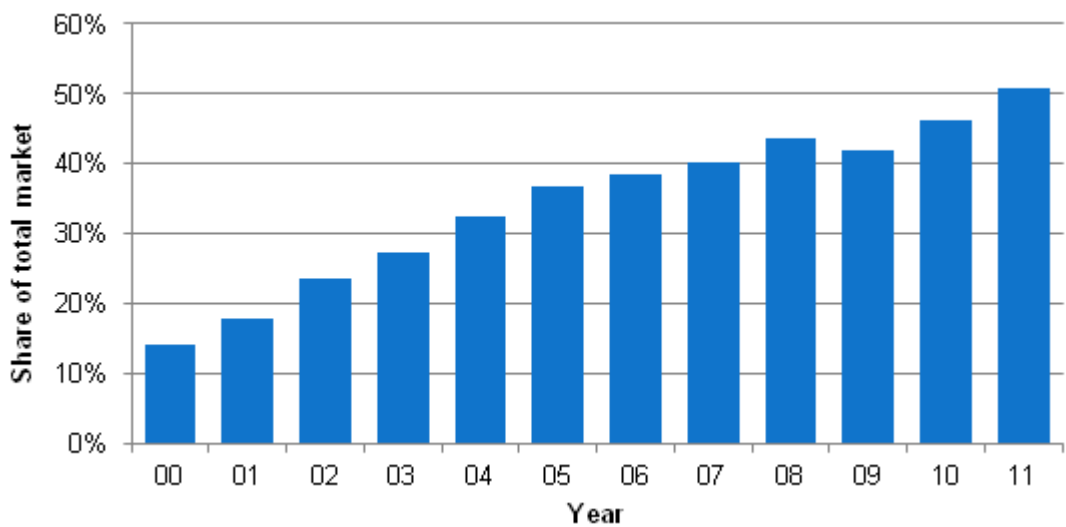


Figure 1-2: Diesel penetration of the UK new car market, 2000-2011 [17]

## Figures

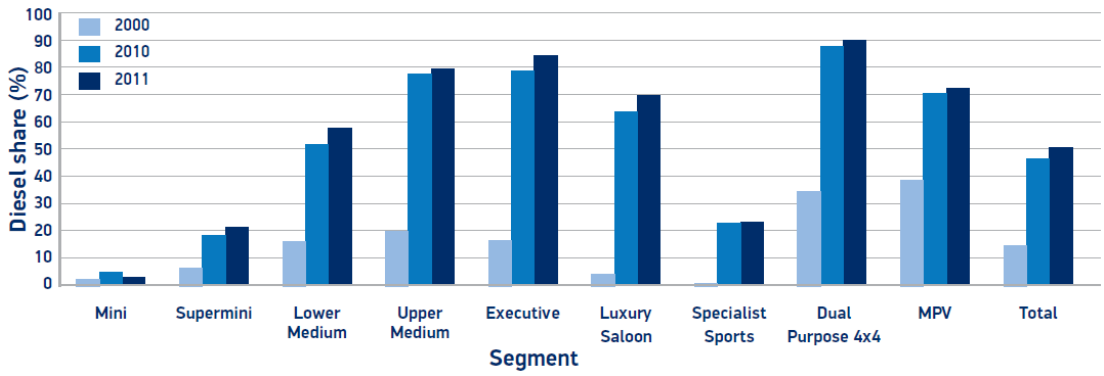


Figure 1-3. Diesel share of the UK new car market by segment in 2000, 2010 and 2011 [17]

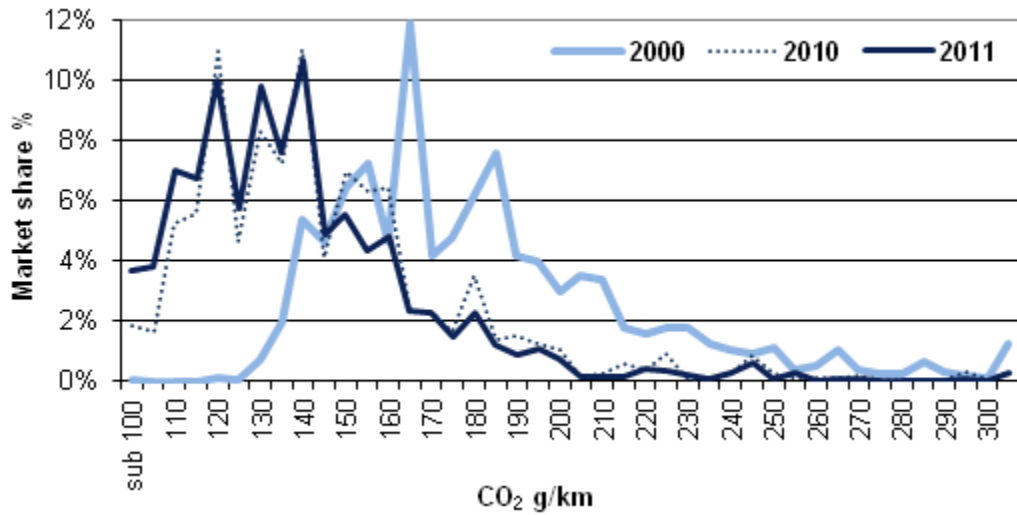


Figure 1-4. Distribution of the UK new car market by CO<sub>2</sub> levels [17]



# Chapter 3

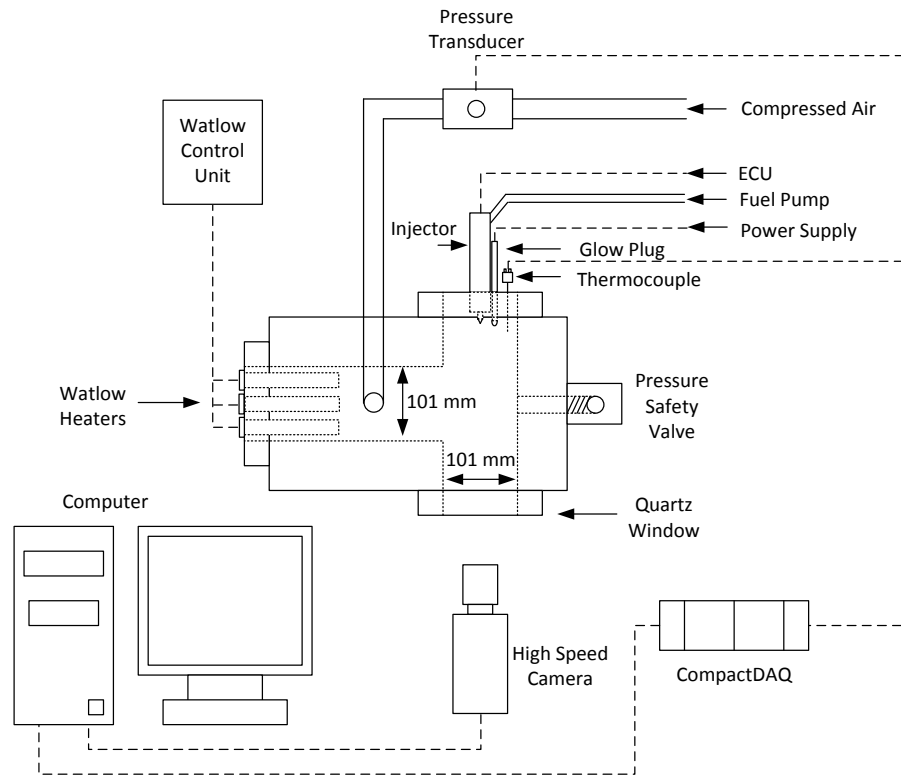


Figure 3-1. Schematic of the optical vessel rig setup

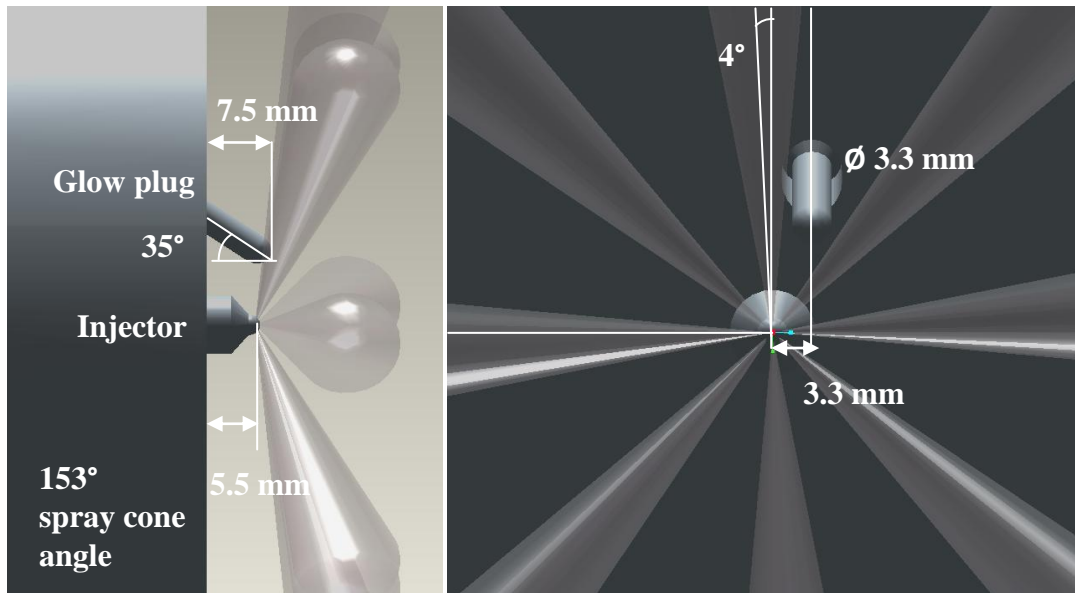
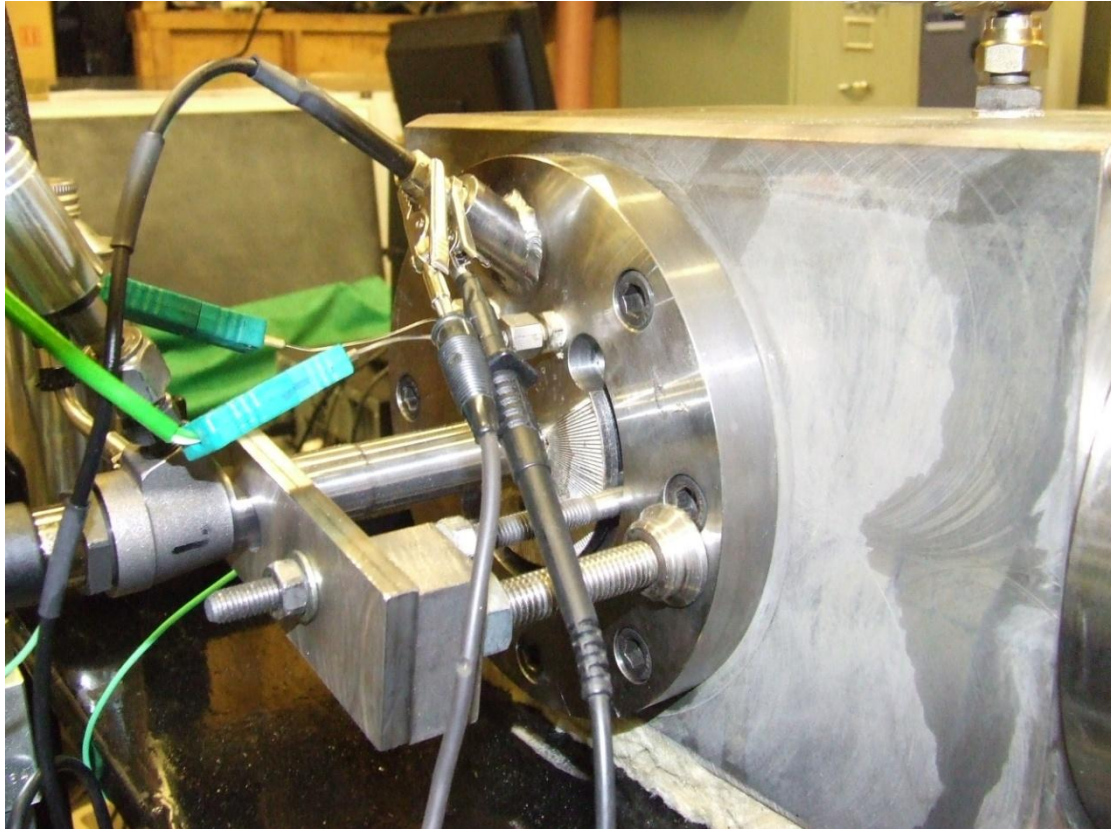

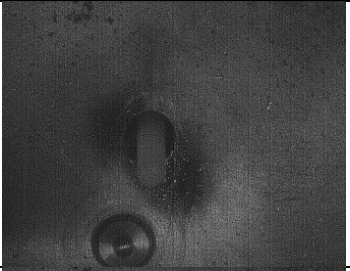





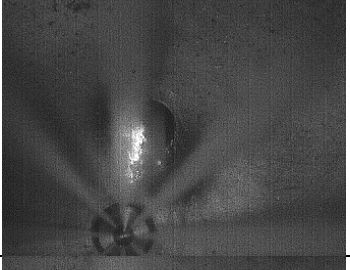




Figure 3-2. Injector spray plume and glow plug position CAD drawing



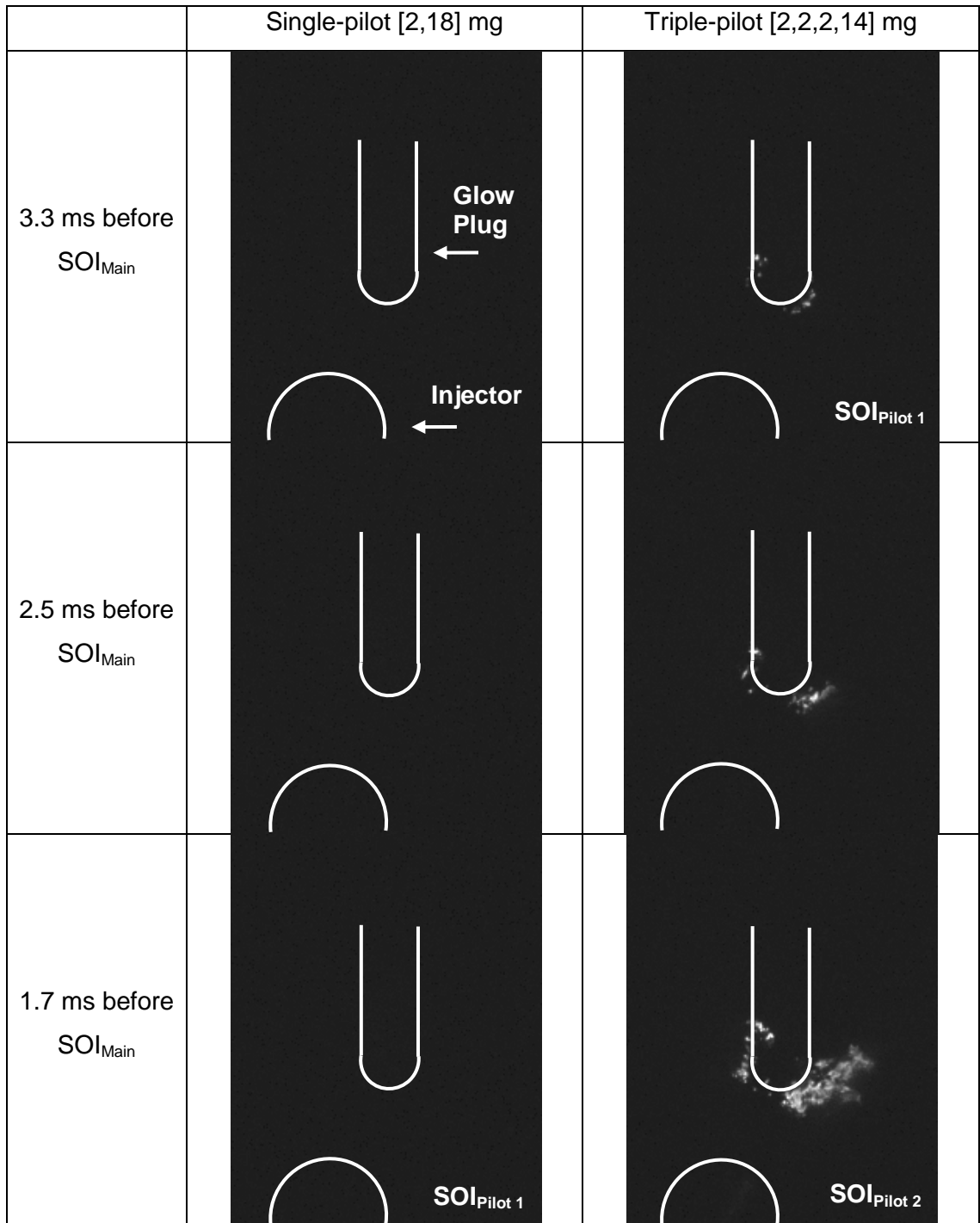
**Figure 3-3. Optical vessel injector and glow plug plate**

Figures

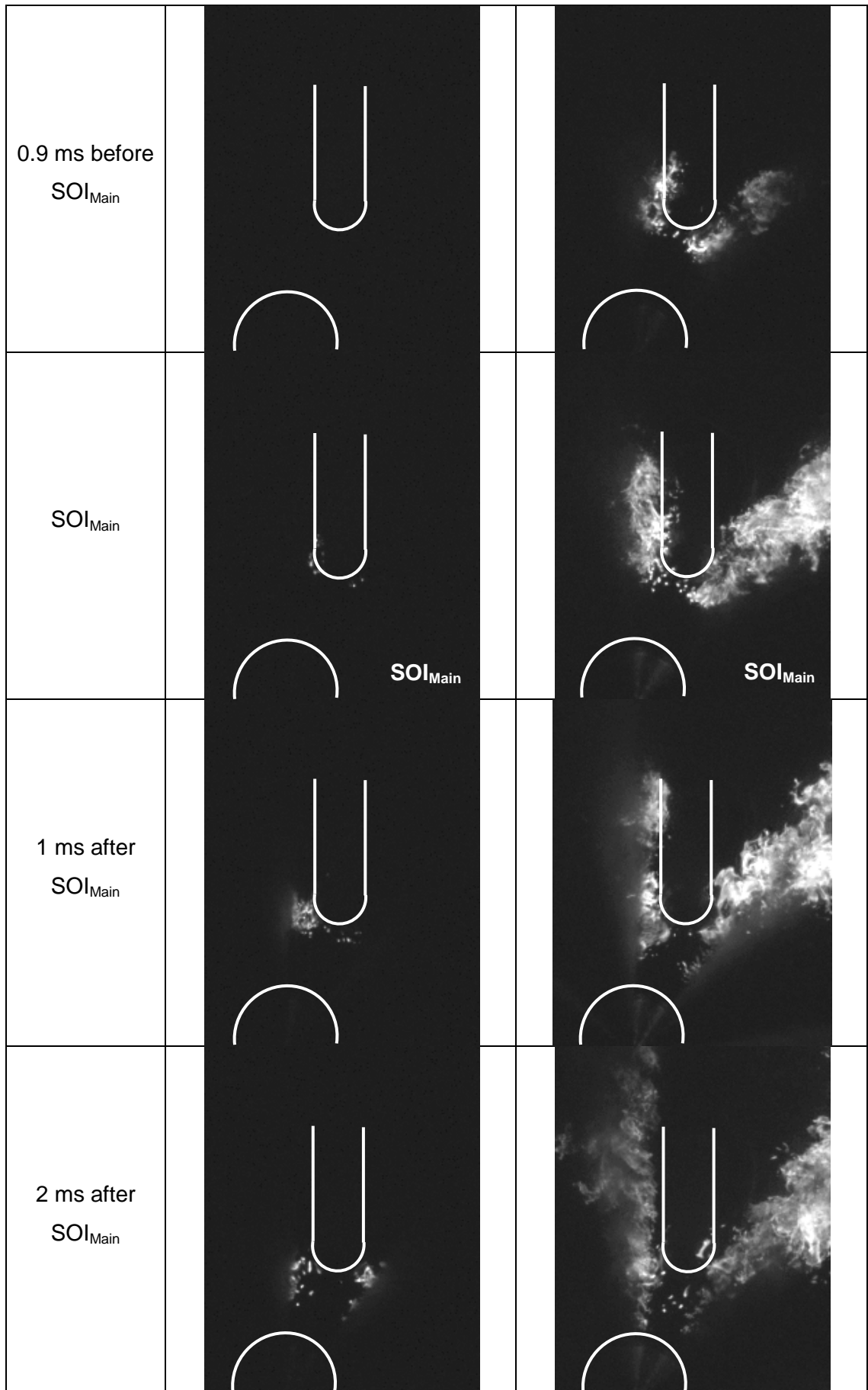
	4° spray position (optimum)	0° spray position
1.7 ms before SOI <sub>Main</sub>		
SOI <sub>Main</sub>		
1 ms after SOI <sub>Main</sub>		
2 ms after SOI <sub>Main</sub>		
3 ms after SOI <sub>Main</sub>		

**Figure 3-4. Combustion initiation evolution for different spray angles. Conditions: [2,18] mg, 35 bar vessel pressure, 100°C vessel temperature, 900°C glow plug, 200 bar rail pressure, 1.7 ms separation**

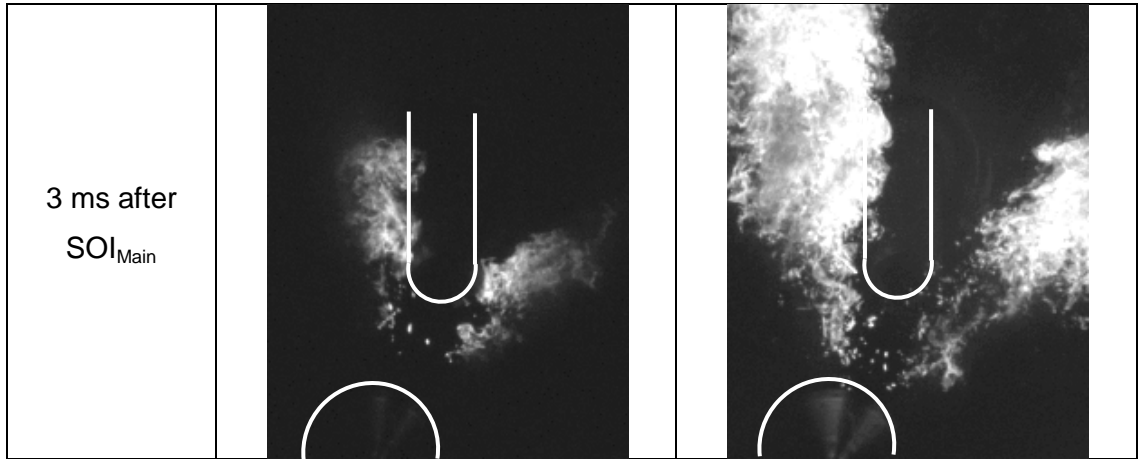
Figures



Figures



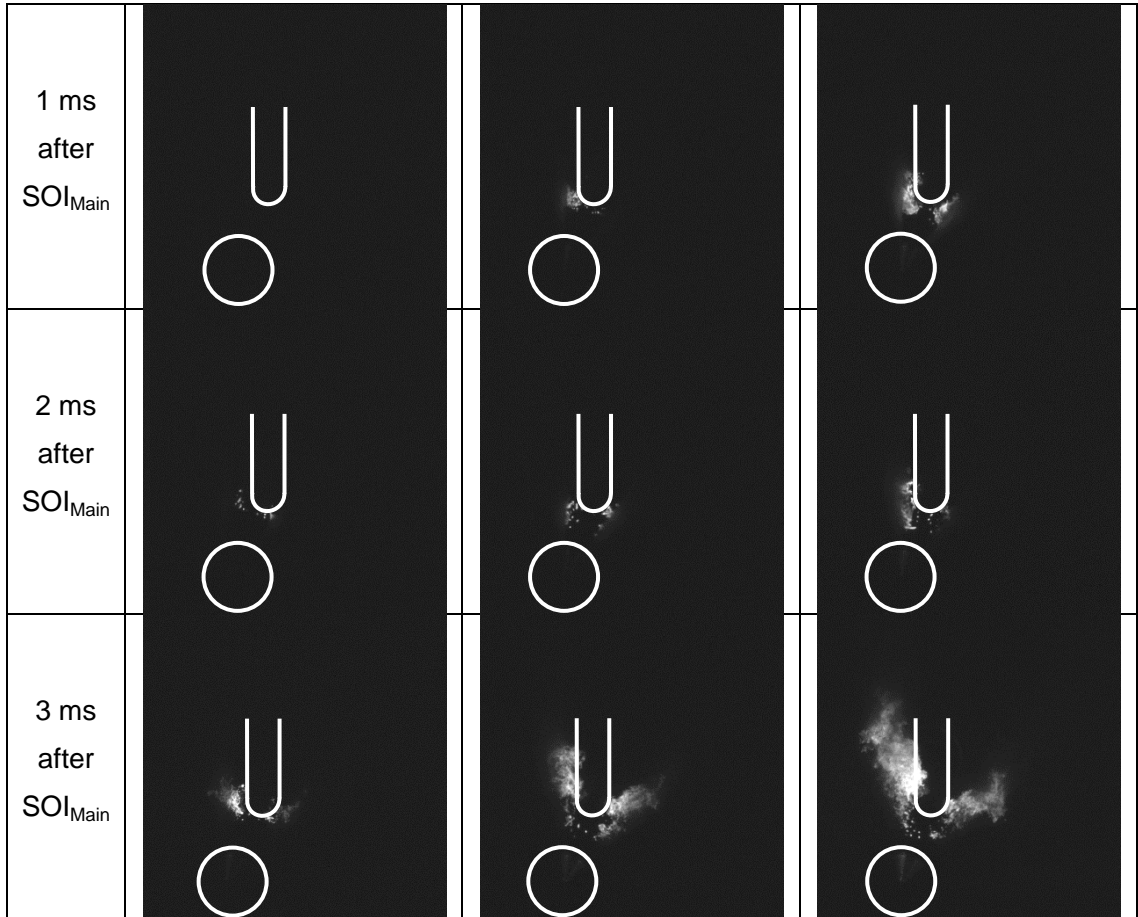
Figures



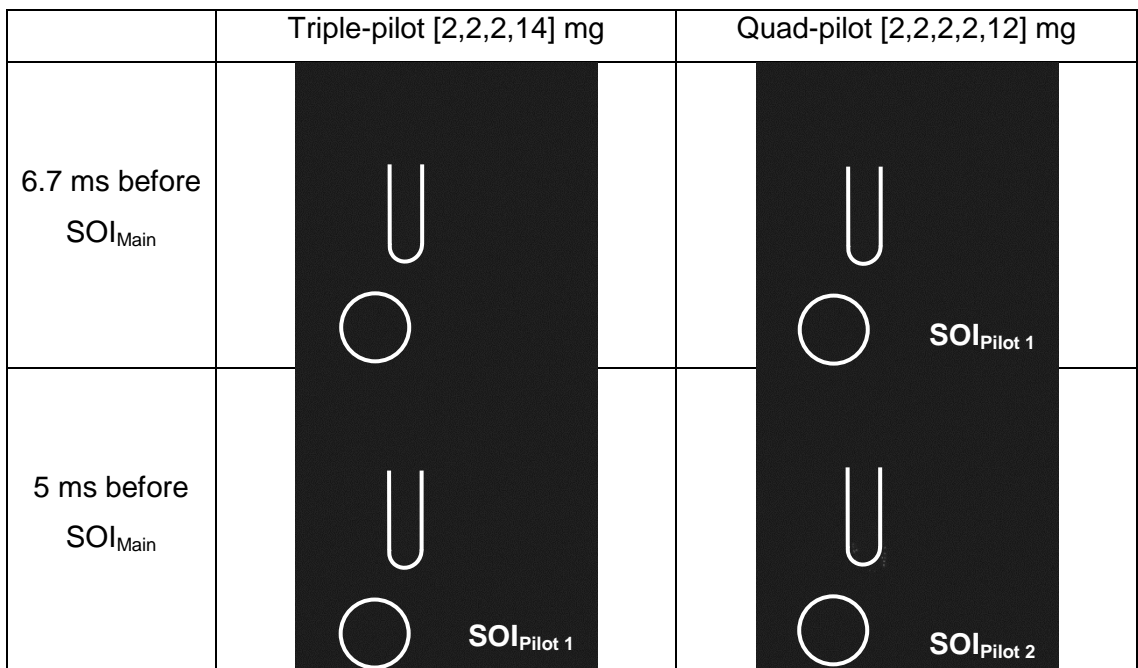
**Figure 3-5. Combustion initiation evolution close up images for single- [2,18] mg and triple-pilot [2,2,2,14] mg strategies. Conditions: 20 mg total fuelling, 35 bar vessel pressure, 100°C vessel temperature, 900°C glow plug, 200 bar rail pressure, 1.7 ms separation**

	No pilot [0,20] mg	Single-pilot [2,18] mg	Twin-pilot [2,2,16] mg
3.3 ms before SOI <sub>Main</sub>			
1.7 ms before SOI <sub>Main</sub>			
SOI <sub>Main</sub>			

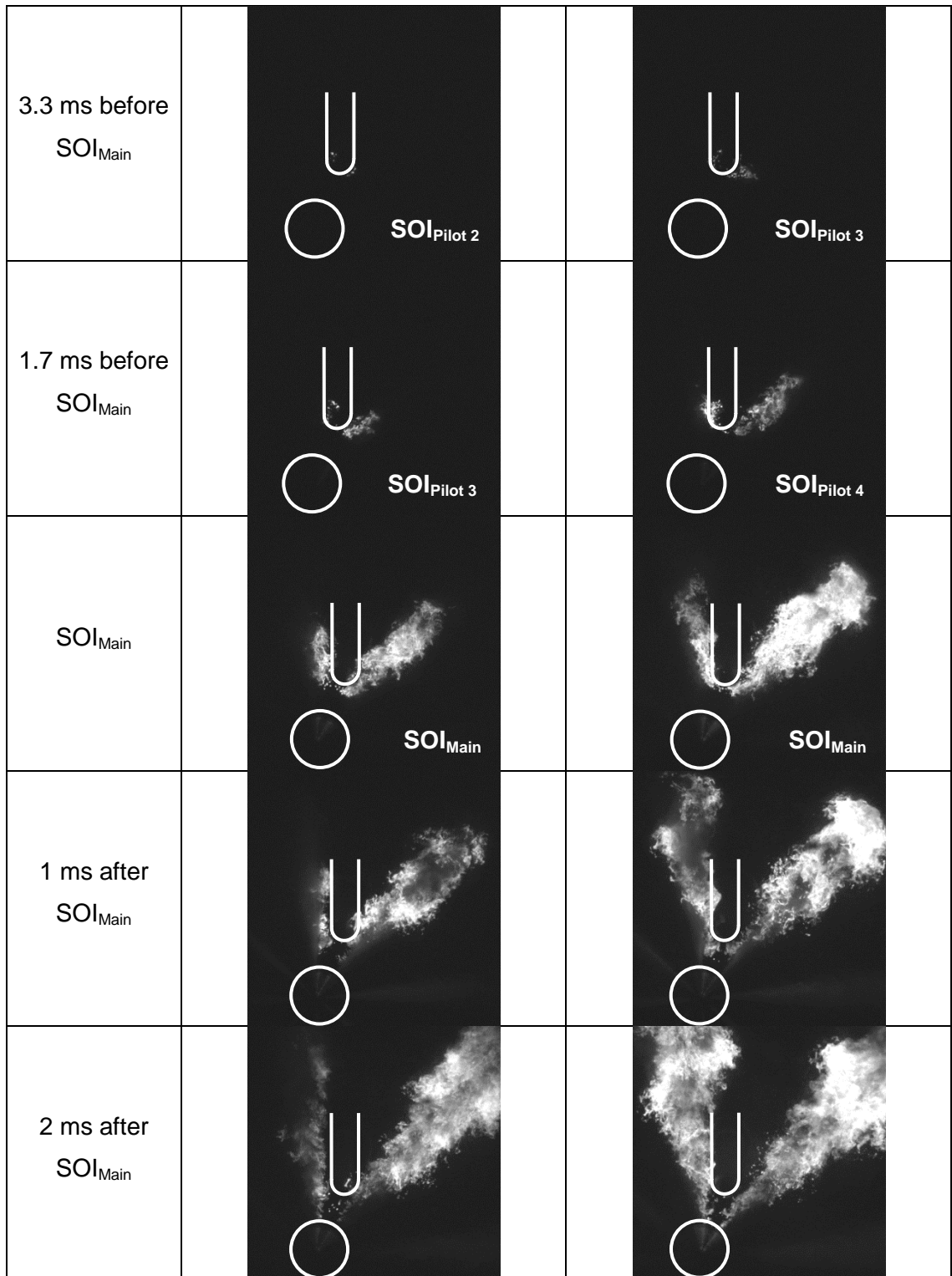
Figures



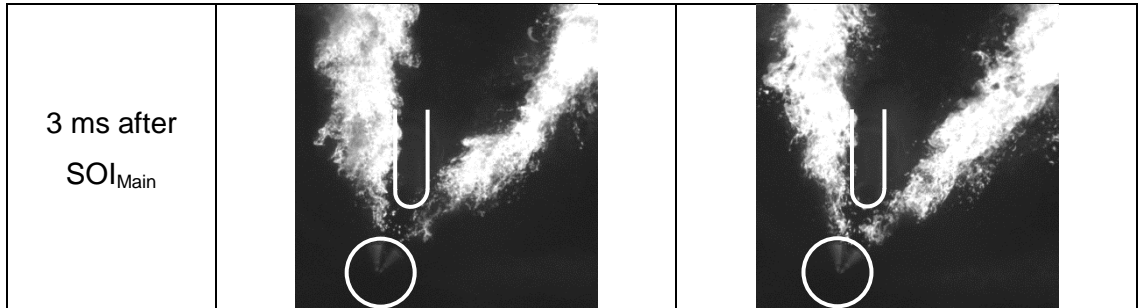
**Figure 3-6. Combustion initiation evolution for no pilot, single- and twin-pilot strategies. Conditions: 20 mg total fuelling, 35 bar vessel pressure, 100°C vessel temperature, 900°C glow plug, 200 bar rail pressure, 1.7 ms separation**



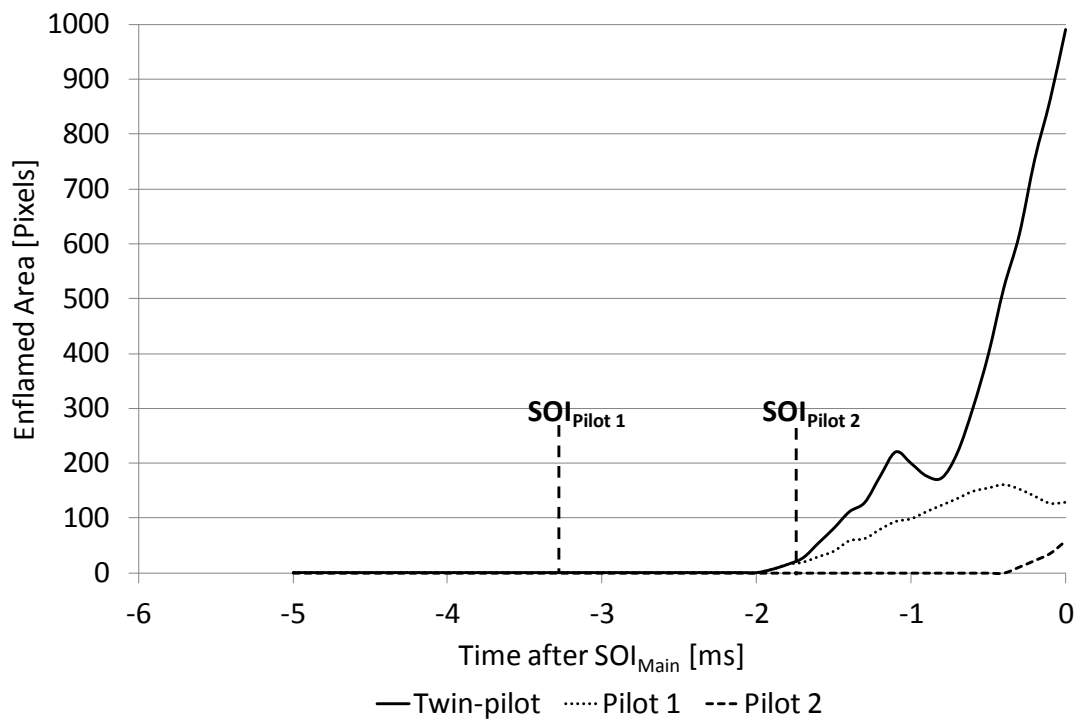
Figures







**Figure 3-7. Combustion initiation evolution for triple- and quad-pilot strategies. Conditions: 20 mg total fuelling, 35 bar vessel pressure, 100°C vessel temperature, 900°C glow plug, 200 bar rail pressure, 1.7 ms separation**



**Figure 3-8. Comparison of the pilot combustion contribution between a twin-pilot strategy and individual pilots injected during separate tests. Conditions: 2 mg per pilot, 35 bar vessel pressure, 100°C vessel temperature, 900°C glow plug, 200 bar rail pressure, 1.7 ms separation**

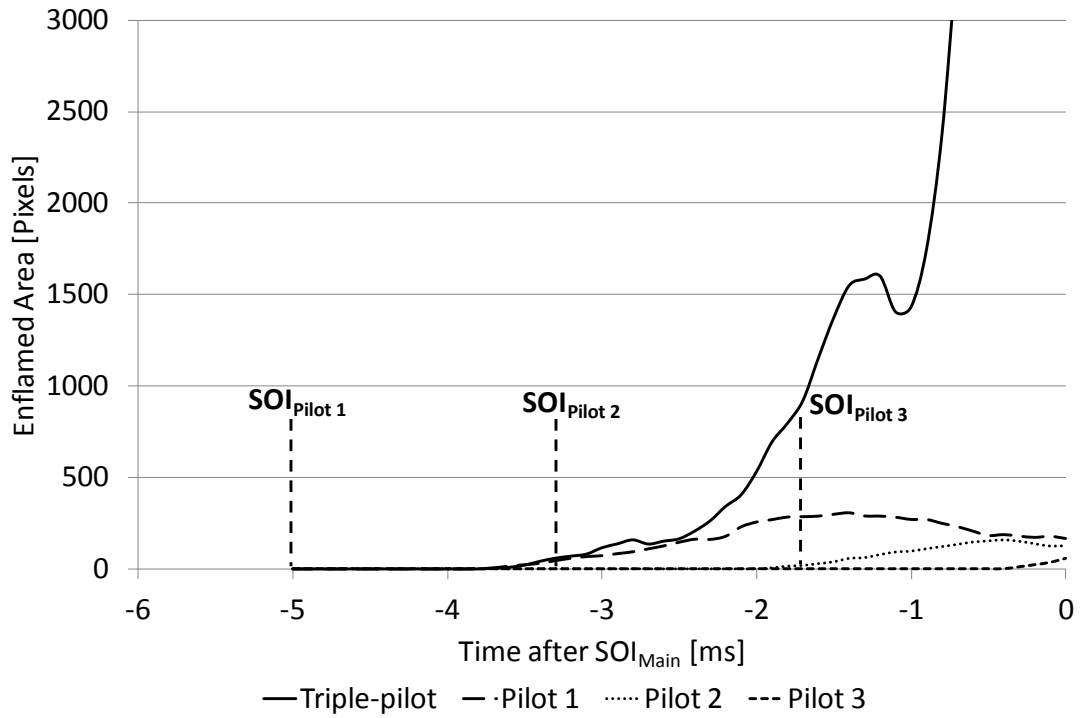
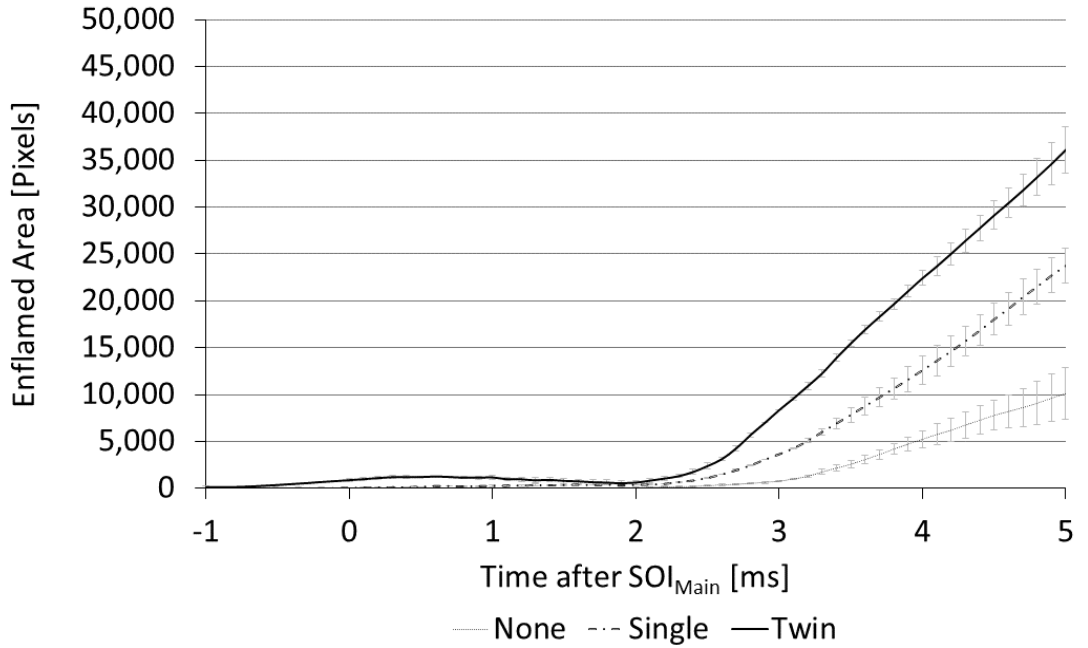
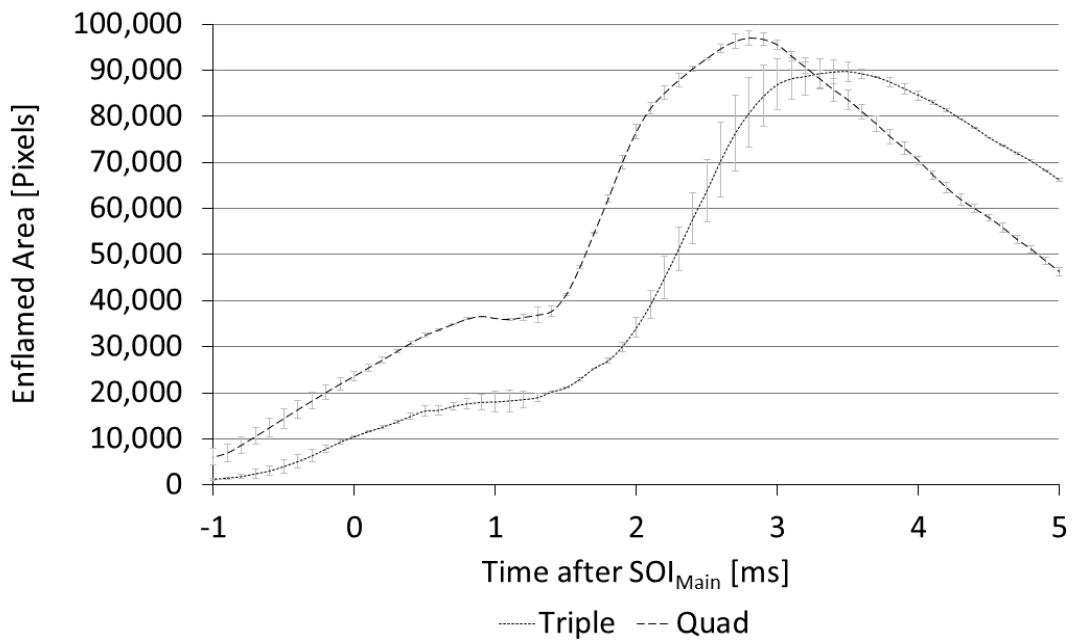


Figure 3-9. Comparison of the pilot combustion contribution between a triple-pilot strategy and individual pilots injected during separate tests. Conditions: 2 mg per pilot, 35 bar vessel pressure, 100°C vessel temperature, 900°C glow plug, 200 bar rail pressure, 1.7 ms separation. The enflamed area reaches 10,500 pixels at  $SOI_{Main}$ , but the scale has been reduced for clarity.



**Figure 3-10. Enflamed area for no pilot, single- and twin-pilot strategies. Conditions: 20 mg total fuelling, 35 bar vessel pressure, 100°C vessel temperature, 900°C glow plug, 200 bar rail pressure, 1.7 ms separation**

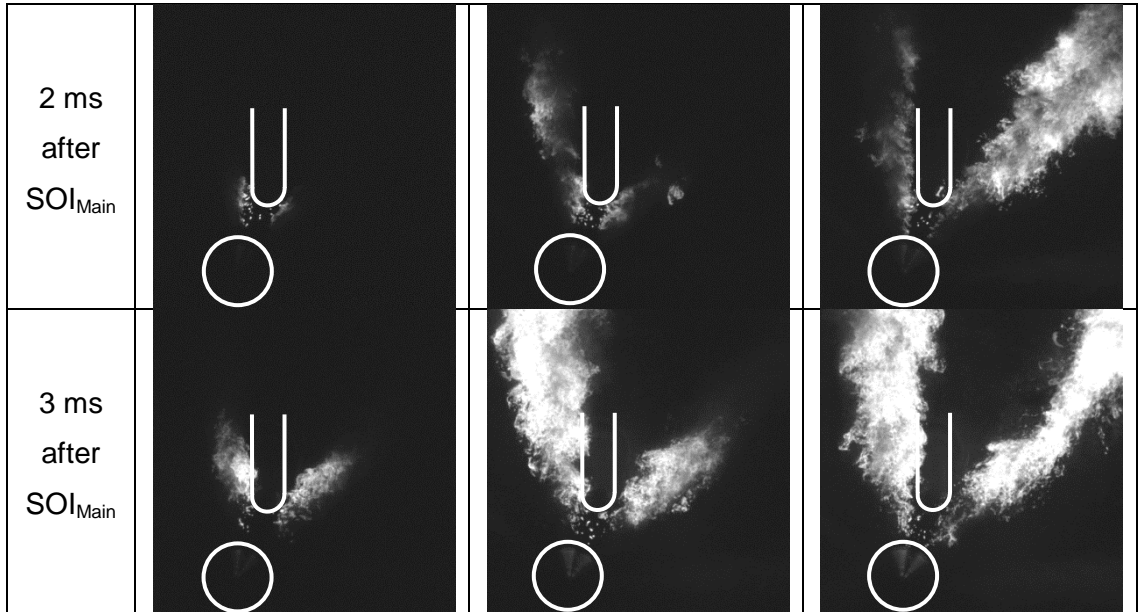


**Figure 3-11. Enflamed area for triple- and quad-pilot strategies. Conditions: 20 mg total fuelling, 35 bar vessel pressure, 100°C vessel temperature, 900°C glow plug, 200 bar rail pressure, 1.7 ms separation**

Figures

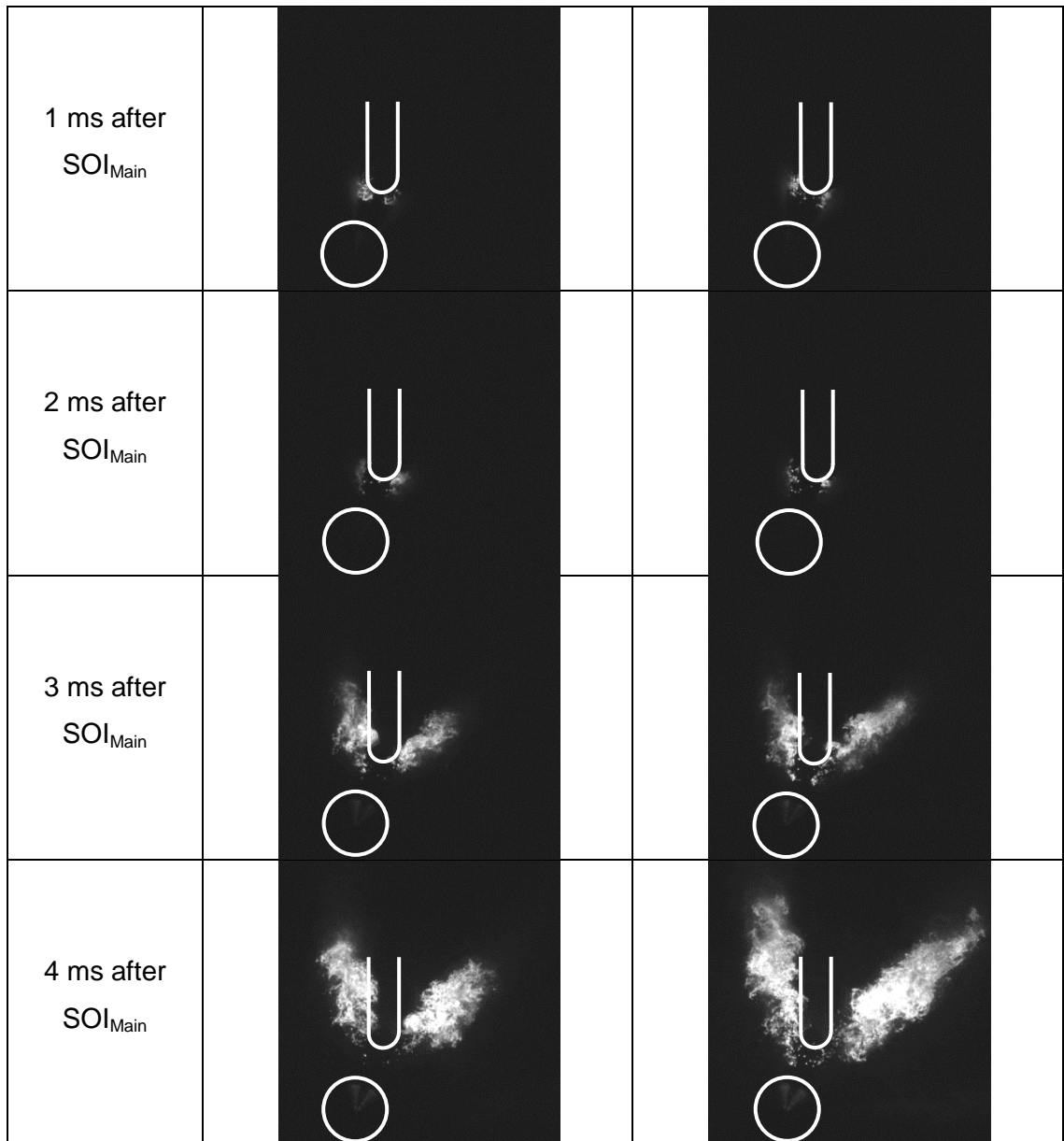
	Single-pilot [6,14] mg	Twin-pilot [3,3,14] mg	Triple-pilot [2,2,2,14] mg
5.0 ms before $SOI_{Main}$			
3.3 ms before $SOI_{Main}$			
1.7 ms before $SOI_{Main}$			
$SOI_{Main}$			
1 ms after $SOI_{Main}$			

Figures

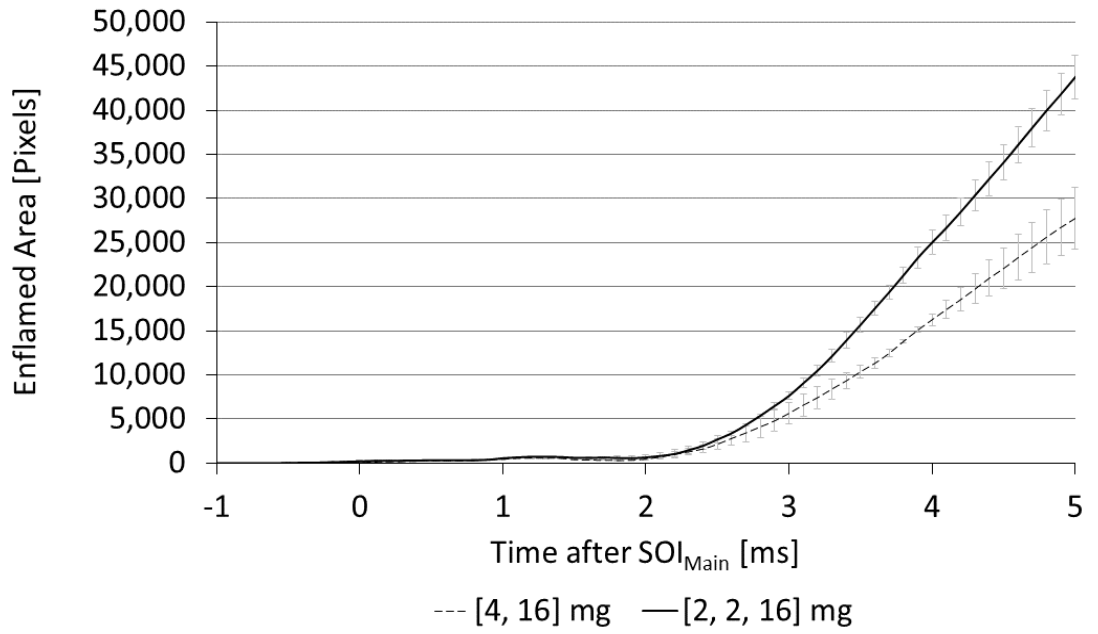


**Figure 3-12. Combustion initiation evolution for different multiple injection strategies with a constant total pilot fuel quantity of 6 mg. Conditions: 35 bar vessel pressure, 100°C vessel temperature, 900°C glow plug, 200 bar rail pressure, 1.7 ms separation**

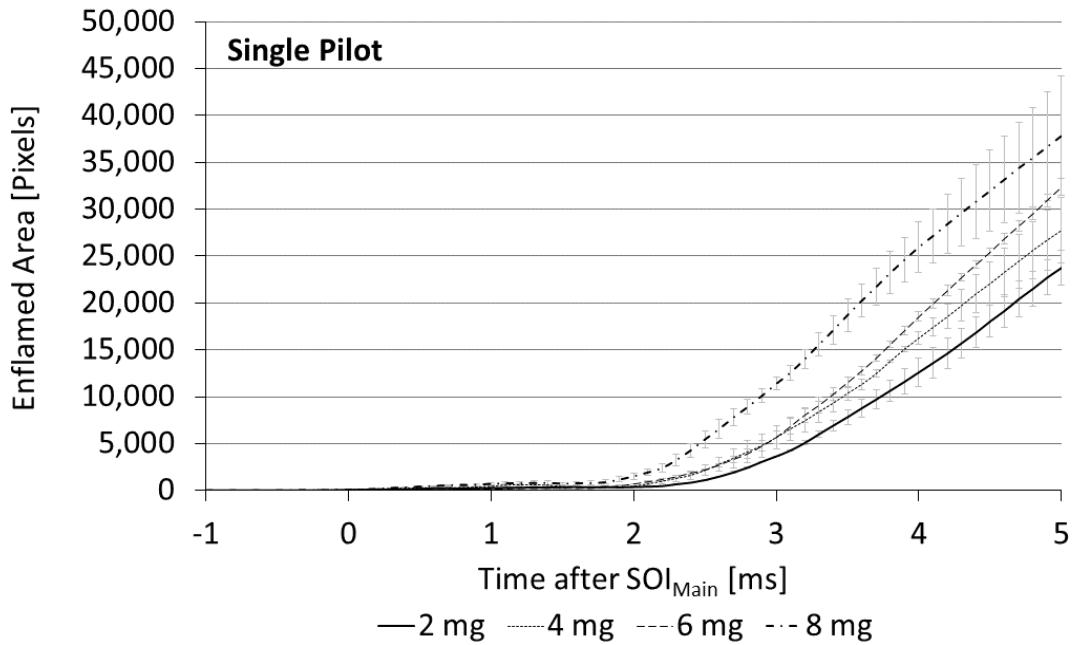
	Single-pilot [4,16] mg	Twin-pilot [2,2,16] mg
1.7 ms before $SOI_{Main}$		
0.83 ms before $SOI_{Main}$		
$SOI_{Main}$		



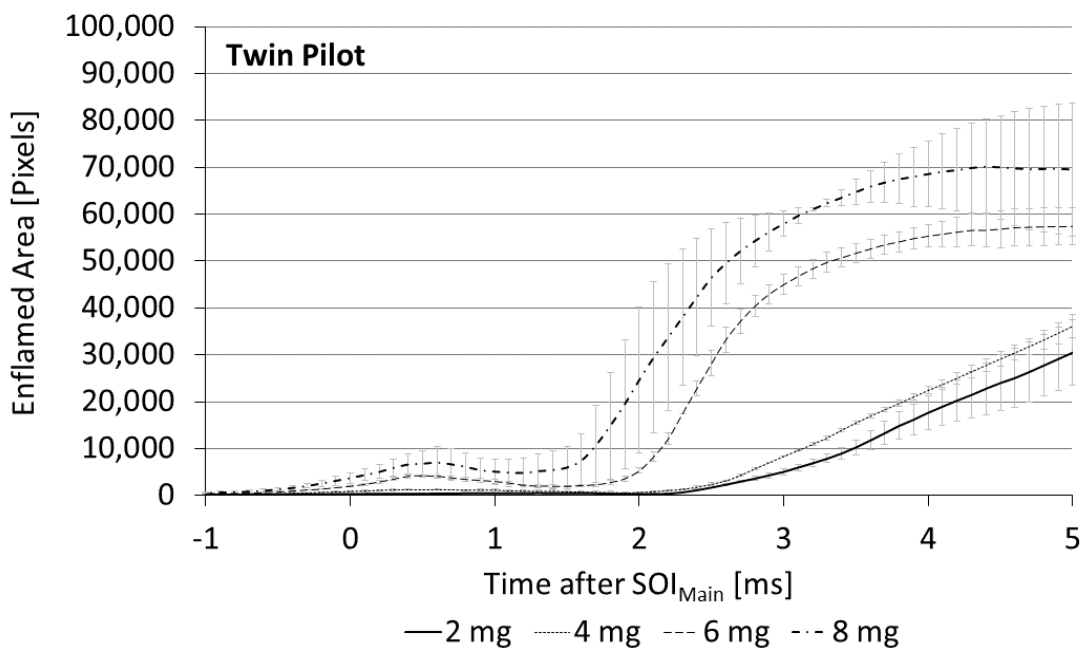
**Figure 3-13. Combustion initiation evolution for single- and twin- pilot strategies with a constant total pilot fuel quantity of 4 mg introduced at the same starting time. Conditions: 35 bar vessel pressure, 100°C vessel temperature, 900°C glow plug, 200 bar rail pressure**



**Figure 3-14. Influence of the number of pilots on enflamed area. Conditions: 20 mg total fuelling, 35 bar vessel pressure, 100°C vessel temperature, 900°C glow plug, 200 bar rail pressure**

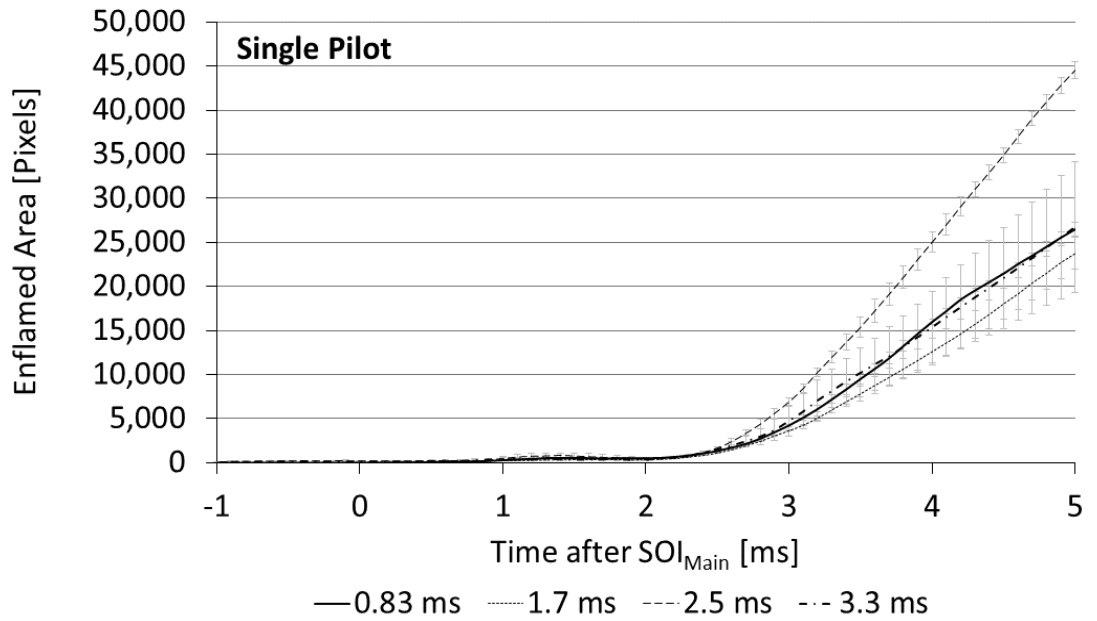


**Figure 3-15. Influence of pilot quantity on enflamed area for a single-pilot strategy. Conditions: 20 mg total fuelling, 35 bar vessel pressure, 100°C vessel temperature, 900°C glow plug, 200 bar rail pressure, 1.7 ms separation**

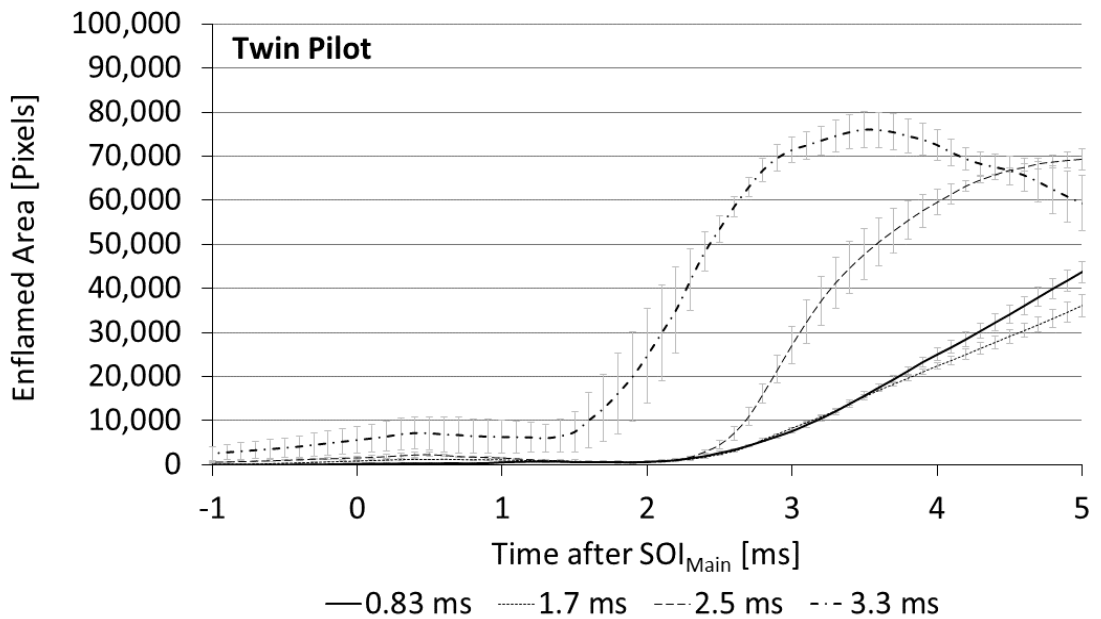


**Figure 3-16. Influence of pilot quantity on enflamed area for a twin-pilot strategy. Conditions: 20 mg total fuelling, 35 bar vessel pressure, 100°C vessel temperature, 900°C glow plug, 200 bar rail pressure, 1.7 ms separation**

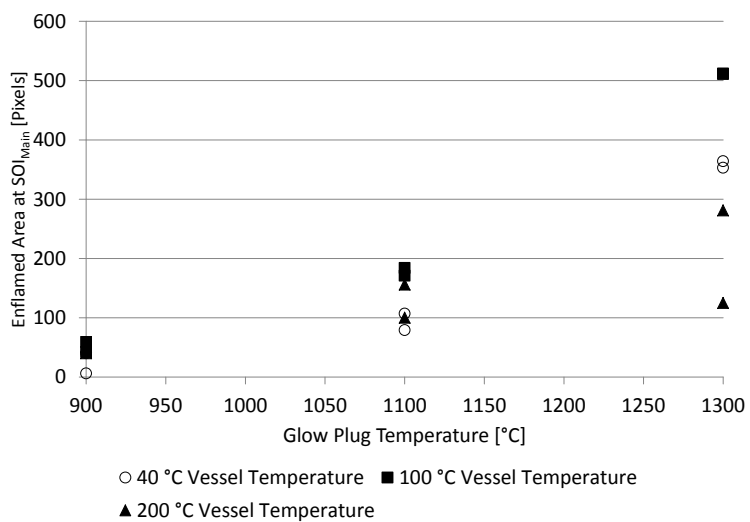
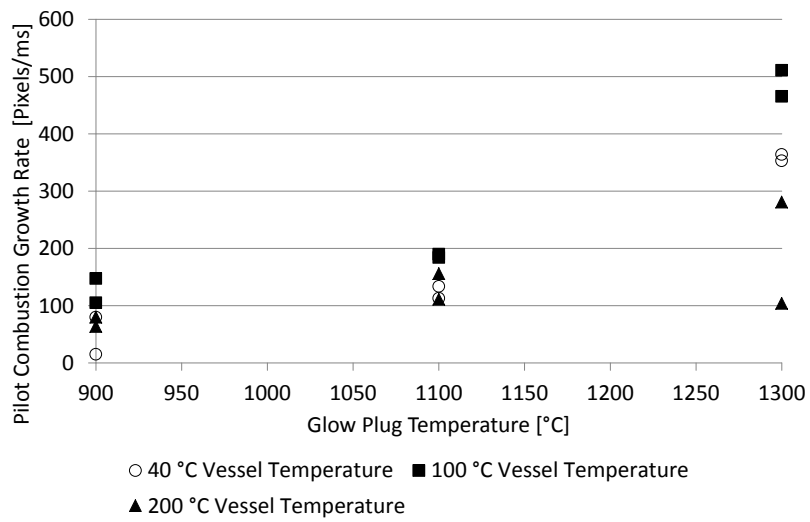
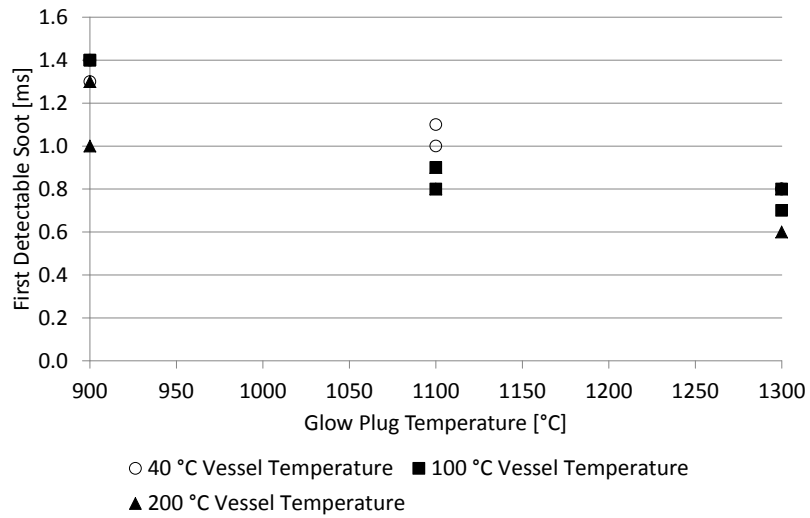


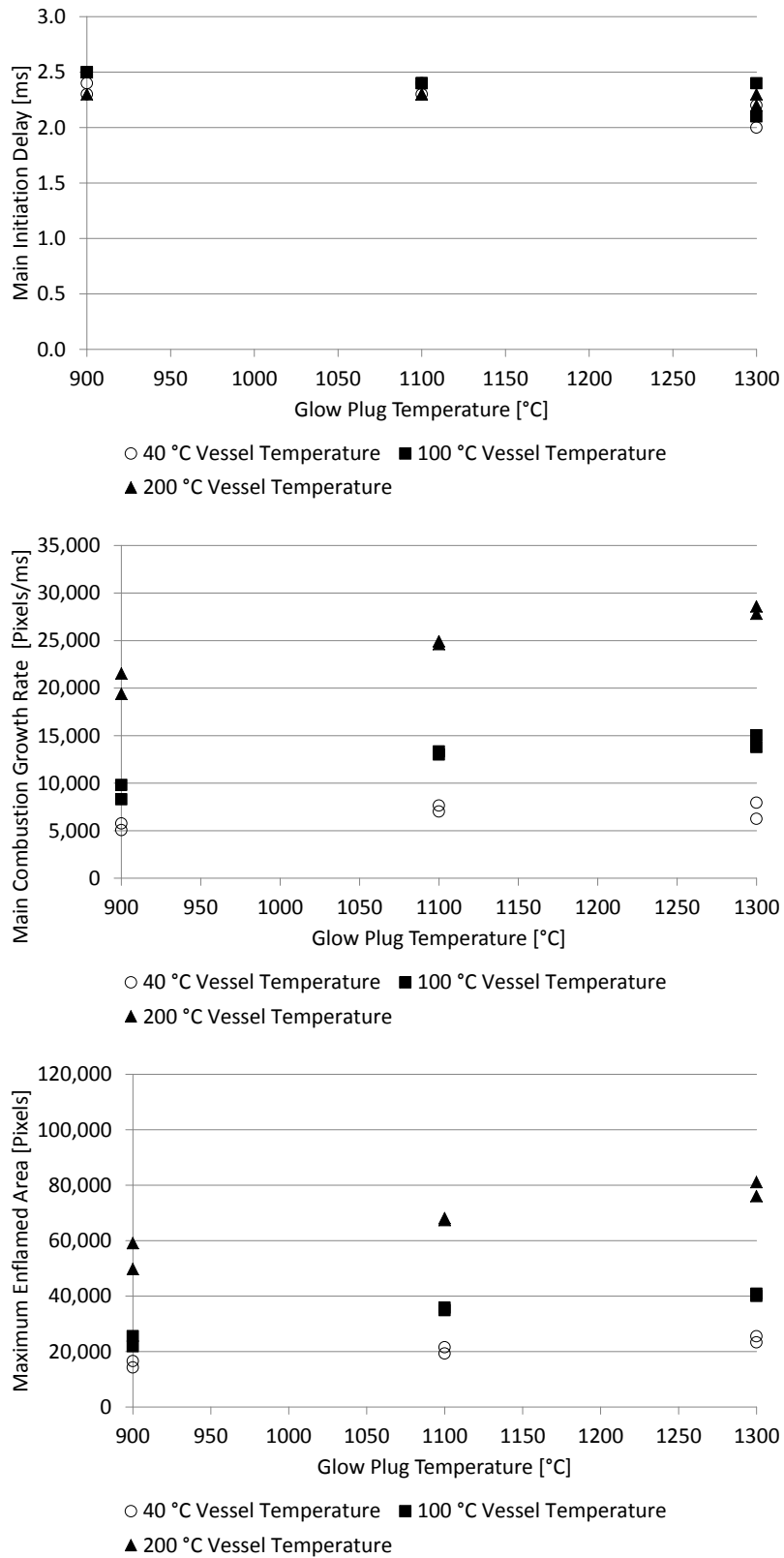


**Figure 3-17. Influence of injection separation on enflamed area for a single-pilot strategy. Conditions: 20 mg total fuelling, 35 bar vessel pressure, 100°C vessel temperature, 900°C glow plug, 200 bar rail pressure**



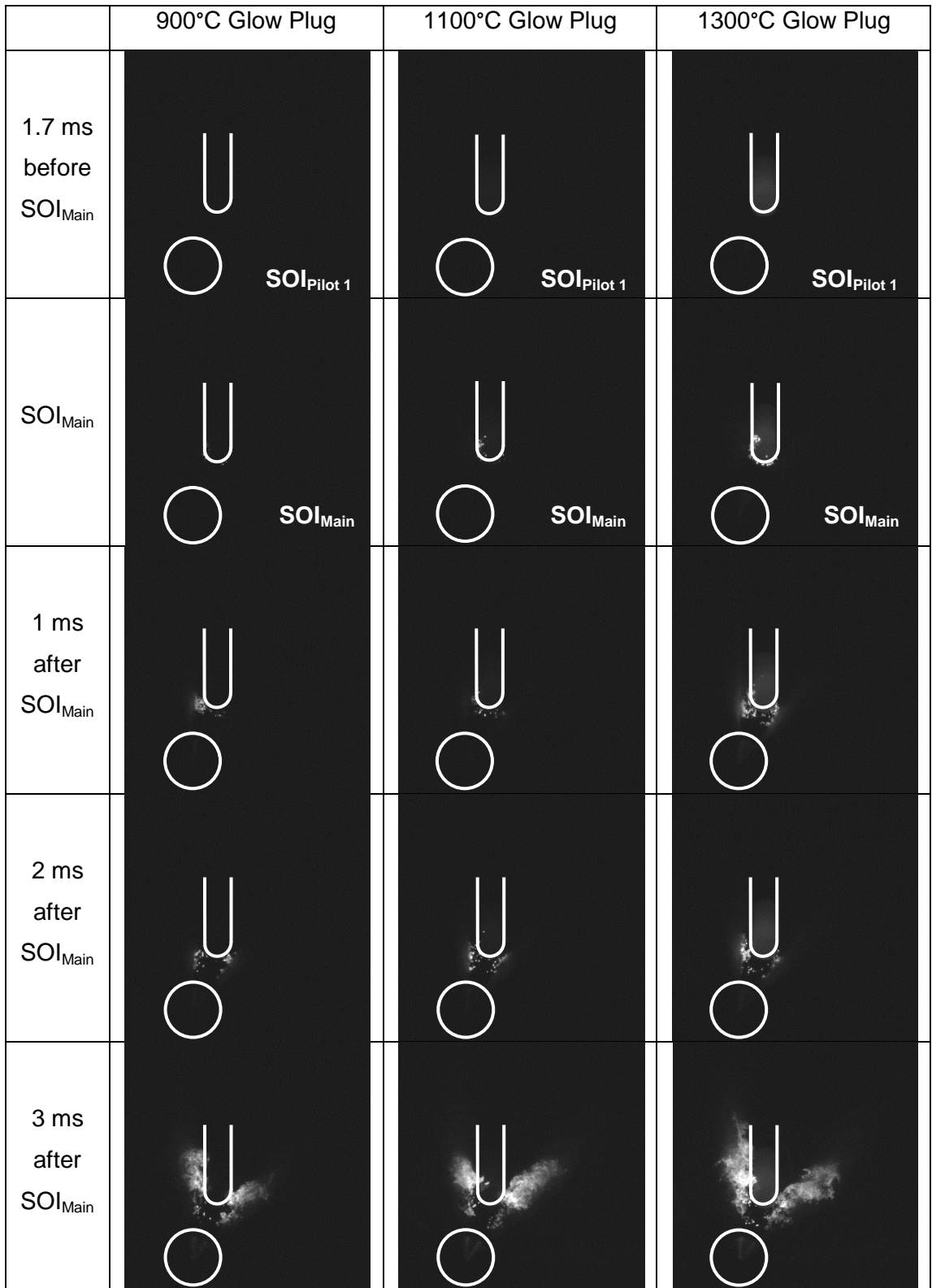
**Figure 3-18. Influence of injection separation on enflamed area for a twin-pilot strategy. Conditions: 20 mg total fuelling, 35 bar vessel pressure, 100°C vessel temperature, 900°C glow plug, 200 bar rail pressure**





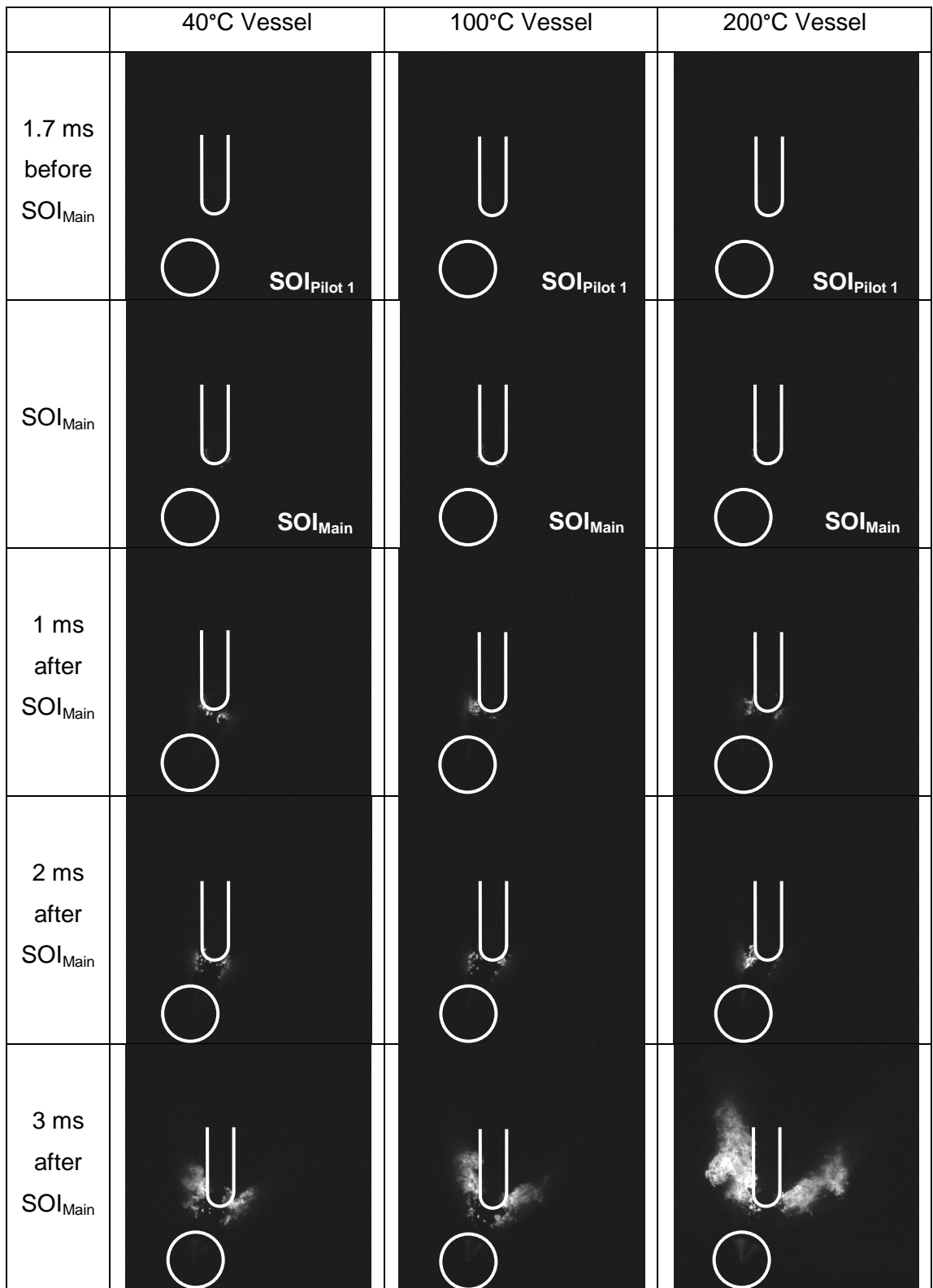
**Figure 3-19. Dependency of indicators on glow plug and vessel temperature for a single-pilot strategy [2,18] mg. Conditions: 35 bar vessel pressure, 200 bar rail pressure, 1.7 ms separation**

Figures



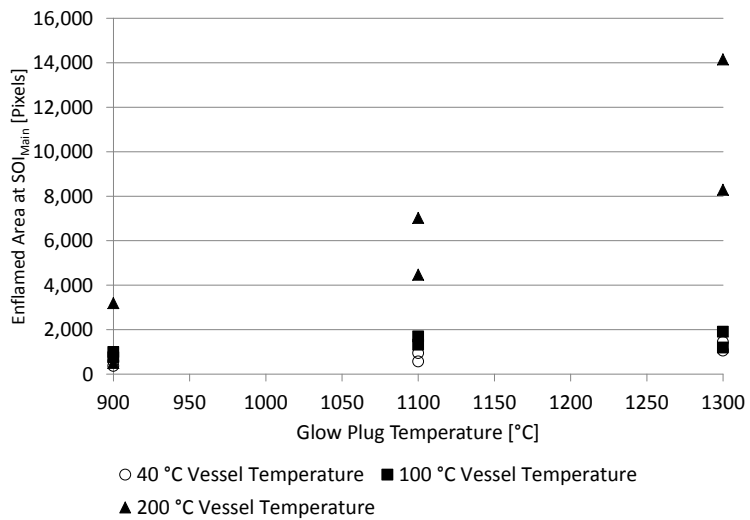
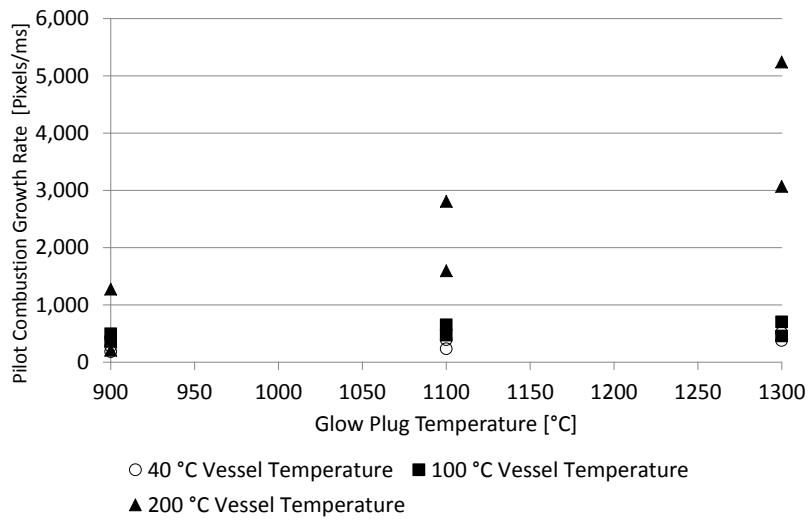
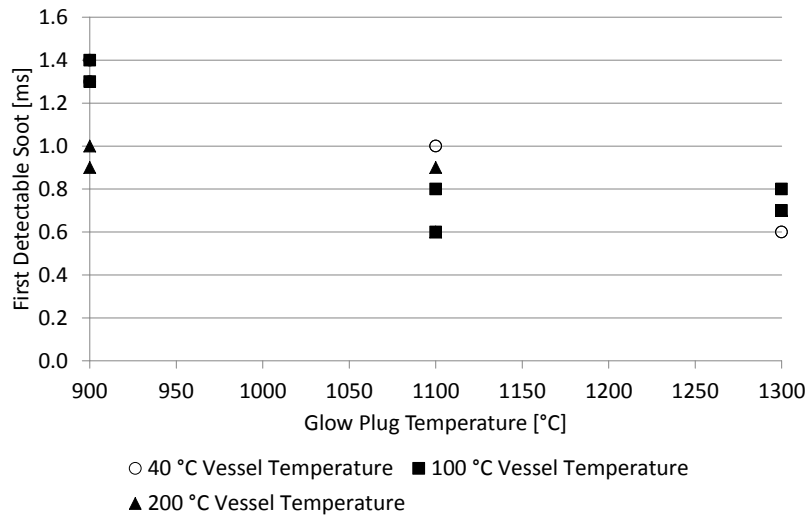
**Figure 3-20. Combustion initiation evolution for different glow plug temperatures using a single-pilot strategy [2,18] mg. Conditions: 35 bar vessel pressure, 100°C vessel temperature, 200 bar rail pressure, 1.7 ms separation**

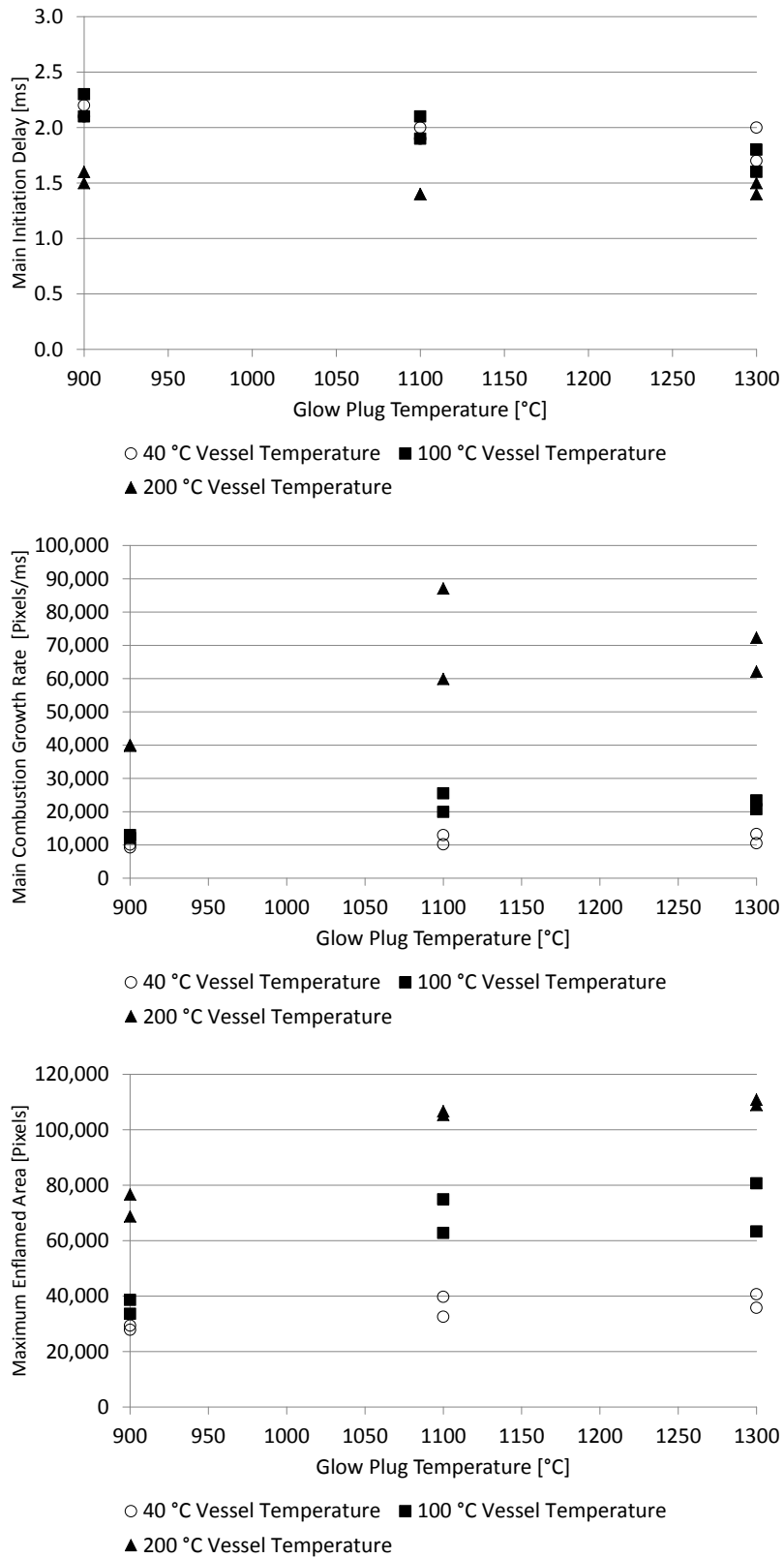
Figures



**Figure 3-21. Combustion initiation evolution for different vessel temperatures using a single-pilot strategy [2,18] mg. Conditions: 35 bar vessel pressure, 900°C glow plug, 200 bar rail pressure, 1.7 ms separation**

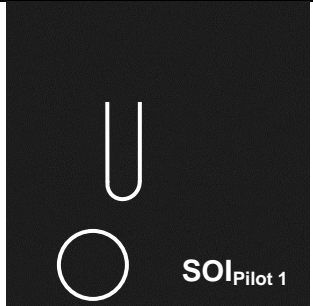
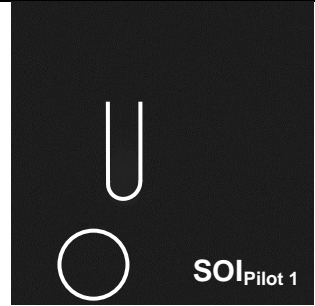
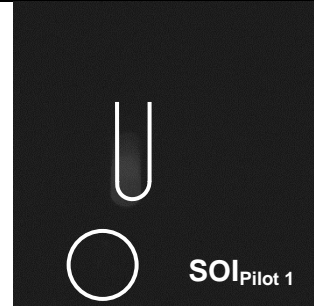
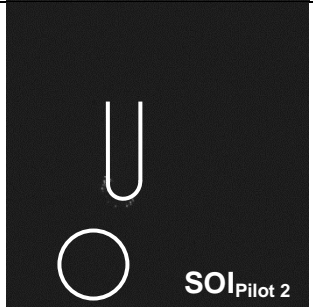
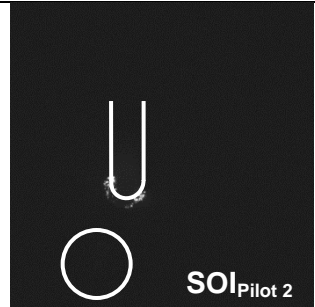
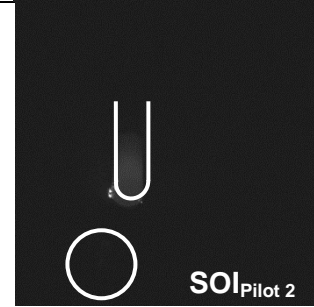
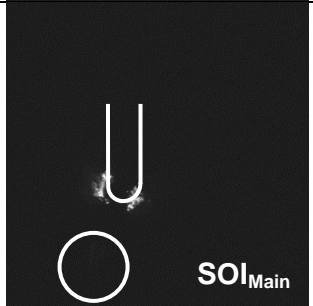

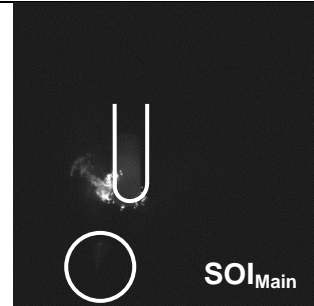
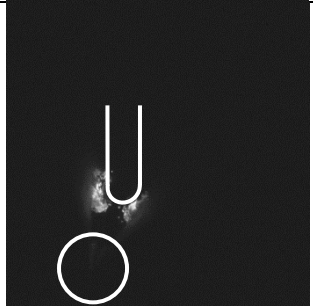
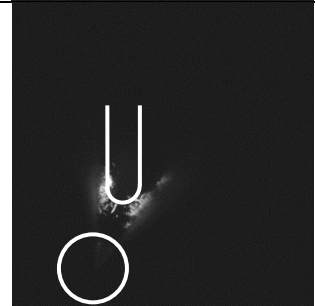
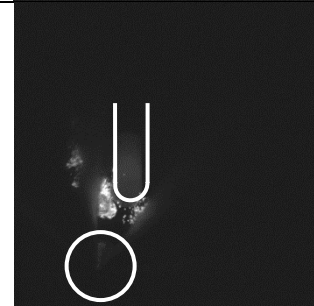
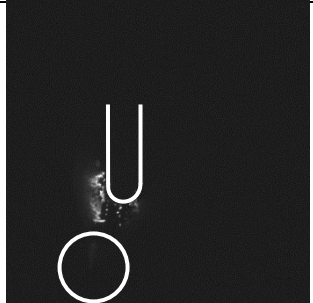
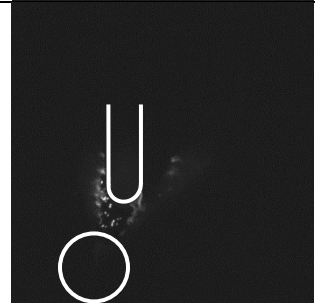
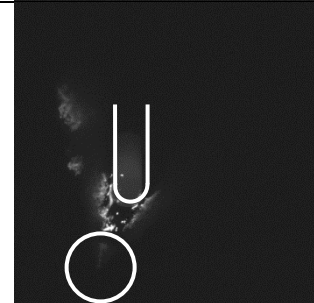
Figures





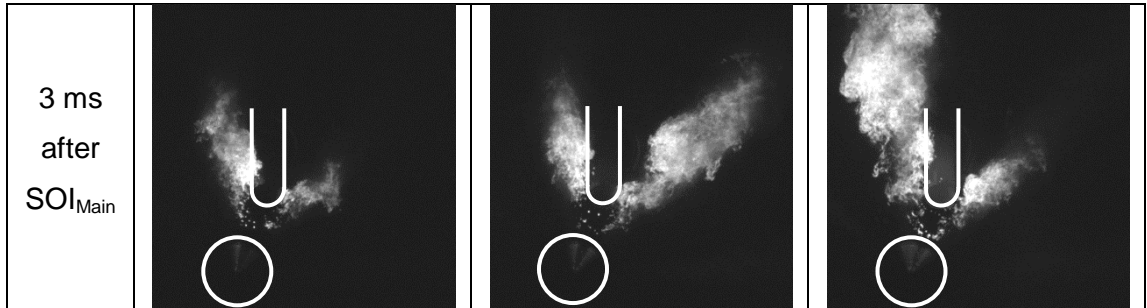
**Figure 3-22. Dependency of indicators on glow plug and vessel temperature for a twin-pilot strategy [2,2,16] mg. Conditions: 35 bar vessel pressure, 200 bar rail pressure, 1.7 ms separation**

Figures

	900°C Glow Plug	1100°C Glow Plug	1300°C Glow Plug
3.3 ms before SOI <sub>Main</sub>			
1.7 ms before SOI <sub>Main</sub>			
SOI <sub>Main</sub>			
1 ms after SOI <sub>Main</sub>			
2 ms after SOI <sub>Main</sub>			

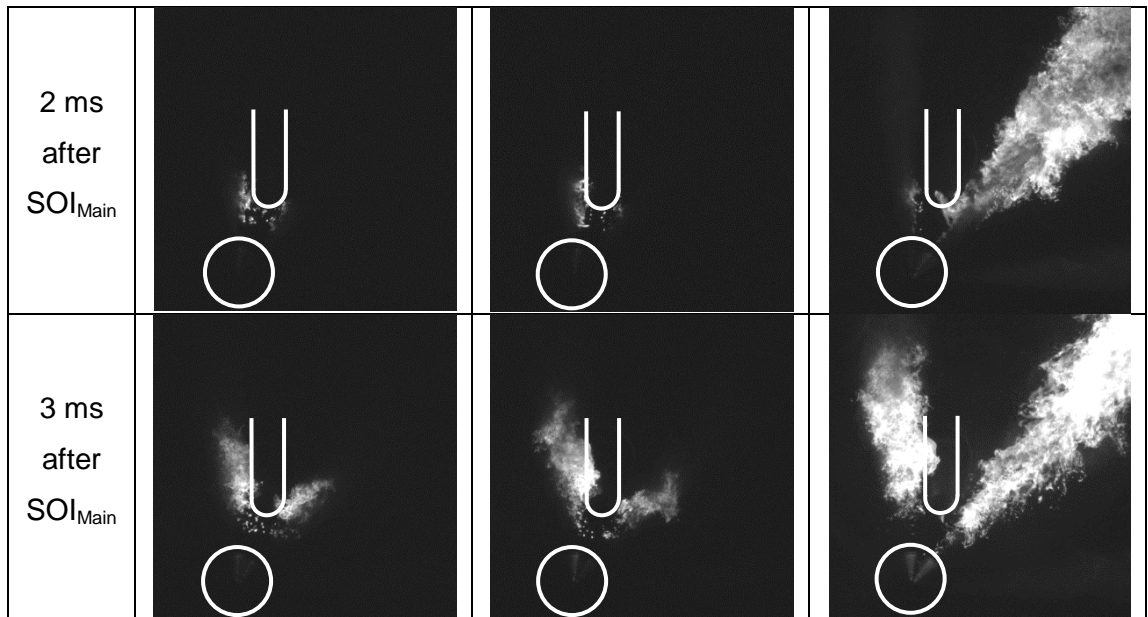


Figures

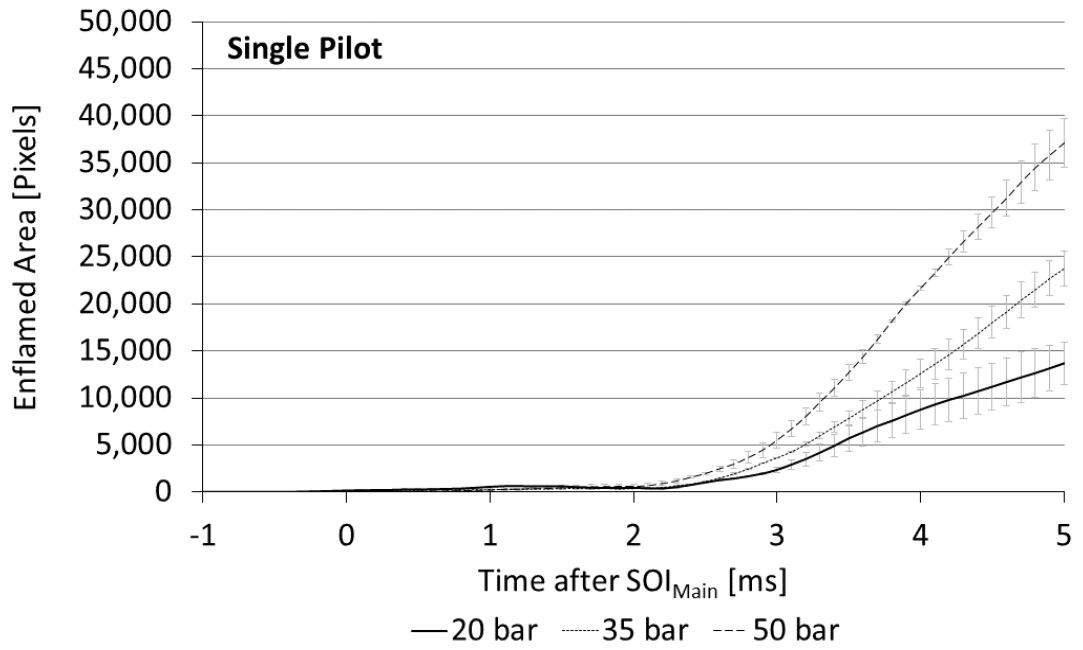


**Figure 3-23. Combustion initiation evolution for different glow plug temperatures using a twin-pilot strategy [2,2,16] mg. Conditions: 35 bar vessel pressure, 100°C vessel temperature, 200 bar rail pressure, 1.7 ms separation**

	40°C Vessel	100°C Vessel	200°C Vessel
3.3 ms before SOI <sub>Main</sub>			
1.7 ms before SOI <sub>Main</sub>			
SOI <sub>Main</sub>			
1 ms after SOI <sub>Main</sub>			



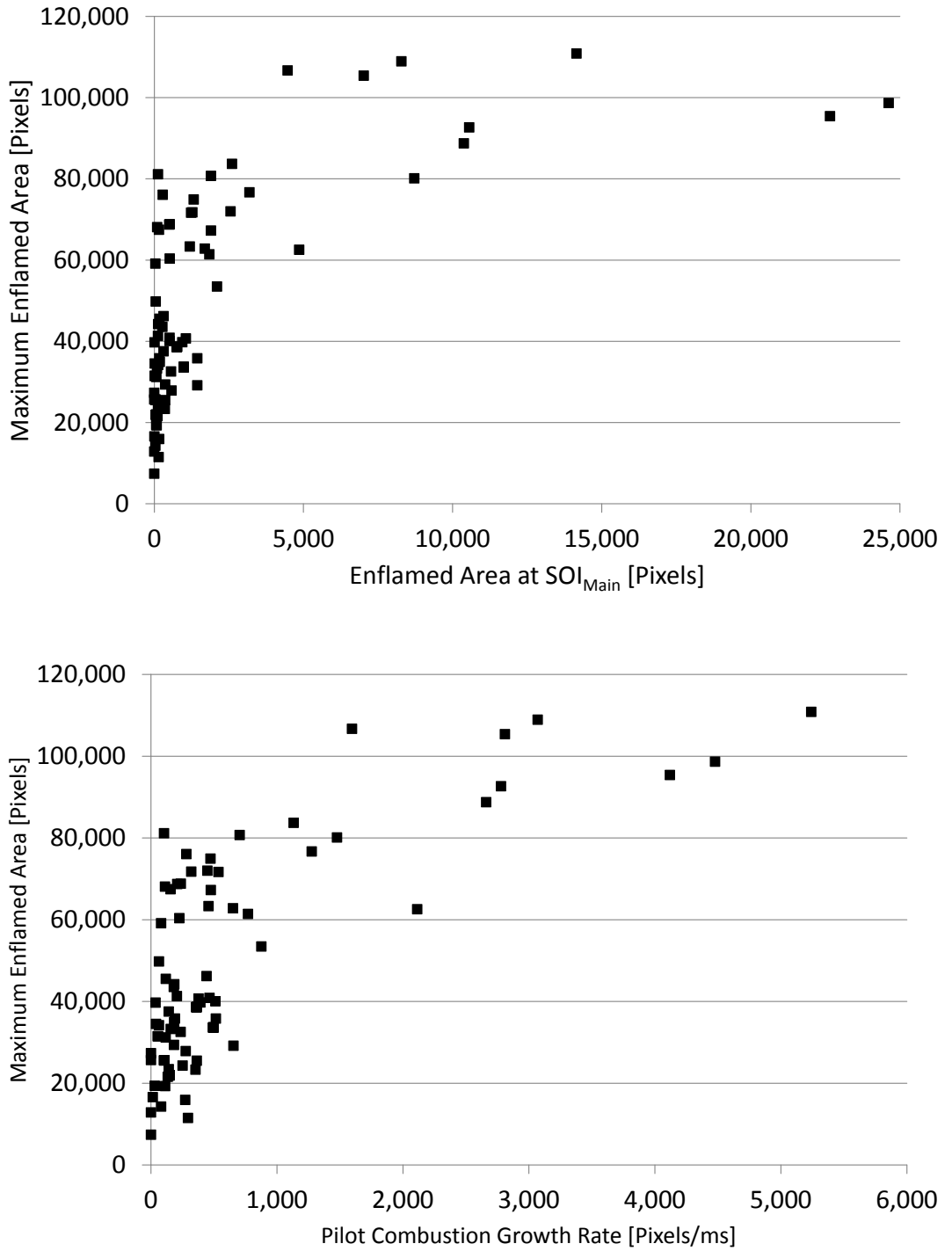
**Figure 3-24. Combustion initiation evolution for different vessel temperatures using a twin-pilot strategy [2,2,16] mg. Conditions: 35 bar vessel pressure, 900°C glow plug, 200 bar rail pressure, 1.7 ms separation**



**Figure 3-25. Influence of vessel pressure on enflamed area for a single-pilot strategy. Conditions: 20 mg total fuelling, 100°C vessel temperature, 900°C glow plug, 200 bar rail pressure, 1.7 ms separation**

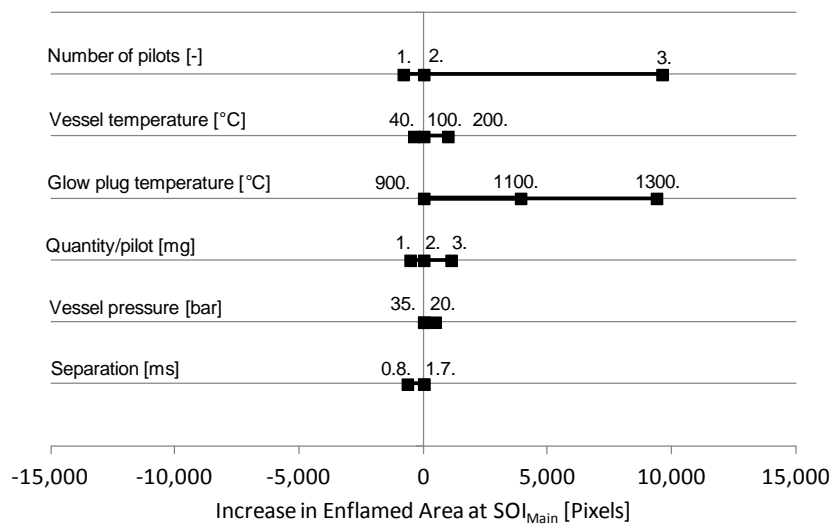
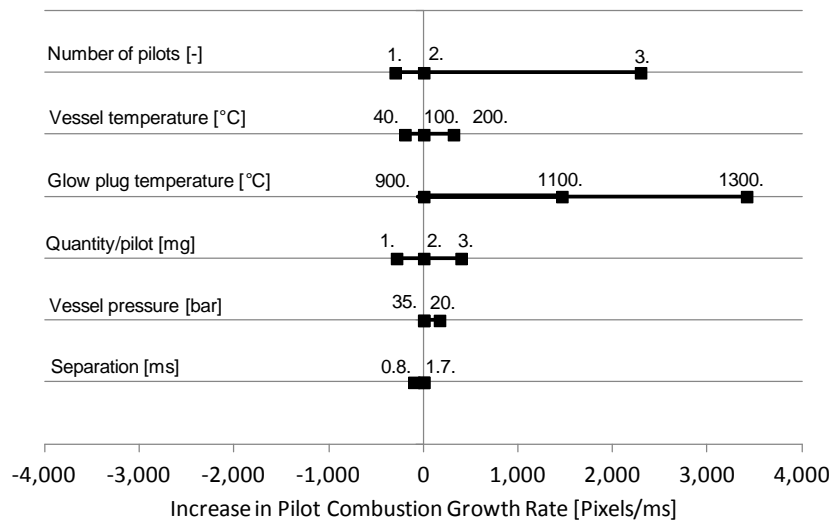
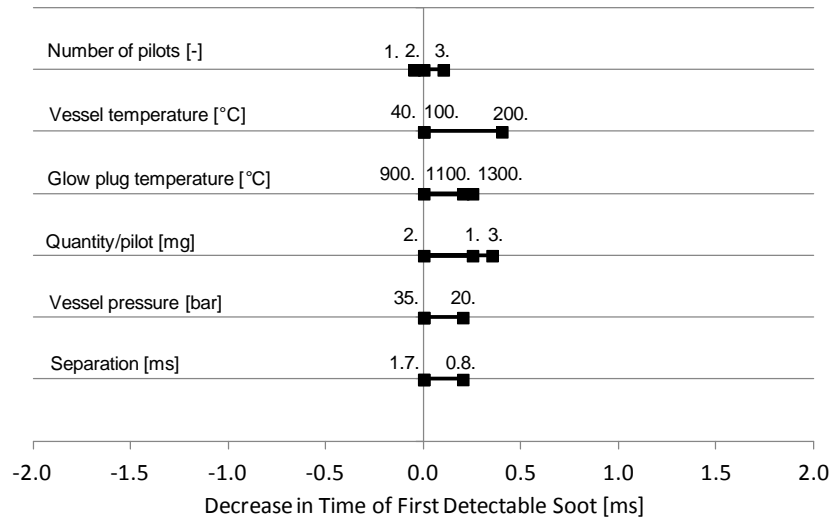


**Figure 3-26. Influence of vessel pressure on enflamed area for a twin-pilot strategy. Conditions: 20 mg total fuelling, 100°C vessel temperature, 900°C glow plug, 200 bar rail pressure, 1.7 ms separation**

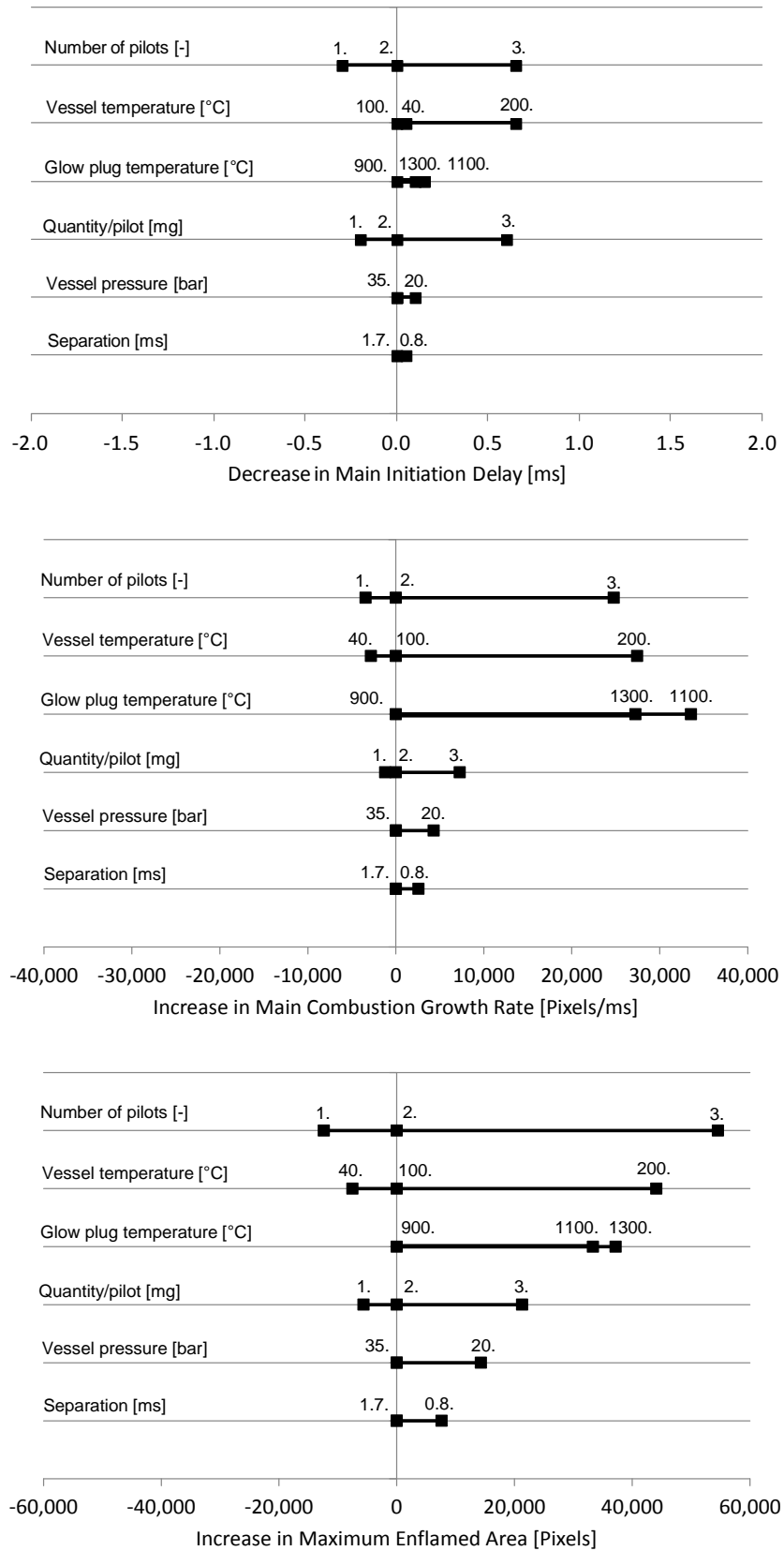


**Figure 3-27. Dependency of the maximum enflamed area on enflamed area at SOI<sub>Main</sub> and the growth rate of the enflamed area of the pilots**

# Figures



# Figures



**Figure 3-28. The effect of a change in each parameter on the indicators**

# Chapter 4



Figure 4-1. Single cylinder engine rig

## Figures

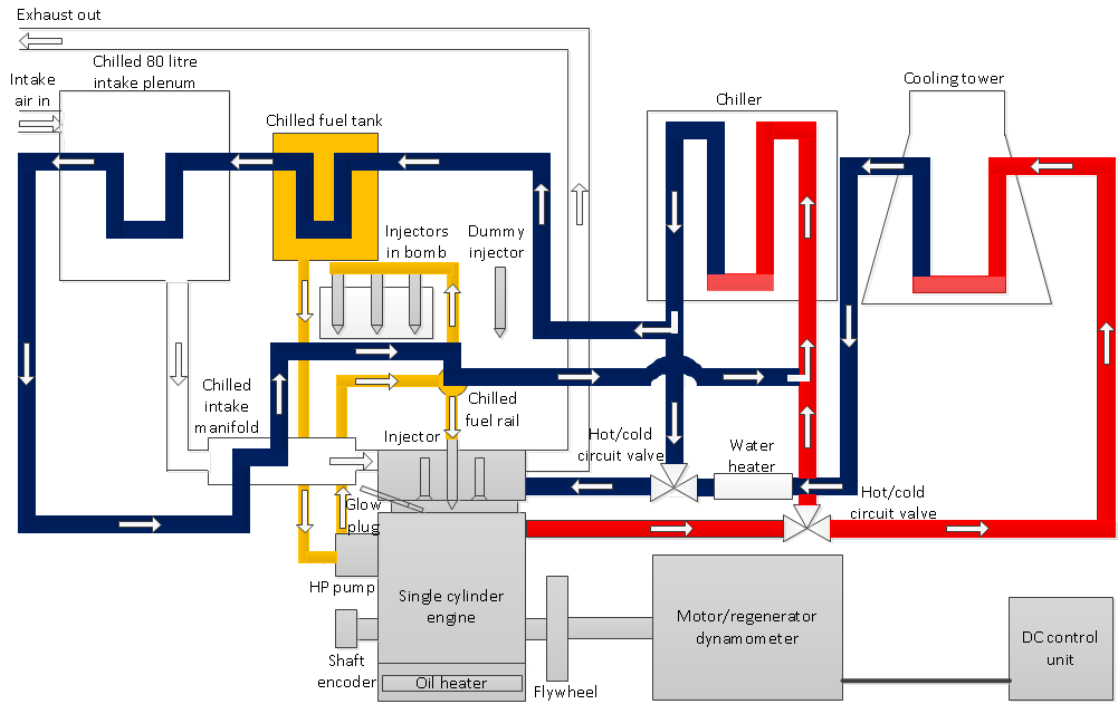


Figure 4-2. Coolant flow circuit

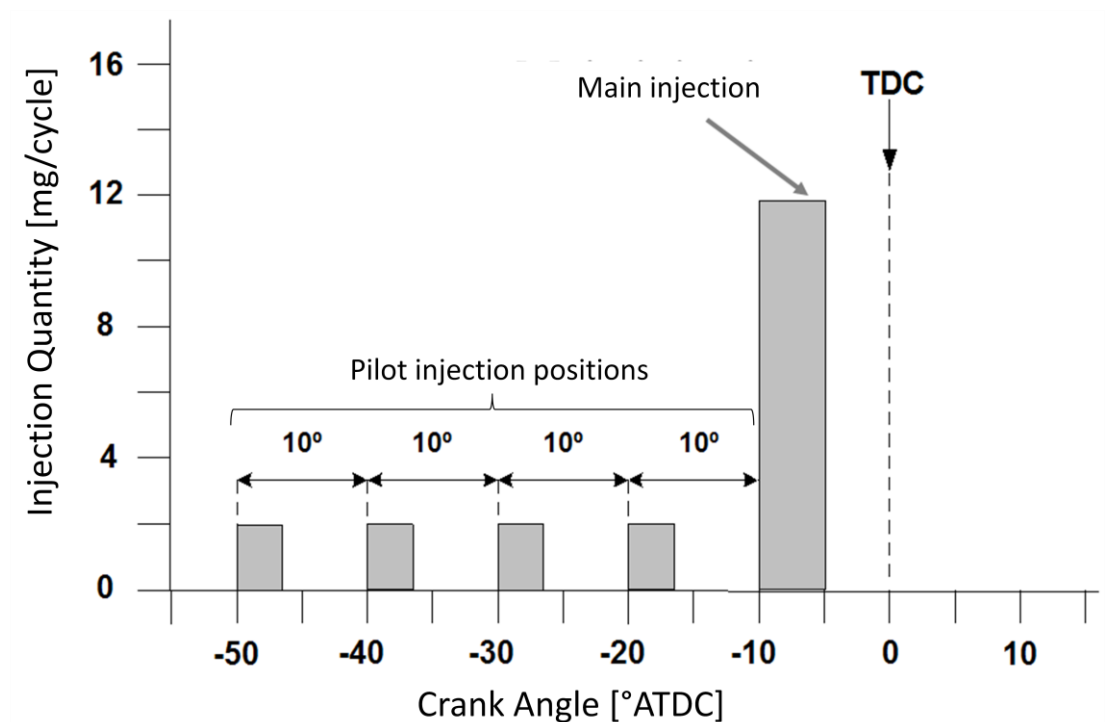


Figure 4-3. Form of injection strategy



## Figures

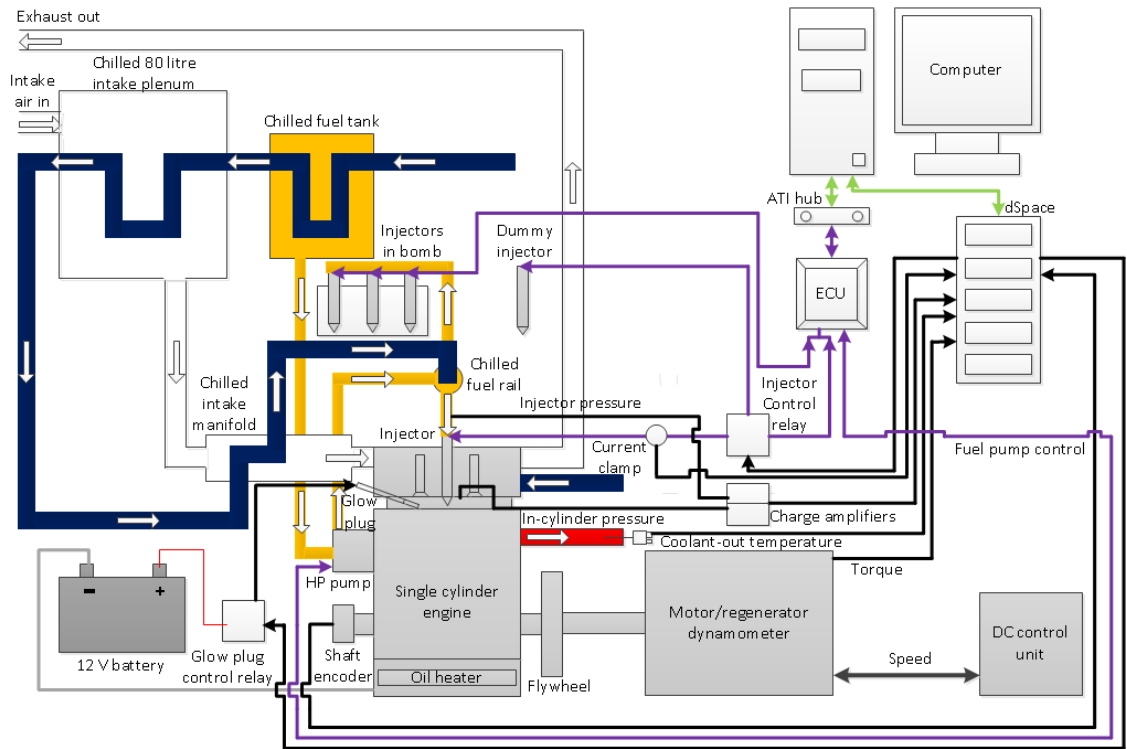


Figure 4-4. Electrical signal rig architecture

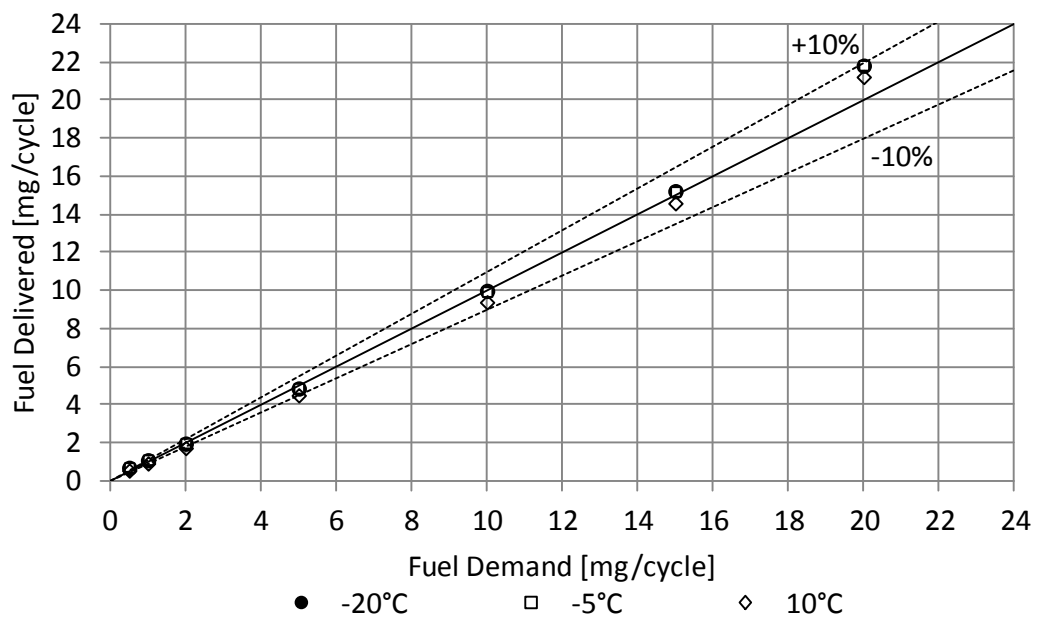
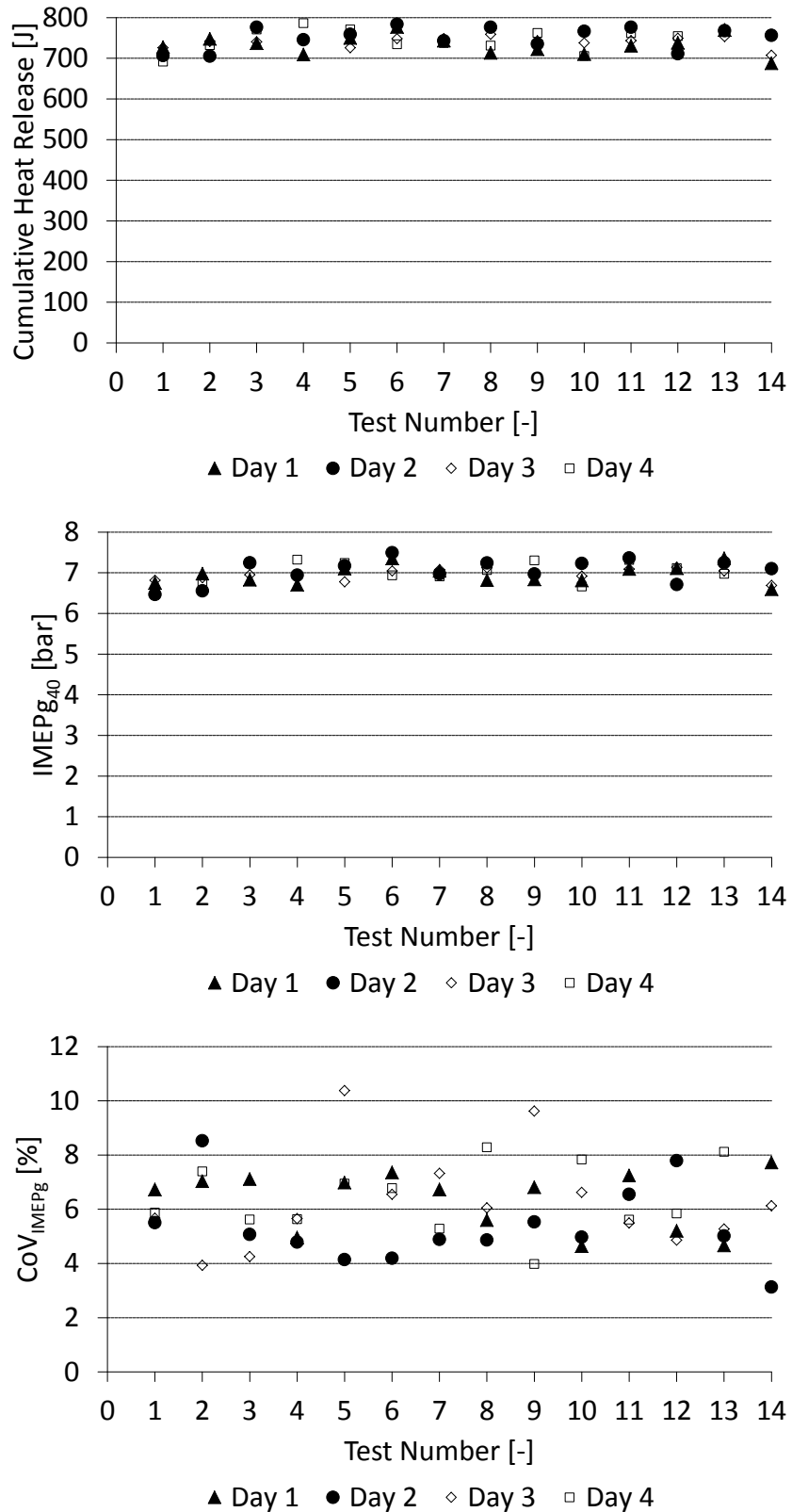
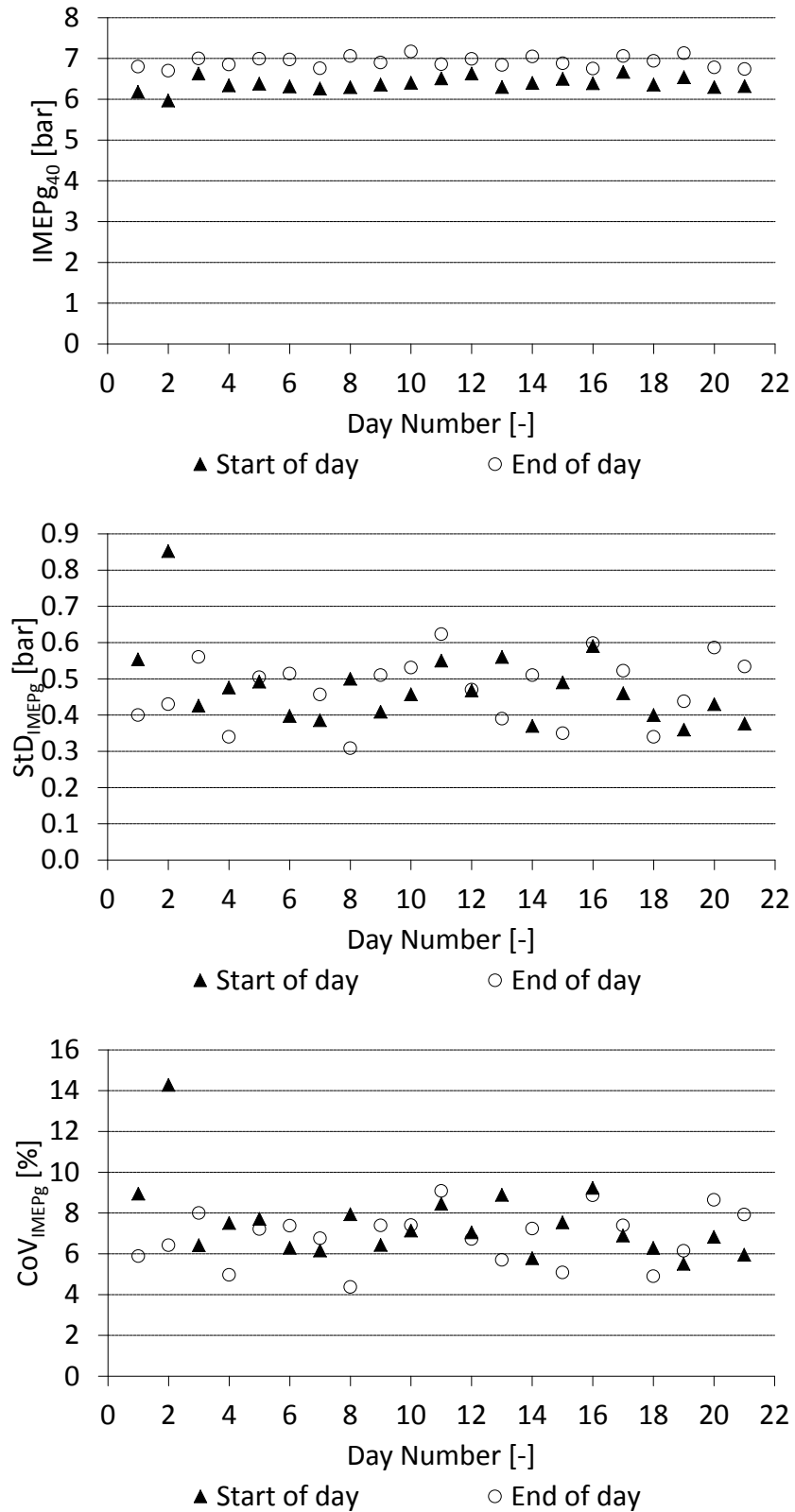


Figure 4-5. Fuelling tests at three soak temperatures



**Figure 4-6. Test-to-test repeatability through the day over four separate days. Conditions: -20°C, SOI<sub>Main</sub> = -4 °ATDC, [2, 2, 2, 18] mg/cycle, 10 °CA separation, 1000 rev/min, 400 bar rail pressure, 850°C glow plug, 24 mg/cycle total fuel**



**Figure 4-7. Long term repeatability of tests at the start and end of the day. Conditions: -20°C, SOI<sub>Main</sub> = -4 °ATDC, [2, 2, 2, 18] mg/cycle, 10 °CA separation, 1000 rev/min, 400 bar rail pressure, 850°C glow plug, 24 mg/cycle total fuel**

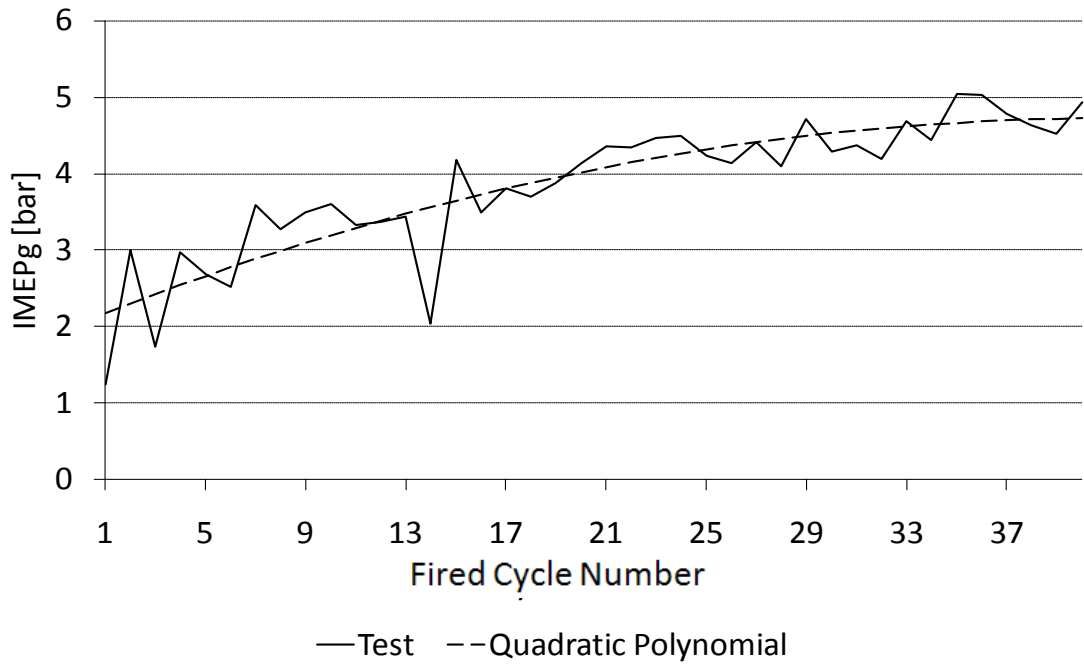


Figure 4-8.  $StD_{IMEPg}$  defined as a deviation from a trend line of best fit

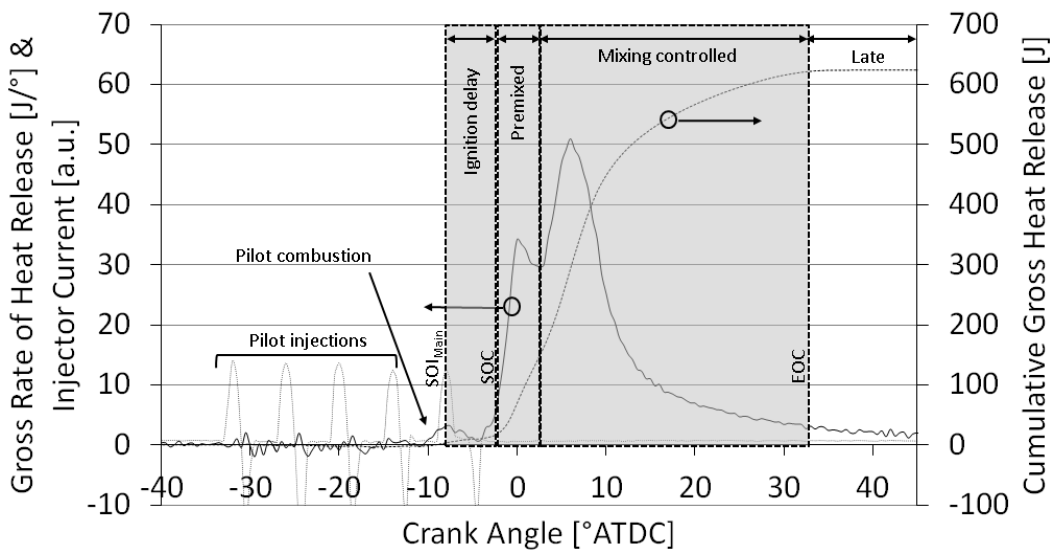
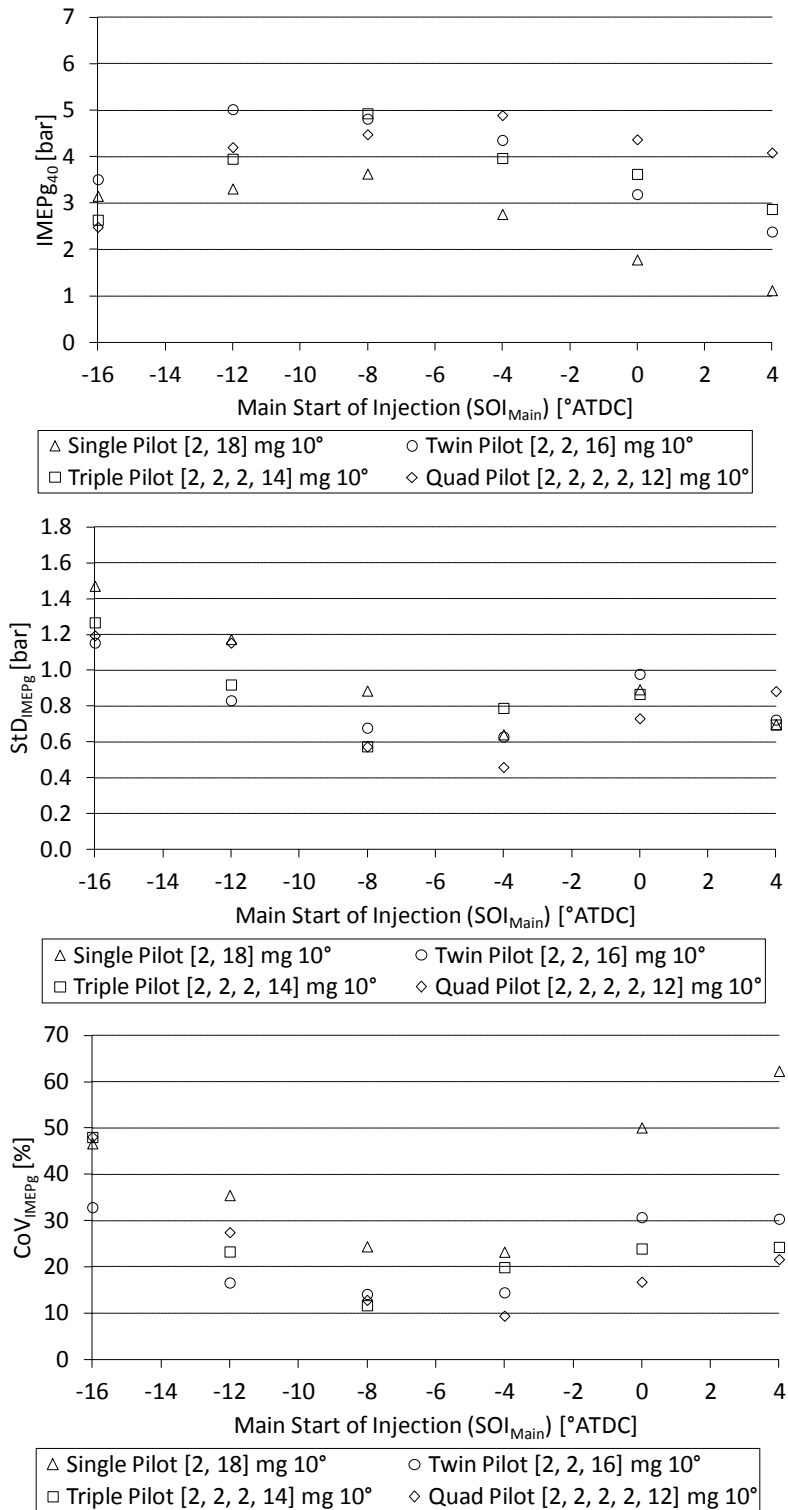
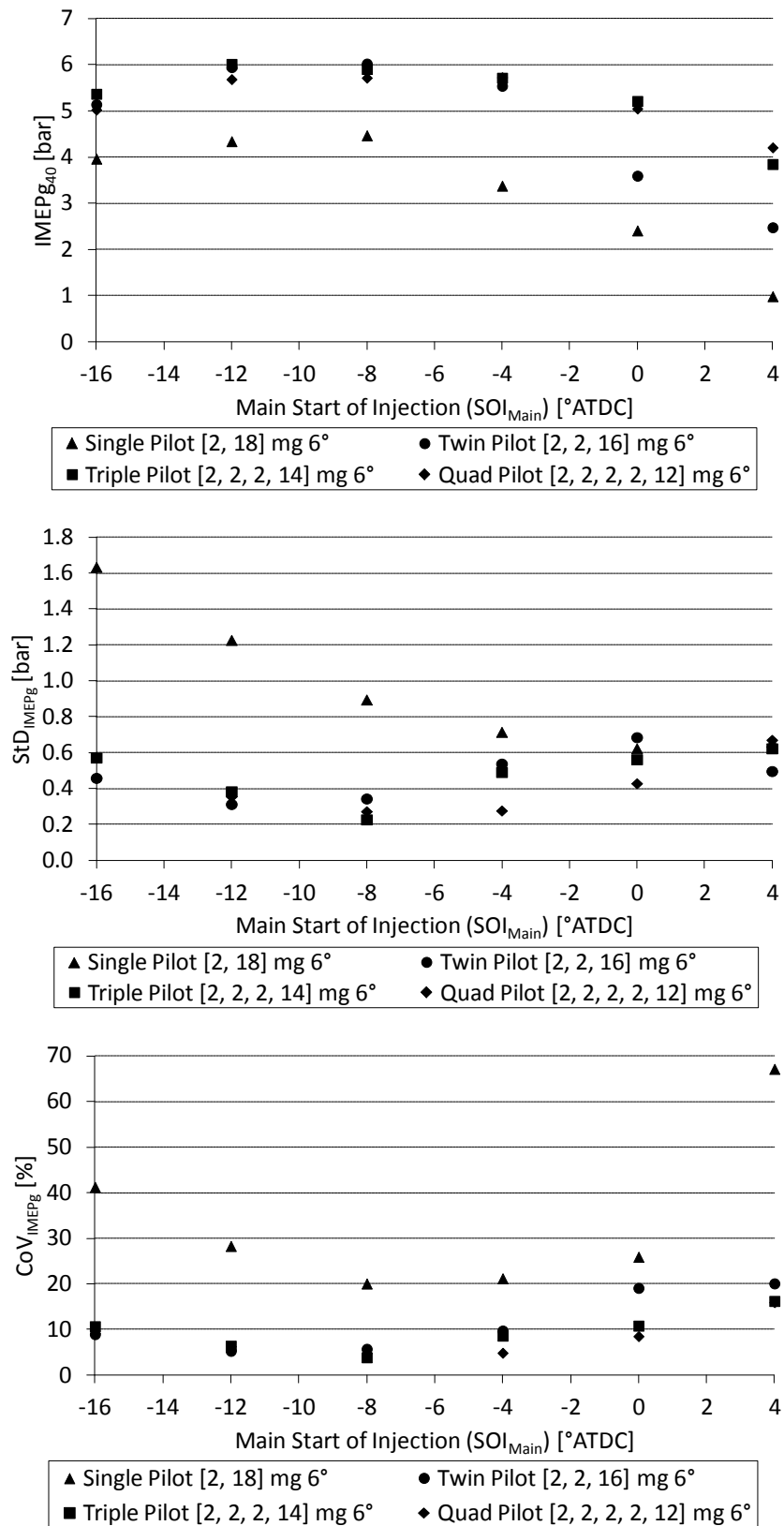


Figure 4-9. Heat release profile illustrating the important phases of combustion for a quad-pilot injection strategy

# Chapter 5



**Figure 5-1. Effect of main injection timing on IMEP<sub>g40</sub>, StD<sub>IMEPg</sub> and CoV<sub>IMEPg</sub> at 10 °CA separation. Conditions: -20 °C, 1000 rev/min, 400 bar rail pressure, 850°C glow plug, 20 mg/cycle total fuel**



**Figure 5-2. Effect of main injection timing on IMEP<sub>g40</sub>, StD<sub>IMEPg</sub> and CoV<sub>IMEPg</sub> at 6 °CA separation. Conditions: -20 °C, 1000 rev/min, 400 bar rail pressure, 850°C glow plug, 20 mg/cycle total fuel**

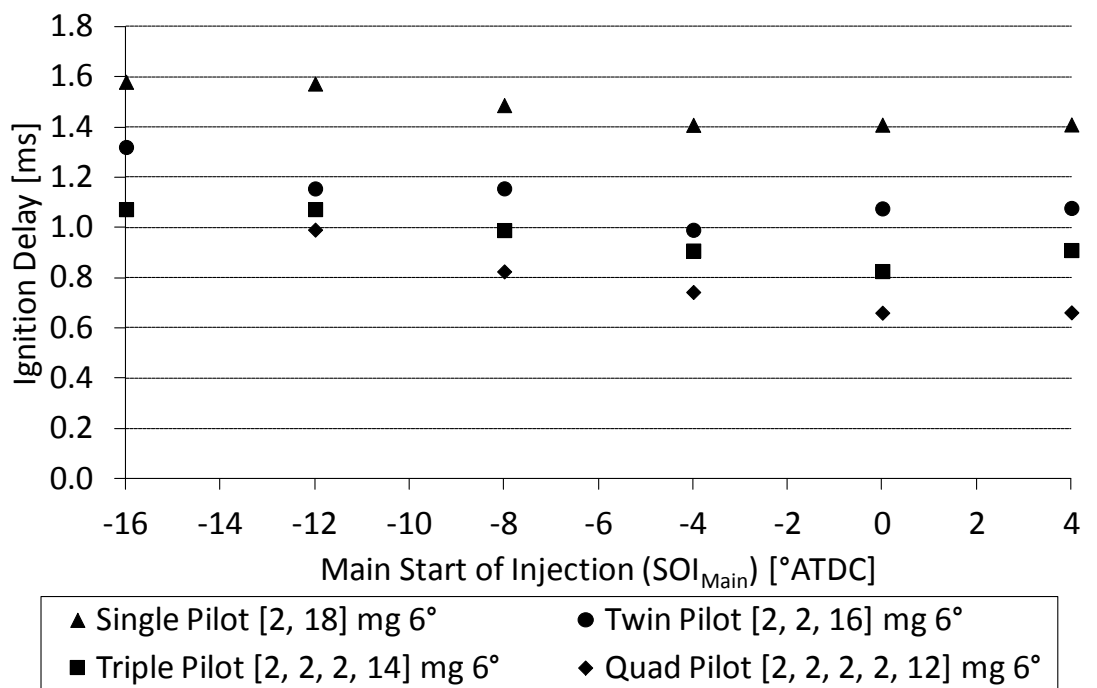
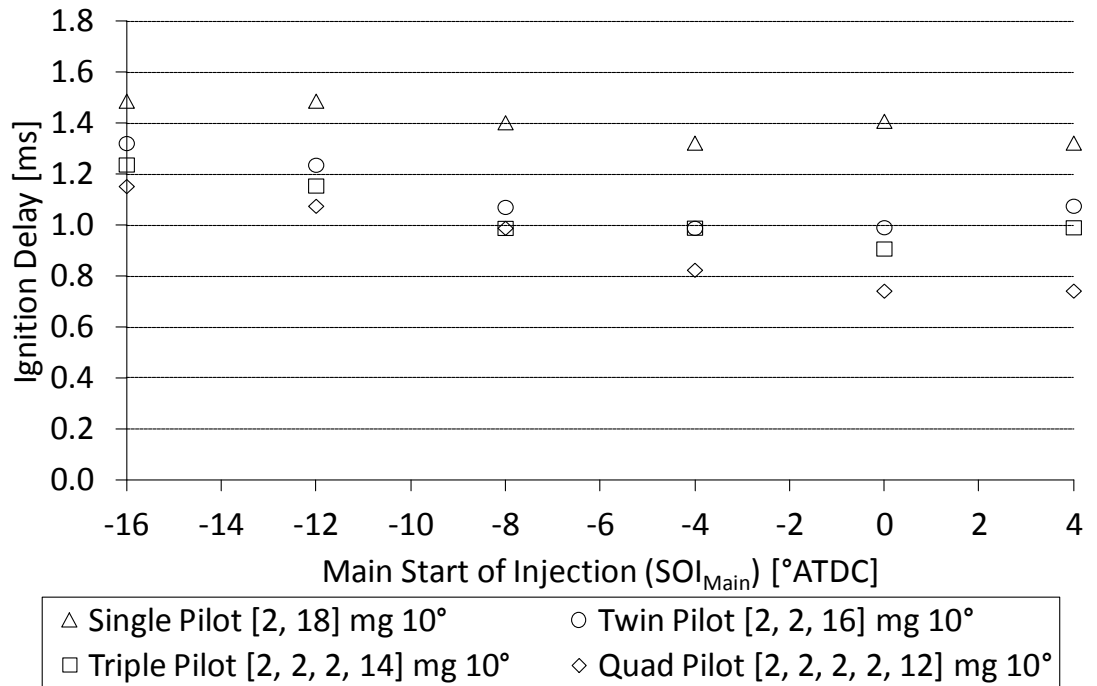


Figure 5-3. Effect of main injection timing on ignition delay (top) 10 °CA separation (bottom) 6 °CA separation. Conditions: -20 °C, 1000 rev/min, 400 bar rail pressure, 850°C glow plug, 20 mg/cycle total fuel

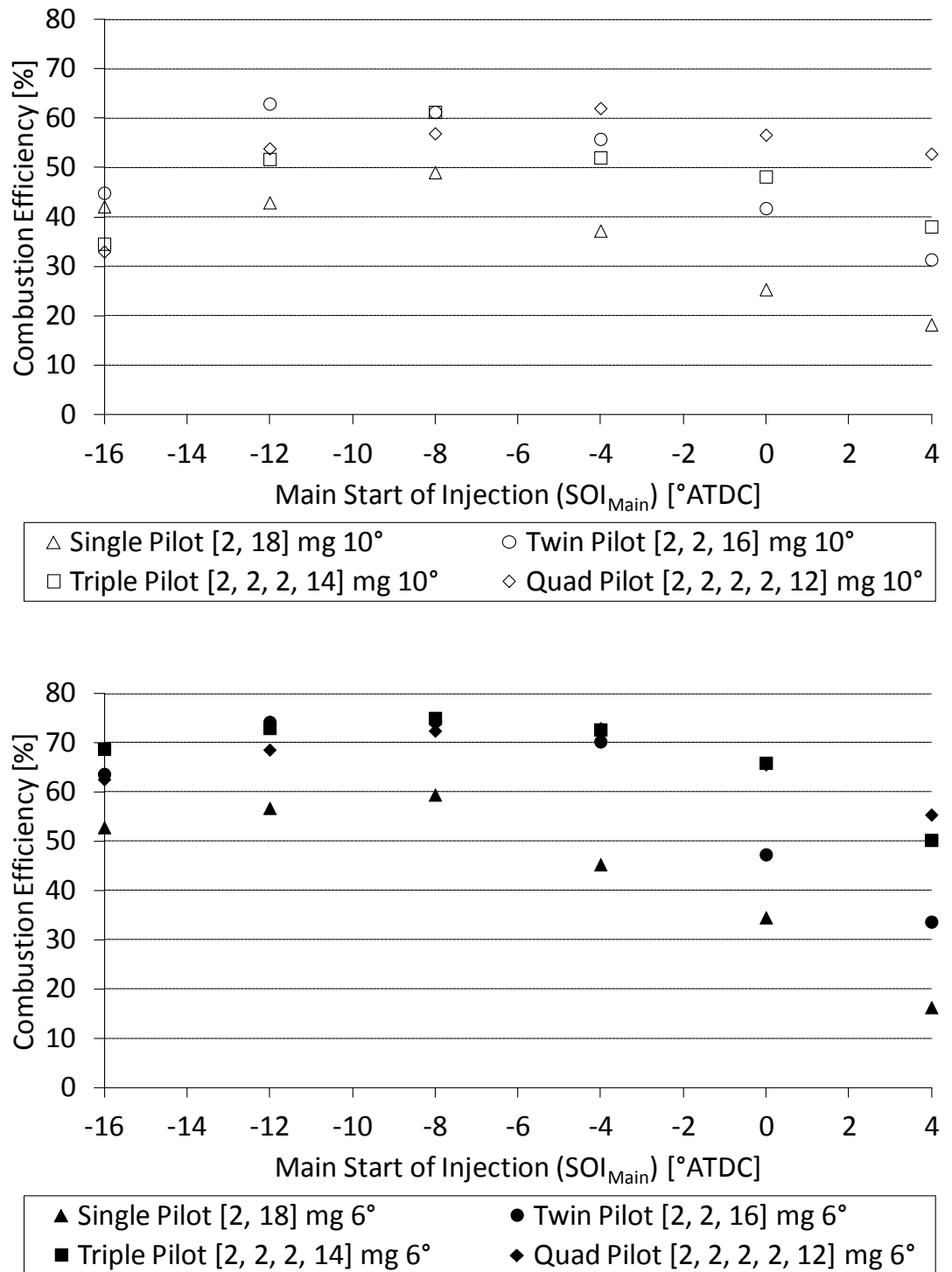


Figure 5-4. Effect of main injection timing on indicated combustion efficiency (top) 10 °CA separation (bottom) 6 °CA separation. Conditions: -20 °C, 1000 rev/min, 400 bar rail pressure, 850°C glow plug, 20 mg/cycle total fuel



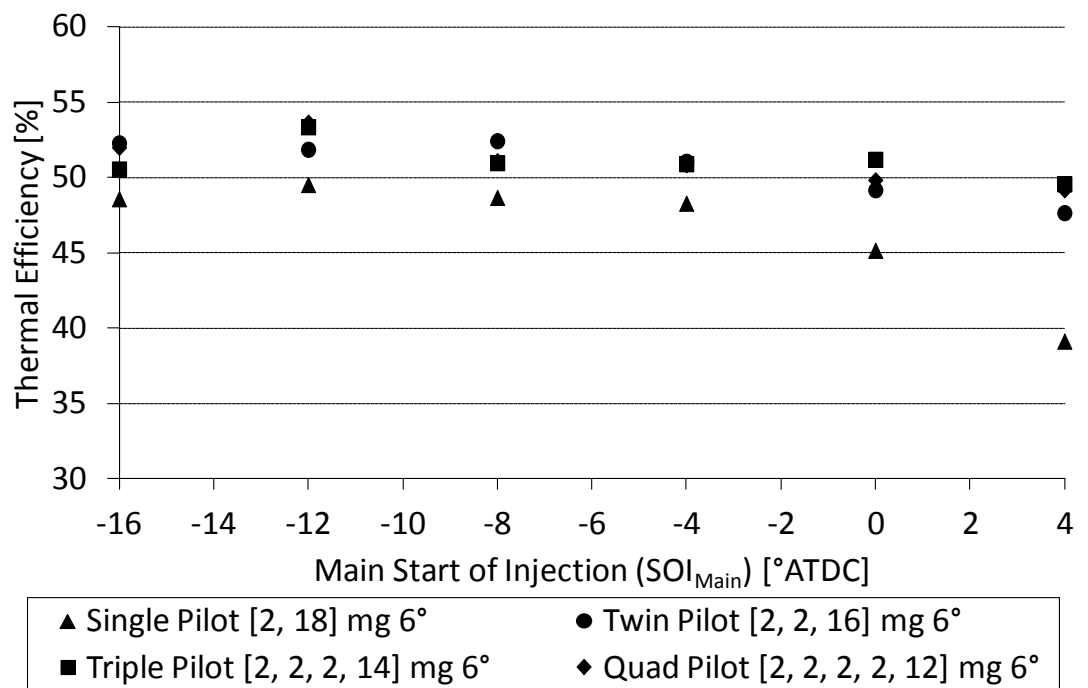
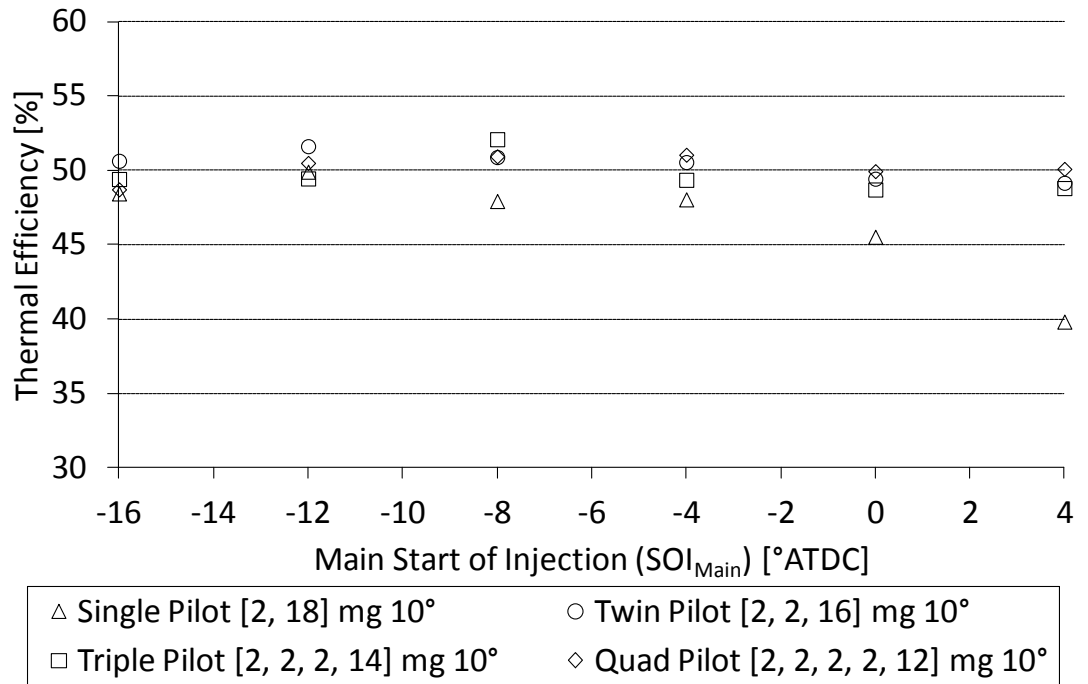


Figure 5-5. Effect of main injection timing on indicated thermal efficiency (top) 10 °CA separation (bottom) 6 °CA separation. Conditions: -20 °C, 1000 rev/min, 400 bar rail pressure, 850°C glow plug, 20 mg/cycle total fuel

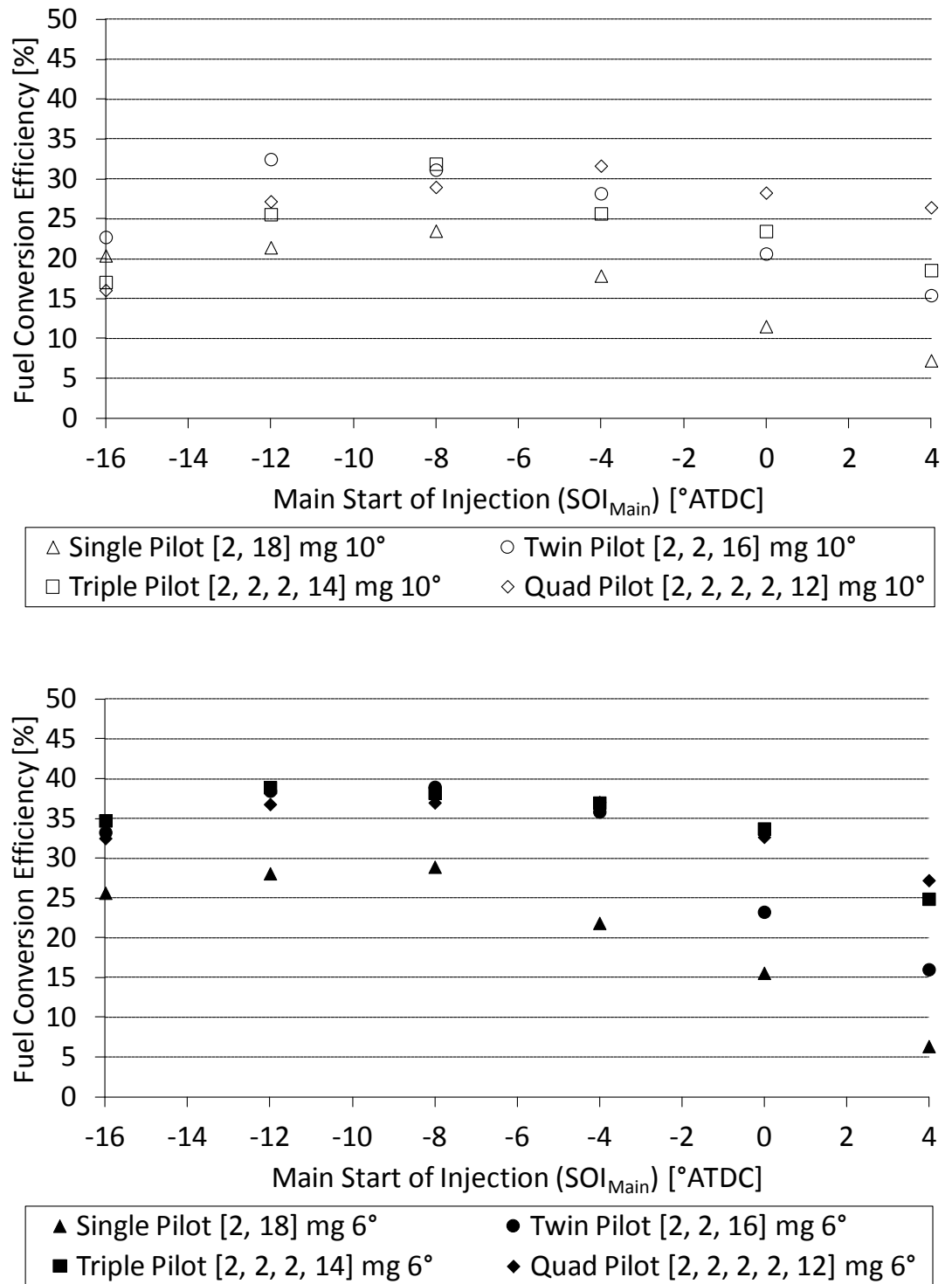


Figure 5-6. Effect of main injection timing on indicated fuel conversion efficiency (top) 10 °CA separation (bottom) 6 °CA separation. Conditions: -20 °C, 1000 rev/min, 400 bar rail pressure, 850°C glow plug, 20 mg/cycle total fuel

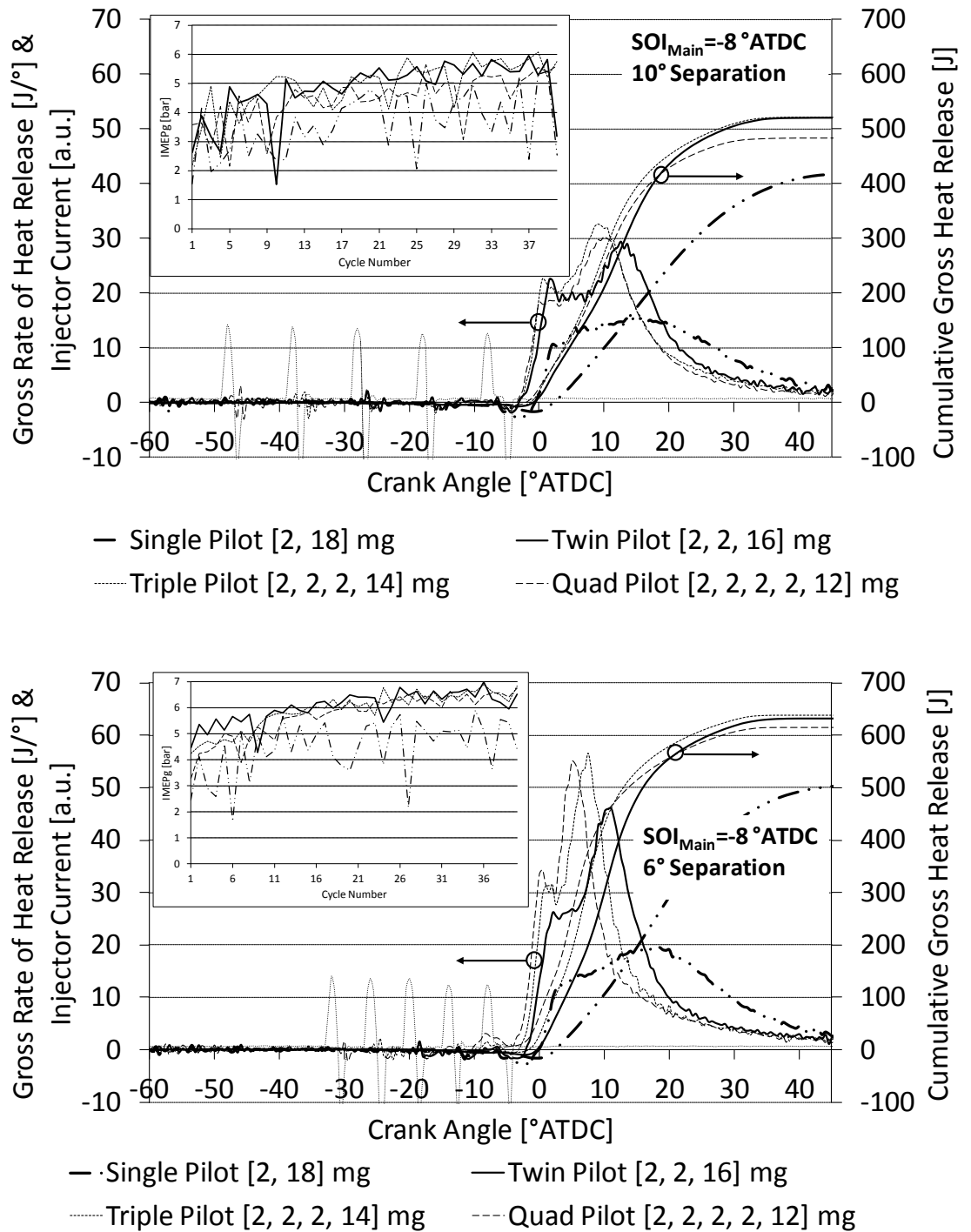


Figure 5-7. The effect of number of pilots on 40 cycle ensemble averaged heat release (top) 10 °CA separation and (bottom) 6 °CA separation. Conditions: -20 °C, SOI<sub>Main</sub> = -8 °ATDC, 1000 rev/min, 400 bar rail pressure, 850°C glow plug, 20 mg/cycle total fuel, injector current shown for quad-pilot case

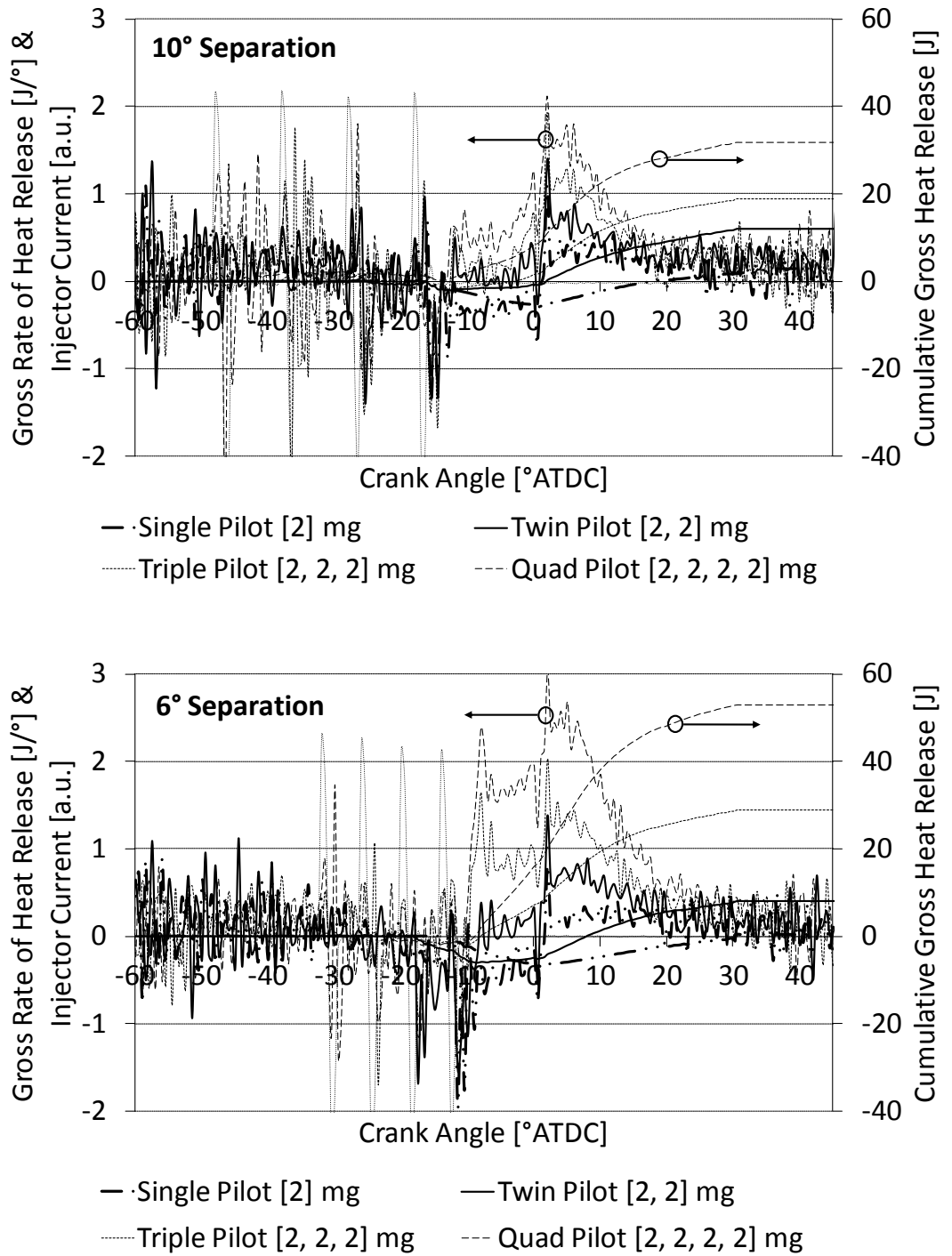


Figure 5-8. 40 cycle ensemble averaged pilot heat release for  $SOI_{Main} = -8$  °ATDC (top) 10 °CA separation (bottom) 6 °CA separation. Conditions: -20 °C, 1000 rev/min, 400 bar rail pressure, 850°C glow plug, injektor current shown for quad-pilot case

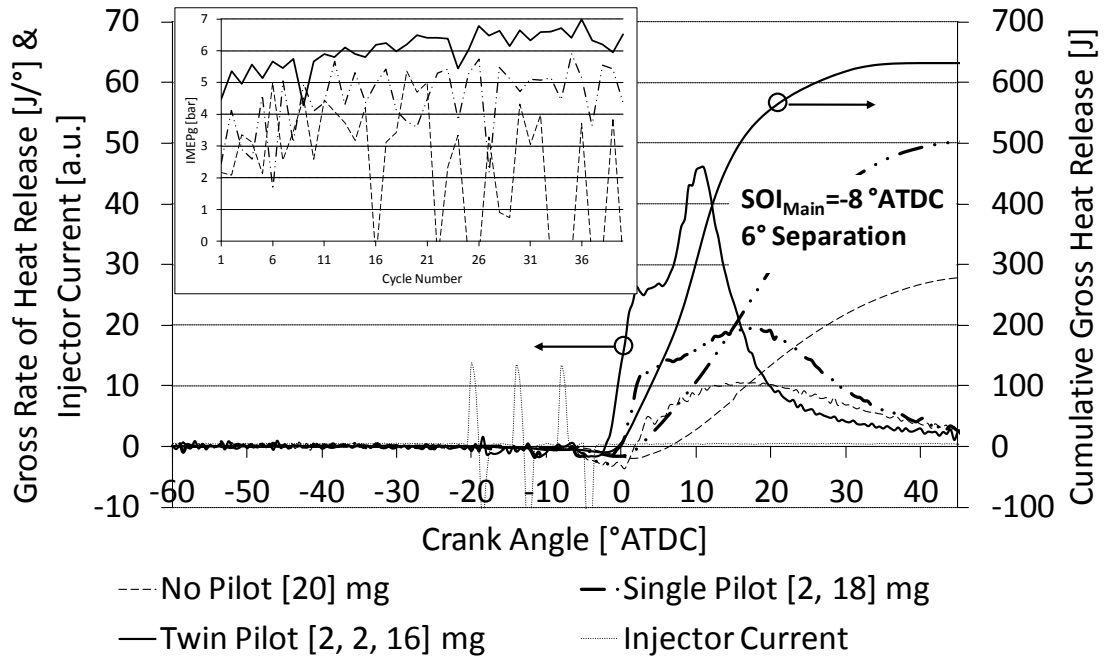


Figure 5-9. Comparison of a single main injection against single- and twin-pilot strategies at 6 °CA separation. Conditions: -20 °C, SOI<sub>Main</sub> = -8 °ATDC, 1000 rev/min, 400 bar rail pressure, 850°C glow plug, 20 mg/cycle total fuel, injector current shown for twin-pilot case

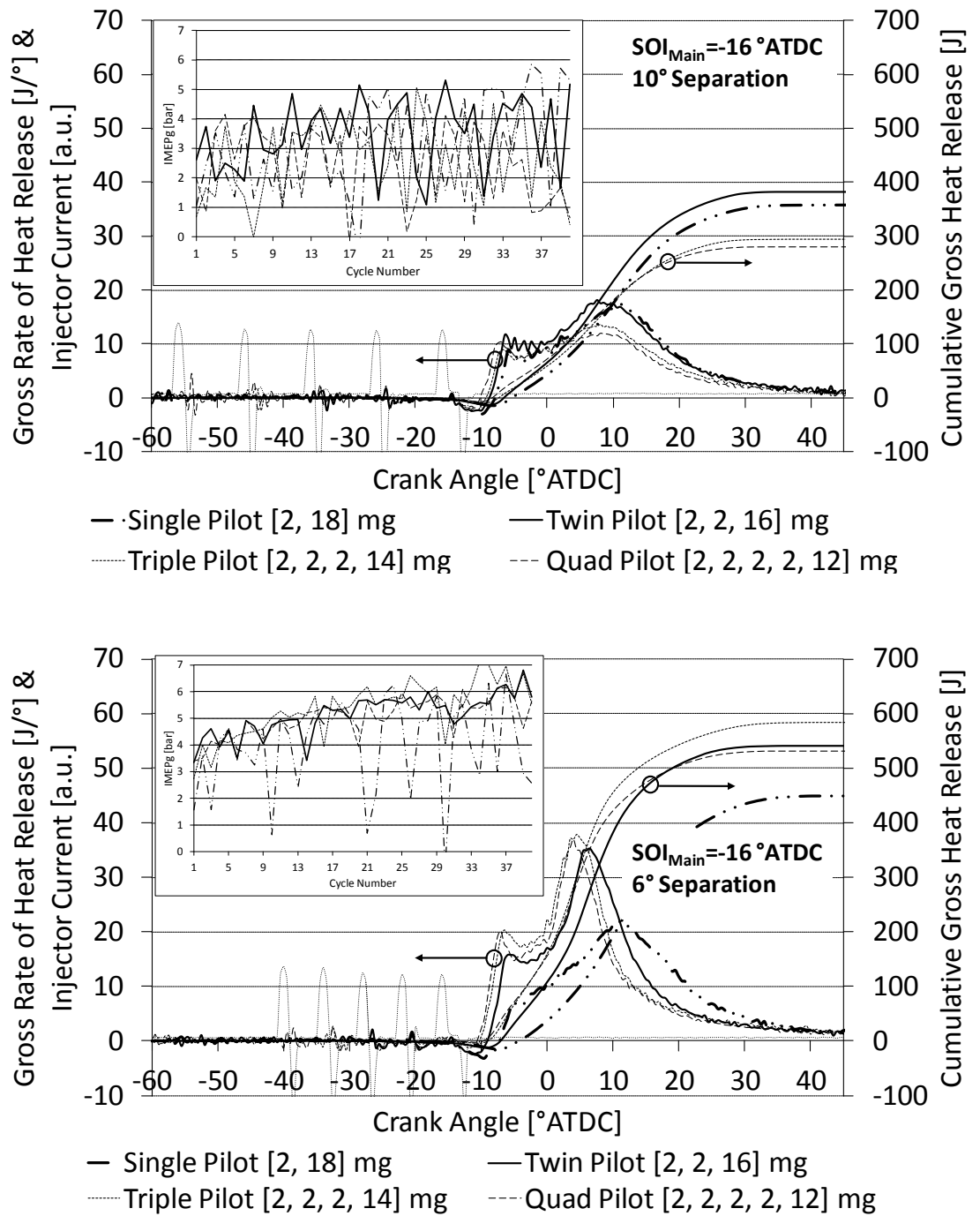


Figure 5-10. The effect of number of pilots on 40 cycle ensemble averaged heat release (top) 10 °CA separation and (bottom) 6 °CA separation. Conditions: -20 °C, SOI<sub>Main</sub> = -16 °ATDC, 1000 rev/min, 400 bar rail pressure, 850°C glow plug, 20 mg/cycle total fuel, injector current shown for quad-pilot case

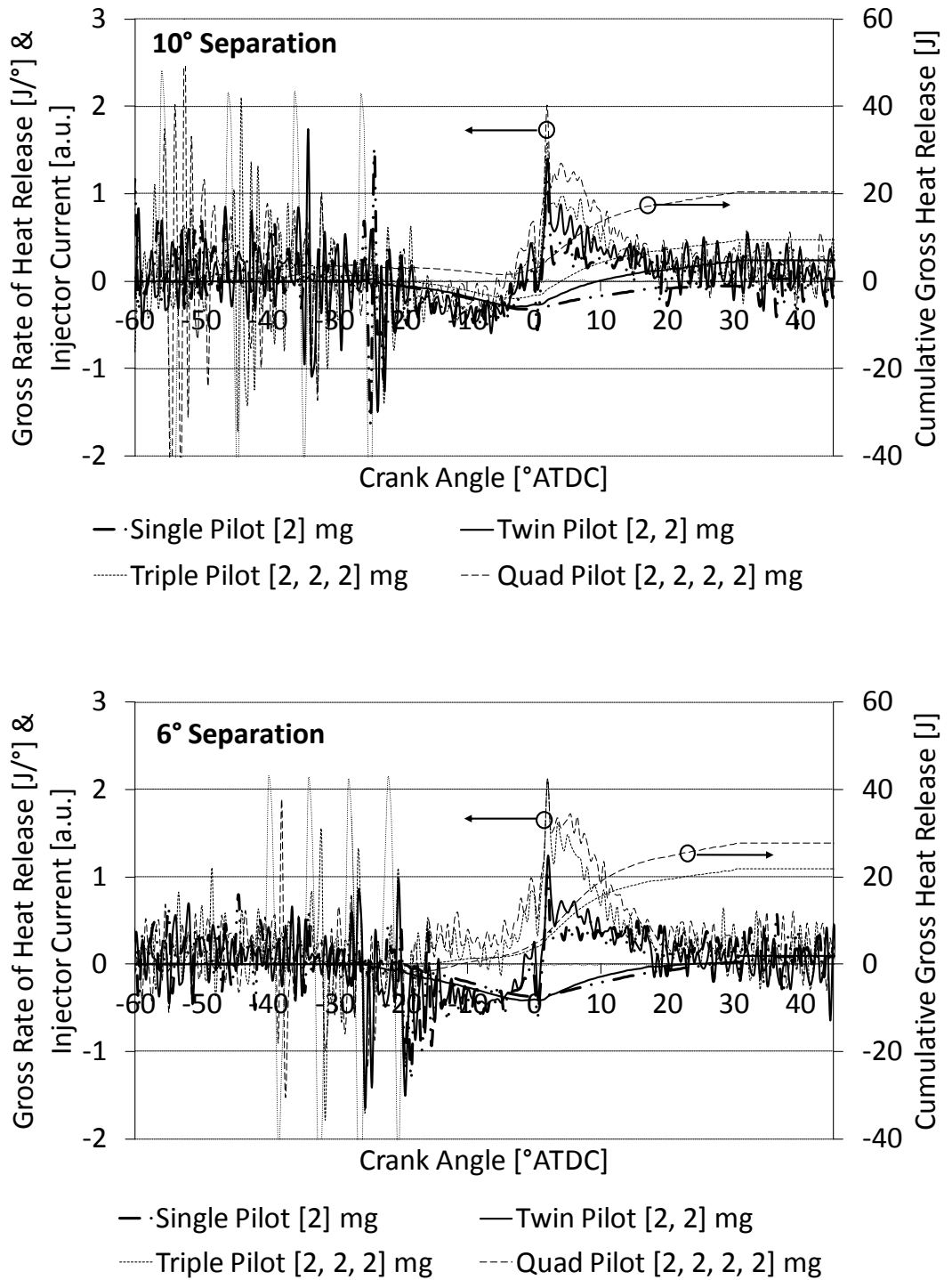


Figure 5-11. 40 cycle ensemble averaged pilot heat release for  $SOI_{Main} = -16$  °ATDC (top) 10 °CA separation (bottom) 6 °CA separation. Conditions: -20 °C, 1000 rev/min, 400 bar rail pressure, 850°C glow plug, injector current shown for quad-pilot case

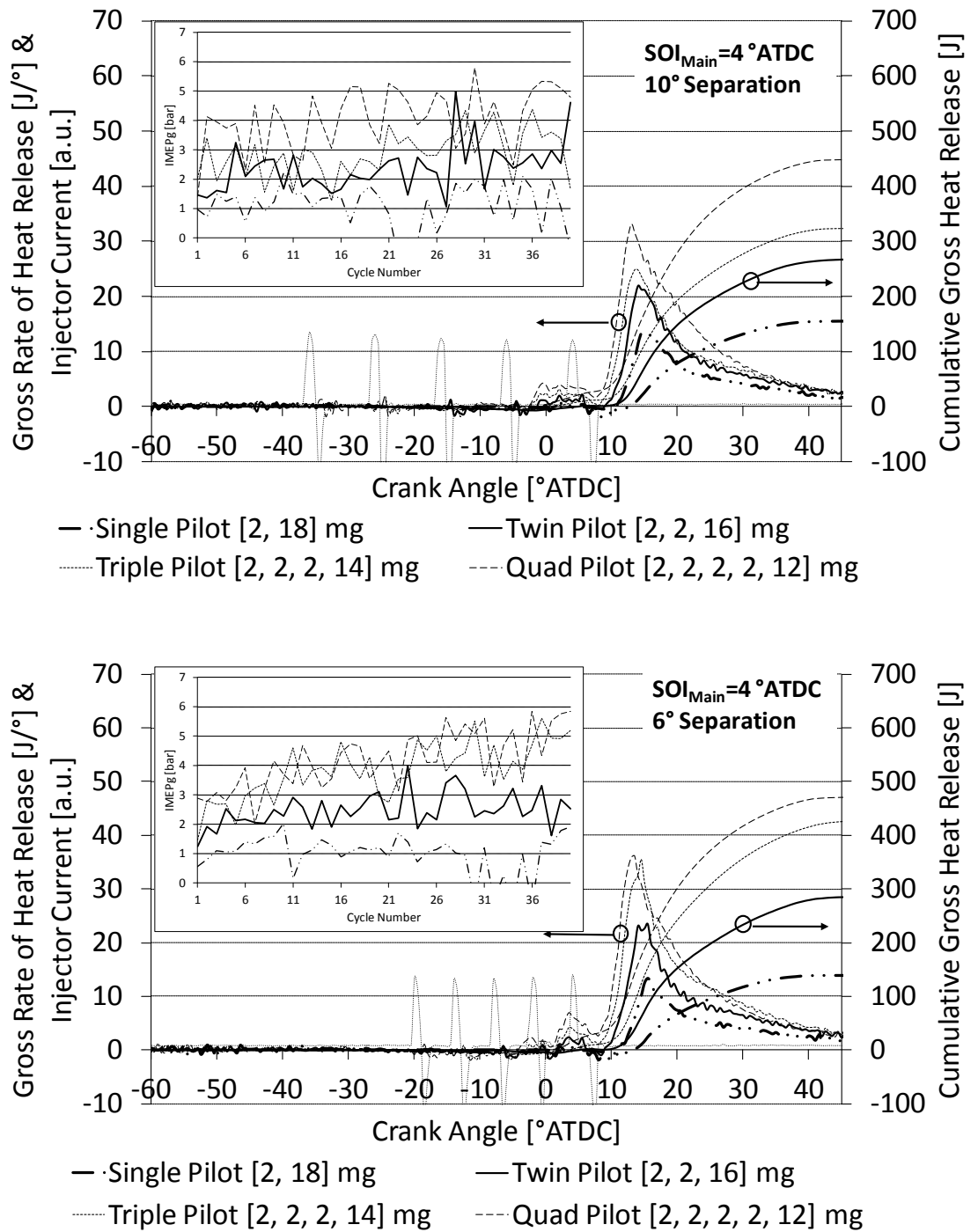


Figure 5-12. The effect of number of pilots on average gross heat release variations (top) 10 °CA separation and (bottom) 6 °CA separation. Conditions: -20 °C, SOI<sub>Main</sub> = 4 °ATDC, 1000 rev/min, 400 bar rail pressure, 850°C glow plug, 20 mg/cycle total fuel, injector current shown for quad-pilot



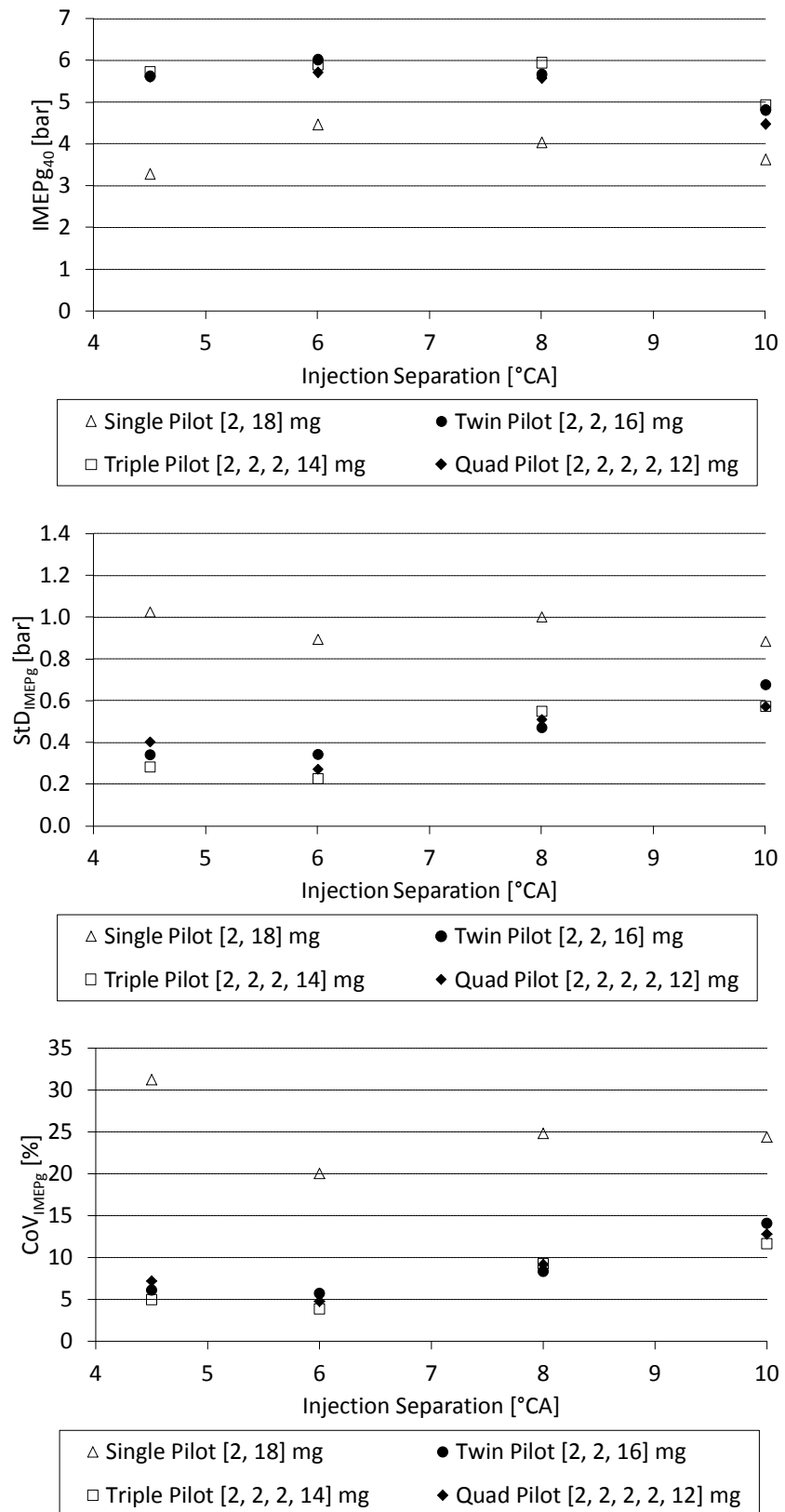


Figure 5-13. The effect of injection separation on IMEP<sub>g</sub>, StD<sub>IMEPg</sub> and CoV<sub>IMEPg</sub> for multiple injection strategies. Conditions: -20°C, SOI<sub>Main</sub> = -8 °ATDC, 1000 rev/min, 400 bar rail pressure, 850°C glow plug, 20 mg/cycle total fuel

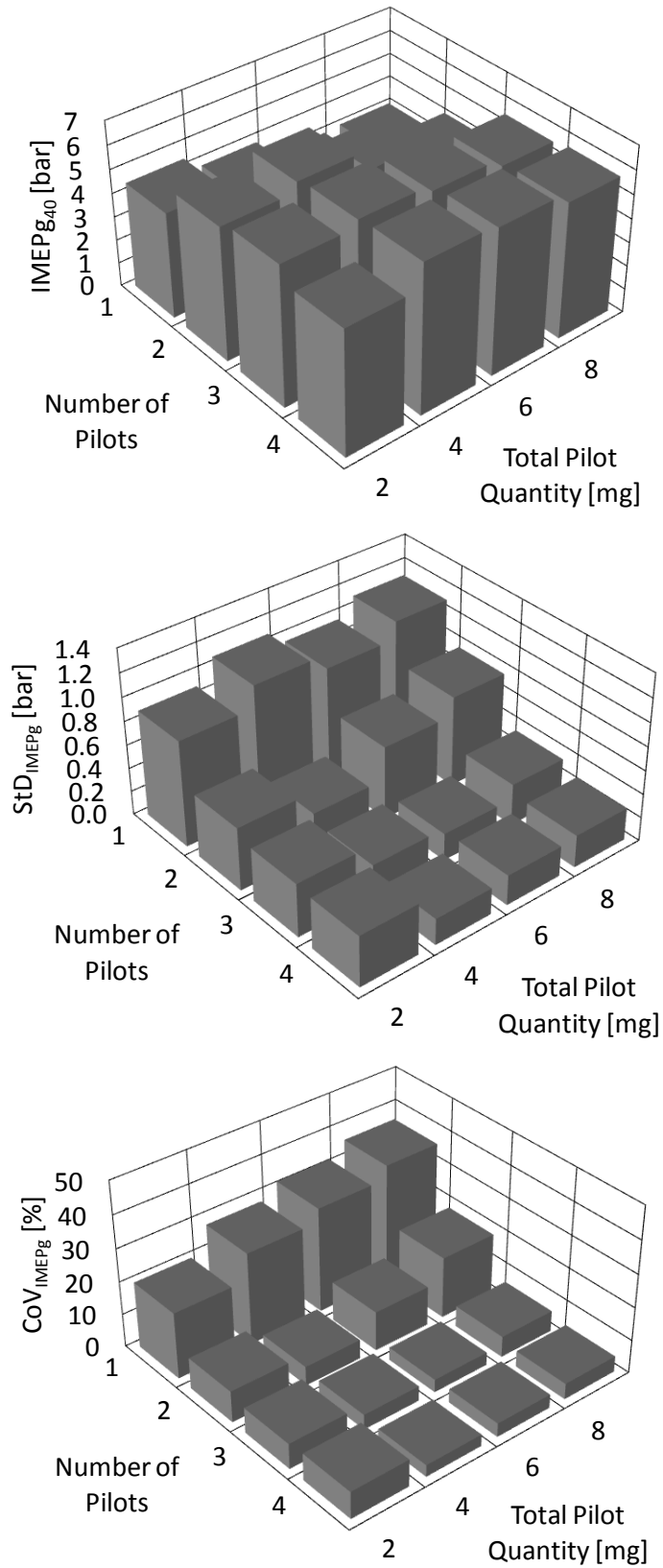
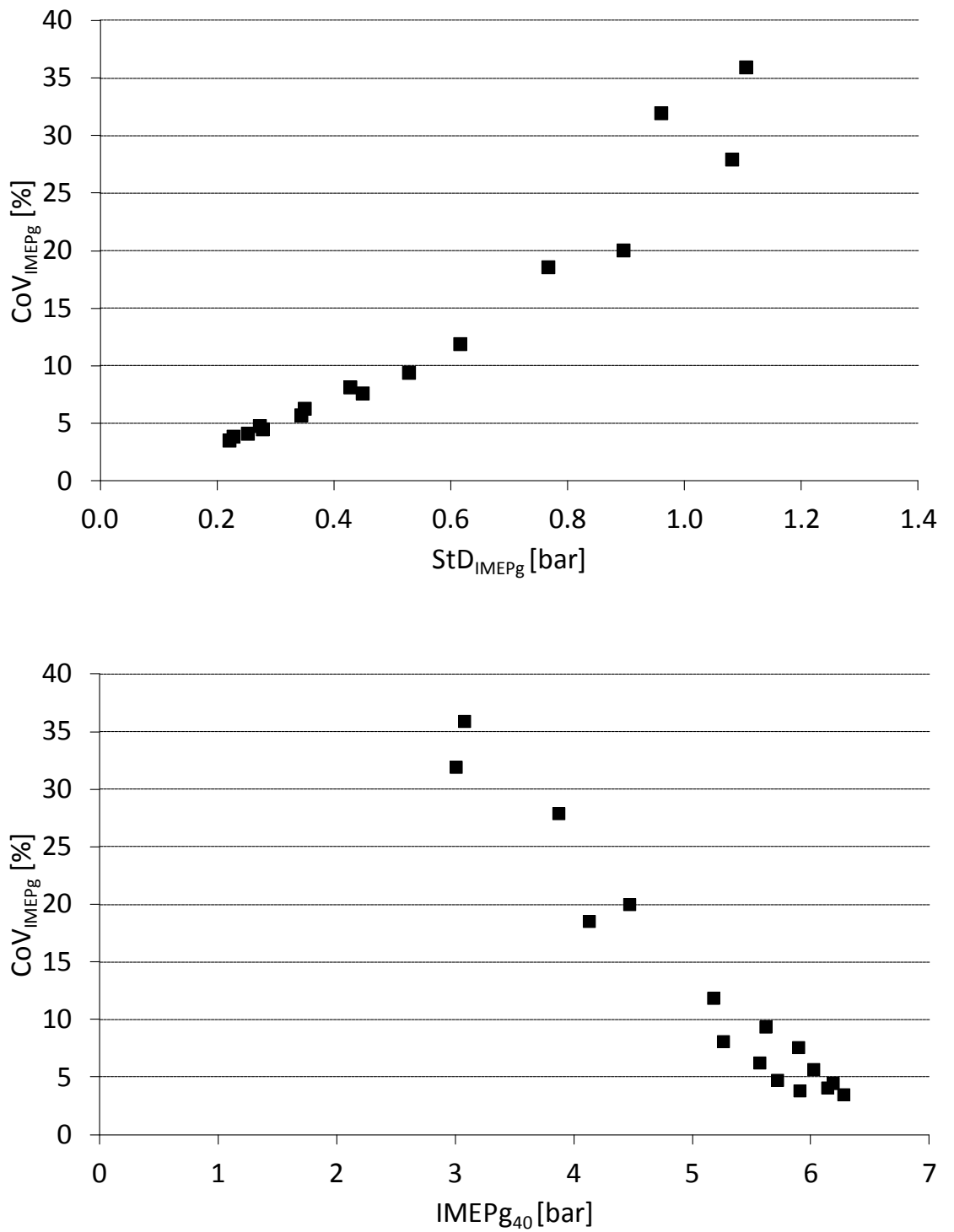


Figure 5-14. The effect of number of pilots and total pilot quantity. Conditions:  $-20^{\circ}\text{C}$ ,  $SOI_{Main} = -8^{\circ}\text{ATDC}$ ,  $6^{\circ}\text{CA}$  separation, 1000 rev/min, 400 bar rail pressure,  $850^{\circ}\text{C}$  glow plug, 20 mg/cycle total fuel



**Figure 5-15. Stability dependency on IMEP<sub>g</sub> and StD<sub>IMEPg</sub>. Conditions: -20°C, SOI<sub>Main</sub> = -8 °ATDC, 6 °CA separation, 1000 rev/min, 400 bar rail pressure, 850°C glow plug, 20 mg/cycle total fuel**

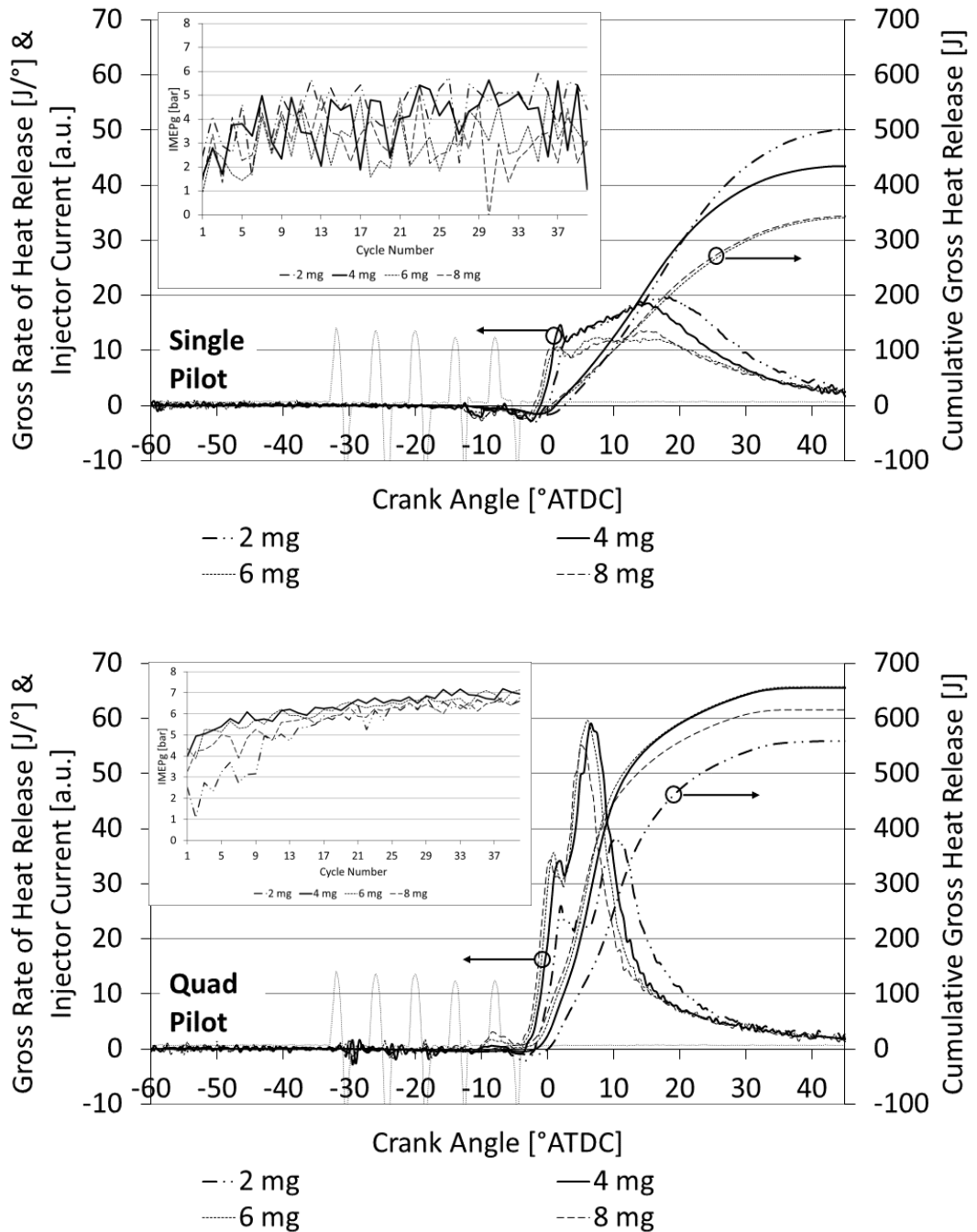
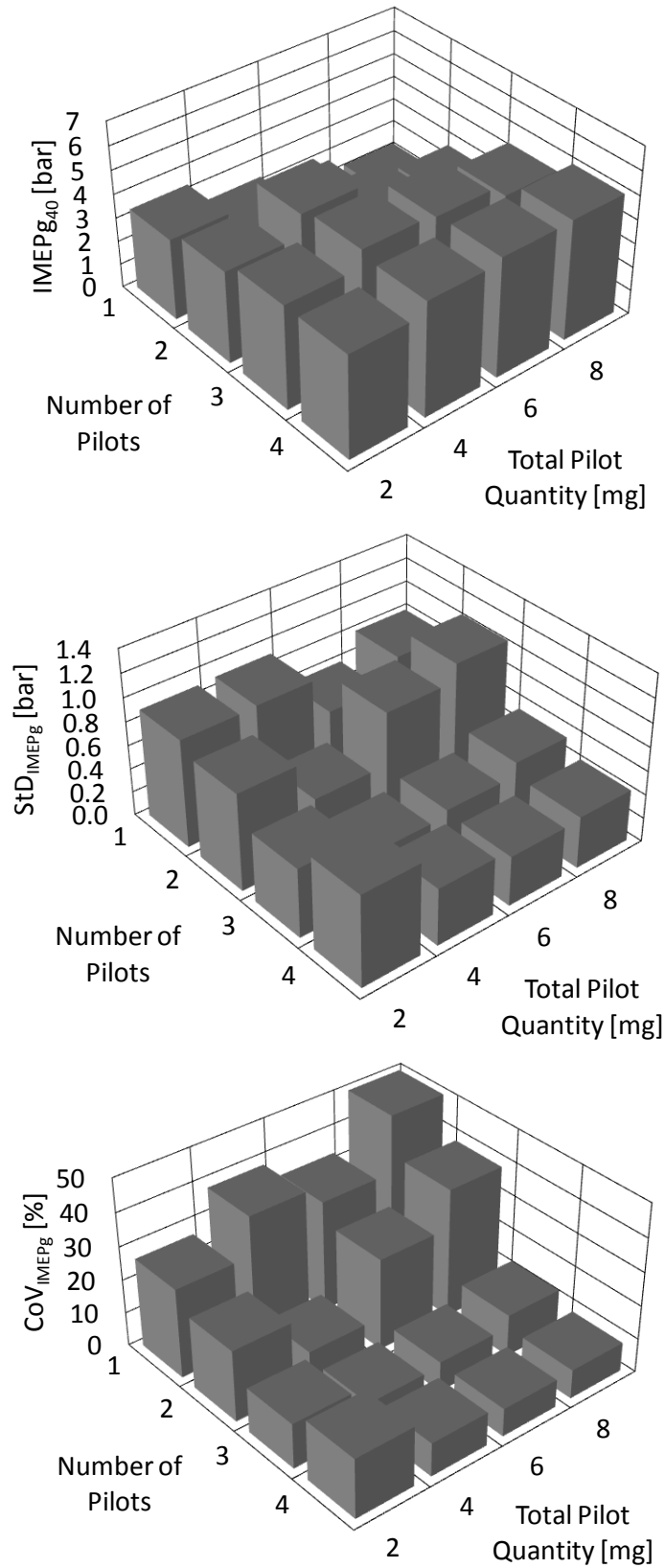
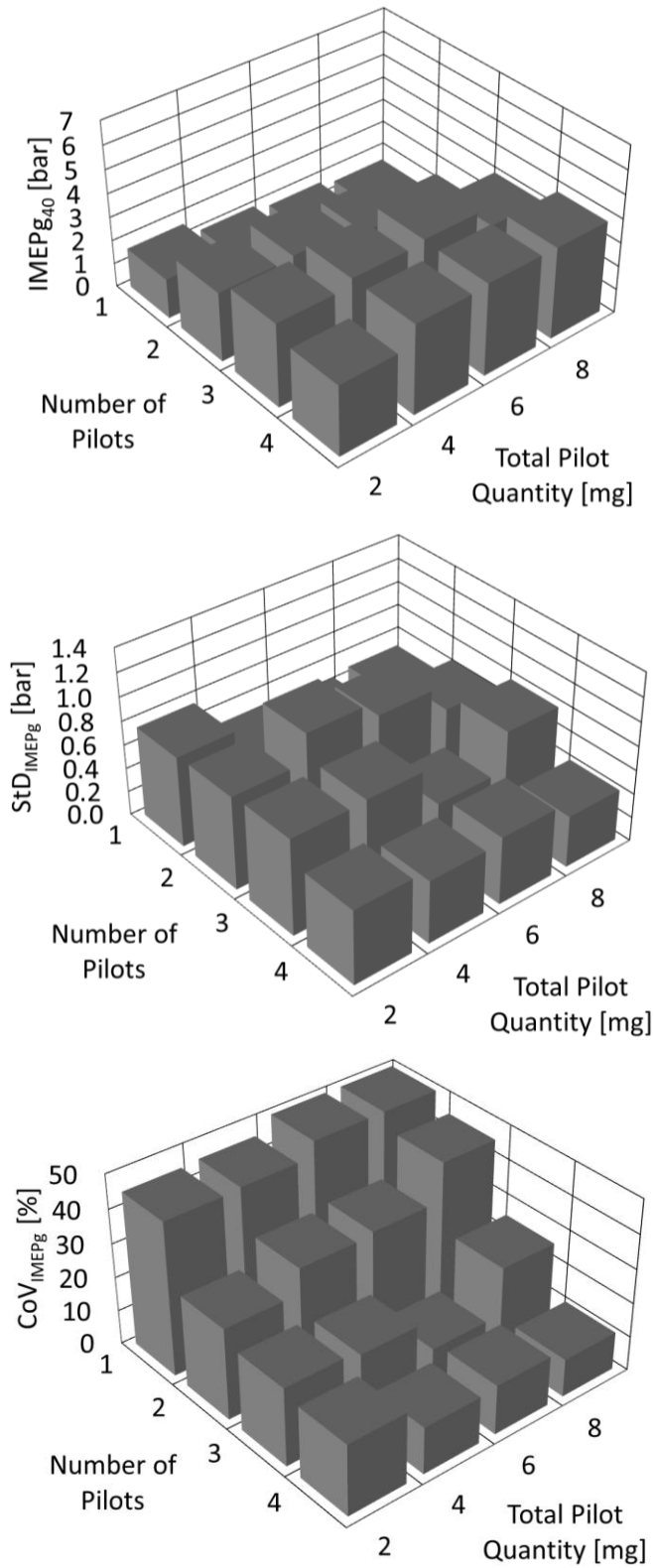


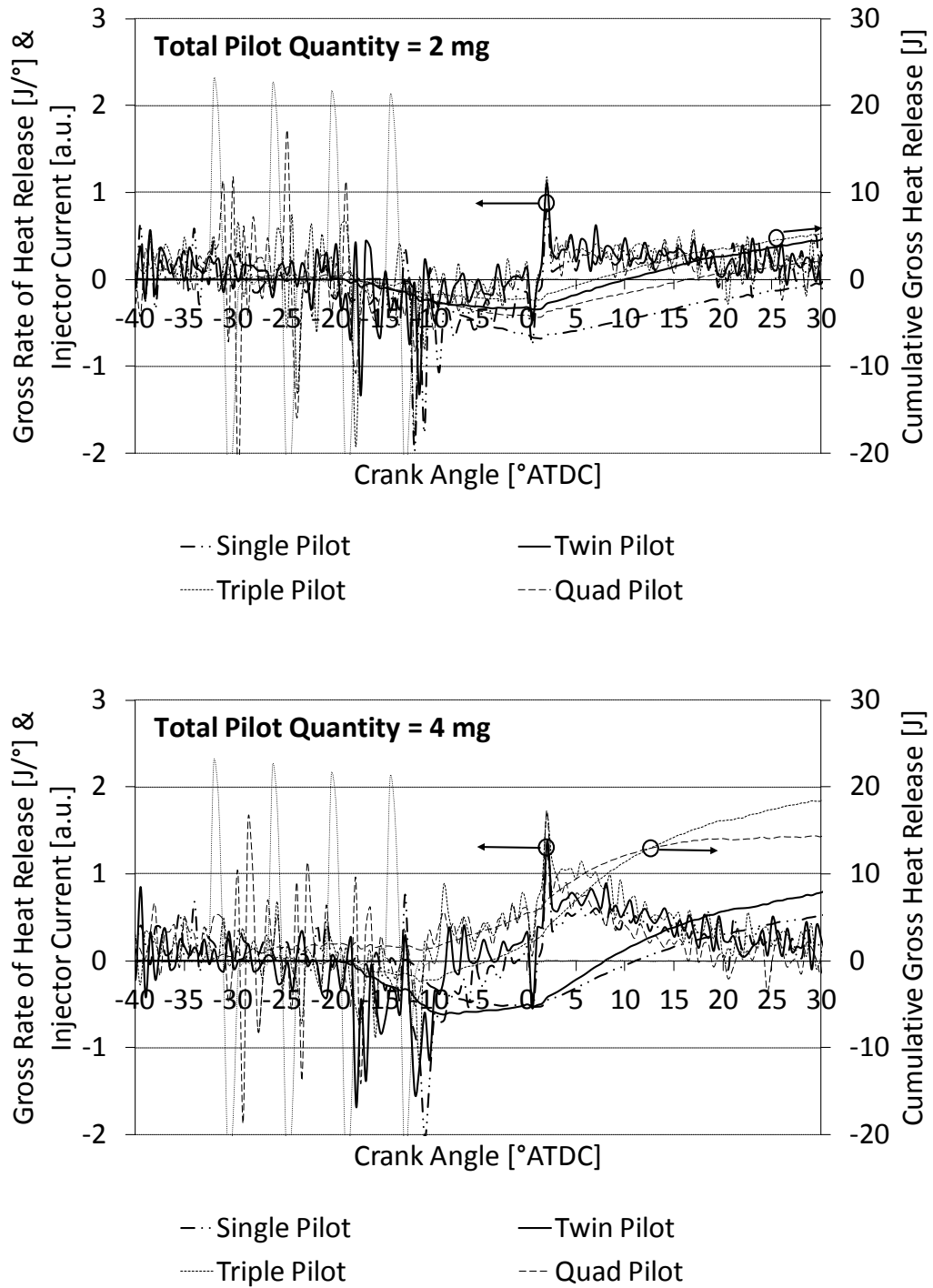
Figure 5-16. Effect of varying total pilot quantity on 40 cycle ensemble averaged heat release (top) single-pilot (bottom) quad-pilot strategy. Conditions:  $-20^{\circ}\text{C}$ ,  $\text{SOI}_{\text{Main}} = -8^{\circ}\text{ATDC}$ ,  $6^{\circ}\text{CA}$  separation, 1000 rev/min, 400 bar rail pressure,  $850^{\circ}\text{C}$  glow plug, 20 mg/cycle total fuel



**Figure 5-17. The effect of number of pilots and total pilot quantity. Conditions: -20°C,  $SOI_{Main} = -8$  °ATDC, 6 °CA separation, 1000 rev/min, 400 bar rail pressure, 850°C glow plug, 18 mg/cycle total fuel**



**Figure 5-18. The effect of number of pilots and total pilot quantity. Conditions: -20°C,  $SOI_{Main} = -8$  °ATDC, 6 °CA separation, 1000 rev/min, 400 bar rail pressure, 850°C glow plug, 16 mg/cycle total fuel ( $CoV_{IMEPg}$  scale has been capped at 50% to maintain clarity, single-pilot results are in the region of 45-90%)**



**Figure 5-19. 40 cycle ensemble averaged pilot heat release (top) 2 mg total pilot quantity (bottom) 4 mg/cycle total pilot quantity. Conditions: -20°C,  $SOI_{Main} = -8$  °ATDC, 6 °CA separation, 1000 rev/min, 400 bar rail pressure, 850°C glow plug, injector current shown for quad-pilot case**

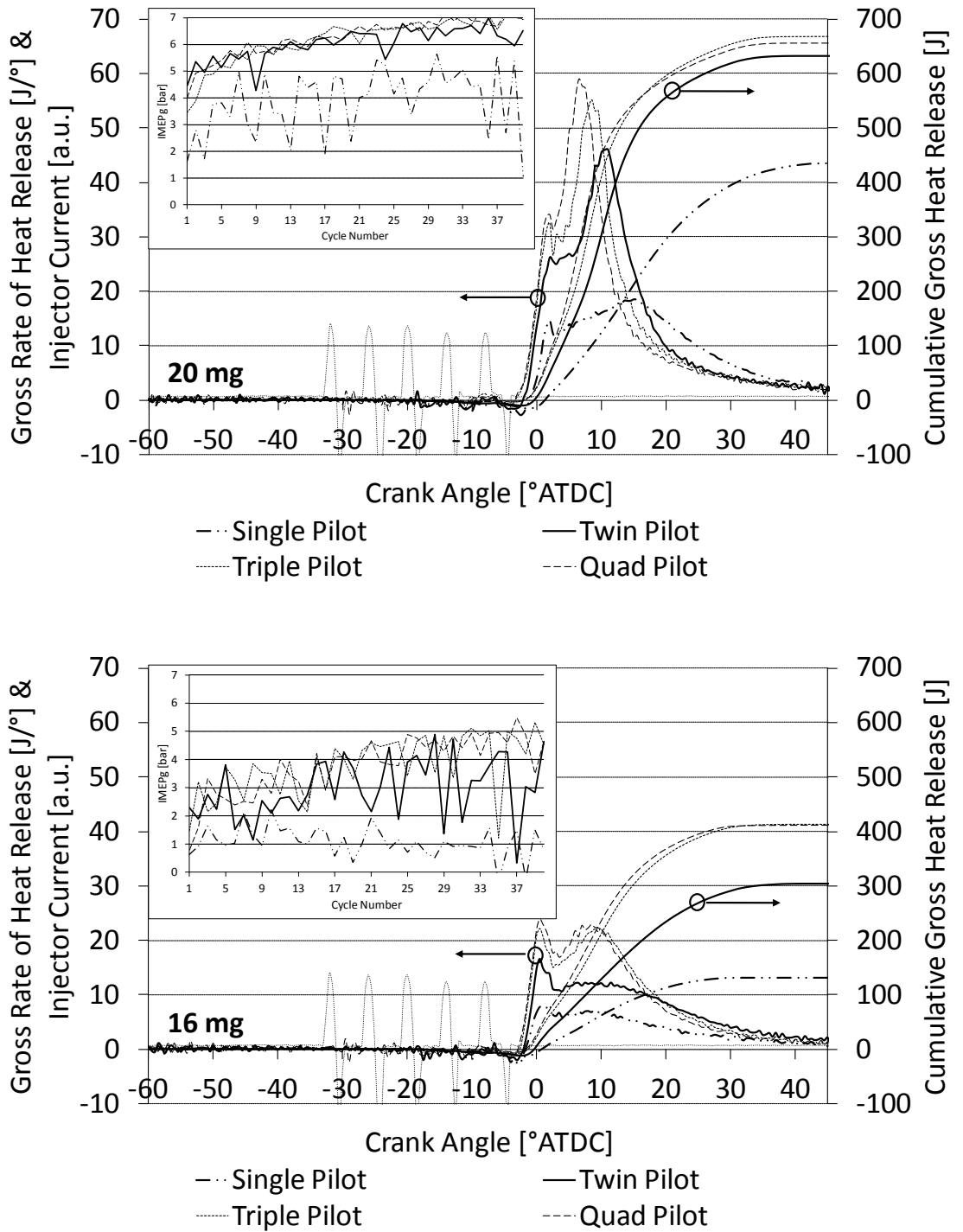


Figure 5-20. 40 cycle ensemble averaged heat release with 4 mg total pilot quantity; (top) 20 mg/cycle total fuel (bottom) 16 mg/cycle total fuel. Conditions:  $-20^{\circ}\text{C}$ ,  $\text{SOI}_{\text{Main}} = -8^{\circ}\text{ATDC}$ ,  $6^{\circ}\text{CA}$  separation, 1000 rev/min, 400 bar rail pressure,  $850^{\circ}\text{C}$  glow plug, injector current shown for quad-pilot case



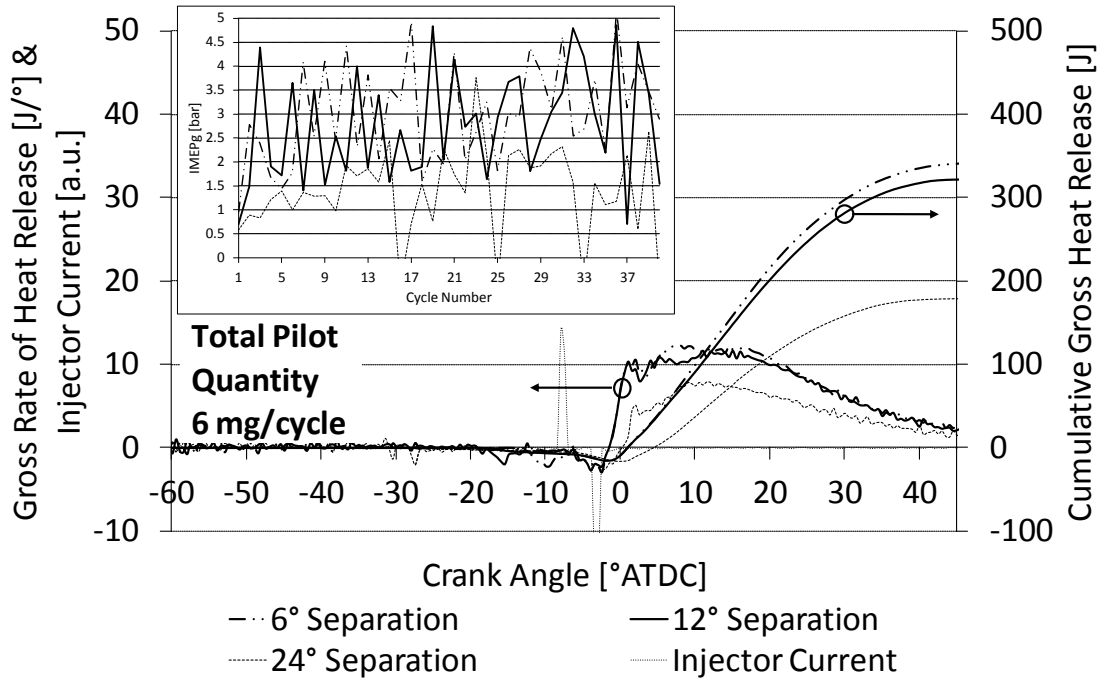


Figure 5-21. 40 cycle ensemble averaged heat release sensitivity to varying the separation of a 6 mg/cycle pilot, 20 mg/cycle total fuel. Conditions: -20°C,  $SOI_{Main} = -8$  °ATDC, 1000 rev/min, 400 bar rail pressure, 850°C glow plug, injector current shown for main injection

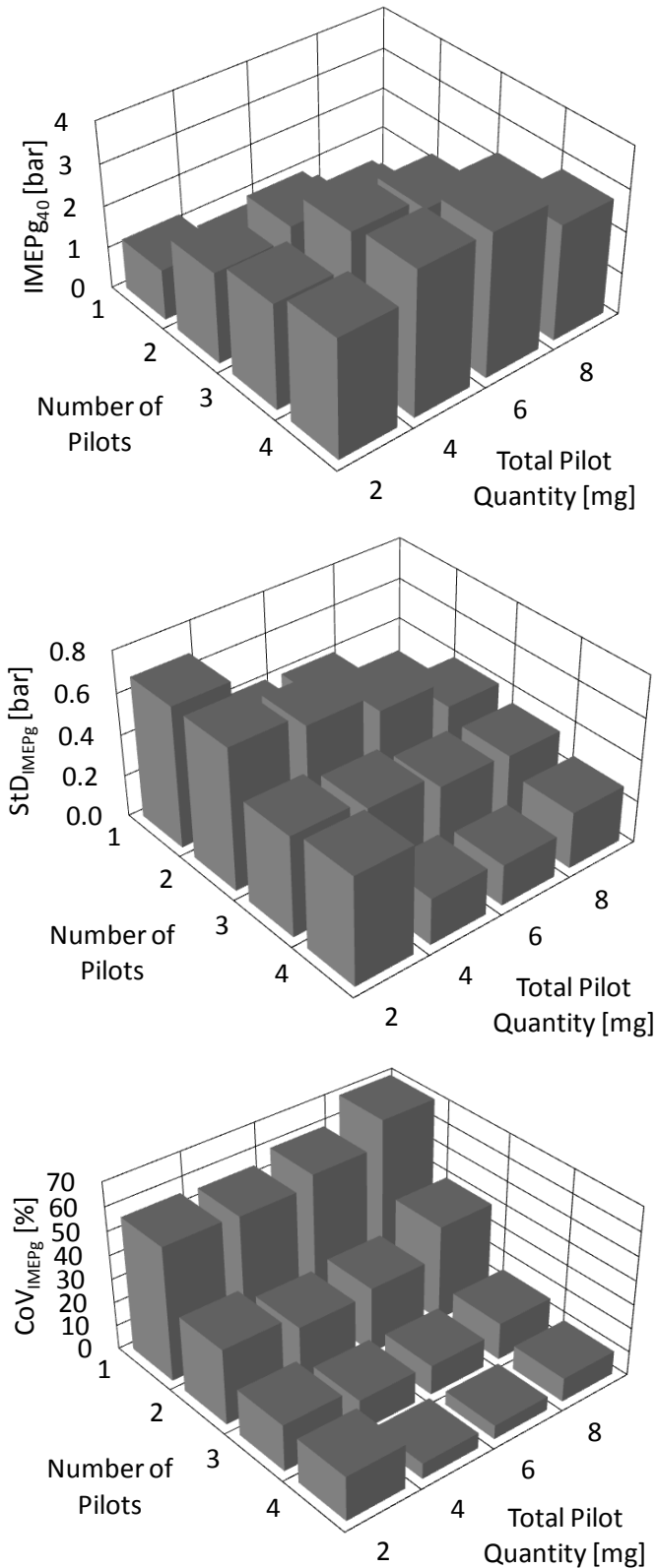


Figure 5-22. The effect of number of pilots and total pilot quantity. Conditions:  $-5^{\circ}\text{C}$ ,  $SOI_{\text{Main}} = -8^{\circ}\text{ATDC}$ ,  $6^{\circ}\text{CA}$  separation, 1000 rev/min, 400 bar rail pressure,  $850^{\circ}\text{C}$  glow plug, 12 mg/cycle total fuel ( $CoV_{IMEPg}$  scale has been capped at 70% to maintain clarity, single-pilot results are in the region of 55-117%)

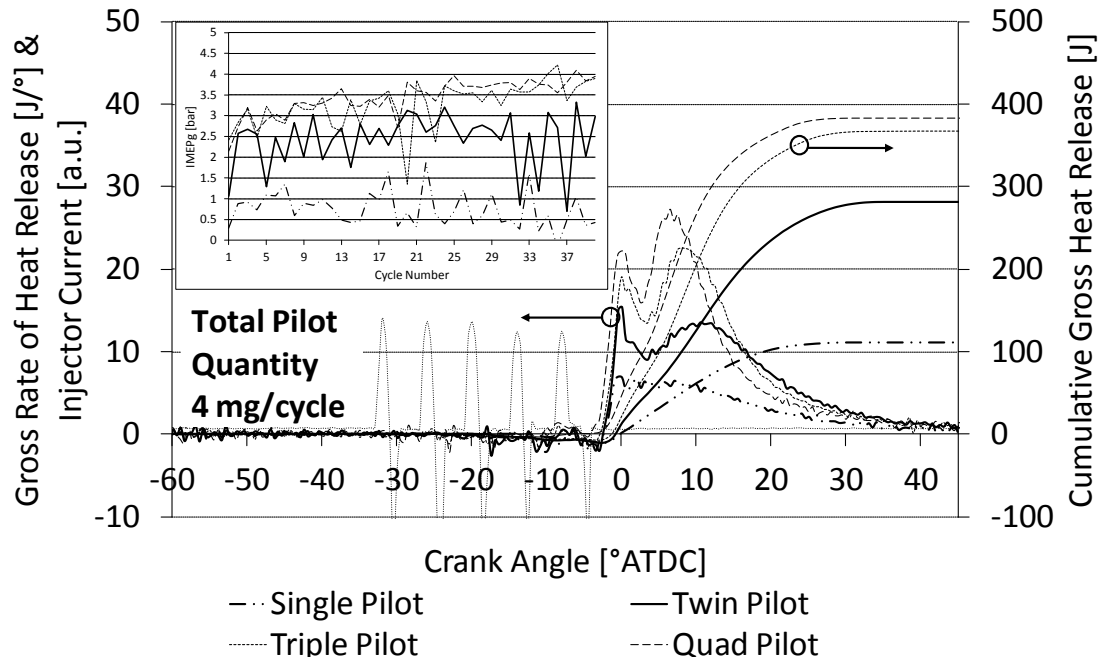


Figure 5-23. 40 cycle ensemble averaged heat release with 4 mg/cycle total pilot quantity. Conditions: -5 °C,  $SOI_{Main} = -8$  °ATDC, 6° separation, 1000 rev/min, 400 bar rail pressure, 850 °C glow plug, 12mg total fuel/cycle, injector current shown for quad-pilot case

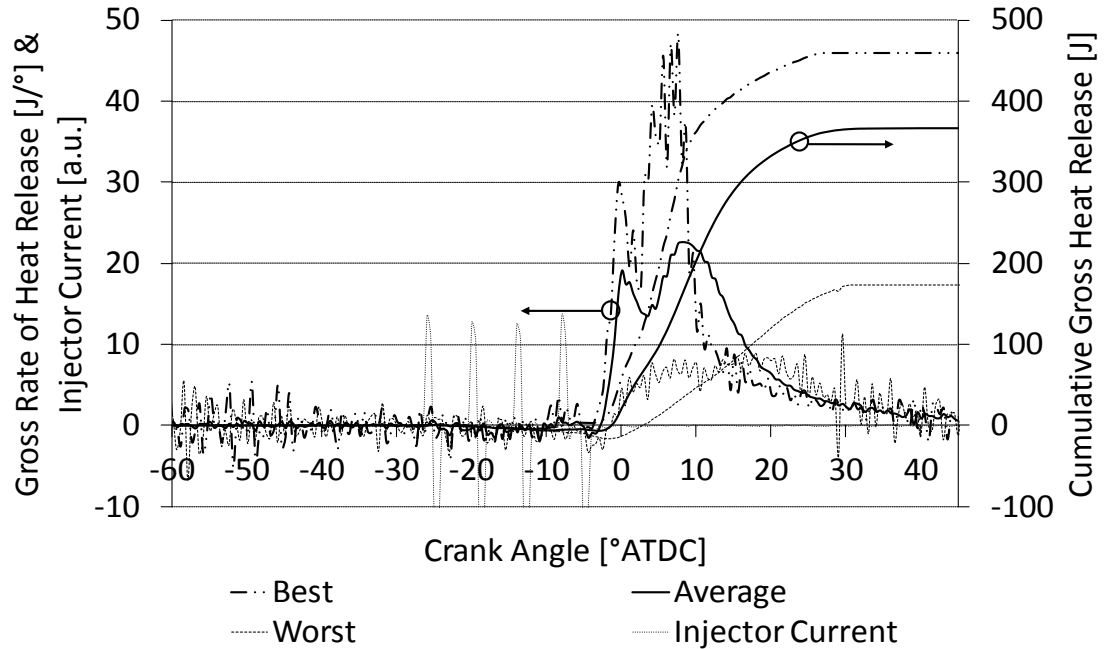


Figure 5-24. Comparison of the best, average and worst heat release profiles for a triple-pilot strategy. Conditions: -5°C,  $SOI_{Main} = -8$  °ATDC, 6 °CA separation, 1000 rev/min, 400 bar rail pressure, 850°C glow plug, 4 mg/cycle total pilot quantity, 12 mg/cycle total fuel, injector current shown for quad-pilot case

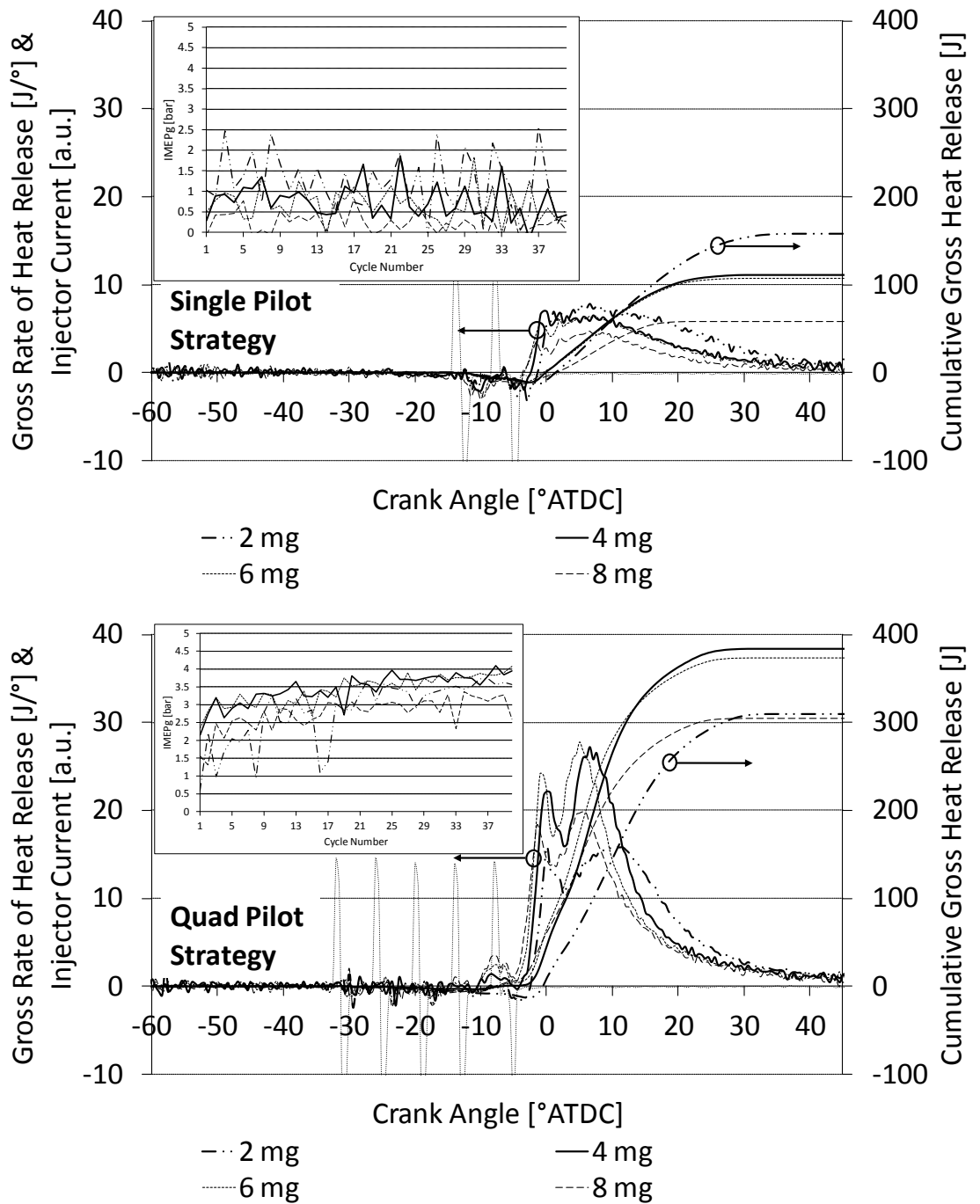
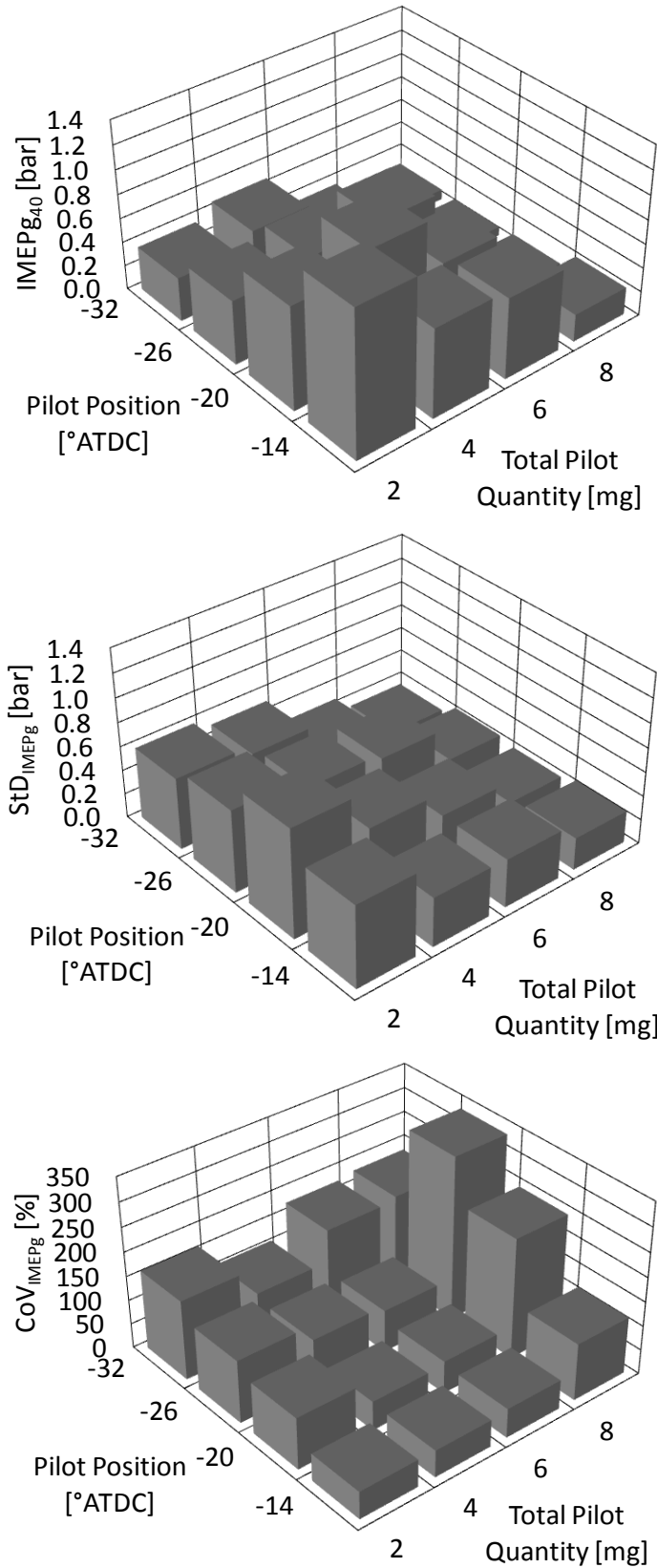
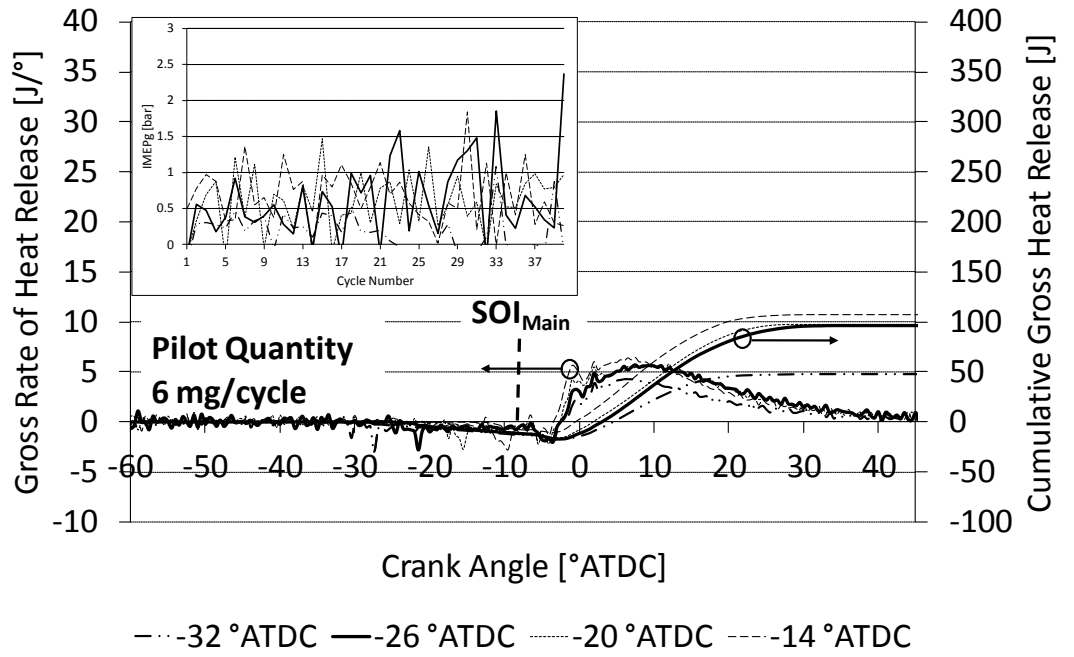


Figure 5-25. Effect of varying total pilot quantity on 40 cycle ensemble averaged heat release (top) single-pilot (bottom) quad-pilot strategy. Conditions:  $-5^{\circ}\text{C}$ ,  $\text{SOI}_{\text{Main}} = -8^{\circ}\text{ATDC}$ ,  $6^{\circ}\text{CA}$  separation, 1000 rev/min, 400 bar rail pressure,  $850^{\circ}\text{C}$  glow plug, 12 mg/cycle total fuel



**Figure 5-26. Effect of pilot fuel distribution and position for a single-pilot strategy. Conditions: -5°C, SOI<sub>Main</sub> = -8 °ATDC, 1000 rev/min, 400 bar rail pressure, 850°C glow plug, 12 mg/cycle total fuel**



**Figure 5-27. Effect of a single 6 mg/cycle pilot injection position on 40 cycle ensemble averaged heat release. Conditions: -5°C,  $SOI_{Main} = -8$  °ATDC, 1000 rev/min, 400 bar rail pressure, 850°C glow plug, 12 mg/cycle total fuel**

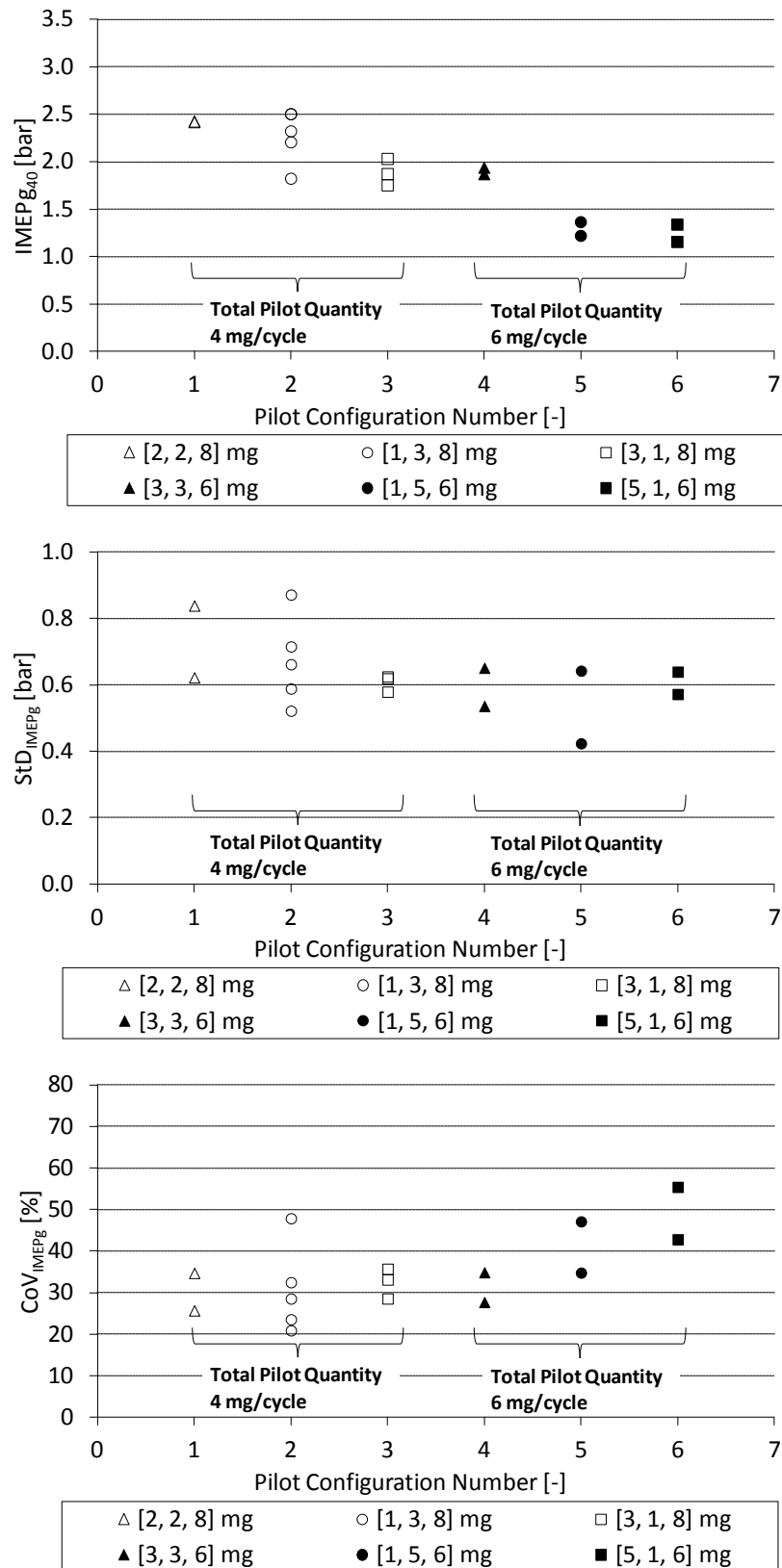


Figure 5-28. Effect of pilot fuel distribution and position for a twin-pilot strategy with the pilots placed at -20 and -14 °ATDC. Conditions: -5°C, SOI<sub>Main</sub> = -8 °ATDC, 1000 rev/min, 400 bar rail pressure, 850°C glow plug, 12 mg/cycle total fuel

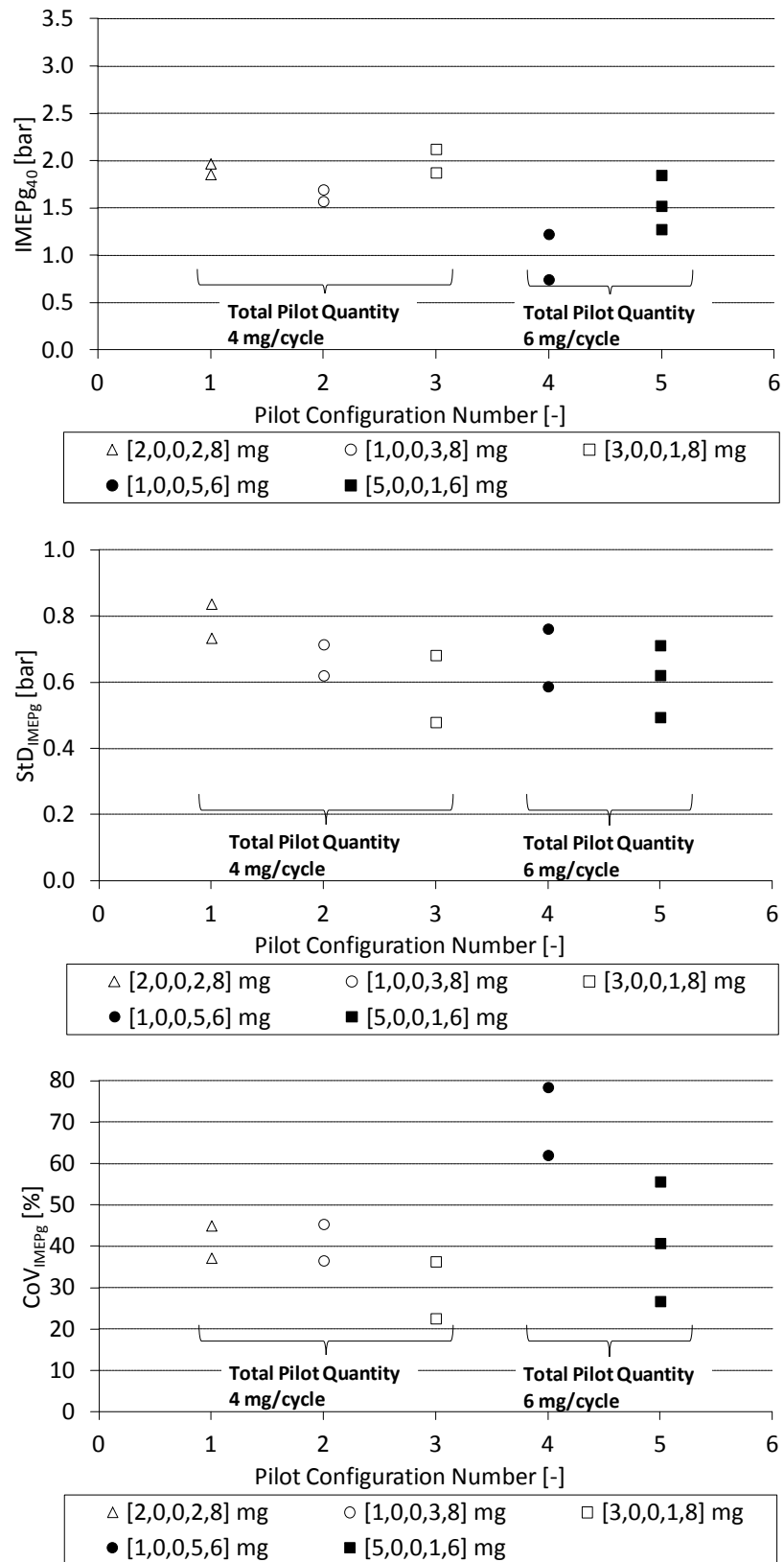


Figure 5-29. Effect of pilot fuel distribution and position for a twin-pilot strategy with the pilots placed at -32 and -14 °ATDC. Conditions: -5°C, SOI<sub>Main</sub> = -8 °ATDC, 1000 rev/min, 400 bar rail pressure, 850°C glow plug, 12 mg/cycle total fuel



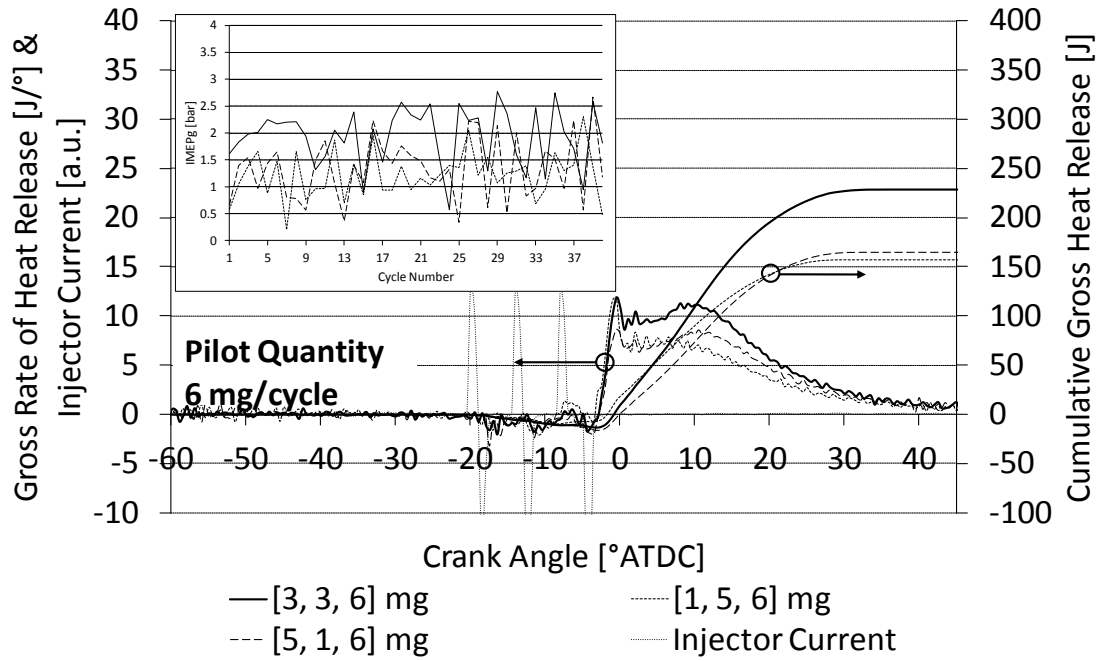


Figure 5-30. Effect of pilot fuel distribution for a twin-pilot strategy with each pilot positioned at -20 and -14 °ATDC. Conditions: -5°C,  $SOI_{Main} = -8$  °ATDC, 1000 rev/min, 400 bar rail pressure, 850°C glow plug, 12 mg/cycle total fuel

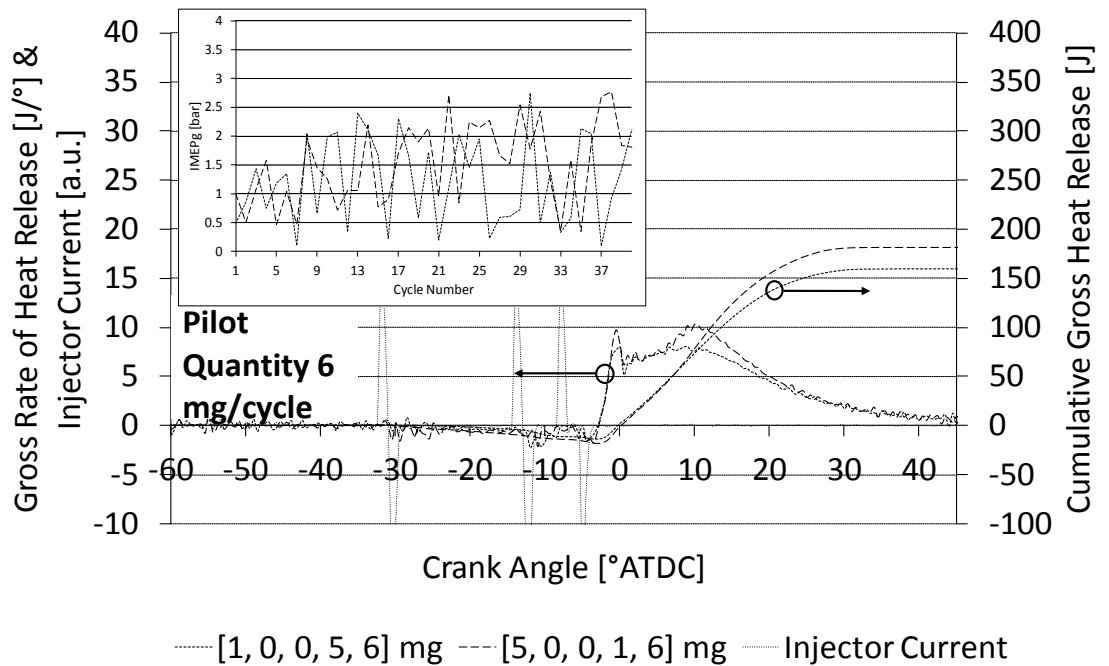
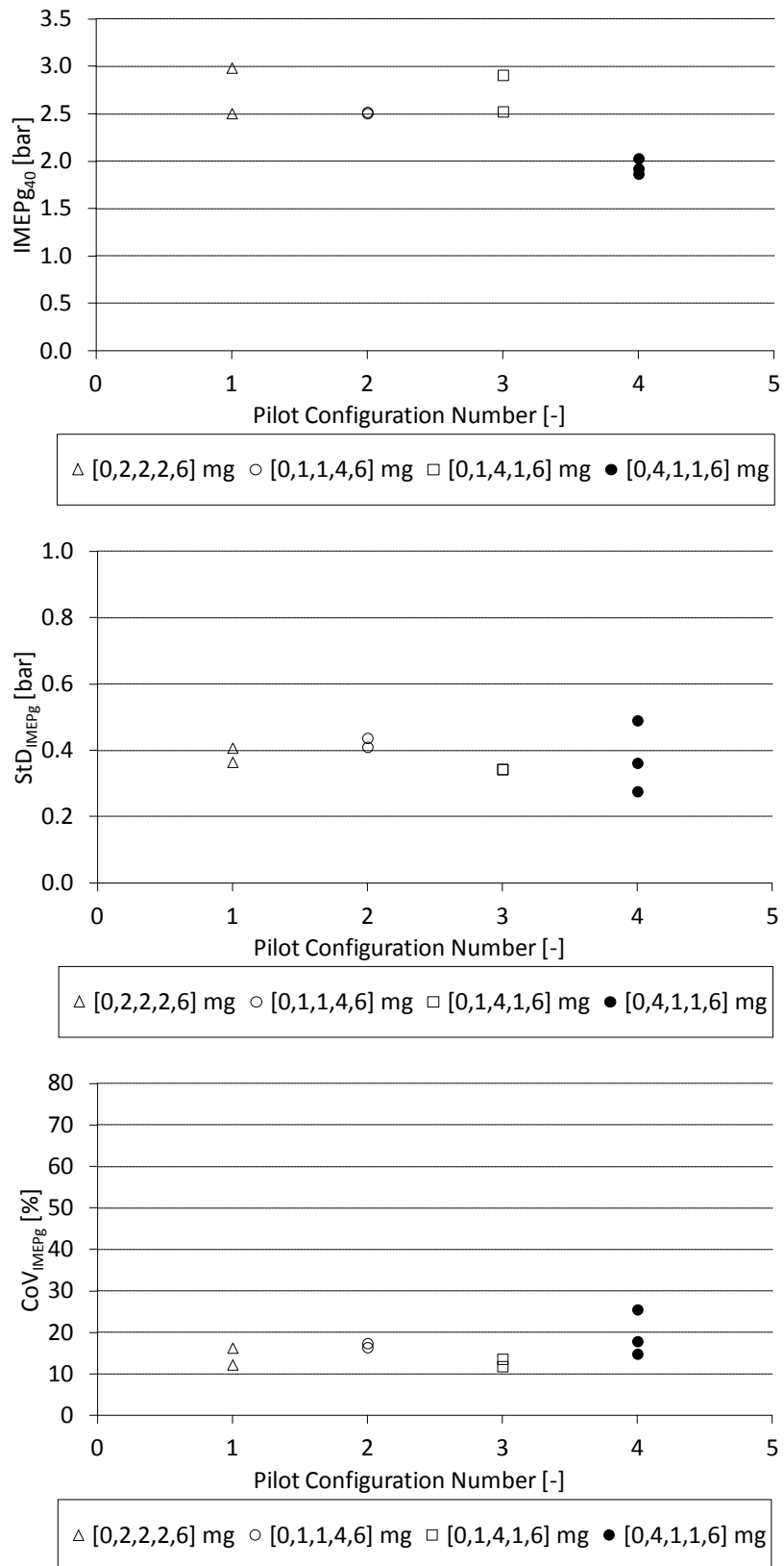


Figure 5-31. Effect of pilot fuel distribution for a twin-pilot strategy with each pilot positioned at -32 and -14 °ATDC. Conditions: -5°C,  $SOI_{Main} = -8$  °ATDC, 1000 rev/min, 400 bar rail pressure, 850°C glow plug, 12 mg/cycle total fuel



**Figure 5-32. Effect of pilot fuel distribution and position for a triple-pilot strategy with the pilots placed at -26, -20 and -14 °ATDC. Conditions: -5°C, SOI<sub>Main</sub> = -8 °ATDC, 1000 rev/min, 400 bar rail pressure, 850°C glow plug, 12 mg/cycle total fuel**

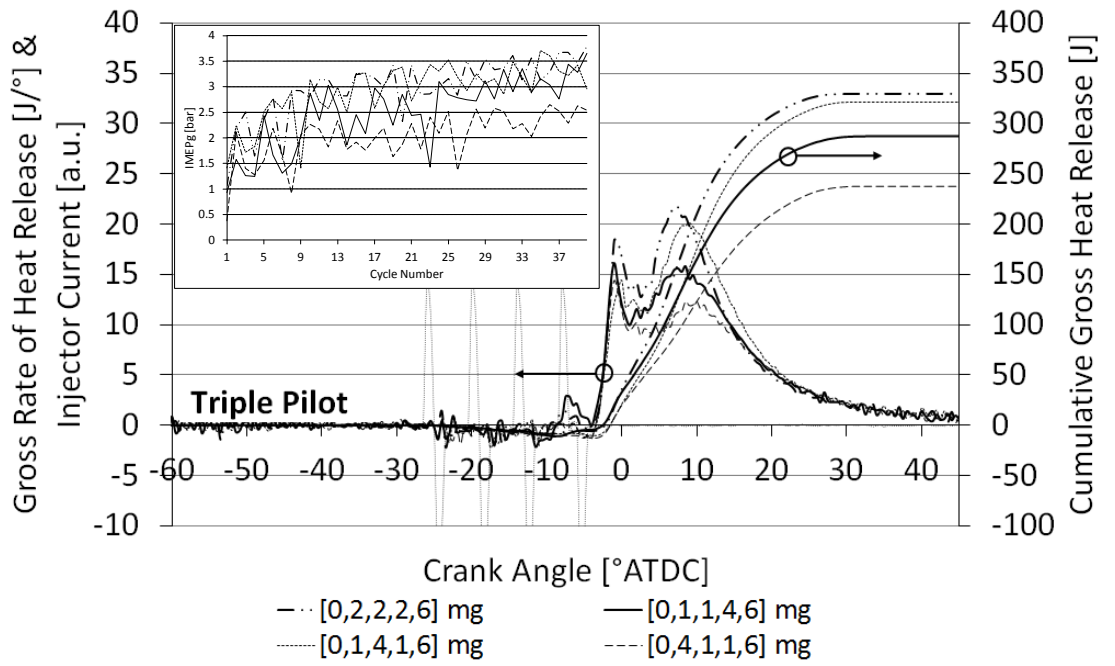


Figure 5-33. Effect of pilot fuel distribution and position on heat release for a triple-pilot strategy with the pilots placed at -26, -20 and -14 °ATDC. Conditions: -5°C,  $SOI_{Main} = -8$  °ATDC, 1000 rev/min, 400 bar rail pressure, 850°C glow plug, 12 mg/cycle total fuel

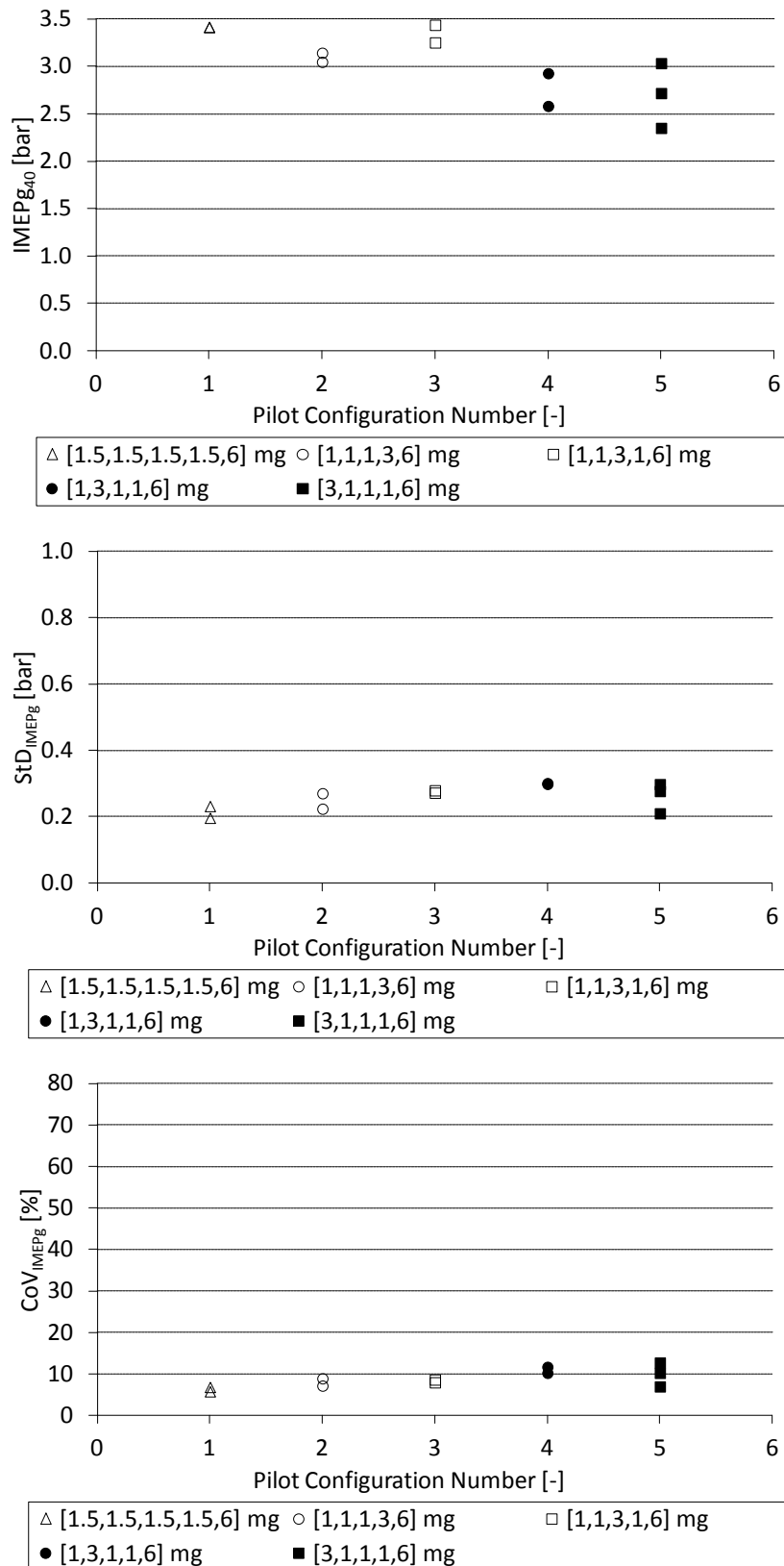
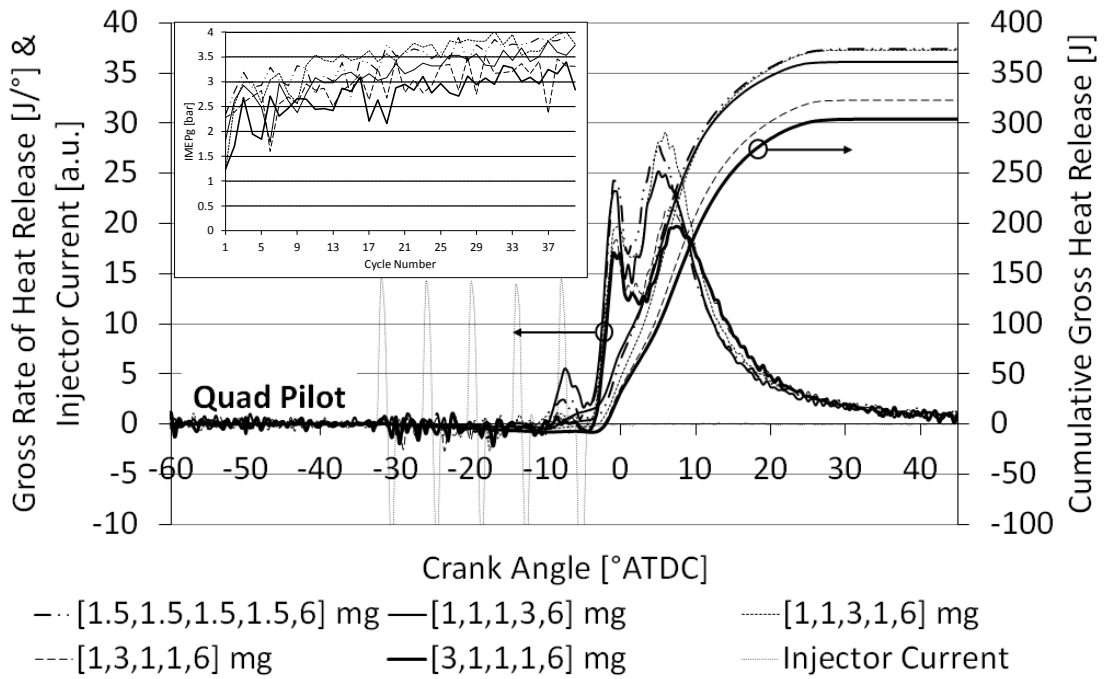
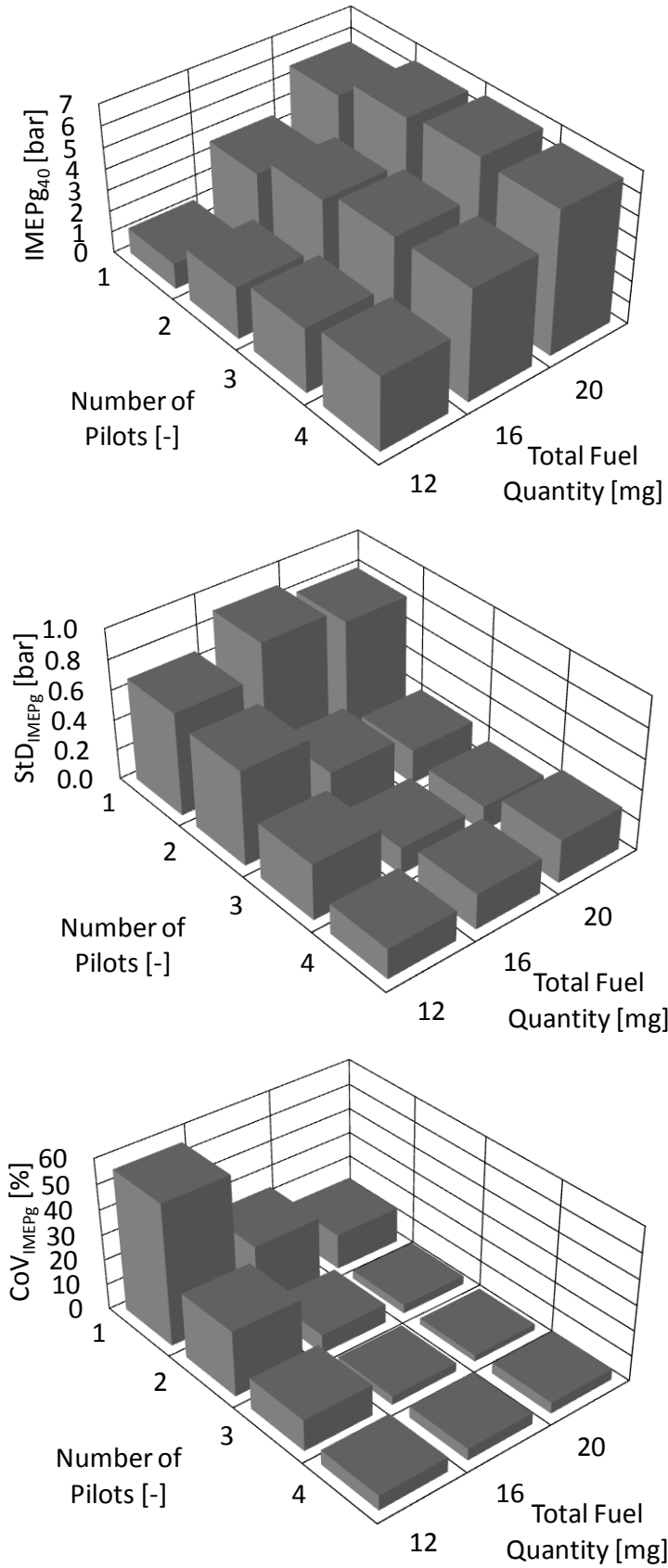


Figure 5-34. Effect of pilot fuel distribution and position for a quad-pilot strategy with the pilots placed at -32, -26, -20 and -14 °ATDC. Conditions: -5°C, SOI<sub>Main</sub> = -8 °ATDC, 1000 rev/min, 400 bar rail pressure, 850°C glow plug, 12 mg/cycle total fuel



**Figure 5-35. Effect of pilot fuel distribution and position on heat release for a quad-pilot strategy with the pilots placed at -32, -26, -20 and -14 °ATDC. Conditions: -5°C,  $SOI_{Main} = -8$  °ATDC, 1000 rev/min, 400 bar rail pressure, 850°C glow plug, 12 mg/cycle total fuel**



**Figure 5-36. Effect of total fuelling level for various injection strategies. Conditions: - 5°C, SOI<sub>Main</sub> = -8 °ATDC, 1000 rev/min, 400 bar rail pressure, 850°C glow plug**

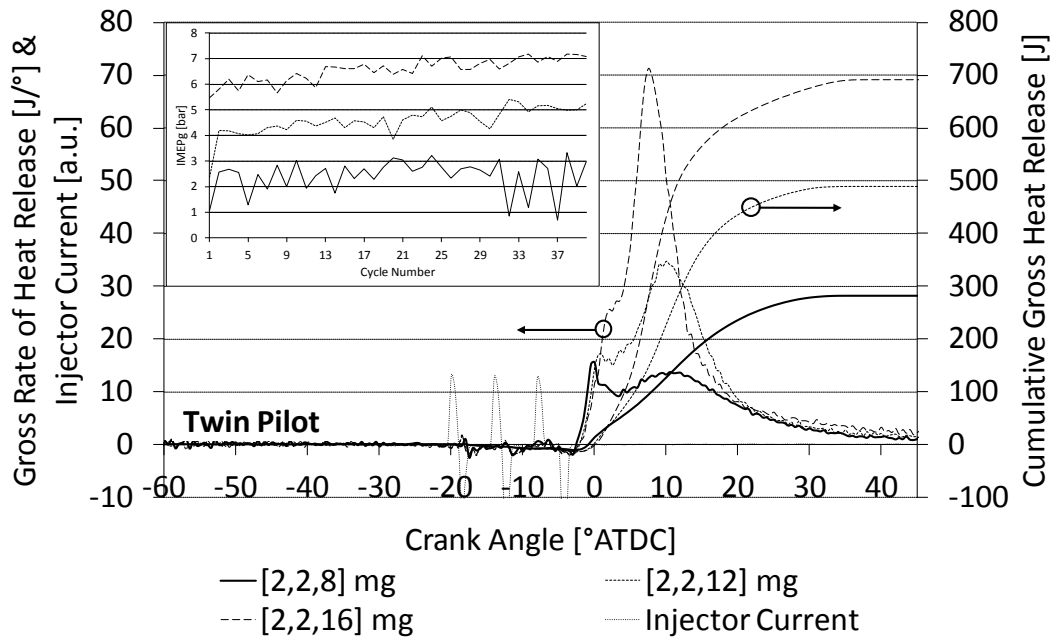


Figure 5-37. Effect of total fuelling level for a twin-pilot strategy. Conditions:  $-5^{\circ}\text{C}$ ,  $\text{SOI}_{\text{Main}} = -8^{\circ}\text{ATDC}$ , 1000 rev/min, 400 bar rail pressure,  $850^{\circ}\text{C}$  glow plug

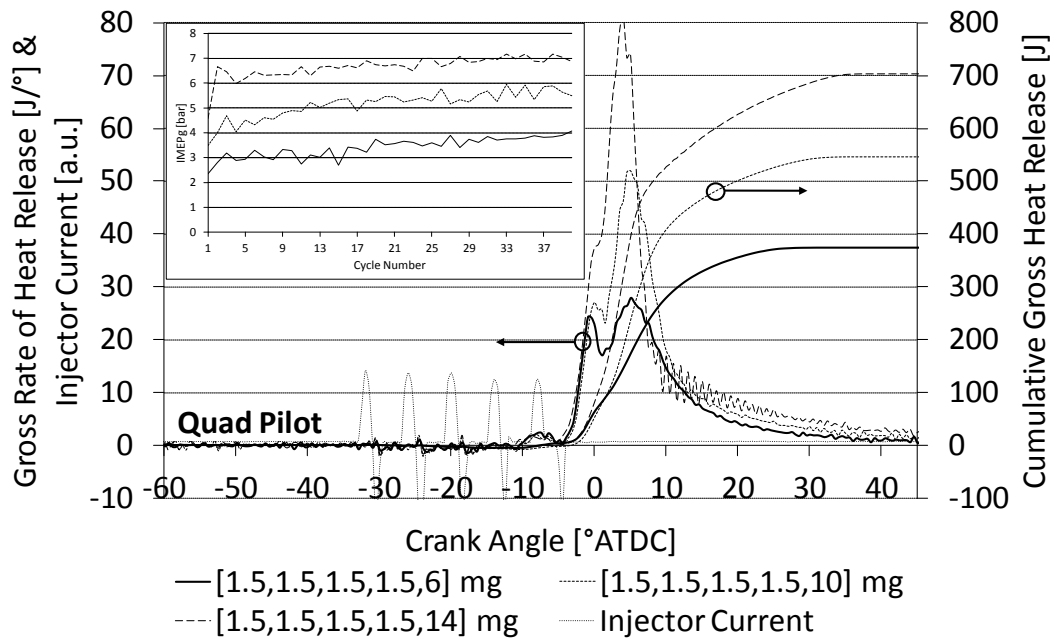


Figure 5-38. Effect of total fuelling level for a quad-pilot strategy. Conditions:  $-5^{\circ}\text{C}$ ,  $\text{SOI}_{\text{Main}} = -8^{\circ}\text{ATDC}$ , 1000 rev/min, 400 bar rail pressure,  $850^{\circ}\text{C}$  glow plug

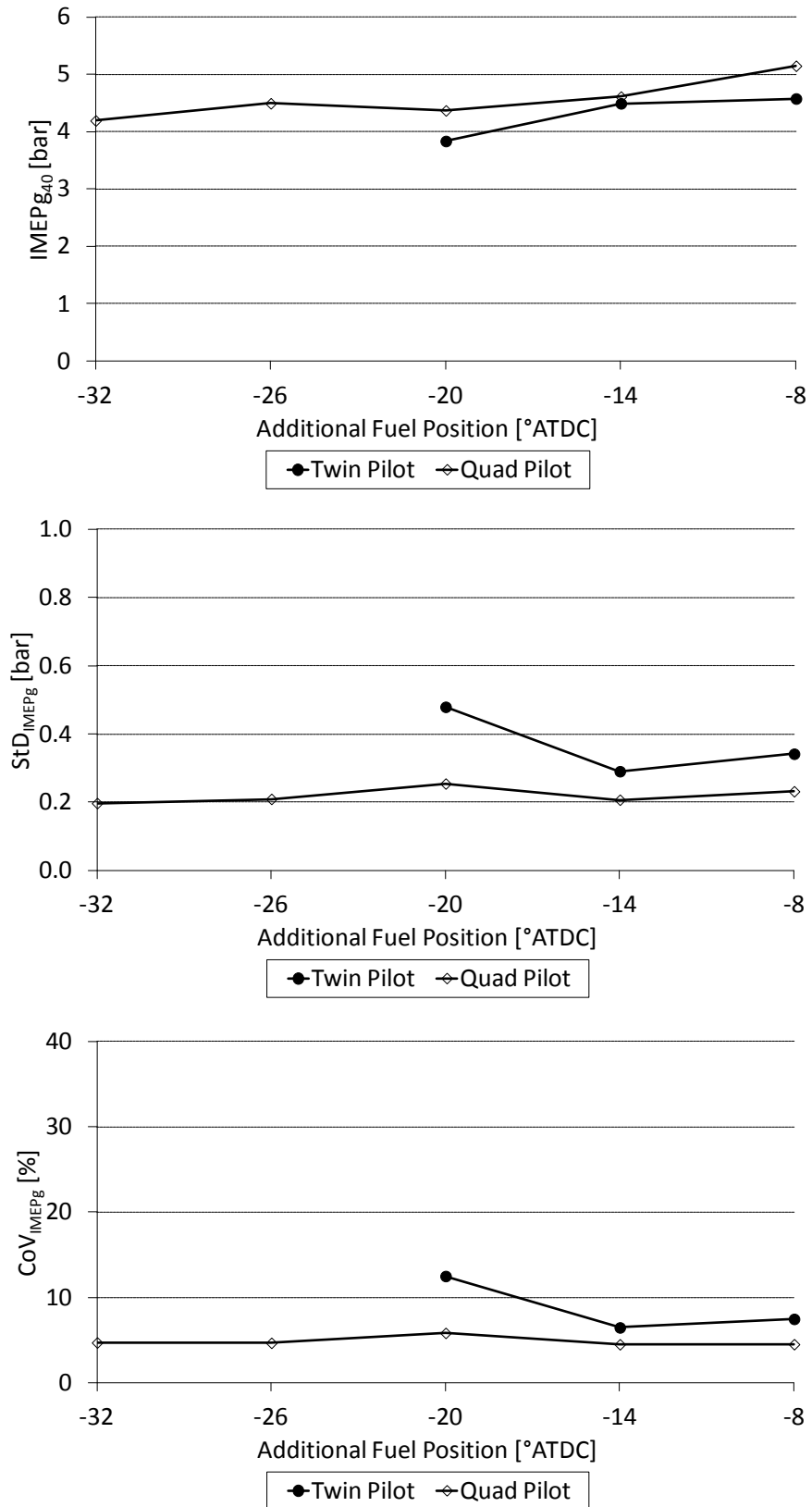


Figure 5-39. Sensitivity to the position of an additional 4 mg/cycle for twin- and quad-pilot strategies. Conditions: -5°C, SOI<sub>Main</sub> = -8 °ATDC, 1000 rev/min, 400 bar rail pressure, 850°C glow plug, 16mg/cycle total fuel



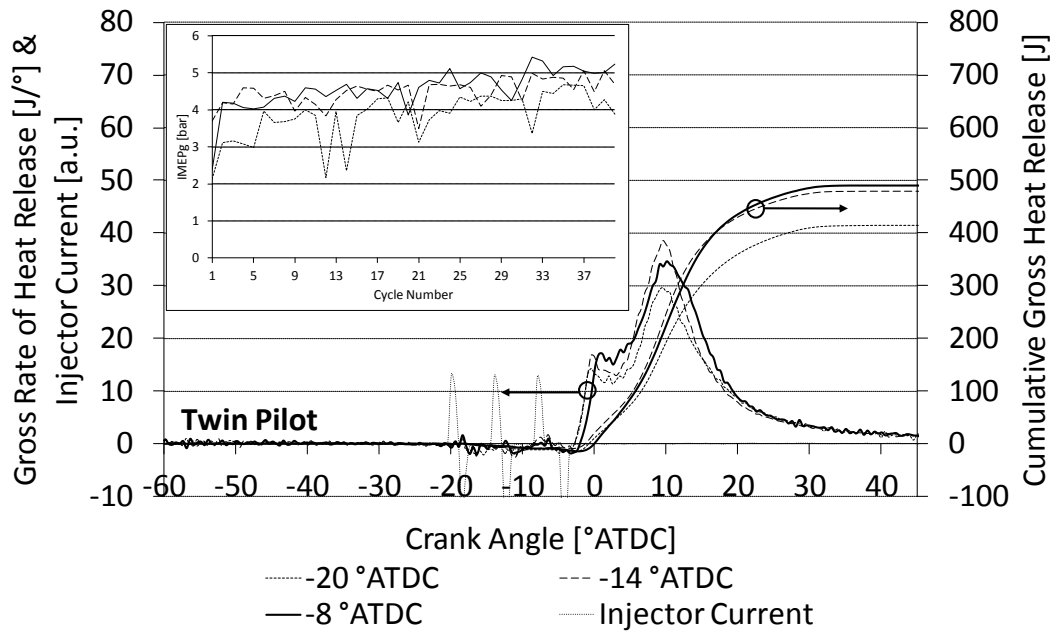


Figure 5-40. Influence of the position of an additional 4 mg/cycle for a twin-pilot strategy on the heat release. Conditions:  $-5^{\circ}\text{C}$ ,  $\text{SOI}_{\text{Main}} = -8^{\circ}\text{ATDC}$ , 1000 rev/min, 400 bar rail pressure,  $850^{\circ}\text{C}$  glow plug, 16 mg/cycle total fuel

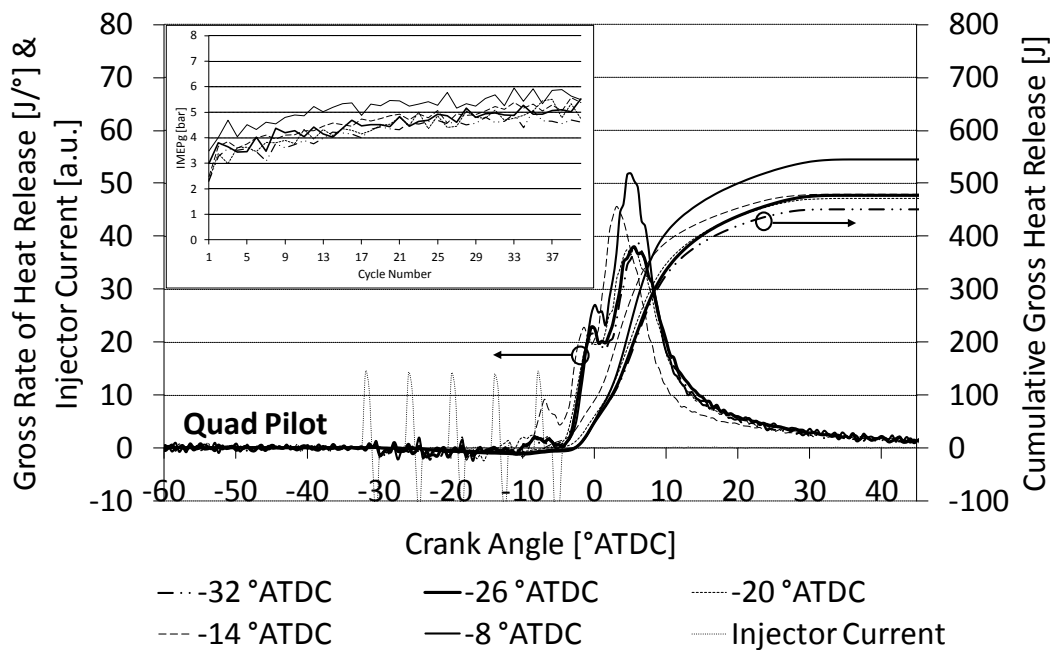


Figure 5-41. Influence of the position of an additional 4 mg/cycle for a quad-pilot strategy on the heat release. Conditions:  $-5^{\circ}\text{C}$ ,  $\text{SOI}_{\text{Main}} = -8^{\circ}\text{ATDC}$ , 1000 rev/min, 400 bar rail pressure,  $850^{\circ}\text{C}$  glow plug, 16 mg/cycle total fuel

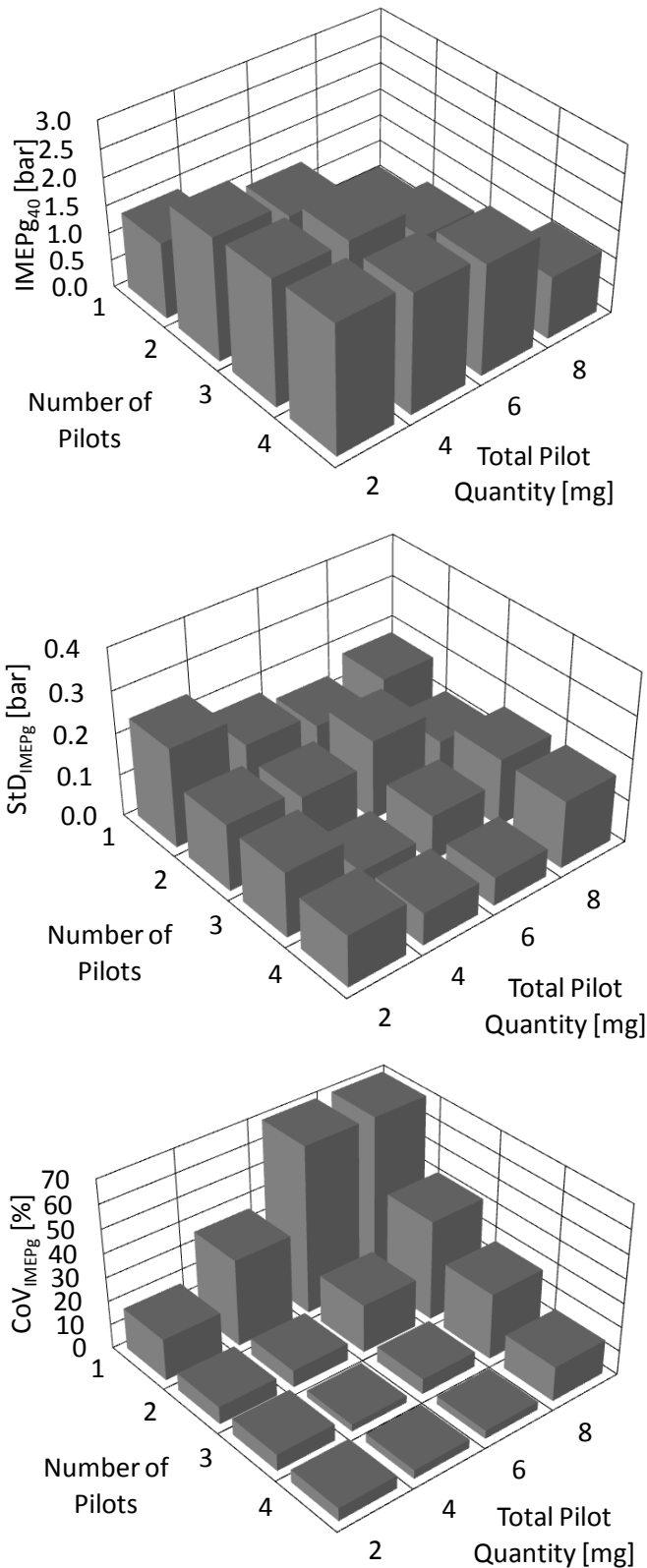


Figure 5-42. The effect of number of pilots and total pilot quantity. Conditions: 10°C, SOI<sub>Main</sub> = -8 °ATDC, 6 °CA separation, 1000 rev/min, 400 bar rail pressure, 850°C glow plug, 9 mg/cycle total fuel (CoV<sub>IMEPg</sub> scale has been capped at 70% to maintain clarity, single-pilot results are in the region of 17-141%)

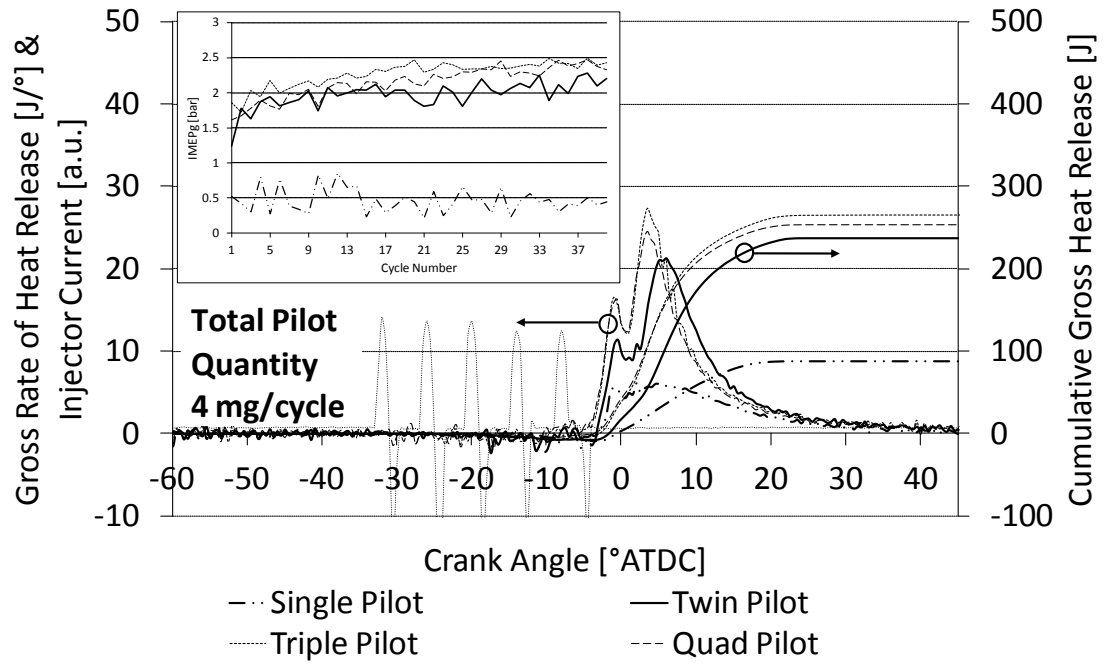


Figure 5-43. 40 cycle ensemble averaged heat release with 4 mg/cycle total pilot quantity. Conditions: 10°C,  $SOI_{Main} = -8$  °ATDC, 6 °CA separation, 1000 rev/min, 400 bar rail pressure, 850°C glow plug, 9 mg/cycle total fuel, injector current shown for quad-pilot case

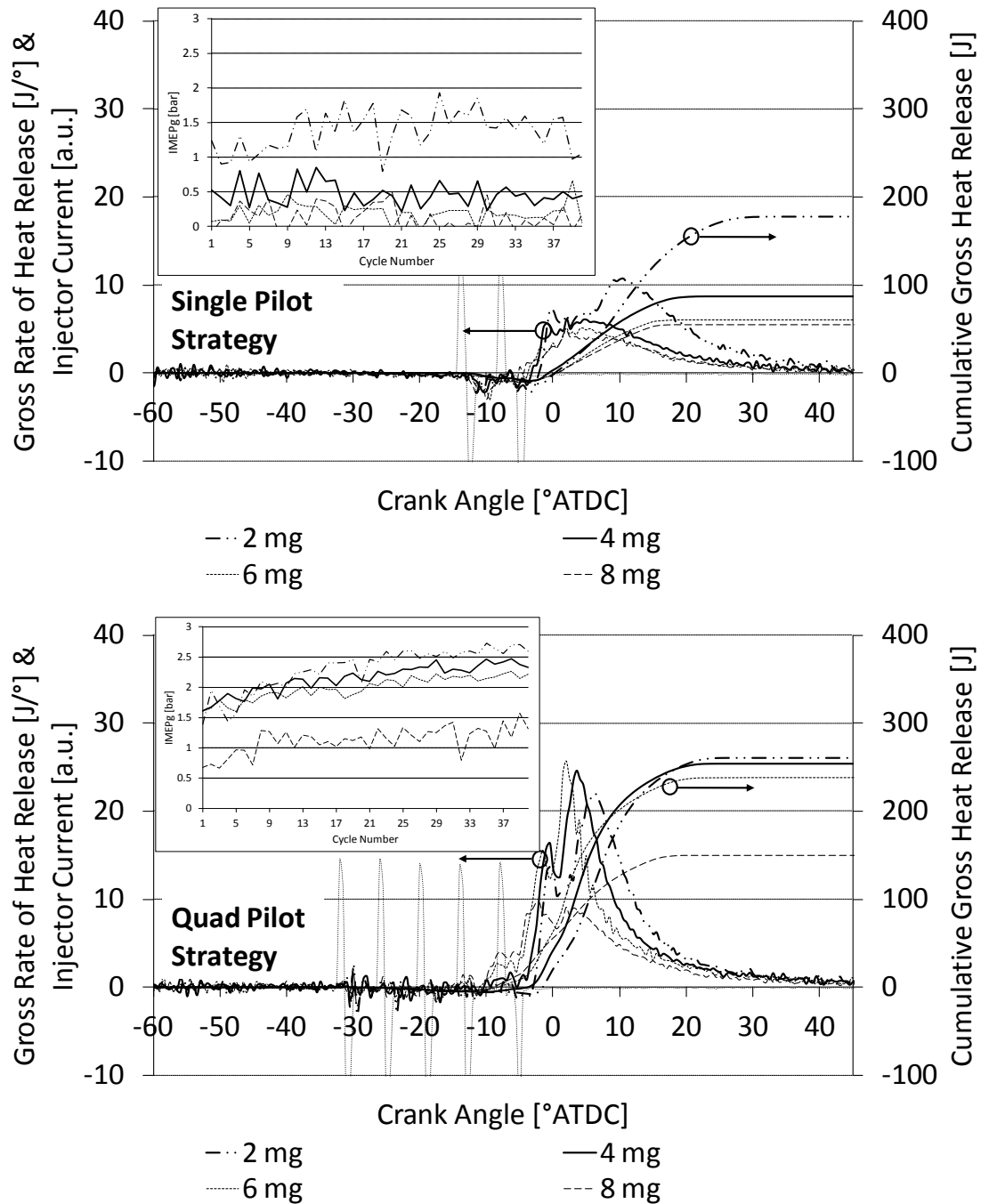


Figure 5-44. Effect of varying total pilot quantity on 40 cycle ensemble averaged heat release (top) single-pilot (bottom) quad-pilot strategy. Conditions: 10°C,  $SOI_{Main} = -8$  °ATDC, 6 °CA separation, 1000 rev/min, 400 bar rail pressure, 850°C glow plug, 9 mg/cycle total fuel

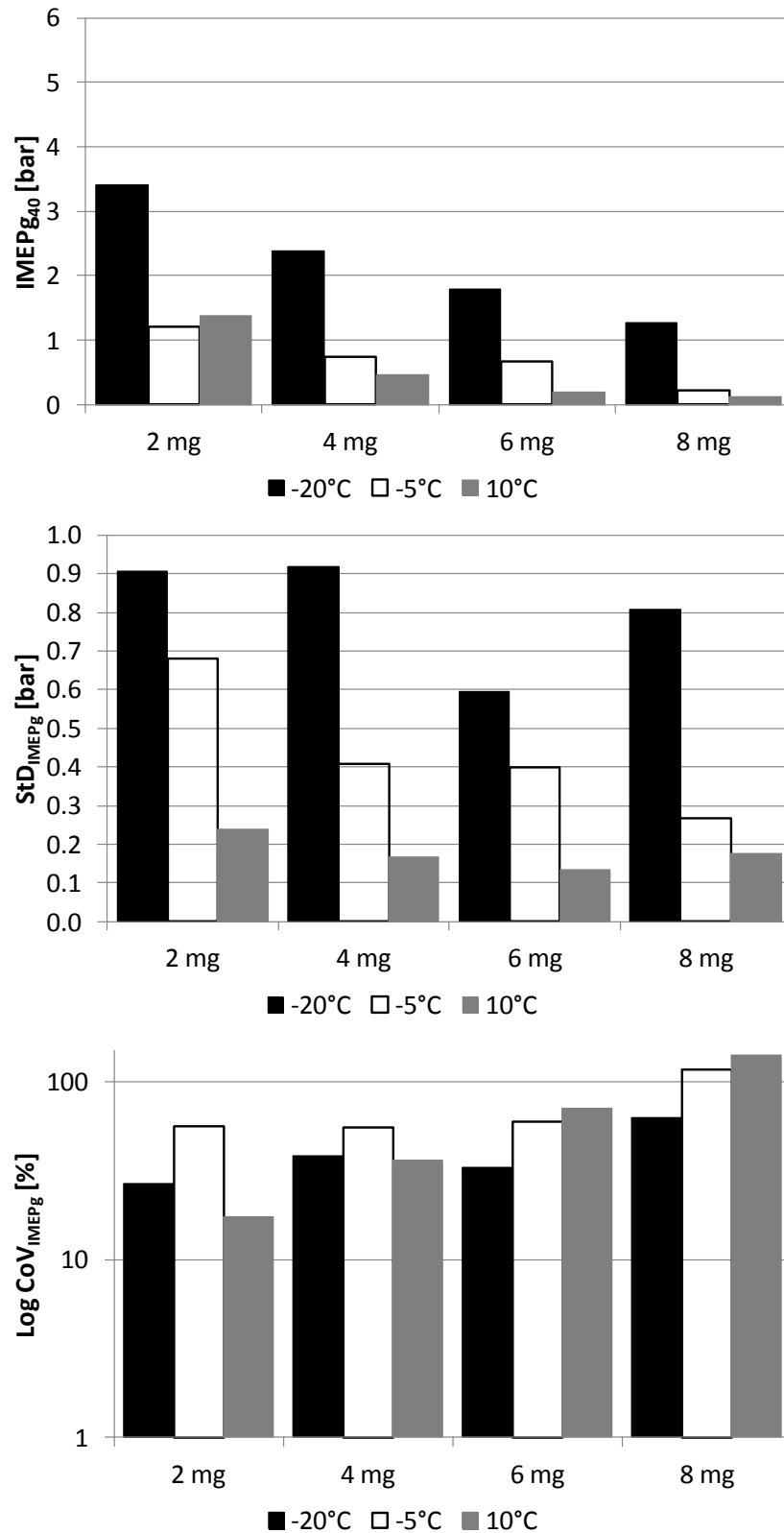


Figure 5-45. Dependency of performance indicators on total pilot quantity at various soak temperatures for a single-pilot strategy. Conditions:  $SOI_{Main} = -8$  °ATDC, 6 °CA separation, 1000 rev/min, 400 bar rail pressure, 850°C glow plug, 18 mg/cycle total fuel at -20°C, 12 mg/cycle total fuel at -5°C and 9 mg/cycle total fuel at 10°C

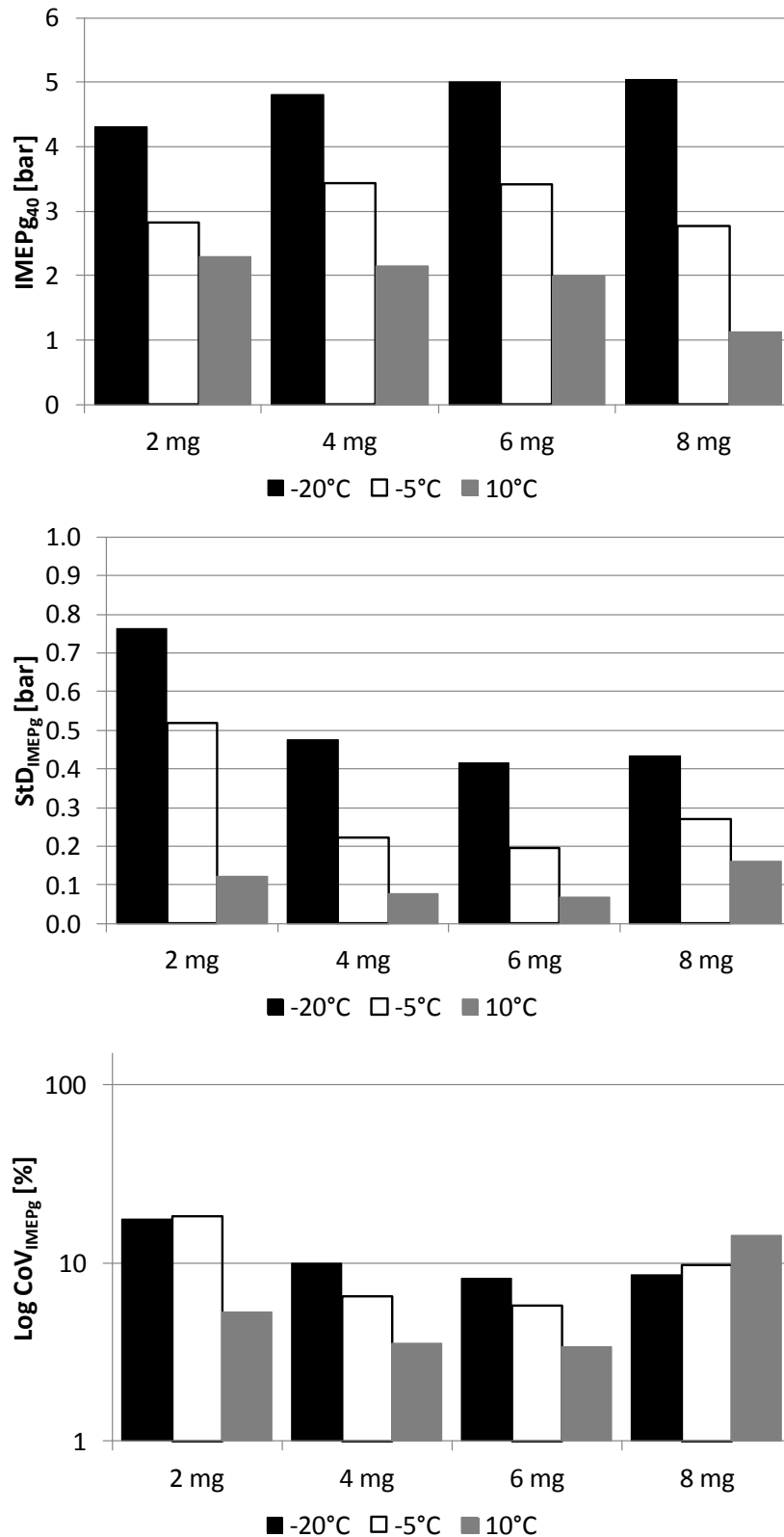
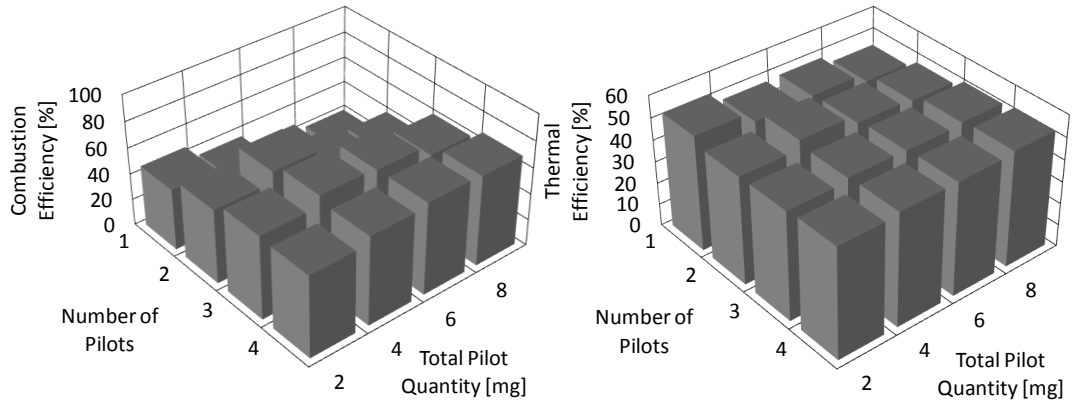
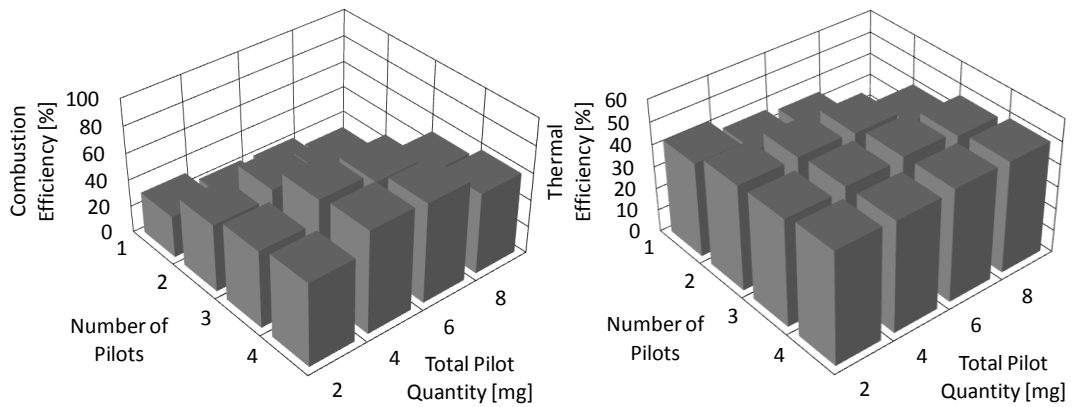


Figure 5-46. Dependency of performance indicators on total pilot quantity at various soak temperatures for a quad-pilot strategy. Conditions: SOI<sub>Main</sub> = -8 °ATDC, 6 °CA separation, 1000 rev/min, 400 bar rail pressure, 850°C glow plug, 18 mg/cycle total fuel at -20°C, 12 mg/cycle total fuel at -5°C and 9 mg/cycle total fuel at 10°C

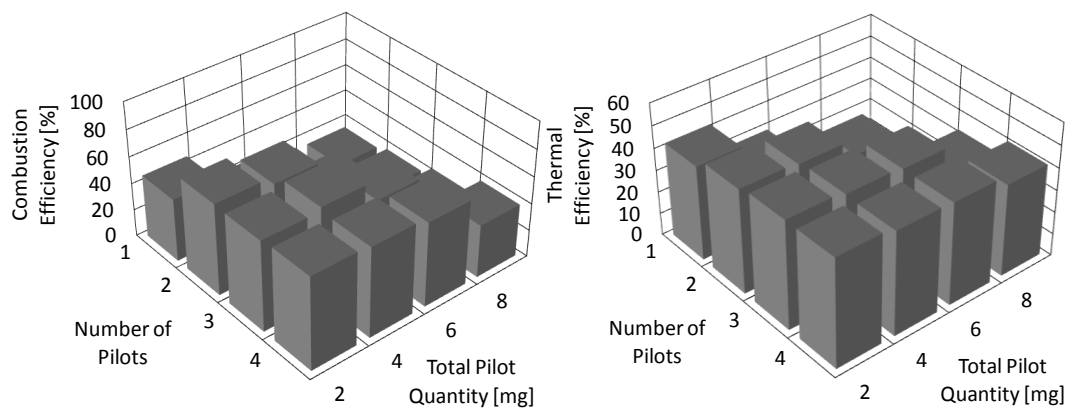
Figures



**Figure 5-47. The effect of injection strategy on indicated combustion and thermal efficiency at -20°C. Conditions:  $SOI_{Main} = -8^\circ$  ATDC, 6 °CA separation, 1000 rev/min, 400 bar rail pressure, 850°C glow plug, 18 mg/cycle total fuel**



**Figure 5-48. The effect of injection strategy on indicated combustion and thermal efficiency at -5°C. Conditions:  $SOI_{Main} = -8^\circ$  ATDC, 6 °CA separation, 1000 rev/min, 400 bar rail pressure, 850°C glow plug, 12 mg/cycle total fuel**



**Figure 5-49. The effect of injection strategy on indicated combustion and thermal efficiency at 10°C. Conditions:  $SOI_{Main} = -8^\circ$  ATDC, 6 °CA separation, 1000 rev/min, 400 bar rail pressure, 850°C glow plug, 9 mg/cycle total fuel**

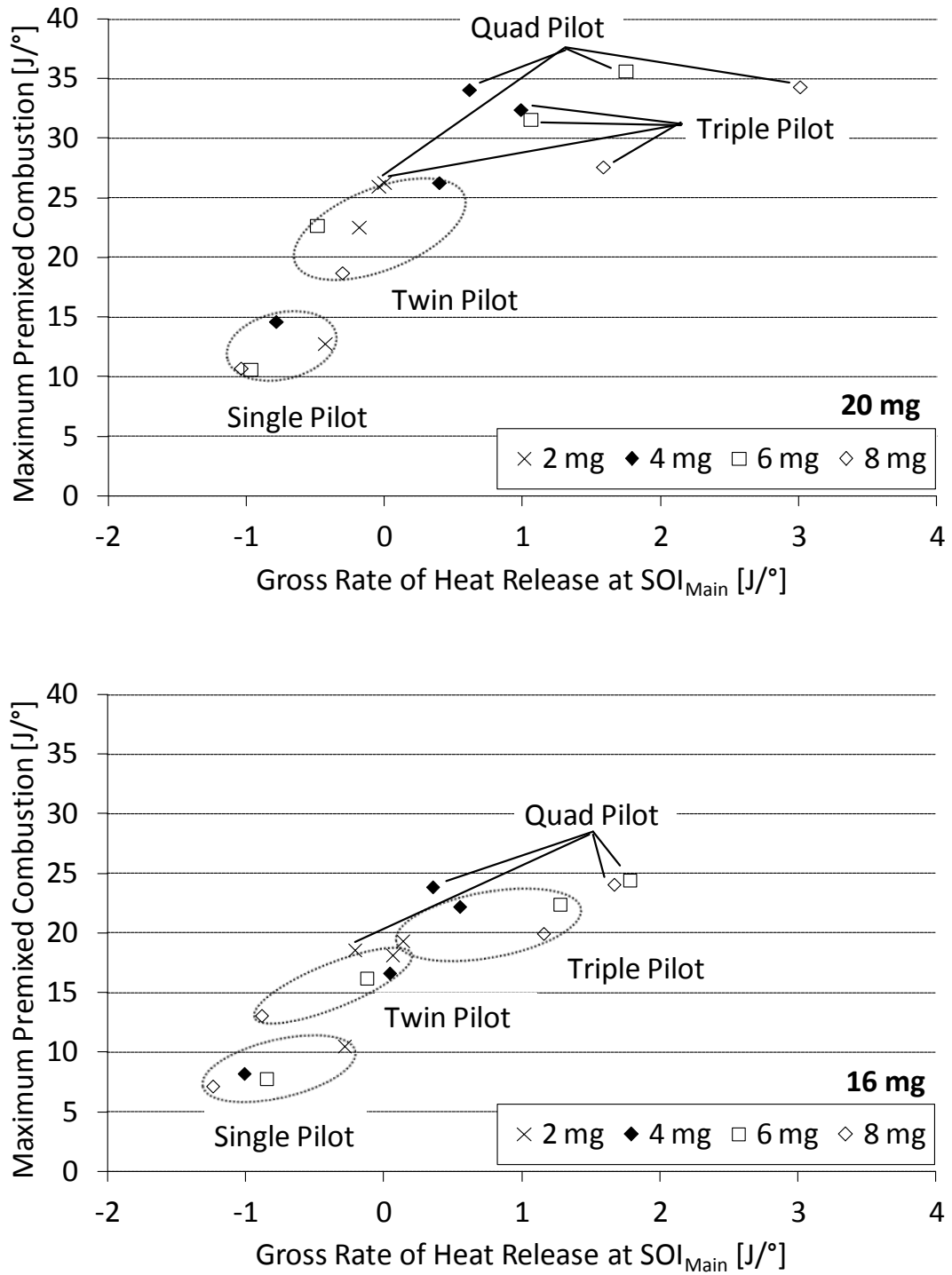


Figure 5-50. 40 cycle ensemble averaged gross rate of heat release around main timing and the influence on maximum premixed combustion with varying total pilot quantities; (top) 20 mg/cycle total fuel (bottom) 16 mg/cycle total fuel. Conditions: - 20°C, SOI<sub>Main</sub> = -8 °ATDC, 6 °CA separation, 1000 rev/min, 400 bar rail pressure, 850°C glow plug



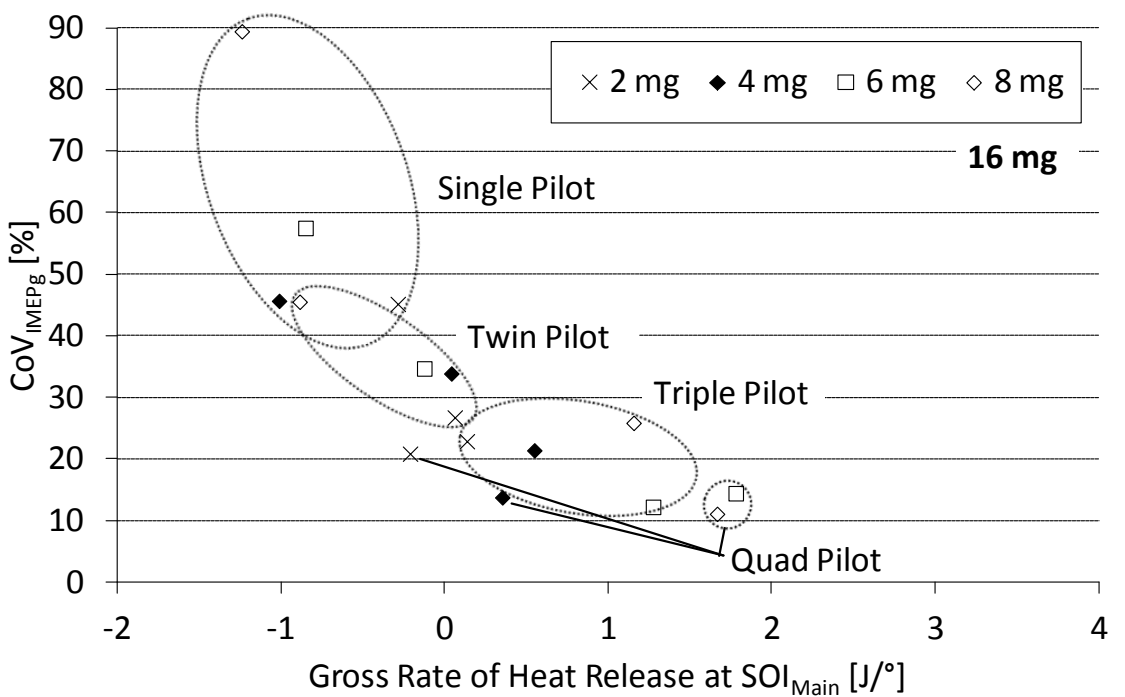
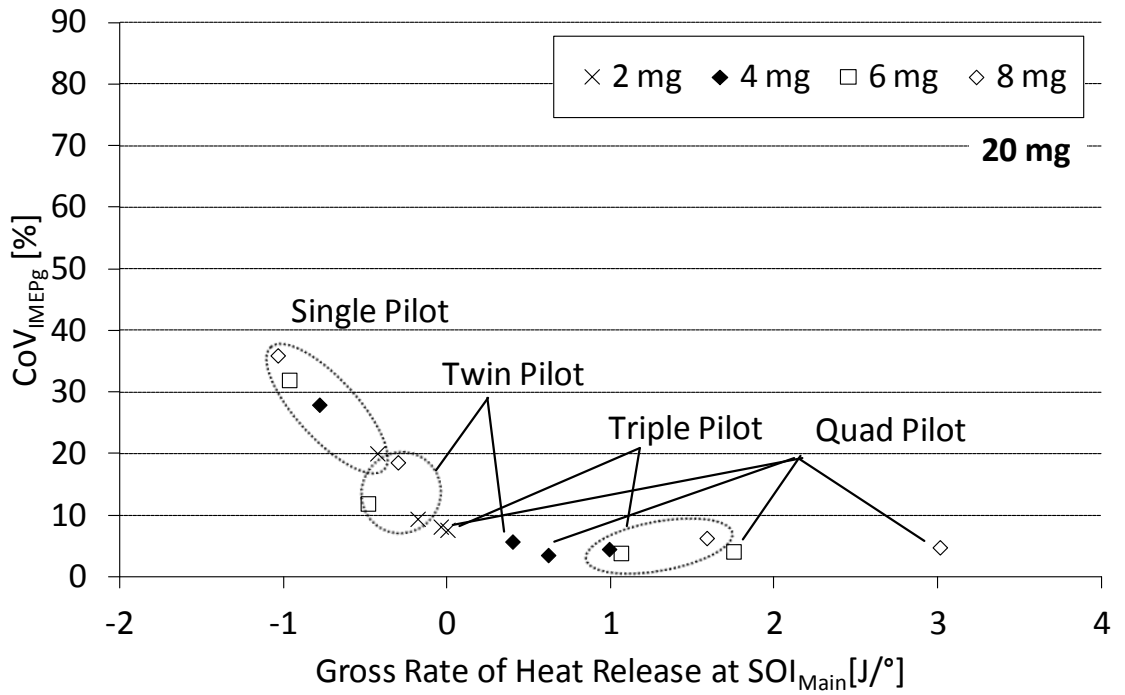


Figure 5-51. The effect of gross rate of heat release at main timing on stability; (top) 20 mg/cycle total fuel (bottom) 16 mg/cycle total fuel. Conditions: -20 °C, SOI<sub>Main</sub> = -8 °ATDC, 6° separation, 1000 rev/min, 400 bar rail pressure, 850°C glow plug

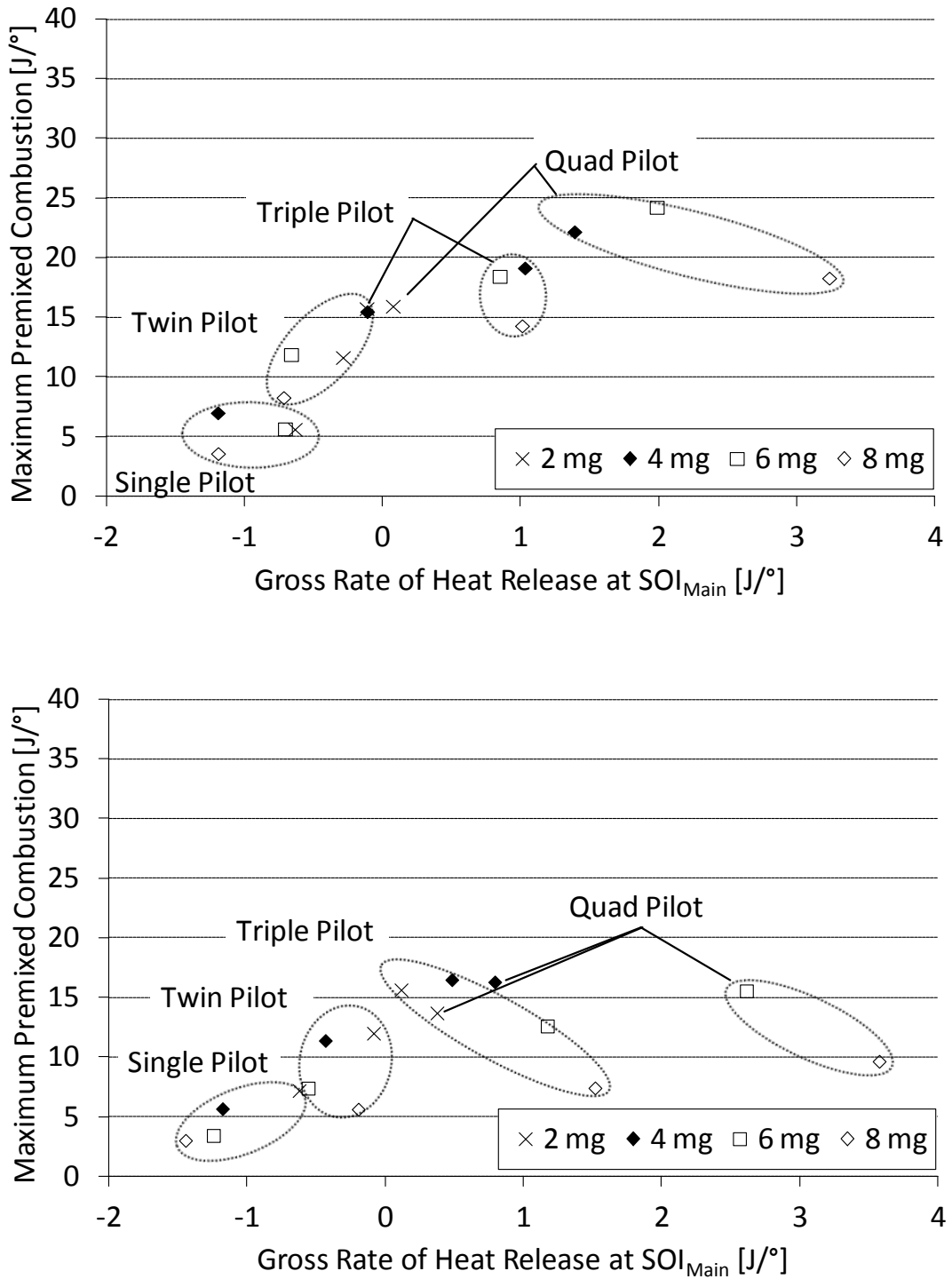


Figure 5-52. 40 cycle ensemble averaged gross rate of heat release around main timing and the influence on maximum premixed combustion with varying total pilot quantities; (top) -5°C, 12 mg/cycle total fuel (bottom) 10°C, 9 mg/cycle total fuel. Conditions: SOI<sub>Main</sub> = -8 °ATDC, 6 °CA separation, 1000 rev/min, 400 bar rail pressure, 850°C glow plug

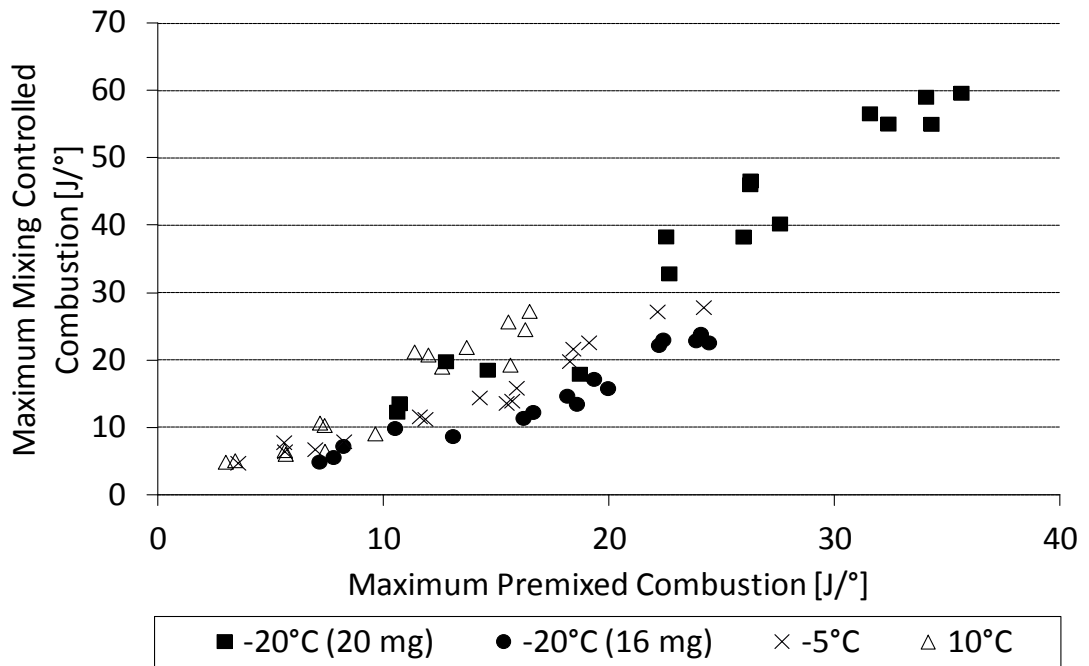


Figure 5-53. Dependency of combustion development on the maximum premixed combustion for various soak temperatures. Conditions:  $SOI_{Main} = -8$  °ATDC, 6 °CA separation, 1000 rev/min, 400 bar rail pressure, 850°C glow plug. Total fuelling levels; 20 mg/cycle at -20°C, 16 mg/cycle at -20°C, 12 mg/cycle at -5°C and 9 mg/cycle at 10°C

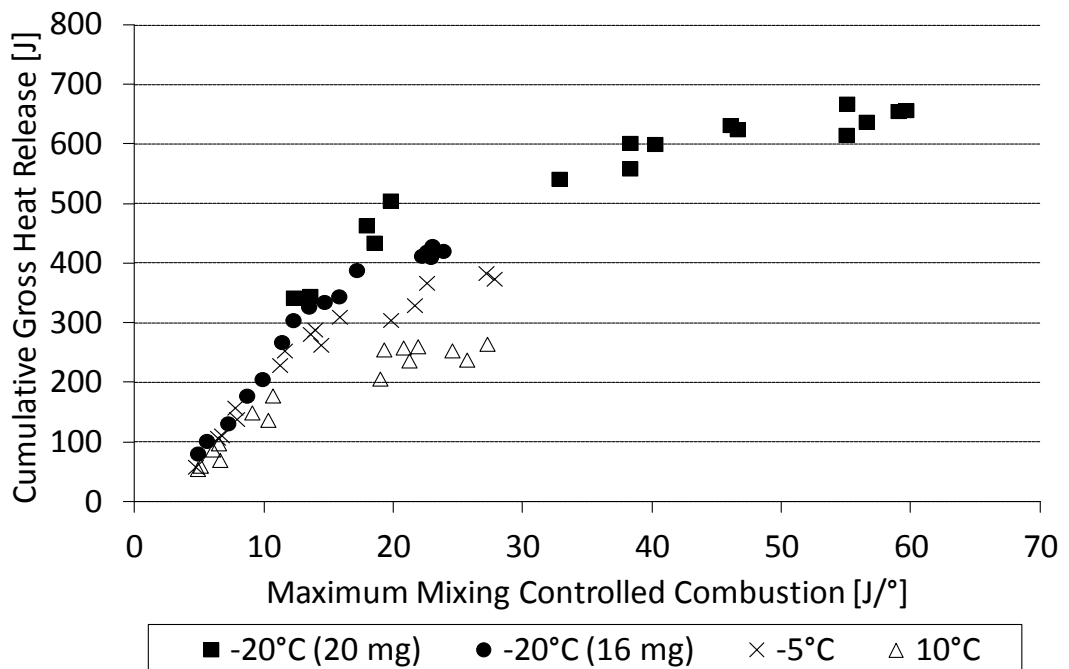
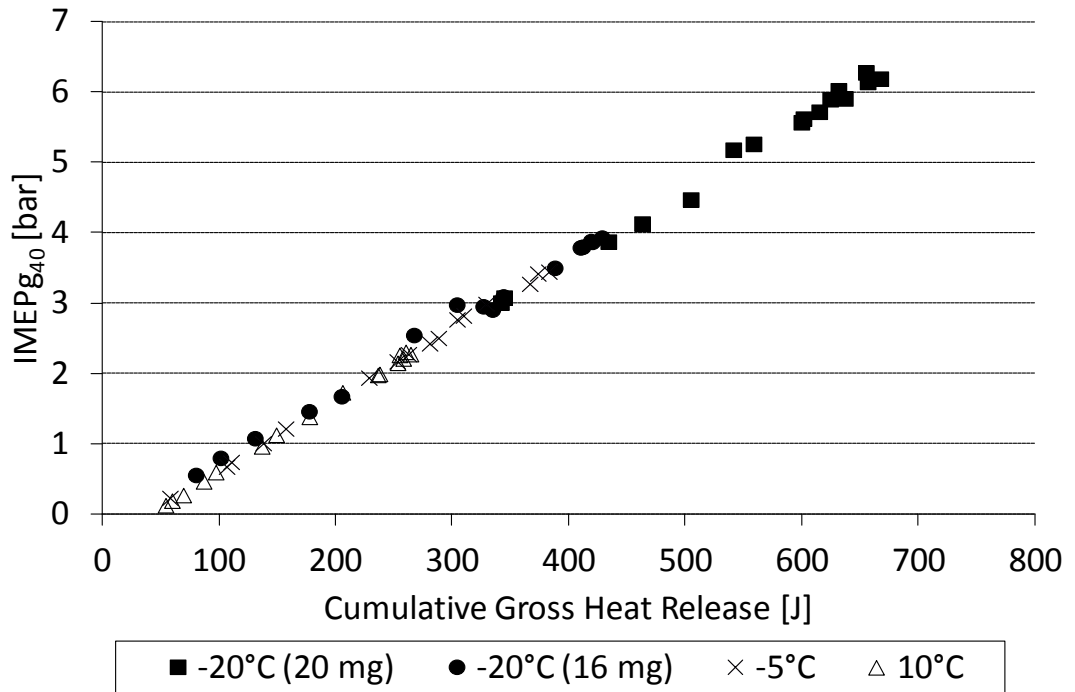


Figure 5-54. Dependency of cumulative gross heat release on combustion development for various soak temperatures. Conditions:  $SOI_{Main} = -8$  °ATDC, 6 °CA separation, 1000 rev/min, 400 bar rail pressure, 850°C glow plug. Total fuelling levels; 20 mg/cycle at -20°C, 16 mg/cycle at -20°C, 12 mg/cycle at -5°C and 9 mg/cycle at 10°C



**Figure 5-55. Dependency of IMEP<sub>g</sub> on cumulative gross heat release for various soak temperatures. Conditions: SOI<sub>Main</sub> = -8 °ATDC, 6 °CA separation, 1000 rev/min, 400 bar rail pressure, 850°C glow plug. Total fuelling levels; 20 mg/cycle at -20°C, 16 mg/cycle at -20°C, 12 mg/cycle at -5°C and 9 mg/cycle at 10°C**

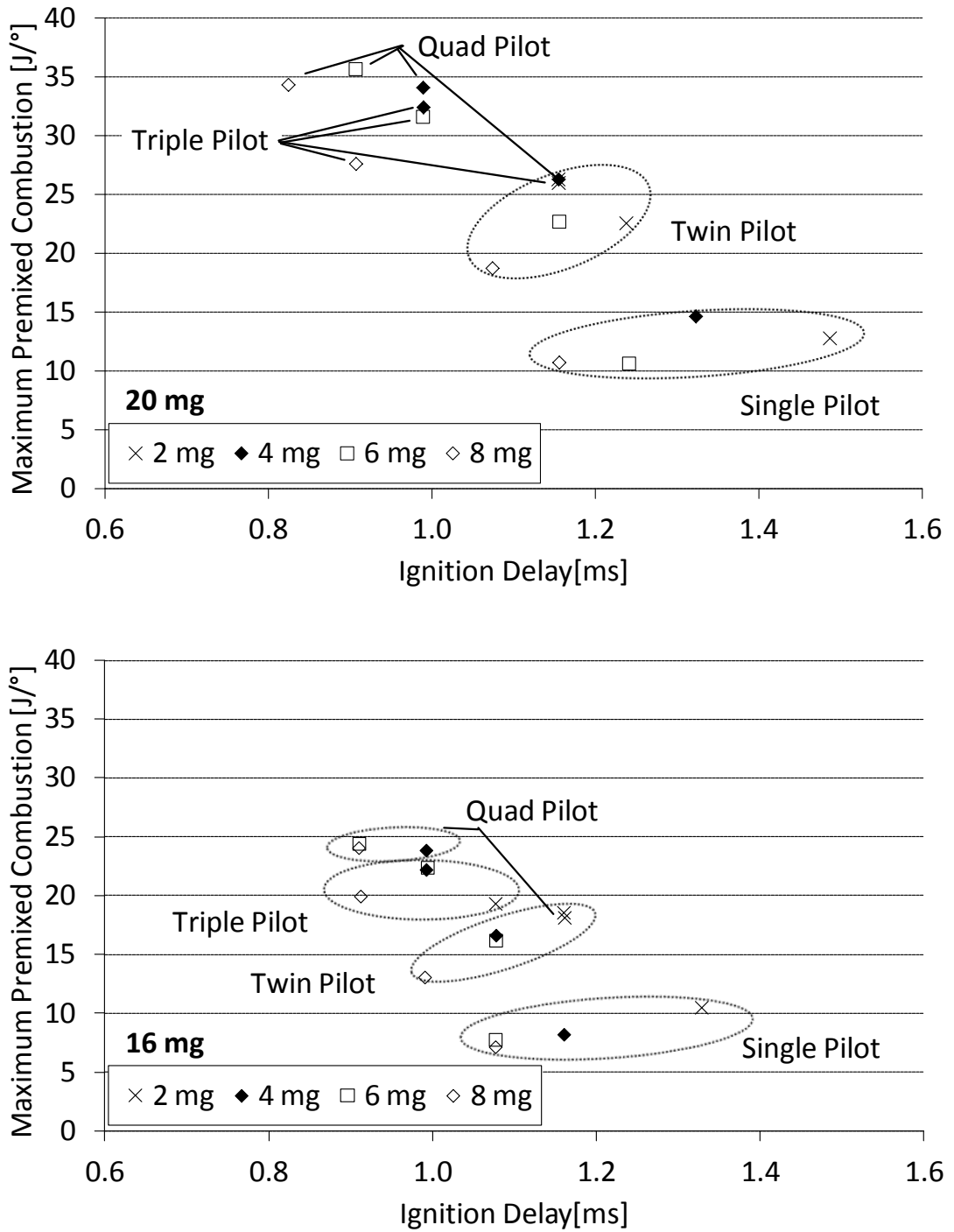


Figure 5-56. The effect of injection strategy and dependency of maximum premixed combustion on ignition delay; (top), 20 mg/cycle total fuel (bottom), 16 mg/cycle total fuel. Conditions:  $-20^{\circ}\text{C}$ ,  $\text{SOI}_{\text{Main}} = -8^{\circ}\text{ATDC}$ ,  $6^{\circ}\text{CA}$  separation, 1000 rev/min, 400 bar rail pressure,  $850^{\circ}\text{C}$  glow plug

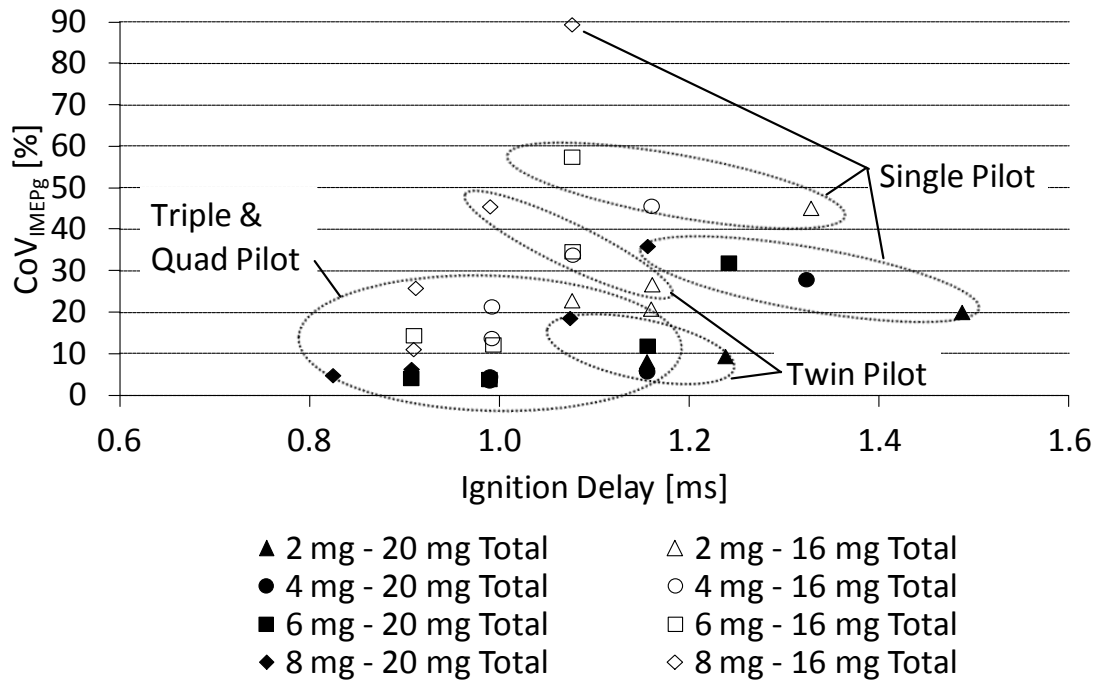


Figure 5-57. 40 cycle ensemble averaged ignition delay with varying total pilot quantities for 20 mg total fuel and 16 mg/cycle total fuel. Conditions: -20°C, SOI<sub>Main</sub> = -8 °ATDC, 6 °CA separation, 1000 rev/min, 400 bar rail pressure, 850°C glow plug

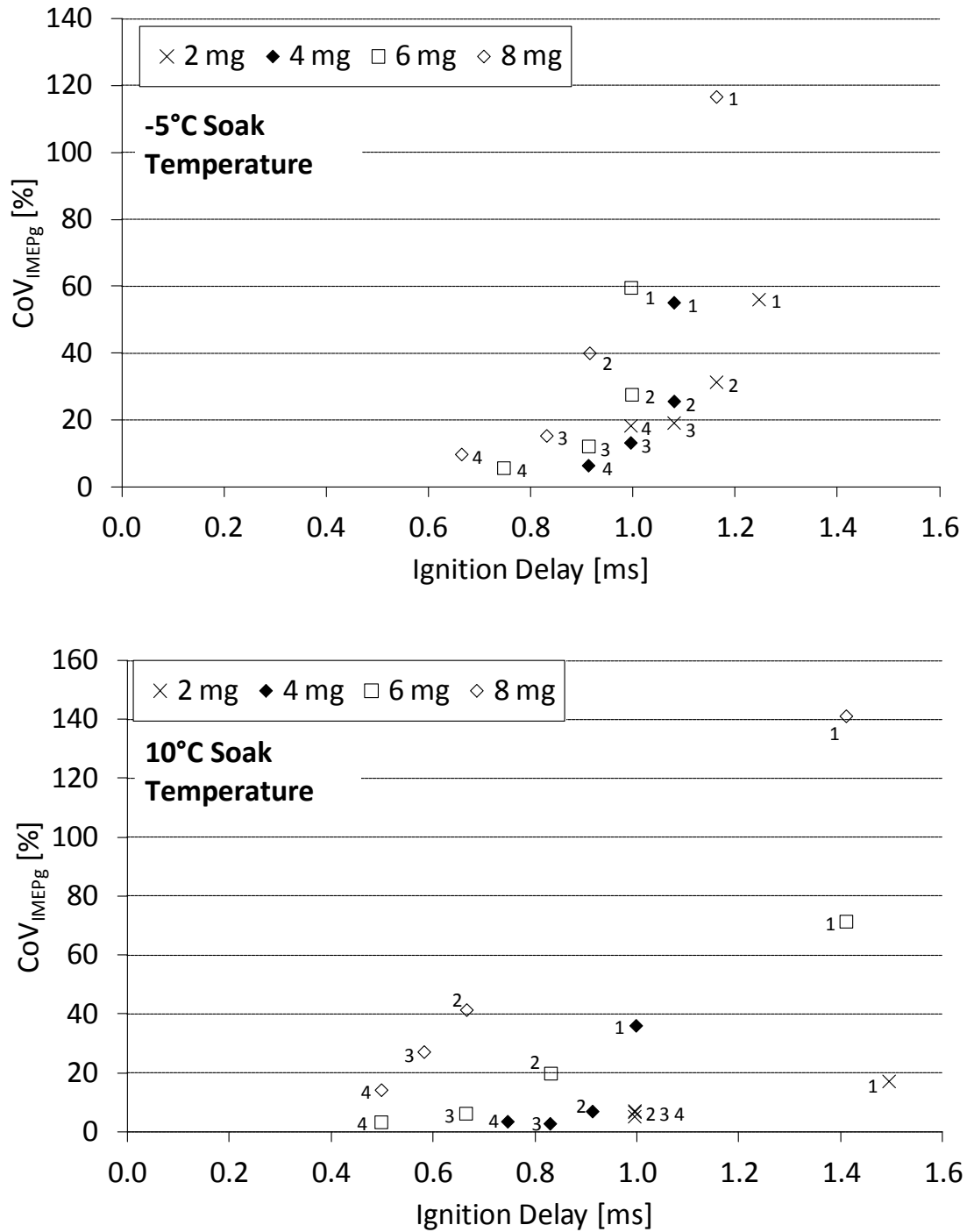


Figure 5-58. Dependence of stability on ignition delay and injection strategy influence at -5°C and 10°C soak temperatures. Conditions:  $SOI_{Main} = -8^\circ ATDC$ ,  $6^\circ CA$  separation, 1000 rev/min, 400 bar rail pressure, 850°C glow plug (numbers on graphs represent the number of pilots)

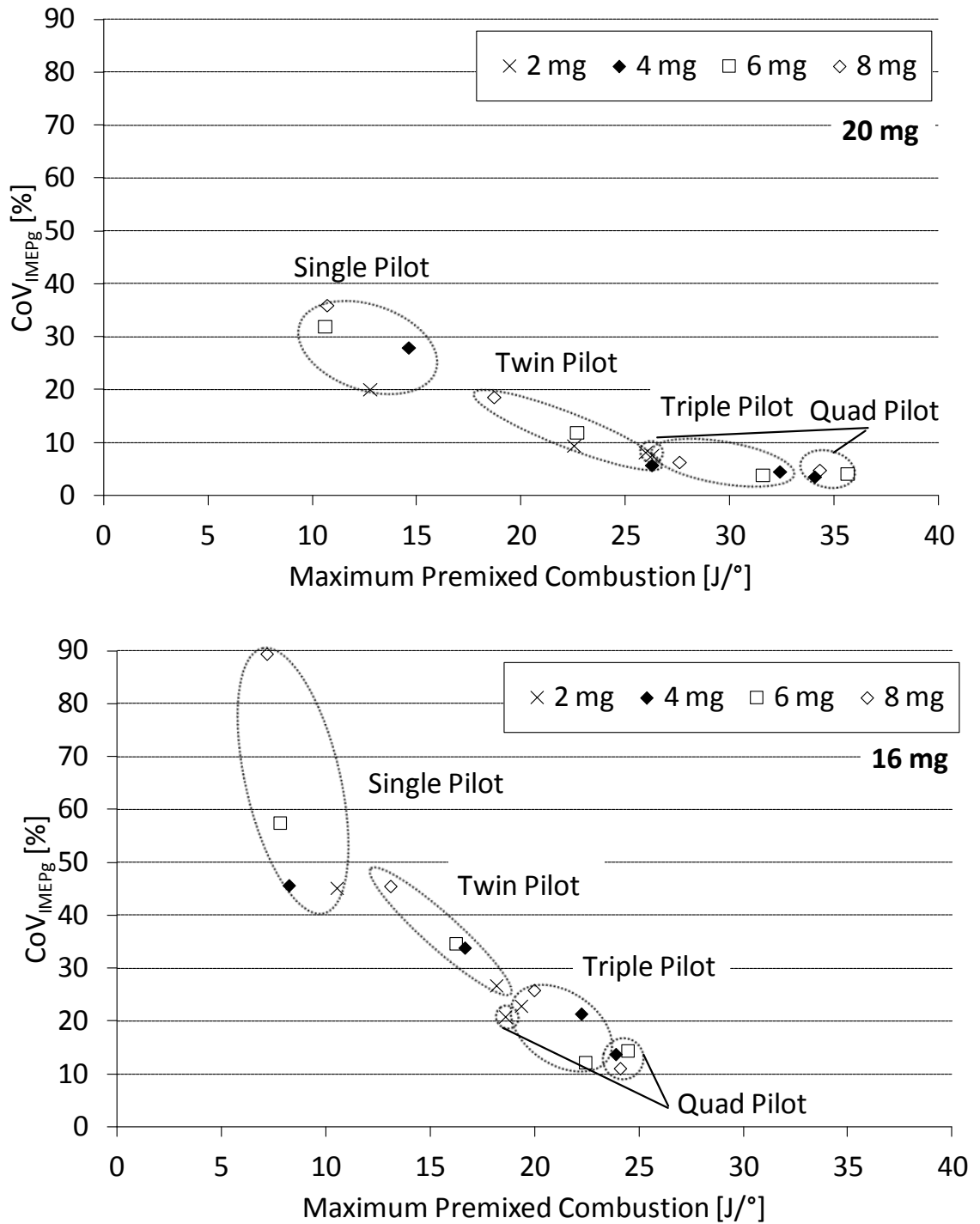


Figure 5-59. 40 cycle ensemble averaged maximum premixed combustion with varying total pilot quantities; (top) 20 mg/cycle total fuel (bottom) 16 mg/cycle total fuel. Conditions: -20°C, SOI<sub>Main</sub> = -8 °ATDC, 6 °CA separation, 1000 rev/min, 400 bar rail pressure, 850°C glow plug



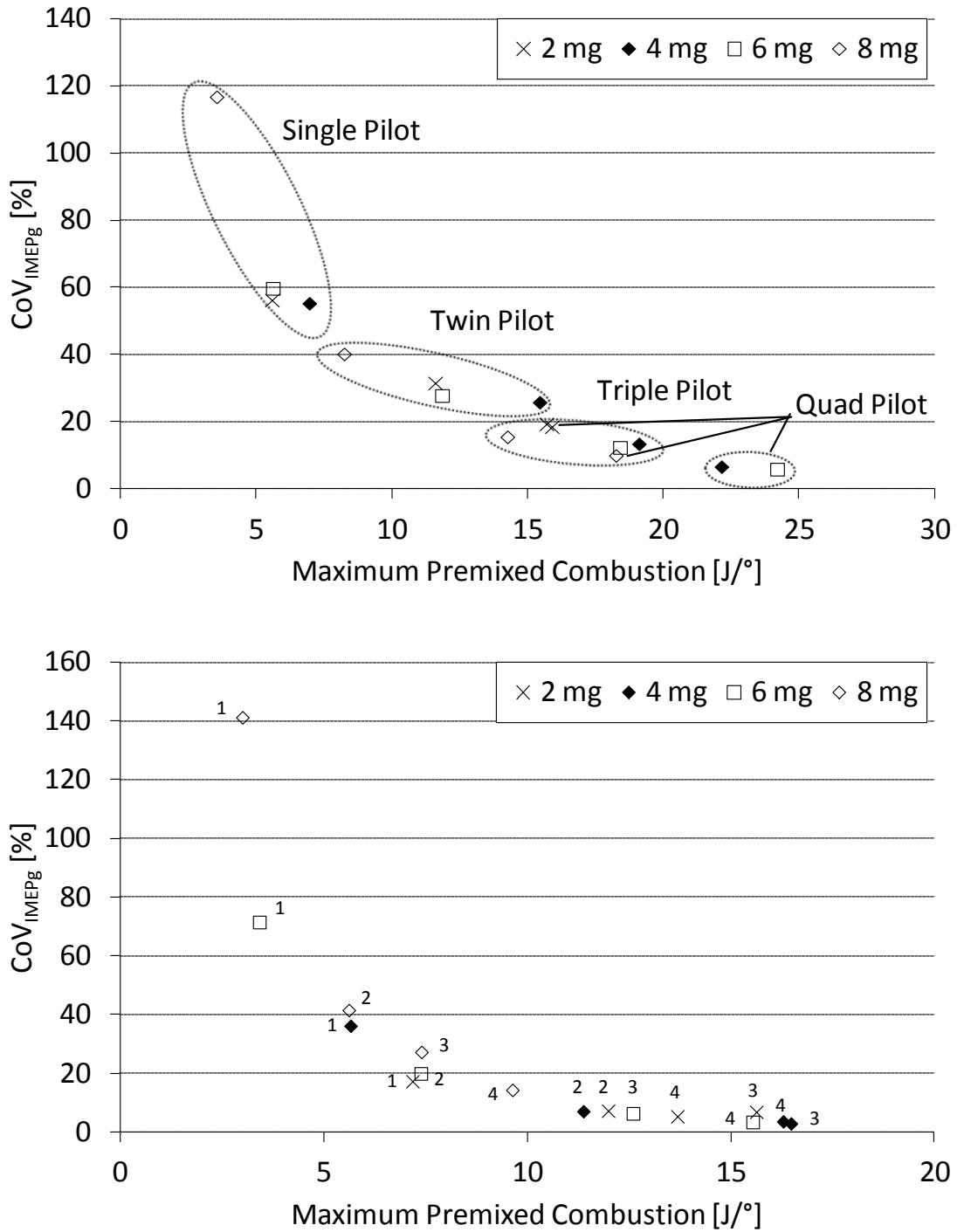


Figure 5-60. 40 cycle ensemble averaged maximum premixed combustion with varying total pilot quantities; (top) -5°C, 12 mg/cycle total fuel (bottom) 10°C, 9 mg/cycle total fuel. Conditions: SOI<sub>Main</sub> = -8 °ATDC, 6 °CA separation, 1000 rev/min, 400 bar rail pressure, 850°C glow plug (numbers on bottom graph represent the number of pilots)

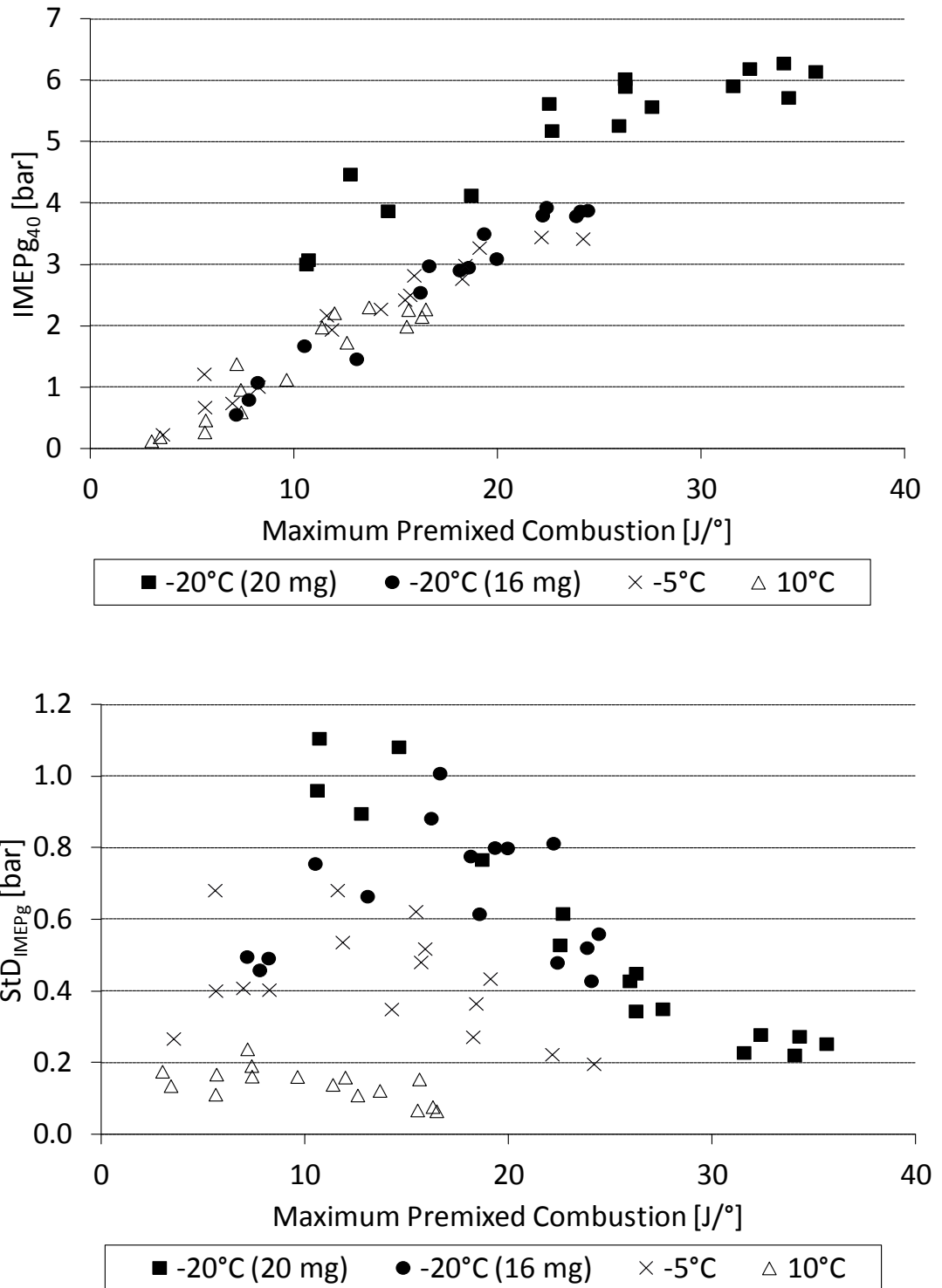


Figure 5-61. Influence of the maximum premixed combustion on IMEP<sub>g</sub> and StD<sub>IMEPg</sub> at different soak temperatures. Conditions: SOI<sub>Main</sub> = -8 °ATDC, 6 °CA separation, 1000 rev/min, 400 bar rail pressure, 850°C glow plug

# Chapter 6

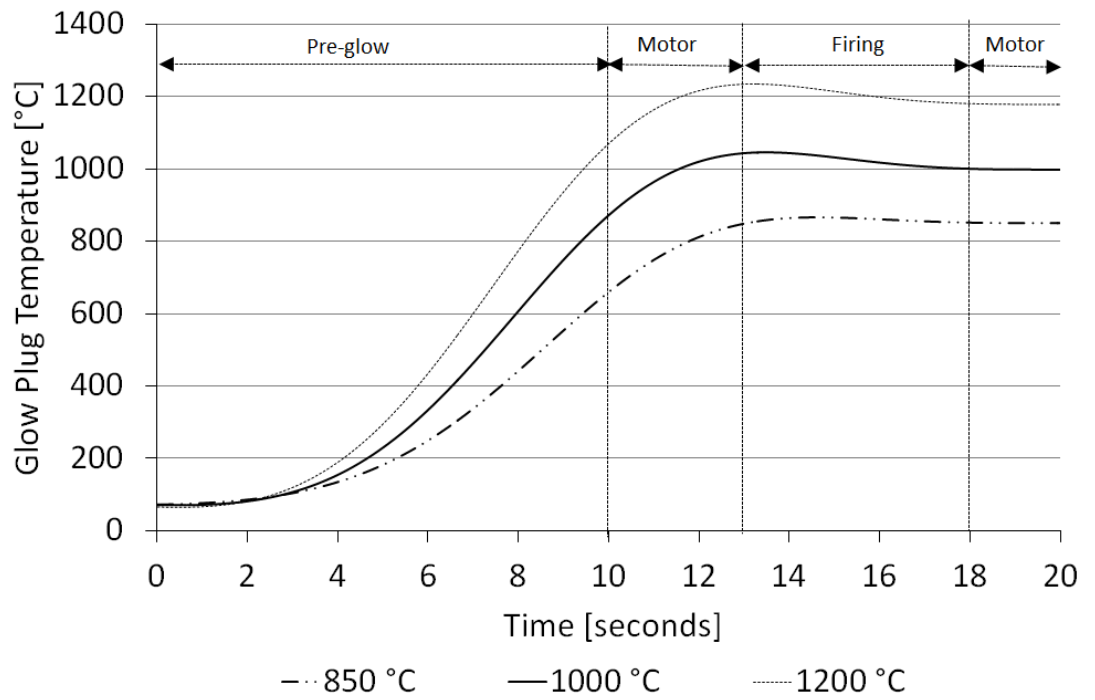


Figure 6-1. Ceramic glow plug internal tip temperature profiles during a typical test period

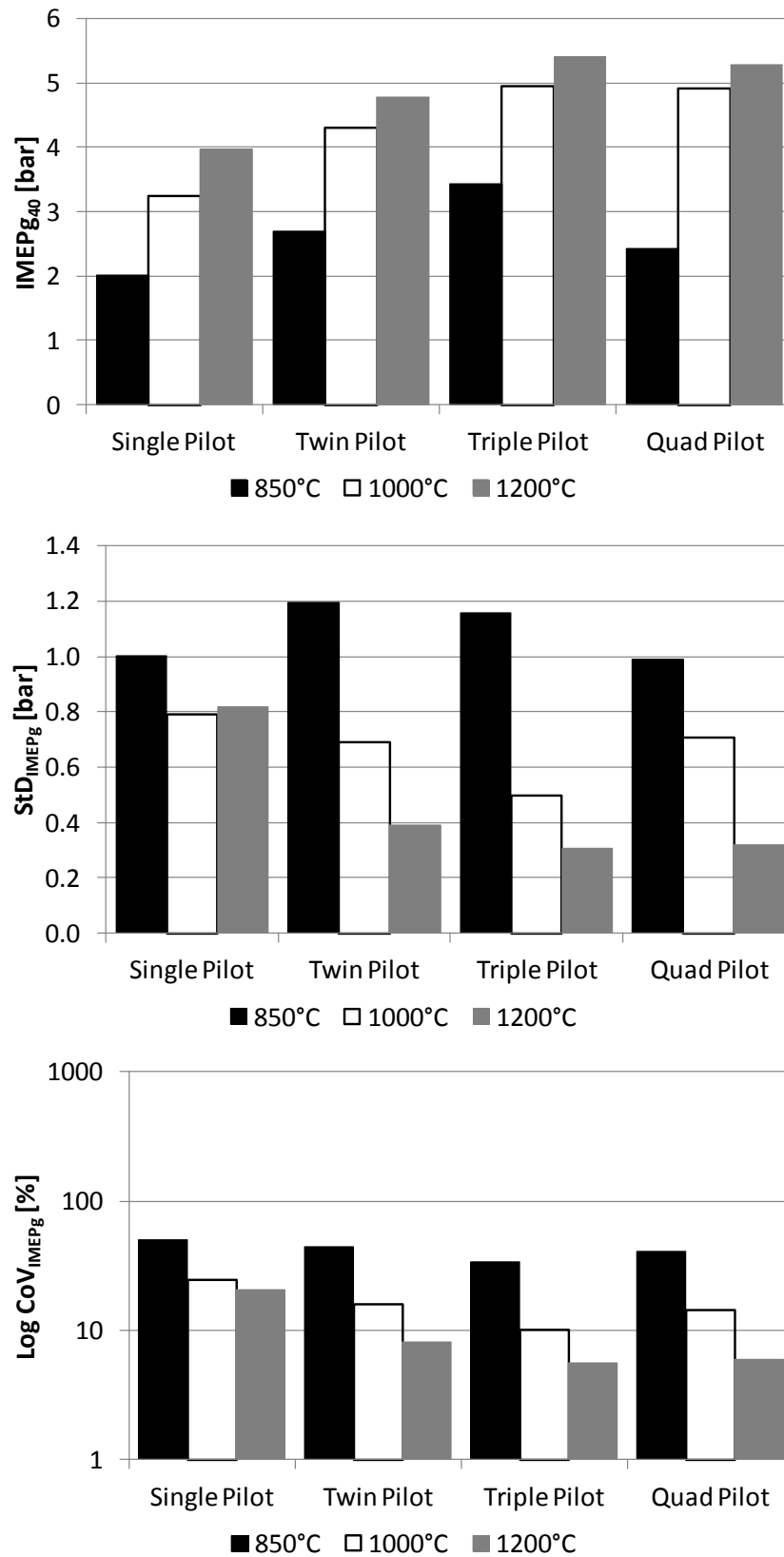


Figure 6-2. Effect of glow plug temperature at -20°C on IMEP<sub>g</sub>, StD<sub>IMEPg</sub> and CoV<sub>IMEPg</sub> for different injection strategies. Conditions: SOI<sub>Main</sub> = -8 °ATDC, 6 °CA separation, 1000 rev/min, 400 bar rail pressure, 18 mg/cycle total fuel

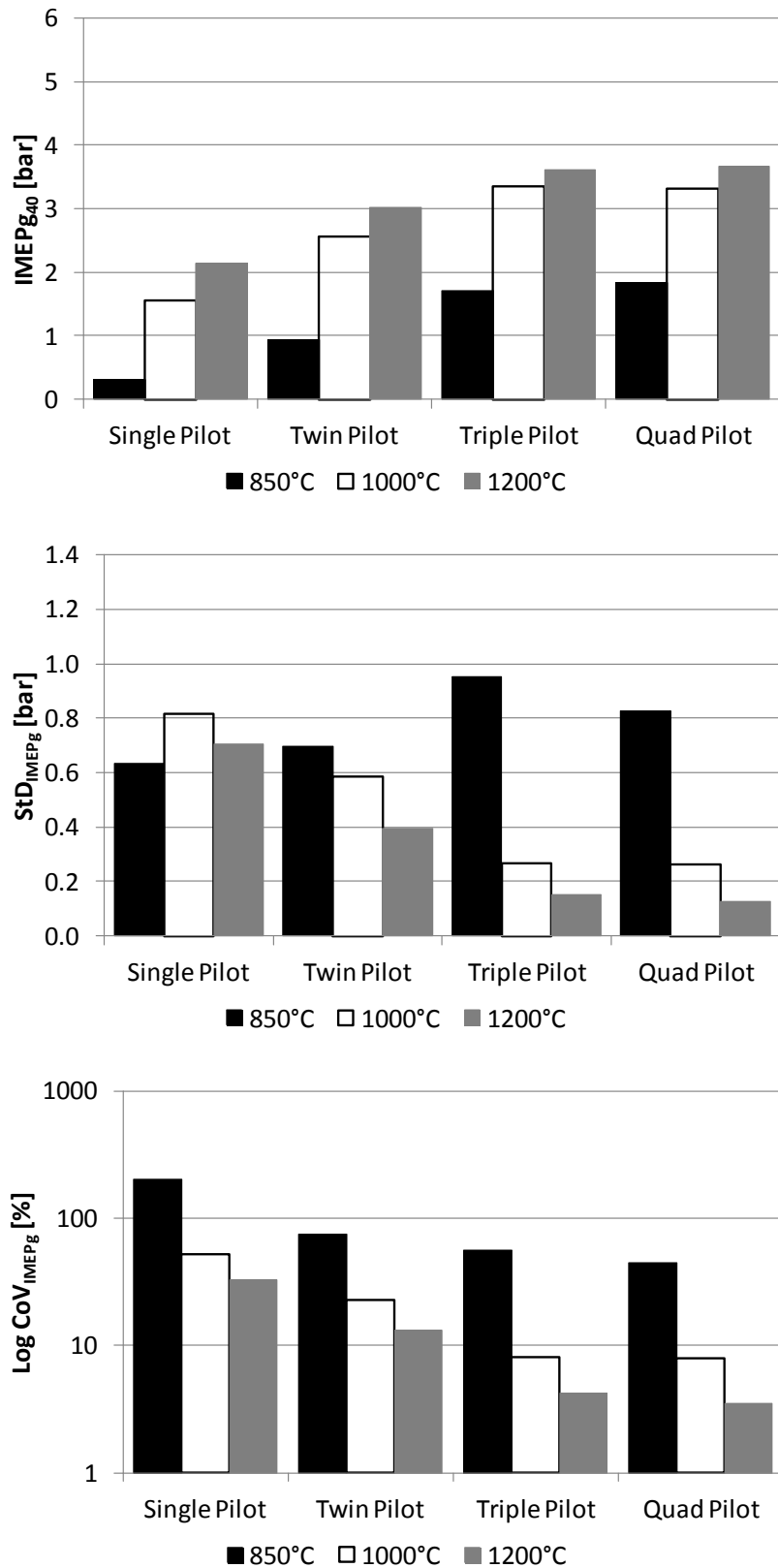


Figure 6-3. Effect of glow plug temperature at -5°C on IMEP<sub>g</sub>, StD<sub>IMEPg</sub> and CoV<sub>IMEPg</sub> for different injection strategies. Conditions: SOI<sub>Main</sub> = -8 °ATDC, 6 °CA separation, 1000 rev/min, 400 bar rail pressure, 12 mg/cycle total fuel

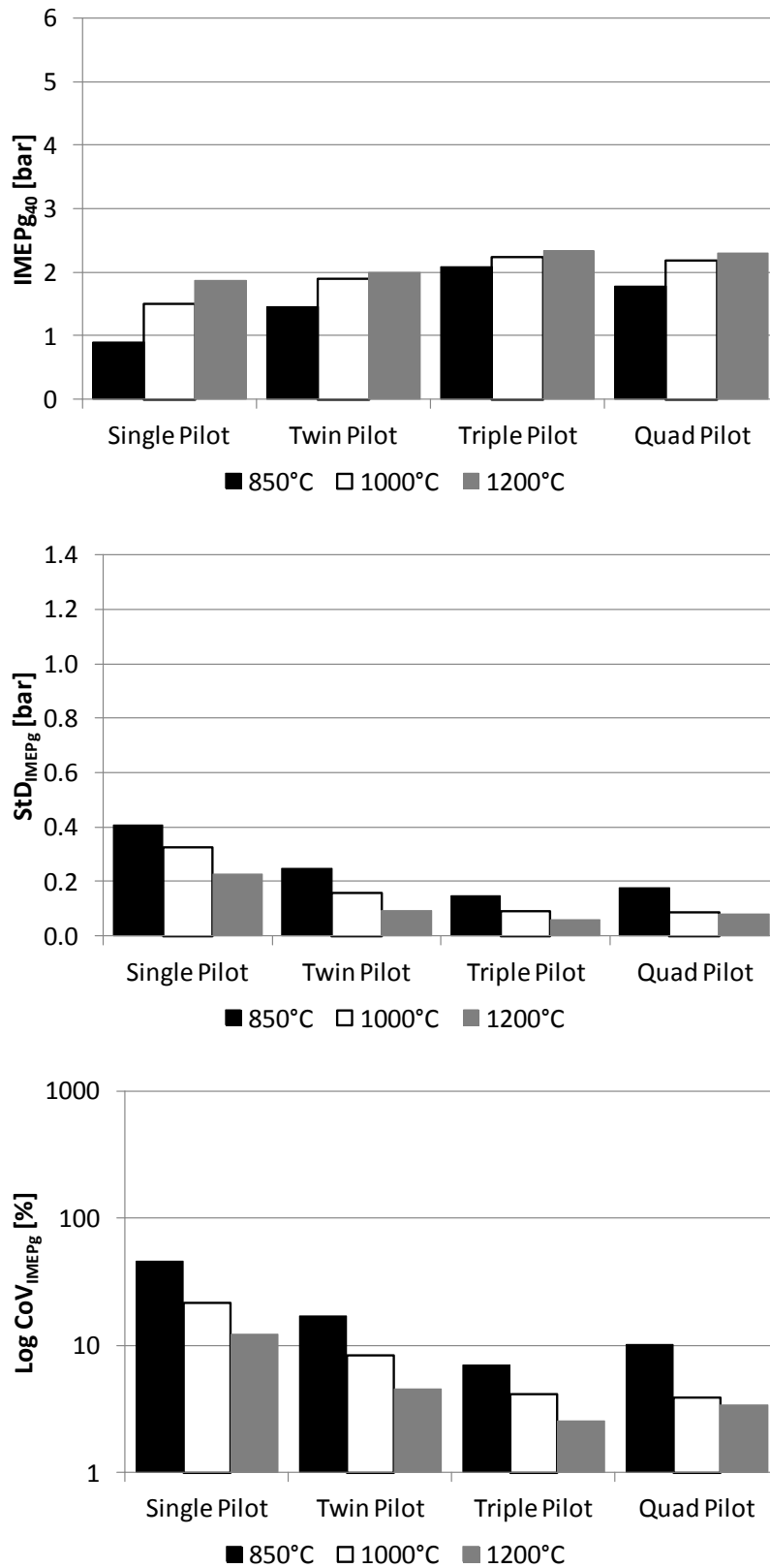


Figure 6-4. Effect of glow plug temperature at 10°C on IMEP<sub>g</sub>, StD<sub>IMEPg</sub> and CoV<sub>IMEPg</sub> for different injection strategies. Conditions: SOI<sub>Main</sub> = -8 °ATDC, 6 °CA separation, 1000 rev/min, 400 bar rail pressure, 9 mg/cycle total fuel

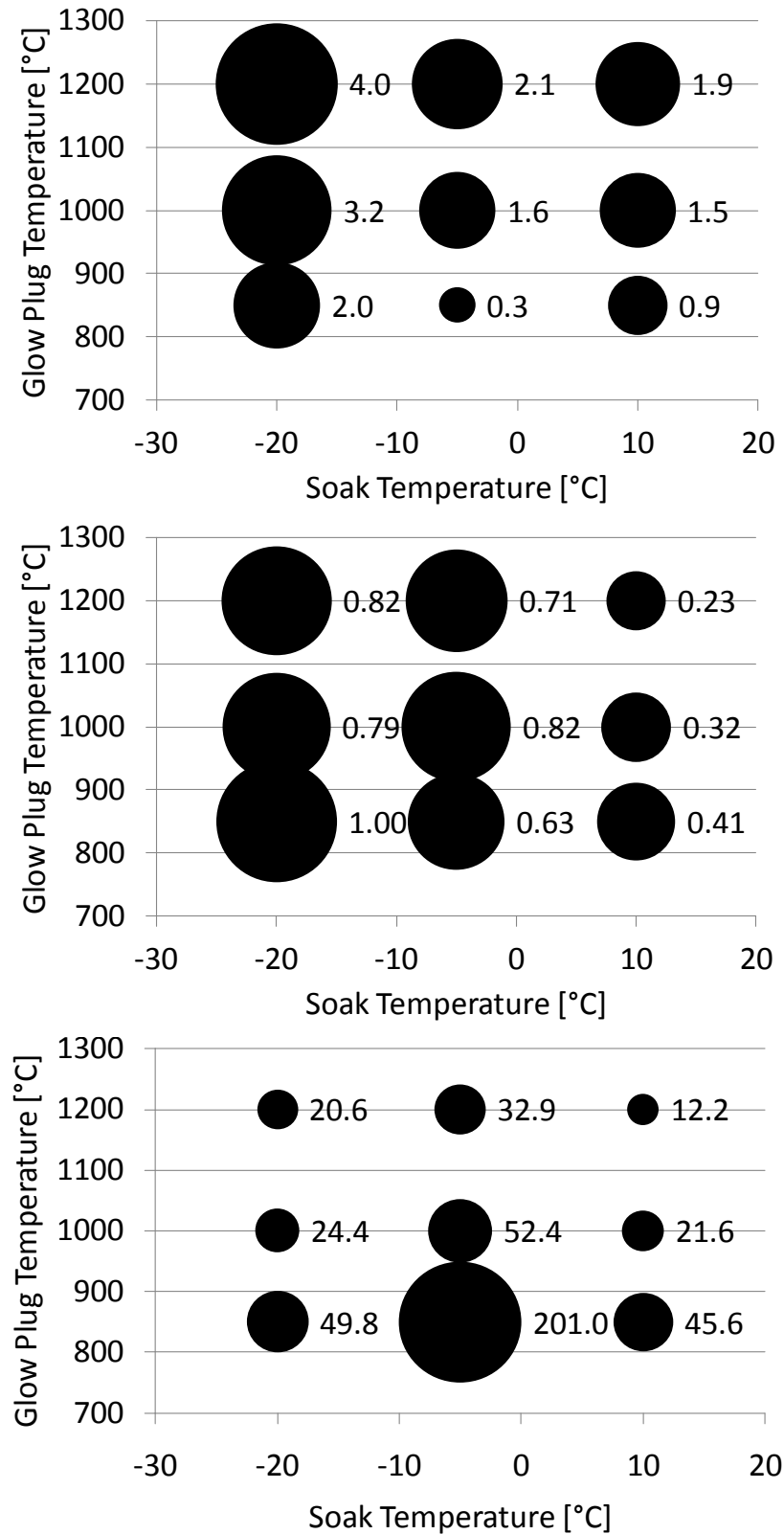


Figure 6-5. Dependence of (top) IMEP<sub>g</sub> (middle) StD<sub>IMEPg</sub> and (bottom) CoV<sub>IMEPg</sub> on glow plug and soak temperature for a single-pilot strategy ( ● size represents 10% CoV<sub>IMEPg</sub>). Conditions: SOI<sub>Main</sub> = -8 °ATDC, 6 °CA separation, 1000 rev/min, 400 bar rail pressure

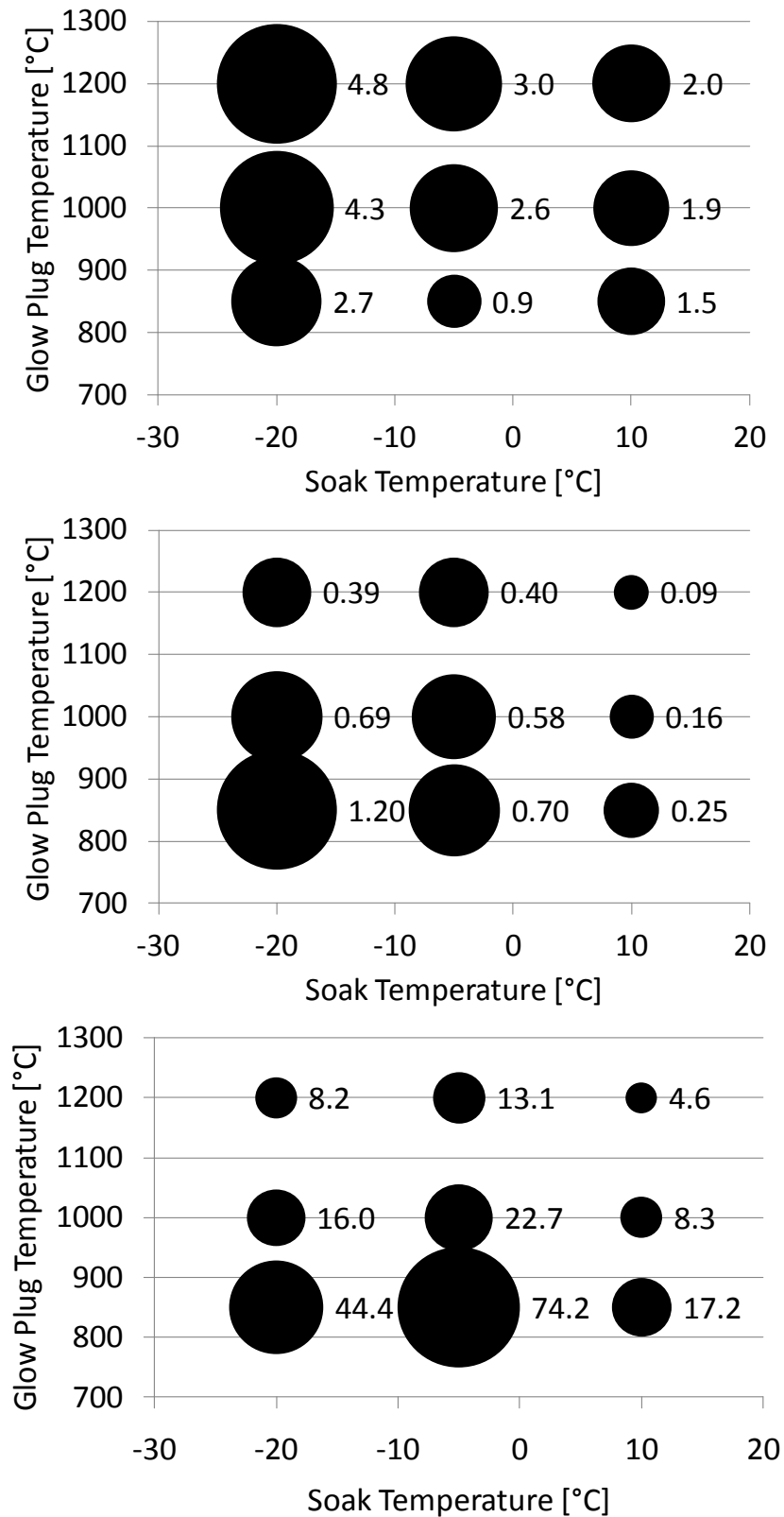


Figure 6-6. Dependence of (top) IMEP<sub>g</sub> (middle) StD<sub>IMEPg</sub> and (bottom) CoV<sub>IMEPg</sub> on glow plug and soak temperature for a twin-pilot strategy (● size represents 10% CoV<sub>IMEPg</sub>). Conditions: SOI<sub>Main</sub> = -8 °ATDC, 6 °CA separation, 1000 rev/min, 400 bar rail pressure



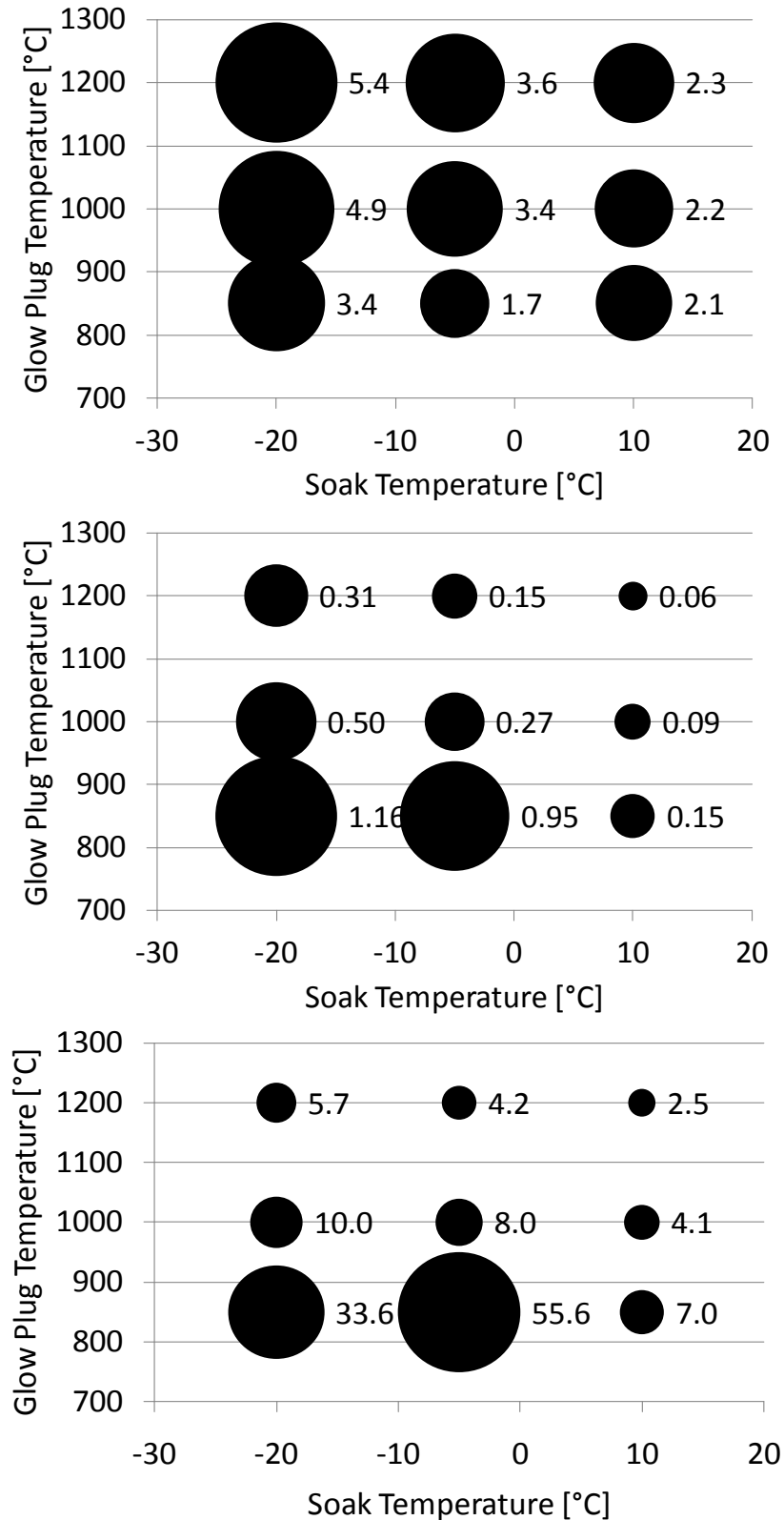


Figure 6-7. Dependence of (top) IMEP<sub>g</sub> (middle) StD<sub>IMEPg</sub> and (bottom) CoV<sub>IMEPg</sub> on glow plug and soak temperature for a triple-pilot strategy ( ● size represents 10% CoV<sub>IMEPg</sub>). Conditions: SOI<sub>Main</sub> = -8 °ATDC, 6 °CA separation, 1000 rev/min, 400 bar rail pressure

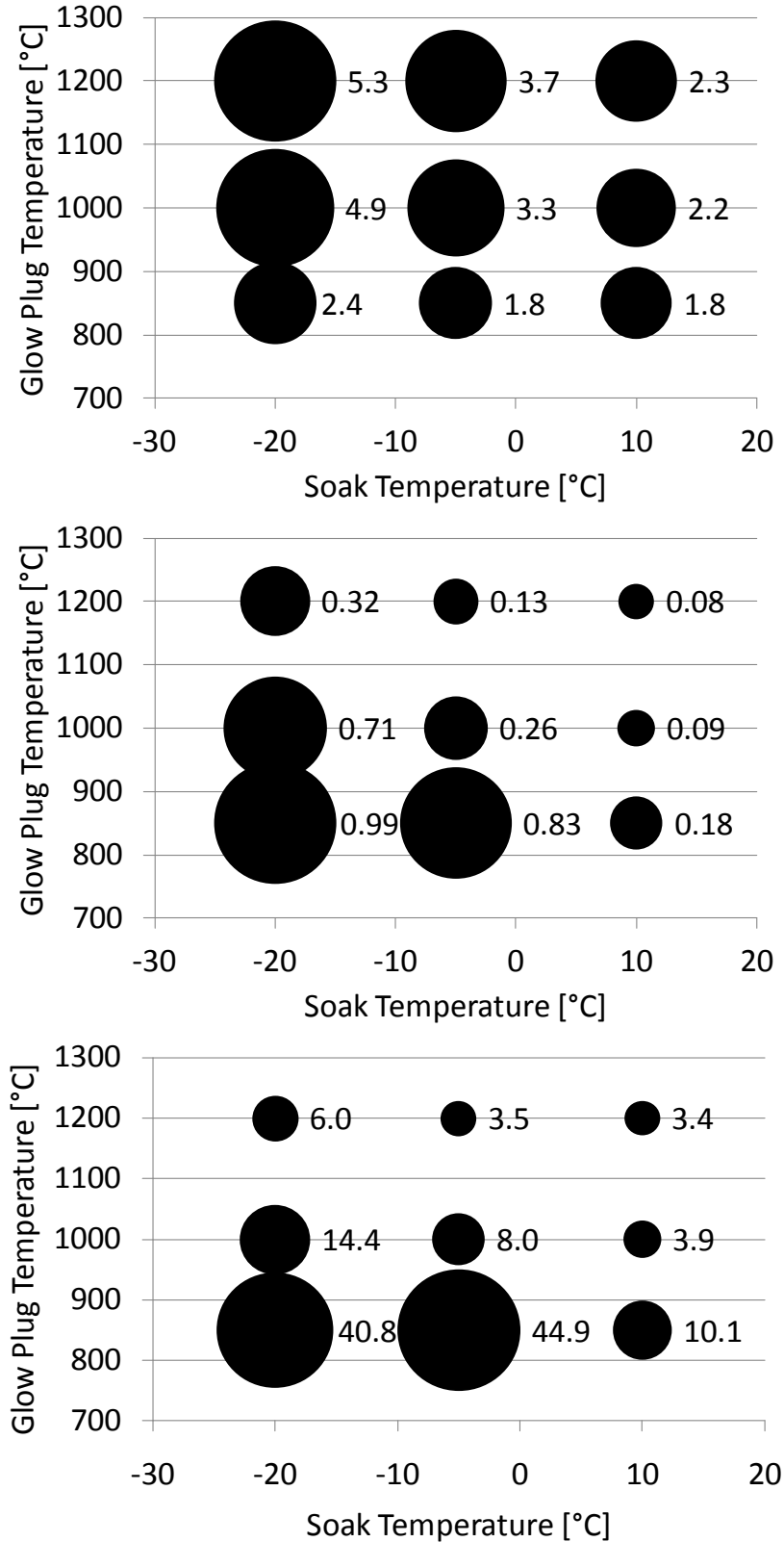
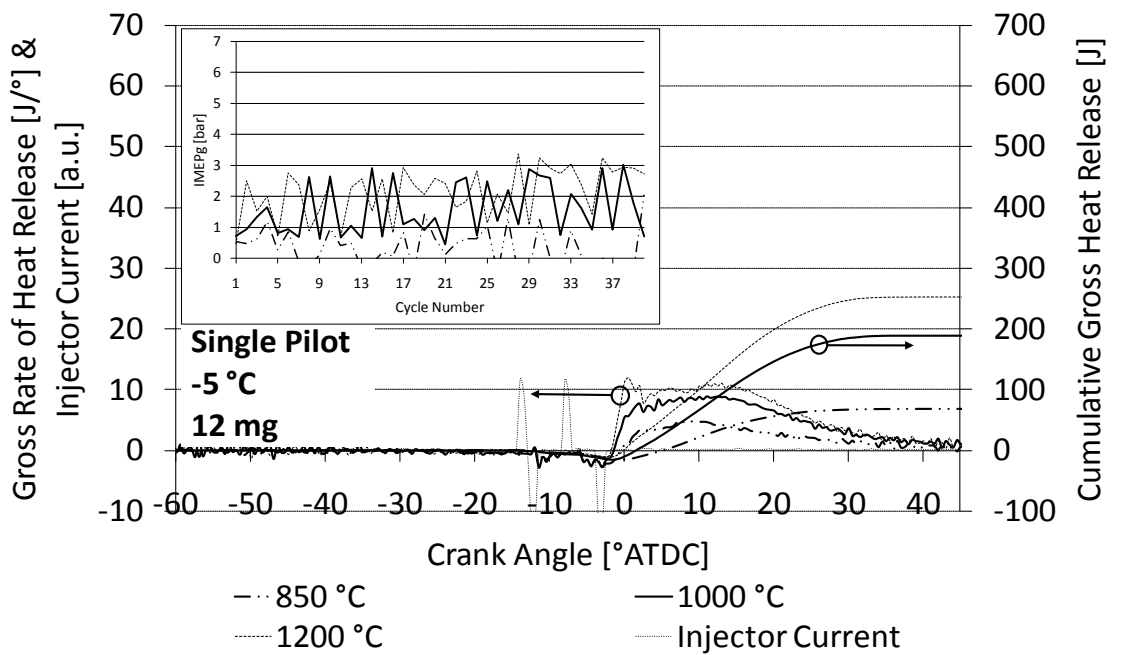
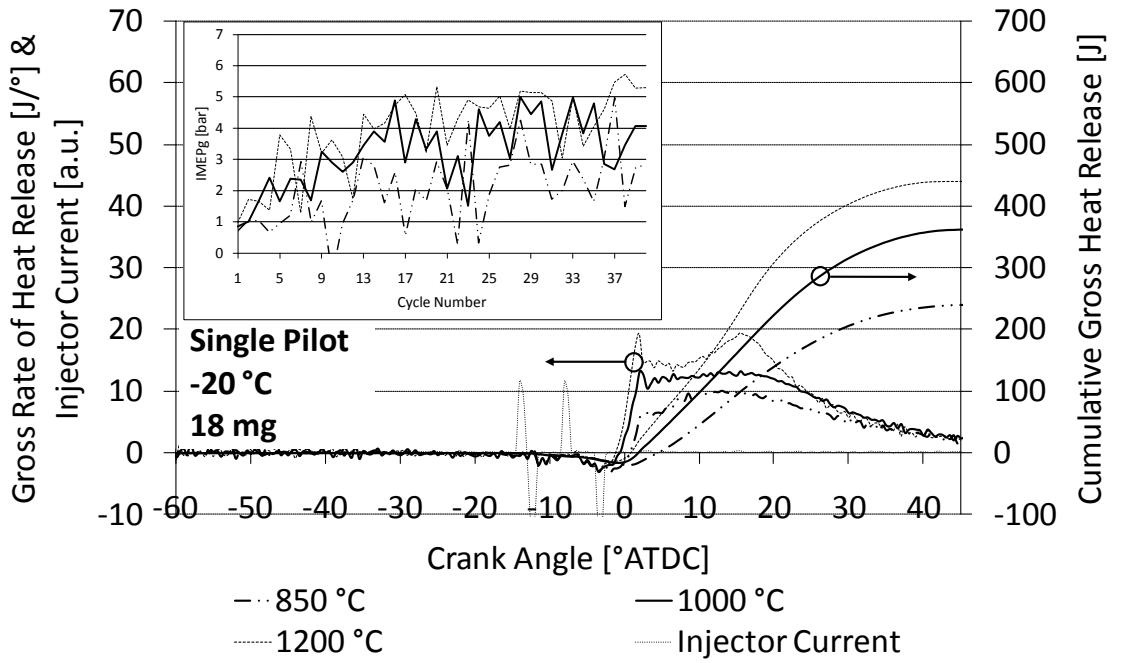


Figure 6-8. Dependence of (top) IMEP<sub>g</sub> (middle) StD<sub>IMEPg</sub> and (bottom) CoV<sub>IMEPg</sub> on glow plug and soak temperature for a quad-pilot strategy ( ● size represents 10% CoV<sub>IMEPg</sub>). Conditions: SOI<sub>Main</sub> = -8 °ATDC, 6 °CA separation, 1000 rev/min, 400 bar rail pressure



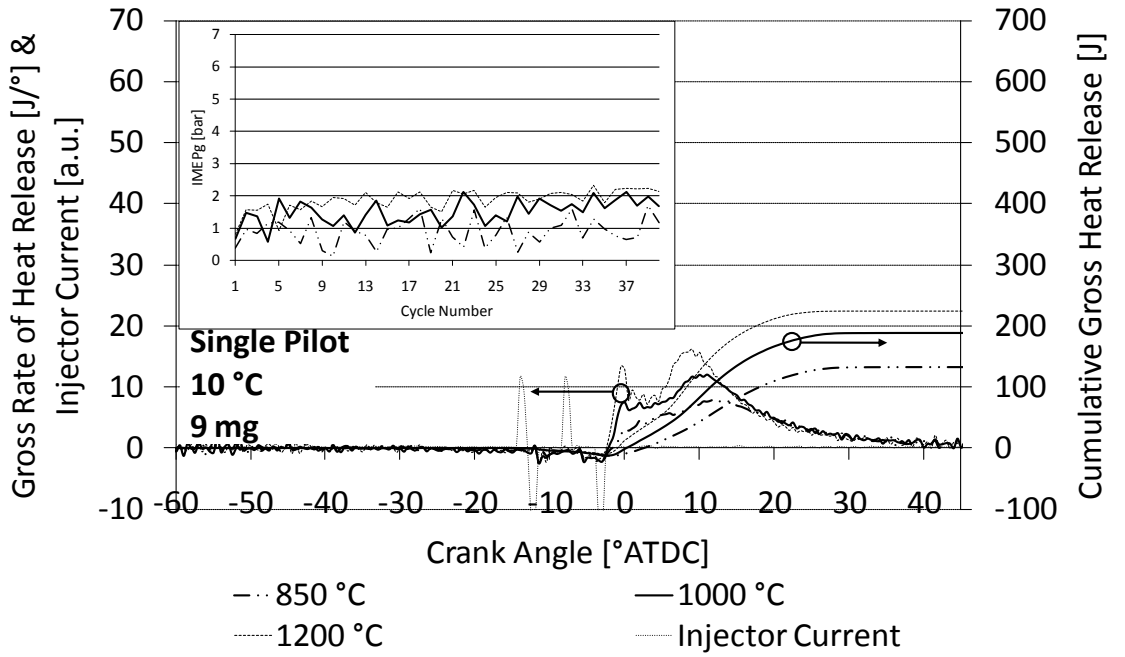
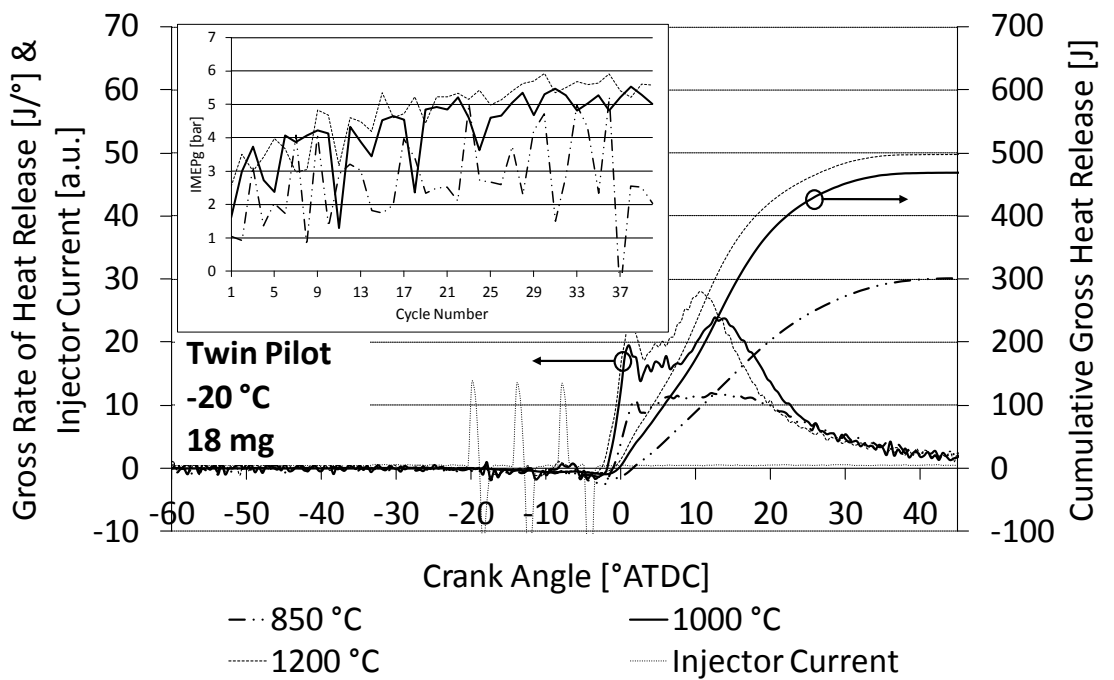


Figure 6-9. Effect of glow plug temperature on 40 cycle ensemble averaged heat release for a single-pilot strategy; (top) -20°C (middle) -5°C (bottom) 10°C. Conditions:  $SOI_{Main} = -8$  °ATDC, 6 °CA separation, 1000 rev/min, 400 bar rail pressure



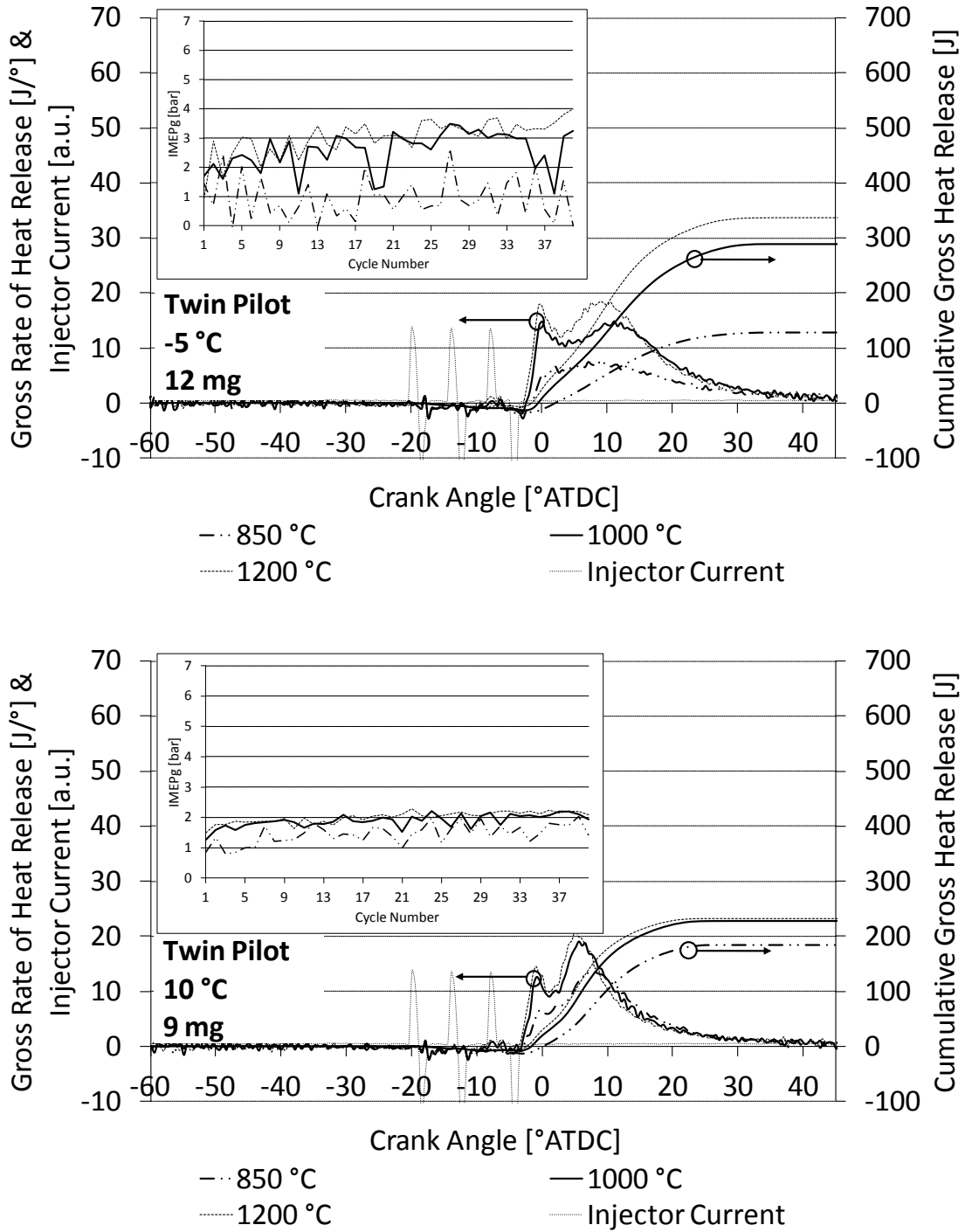
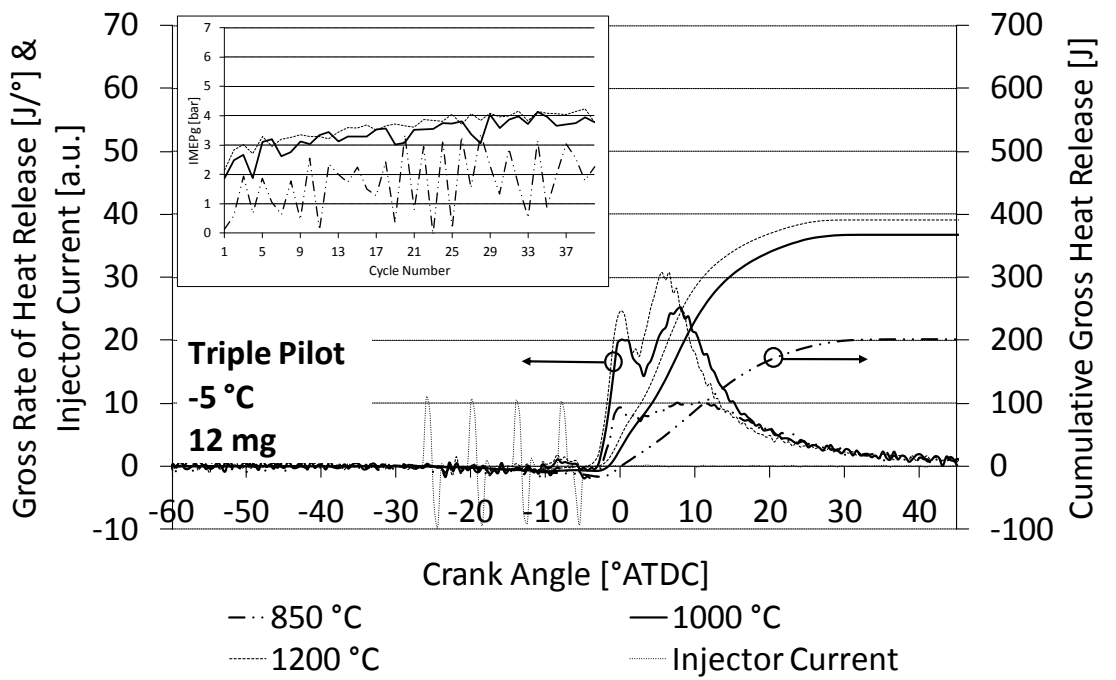
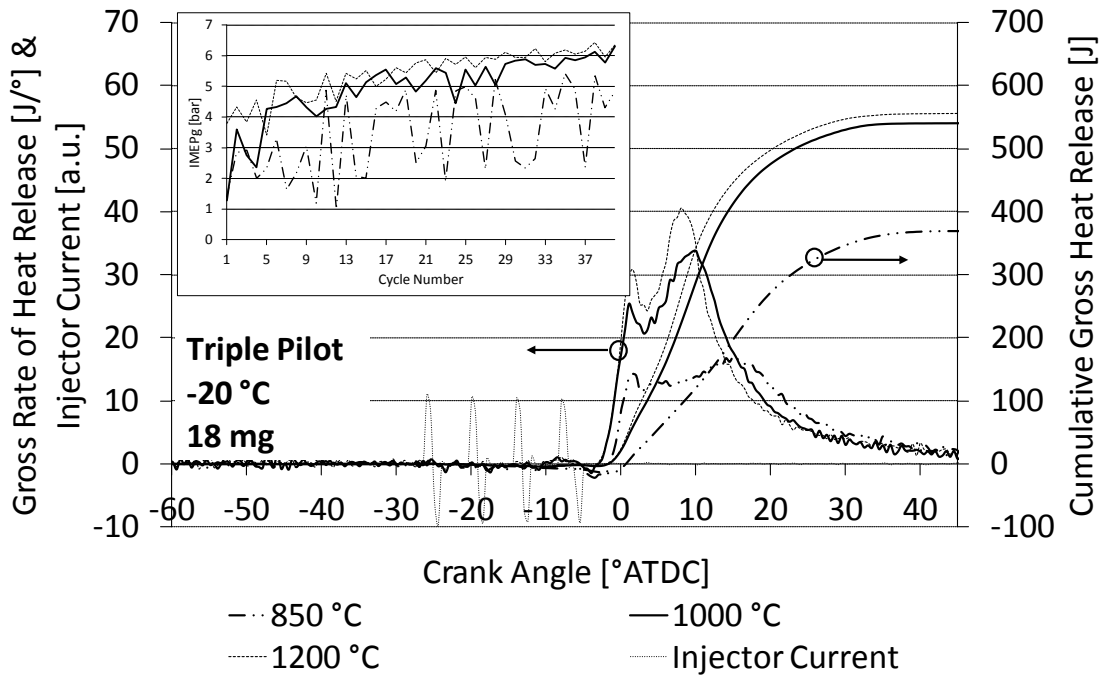


Figure 6-10. Effect of glow plug temperature on 40 cycle ensemble averaged heat release for a twin-pilot strategy; (top) -20°C (middle) -5°C (bottom) 10°C. Conditions:  $SOI_{Main} = -8$  °ATDC, 6 °CA separation, 1000 rev/min, 400 bar rail pressure



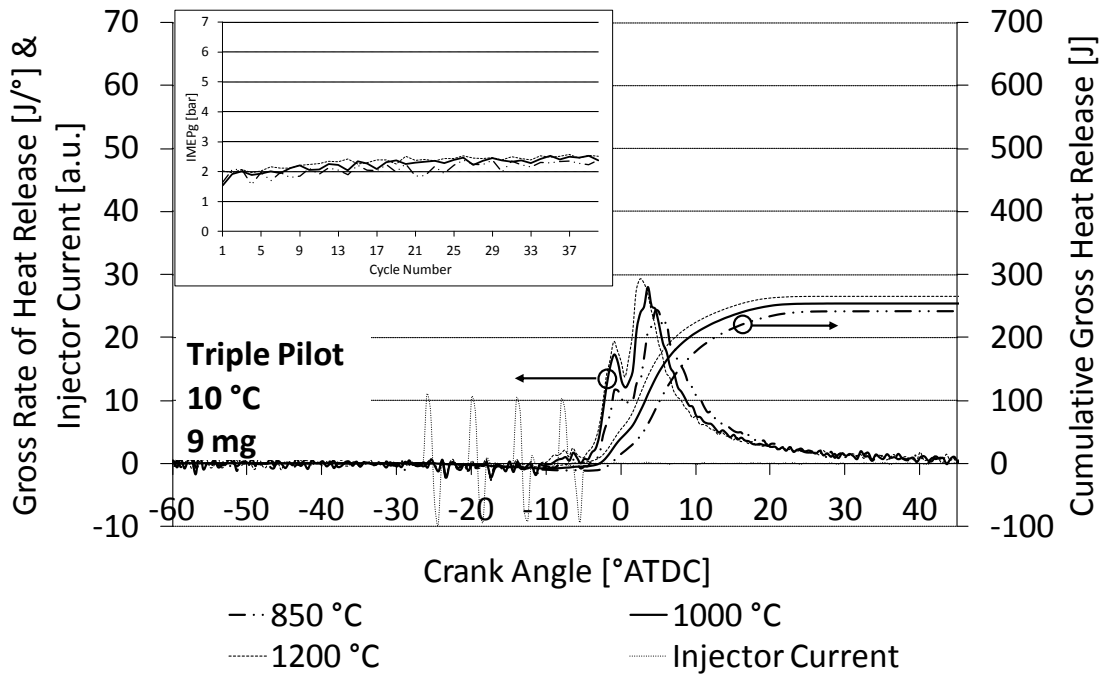
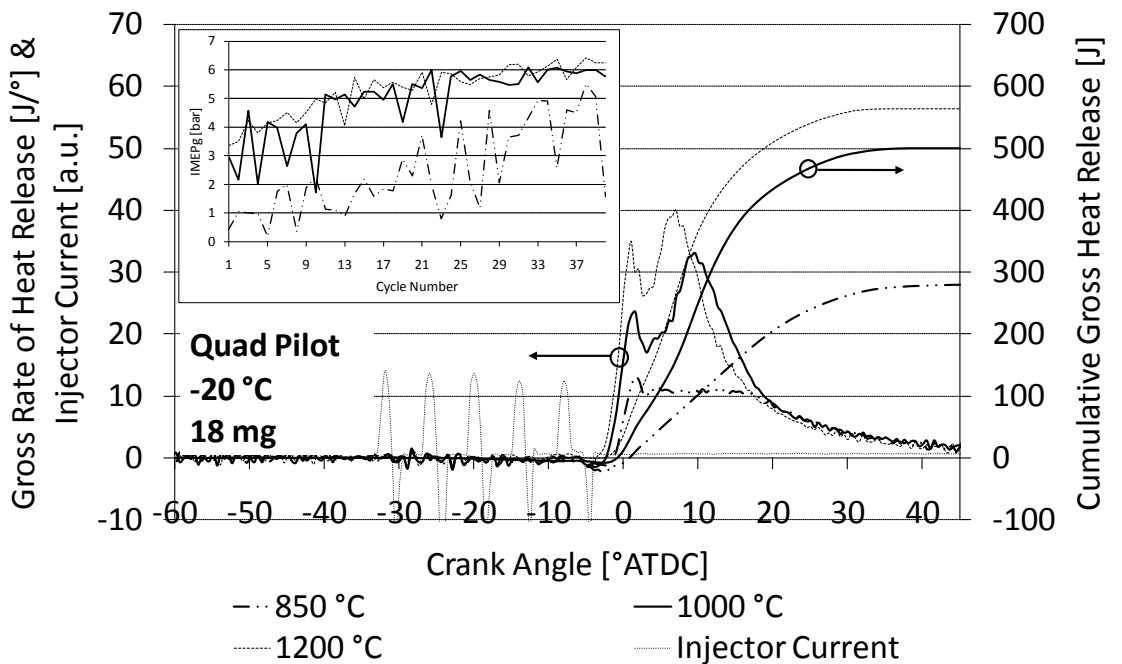


Figure 6-11. Effect of glow plug temperature on 40 cycle ensemble averaged heat release for a triple-pilot strategy; (top) -20°C (middle) -5°C (bottom) 10°C. Conditions:  $SOI_{Main} = -8$  °ATDC, 6 °CA separation, 1000 rev/min, 400 bar rail pressure



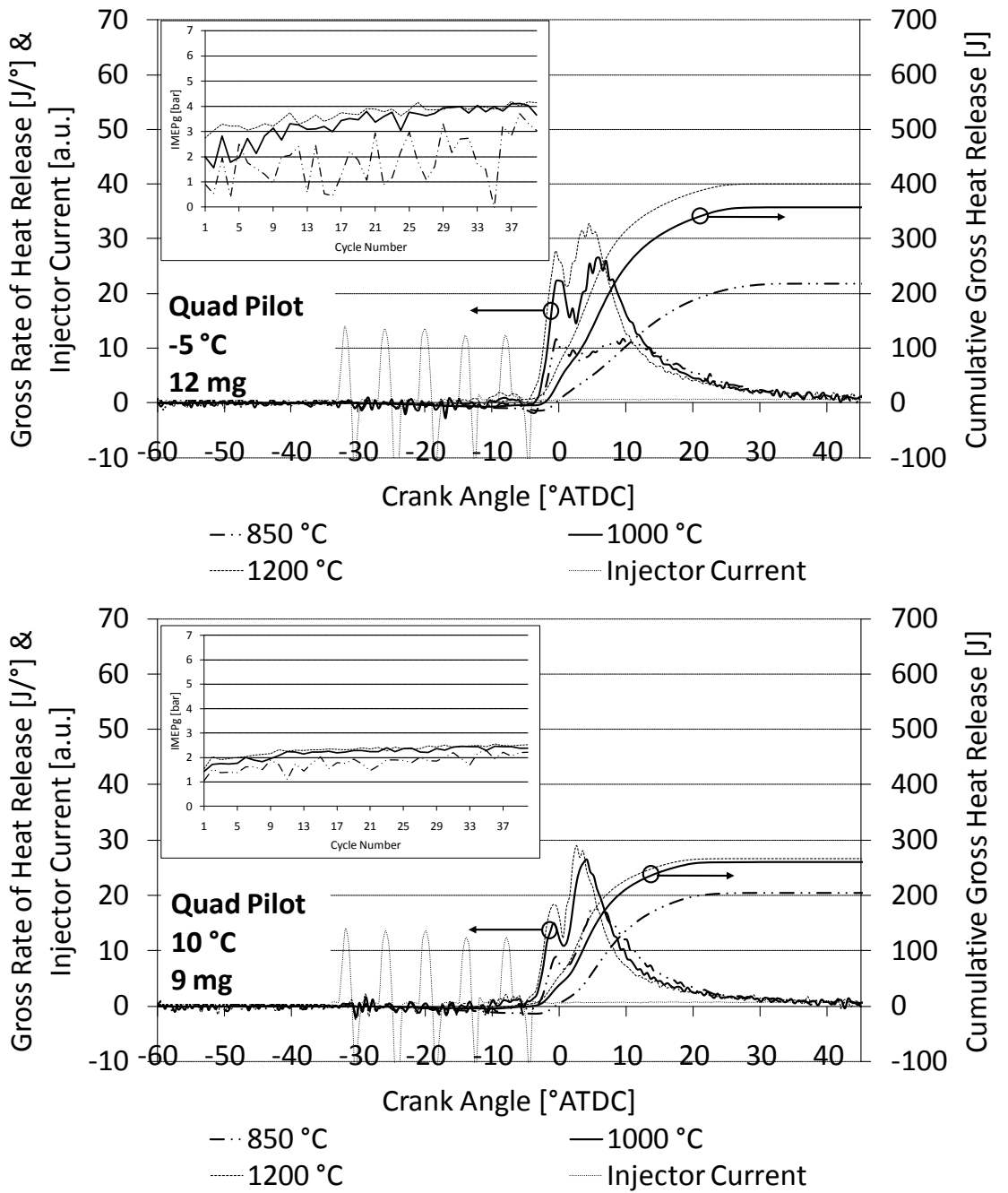


Figure 6-12. Effect of glow plug temperature on 40 cycle ensemble averaged heat release for a quad-pilot strategy; (top) -20°C (middle) -5°C (bottom) 10°C. Conditions:  $SOI_{Main} = -8$  °ATDC, 6 °CA separation, 1000 rev/min, 400 bar rail pressure



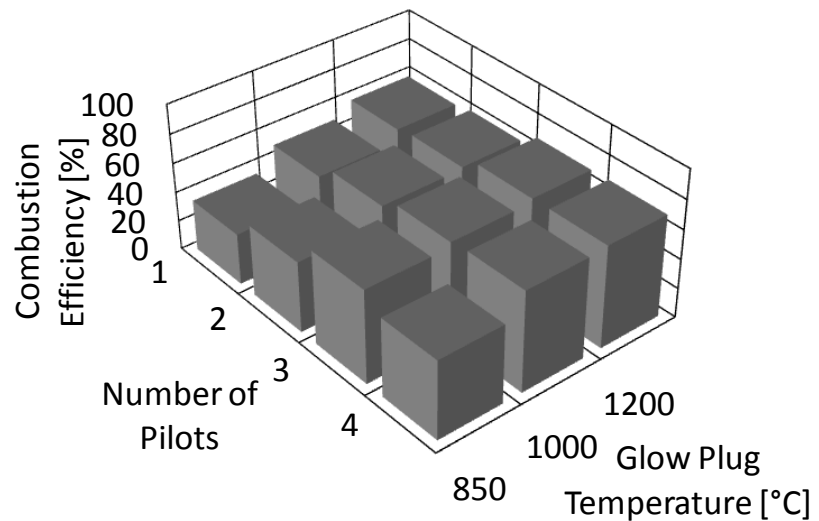
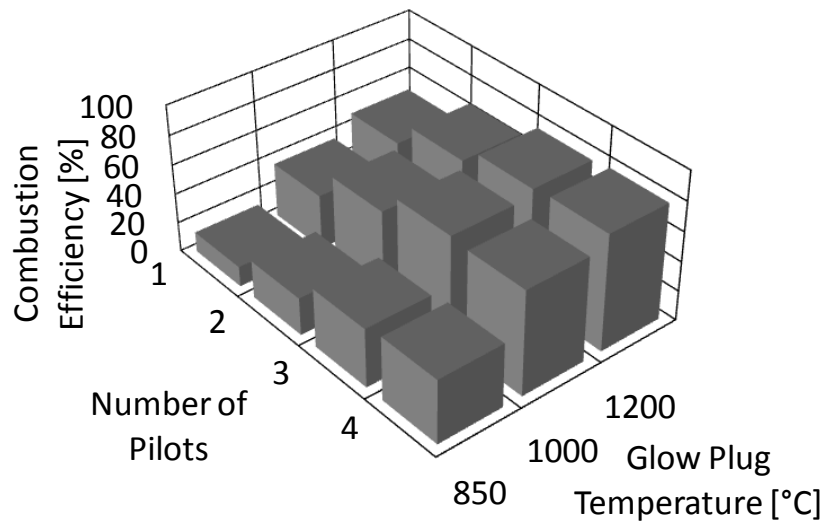
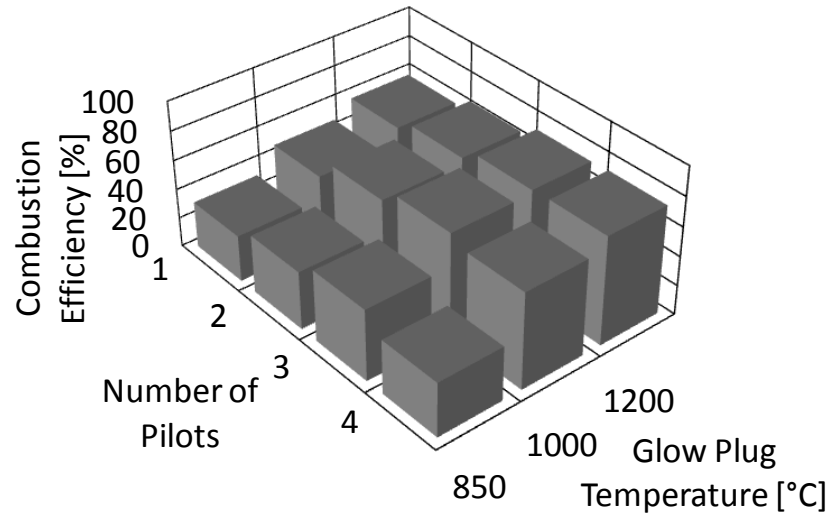


Figure 6-13. Effect of glow plug temperature and number of pilots on indicated combustion efficiency; (top) -20°C, 18 mg/cycle total fuel (middle) -5°C, 12 mg/cycle total fuel (bottom) 10°C, 9 mg/cycle total fuel. Conditions:  $SOI_{Main} = -8$  °ATDC, 6 °CA separation, 1000 rev/min, 400 bar rail pressure

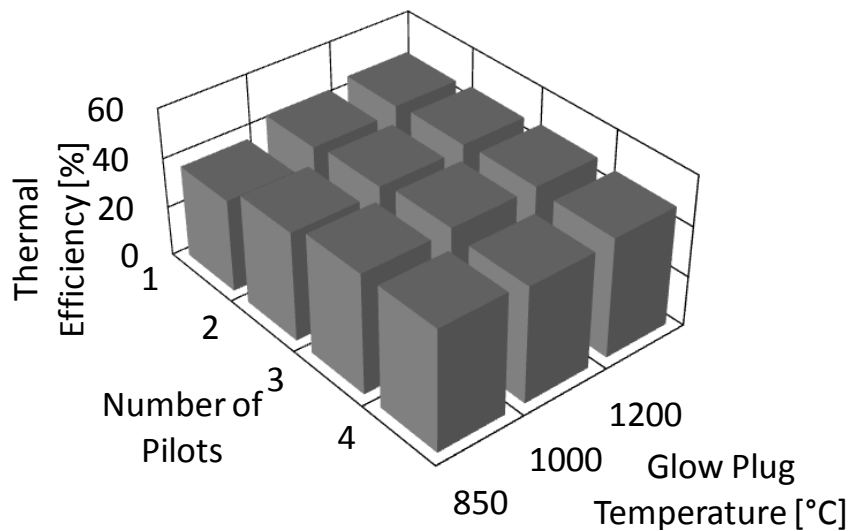
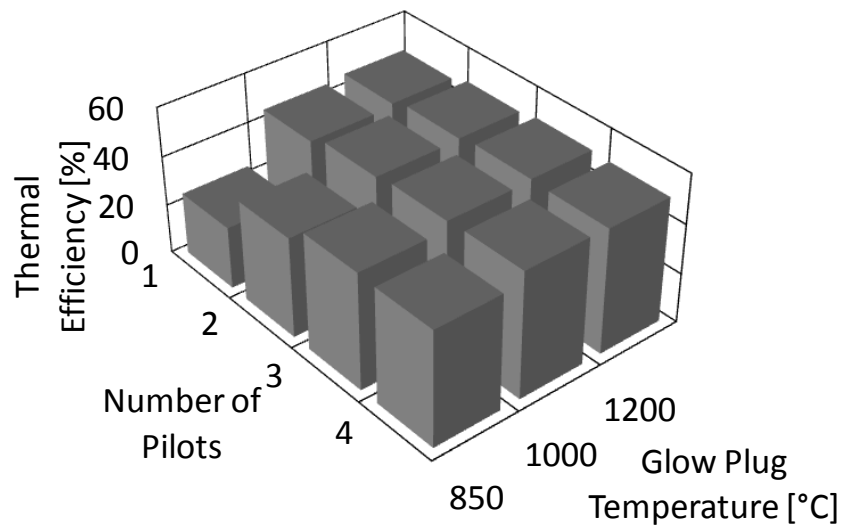
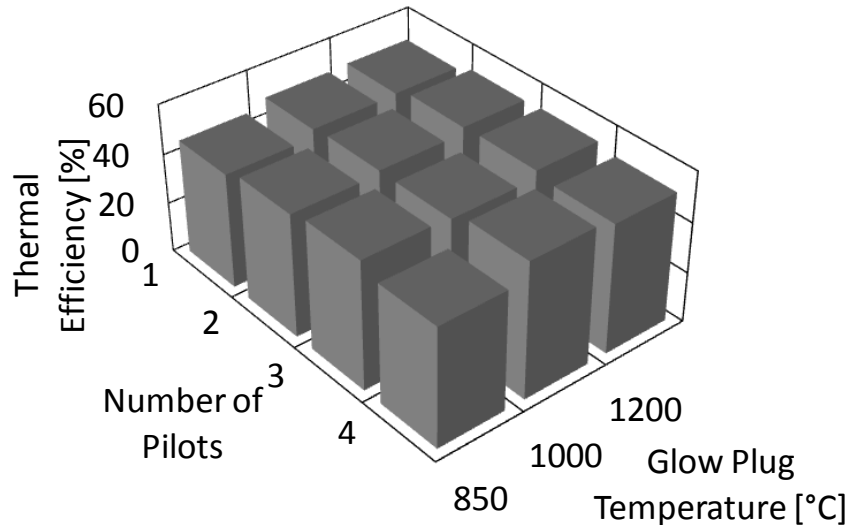


Figure 6-14. Effect of glow plug temperature and number of pilots on indicated thermal efficiency; (top) -20°C, 18 mg/cycle total fuel (middle) -5°C, 12 mg/cycle total fuel (bottom) 10°C, 9 mg/cycle total fuel. Conditions:  $SOI_{Main} = -8^\circ \text{ATDC}$ , 6 °CA separation, 1000 rev/min, 400 bar rail pressure

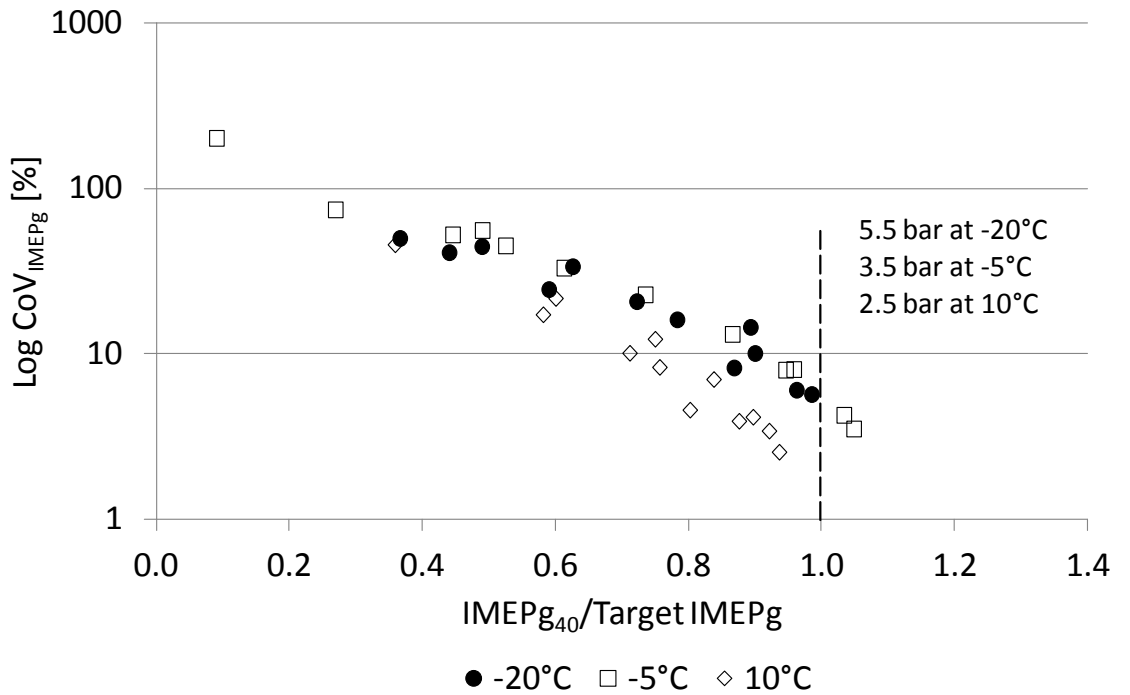


Figure 6-15. Dependence of stability on IMEP<sub>g</sub> normalised against target IMEP<sub>g</sub> at soak temperatures of -20°C, -5°C and 10°C. Conditions: SOI<sub>Main</sub> = -8 °ATDC, 6 °CA separation, 1000 rev/min, 400 bar rail pressure

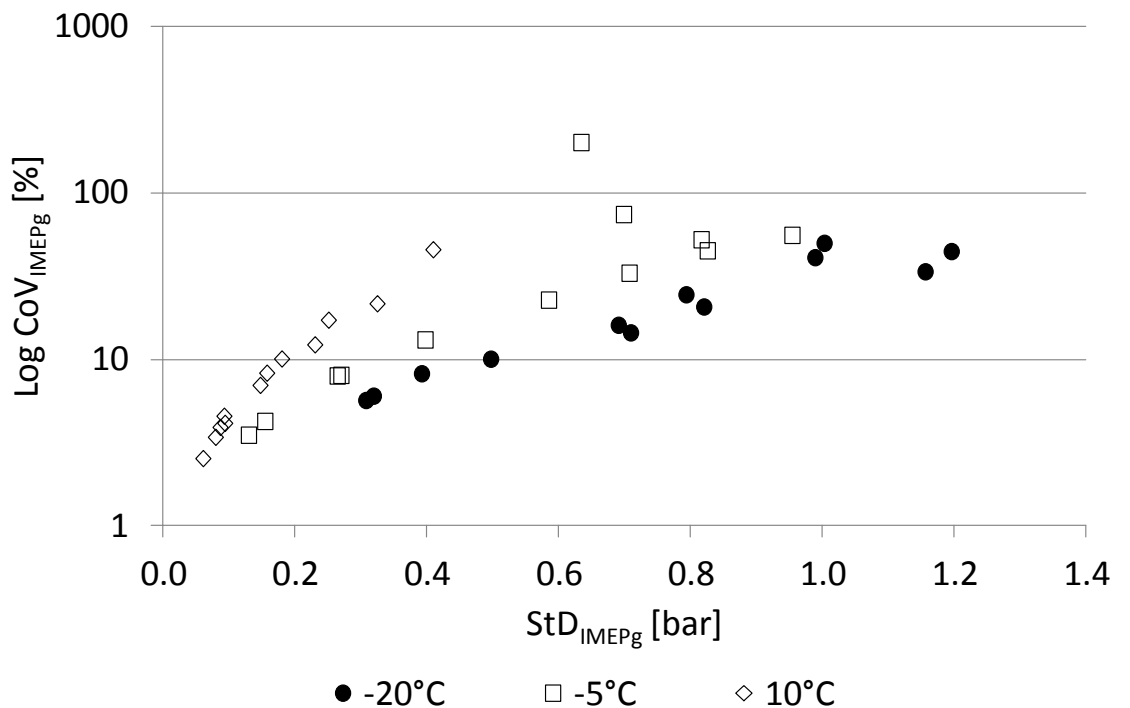


Figure 6-16. Dependence of CoV<sub>IMEPg</sub> on StD<sub>IMEPg</sub> at soak temperatures of -20°C, -5°C and 10°C. Conditions: SOI<sub>Main</sub> = -8 °ATDC, 6 °CA separation, 1000 rev/min, 400 bar rail pressure

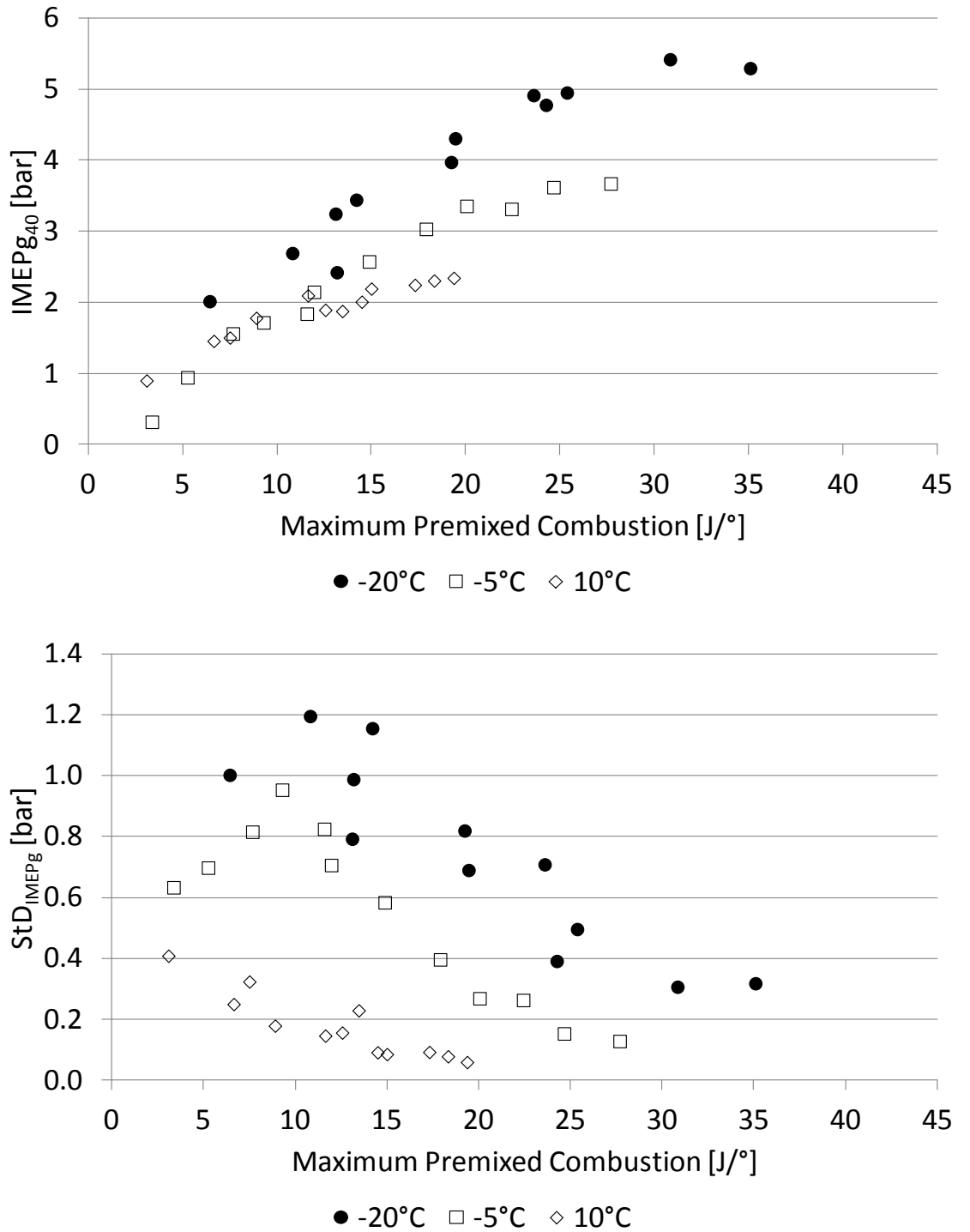
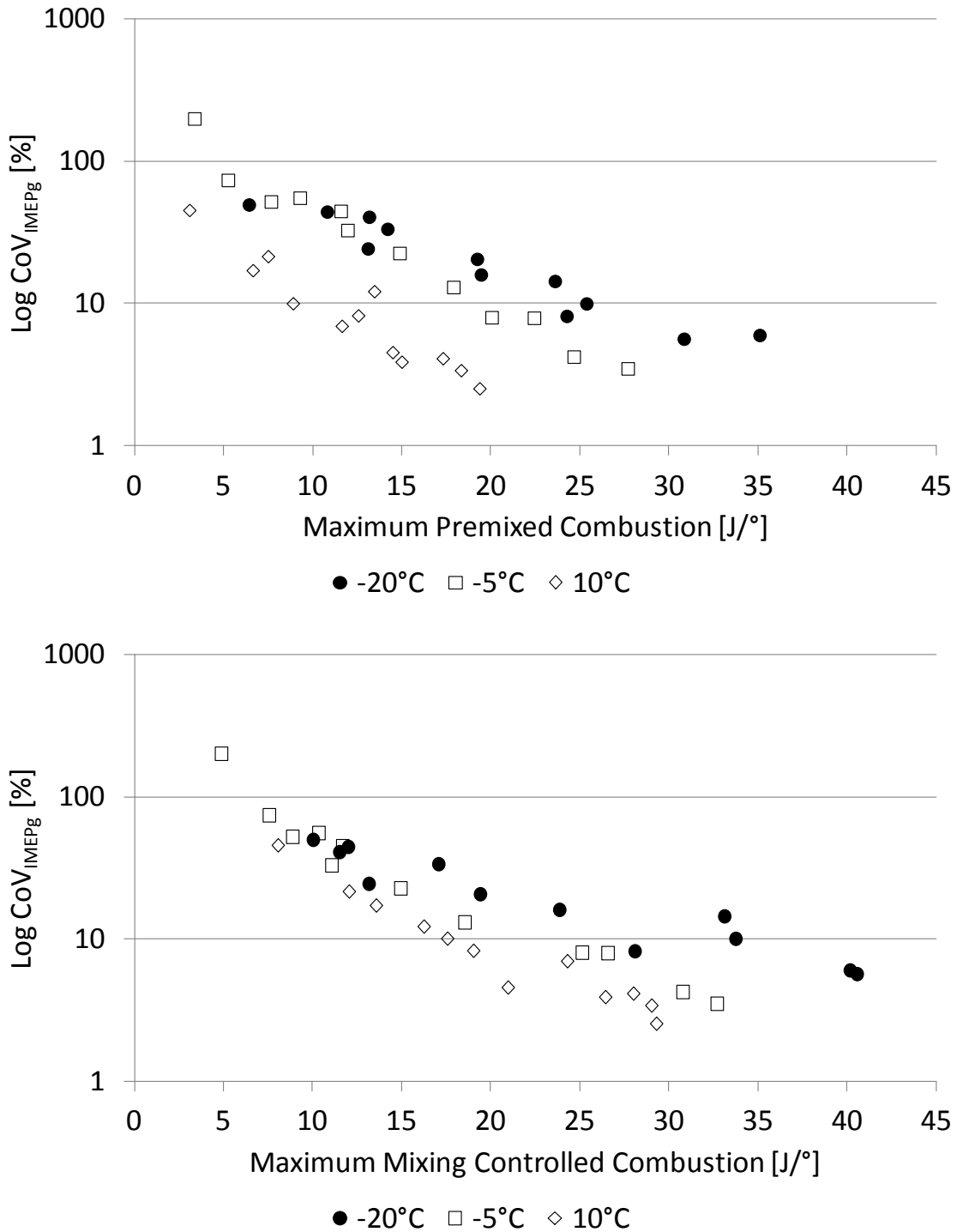


Figure 6-17. Dependence of IMEPg and StD<sub>IMEPg</sub> on 40 cycle ensemble averaged maximum premixed combustion at soak temperatures of -20°C, -5°C and 10°C. Conditions: SOI<sub>Main</sub> = -8 °ATDC, 6 °CA separation, 1000 rev/min, 400 bar rail pressure



**Figure 6-18. Dependence of stability on 40 cycle ensemble averaged maximum premixed and mixing controlled combustion at soak temperatures of -20°C, -5°C and 10°C. Conditions: SOI<sub>Main</sub> = -8 °ATDC, 6 °CA separation, 1000 rev/min, 400 bar rail pressure**

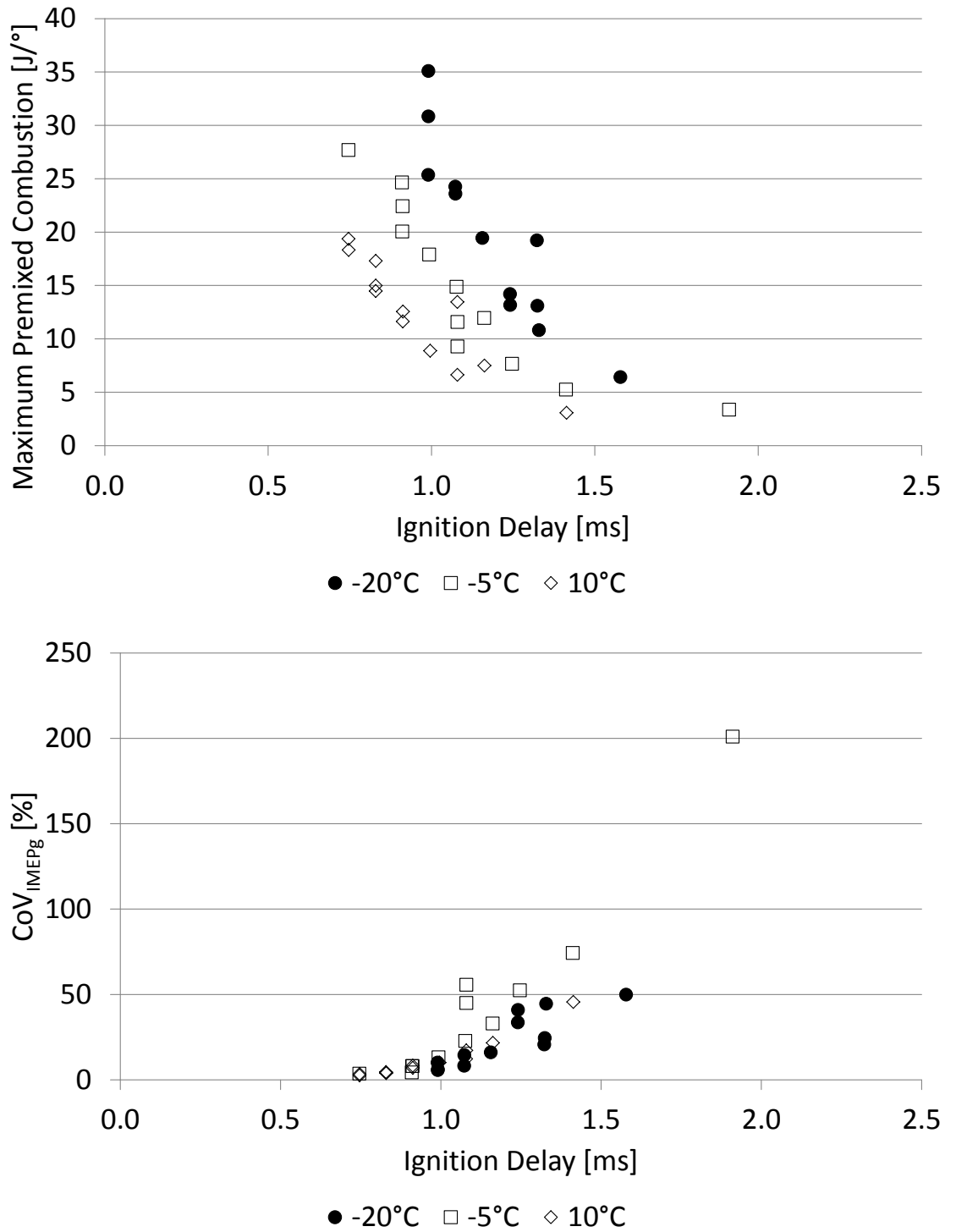


Figure 6-19. Dependence of stability and premixed combustion on ignition delay at -20°C, -5°C and 10°C. Conditions:  $SOI_{Main} = -8$  °ATDC, 6 °CA separation, 1000 rev/min, 400 bar rail pressure

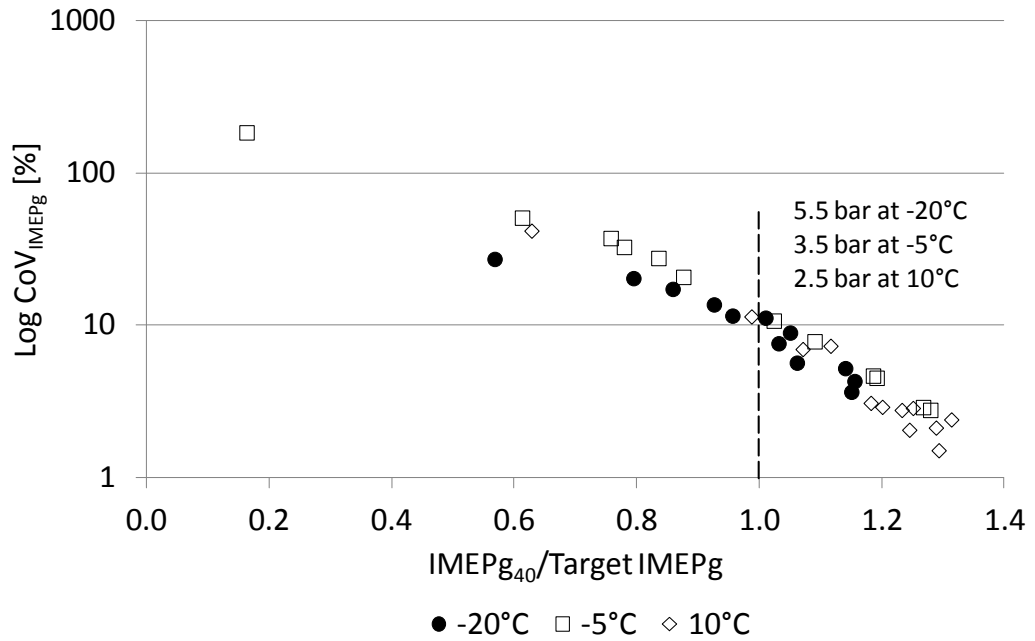


Figure 6-20. Dependence of stability on IMEPg normalised against target IMEPg at soak temperatures of -20°C (20 mg/cycle total fuel), -5°C (14 mg/cycle total fuel) and 10°C (11 mg/cycle total fuel). Conditions:  $SOI_{Main} = -8$  °ATDC, 6 °CA separation, 1000 rev/min, 400 bar rail pressure

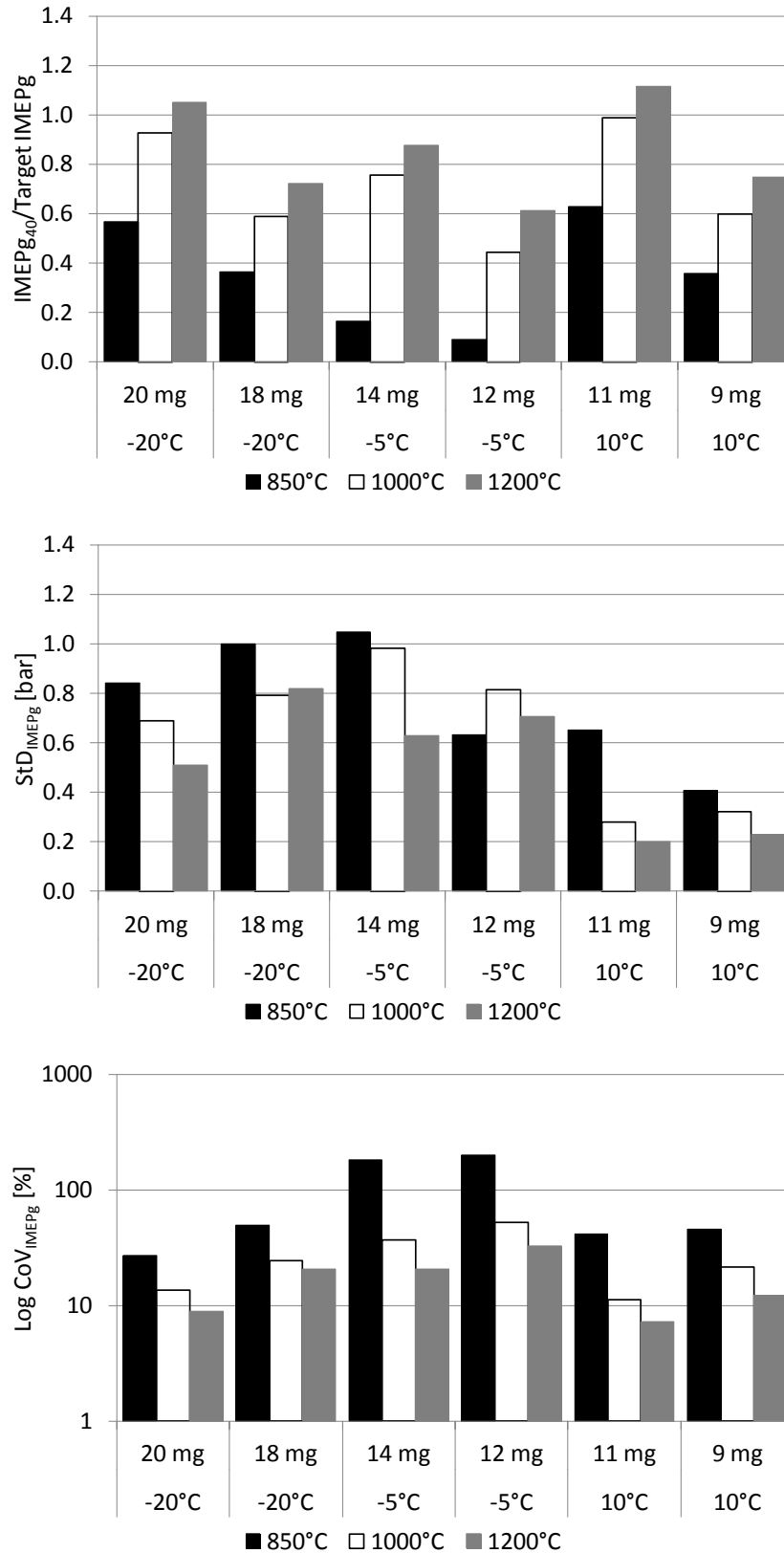


Figure 6-21. IMEP<sub>g</sub>, StD<sub>IMEPg</sub> and CoV<sub>IMEPg</sub> dependency on fuelling level and glow plug temperature at different soak temperatures for a single-pilot strategy. Conditions: SOI<sub>Main</sub> = -8 °ATDC, 6 °CA separation, 1000 rev/min, 400 bar rail pressure



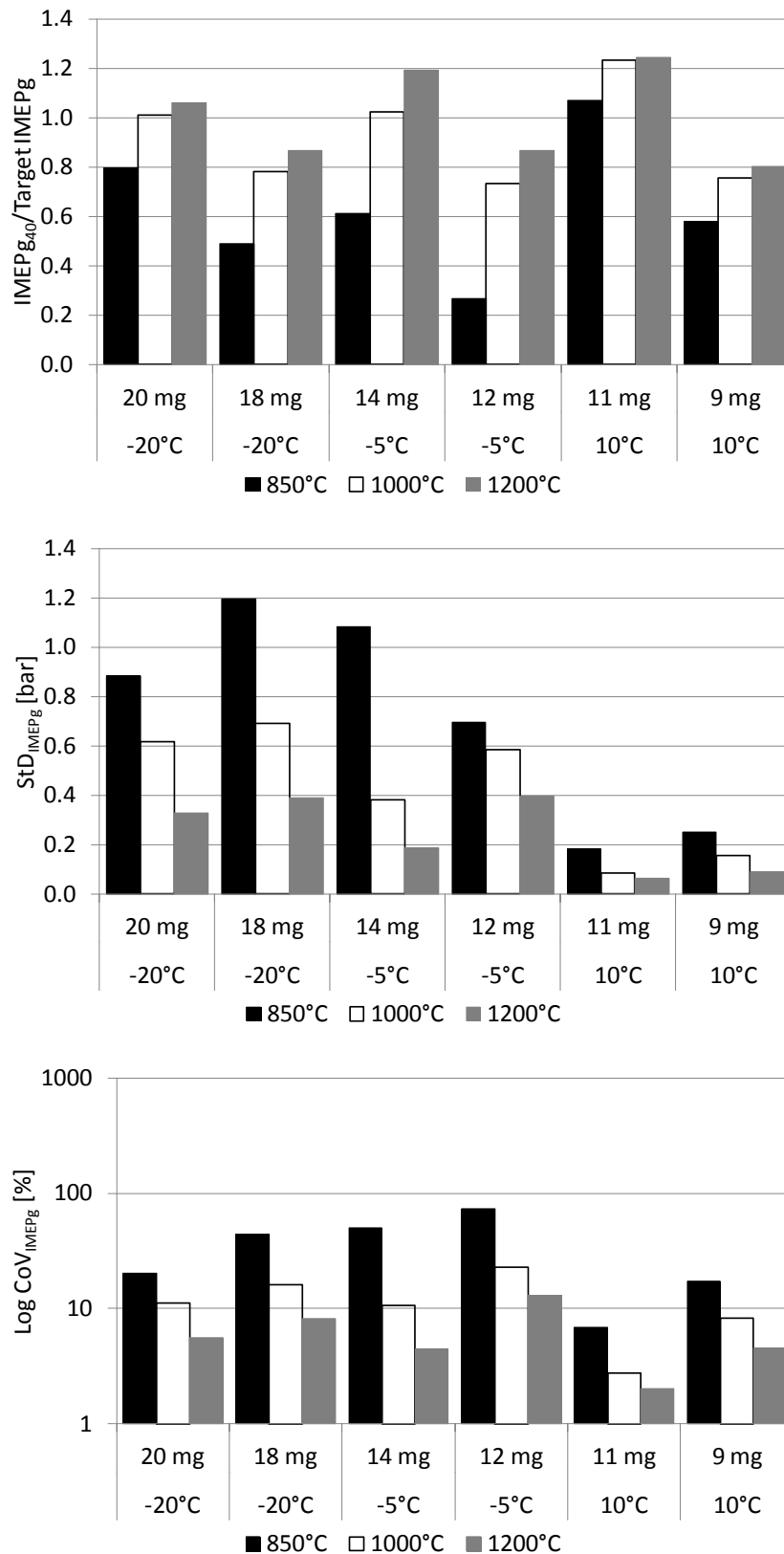


Figure 6-22. IMEP<sub>g</sub>, StD<sub>IMEPg</sub> and CoV<sub>IMEPg</sub> dependency on fuelling level and glow plug temperature at different soak temperatures for a twin-pilot strategy. Conditions: SOI<sub>Main</sub> = -8 °ATDC, 6 °CA separation, 1000 rev/min, 400 bar rail pressure

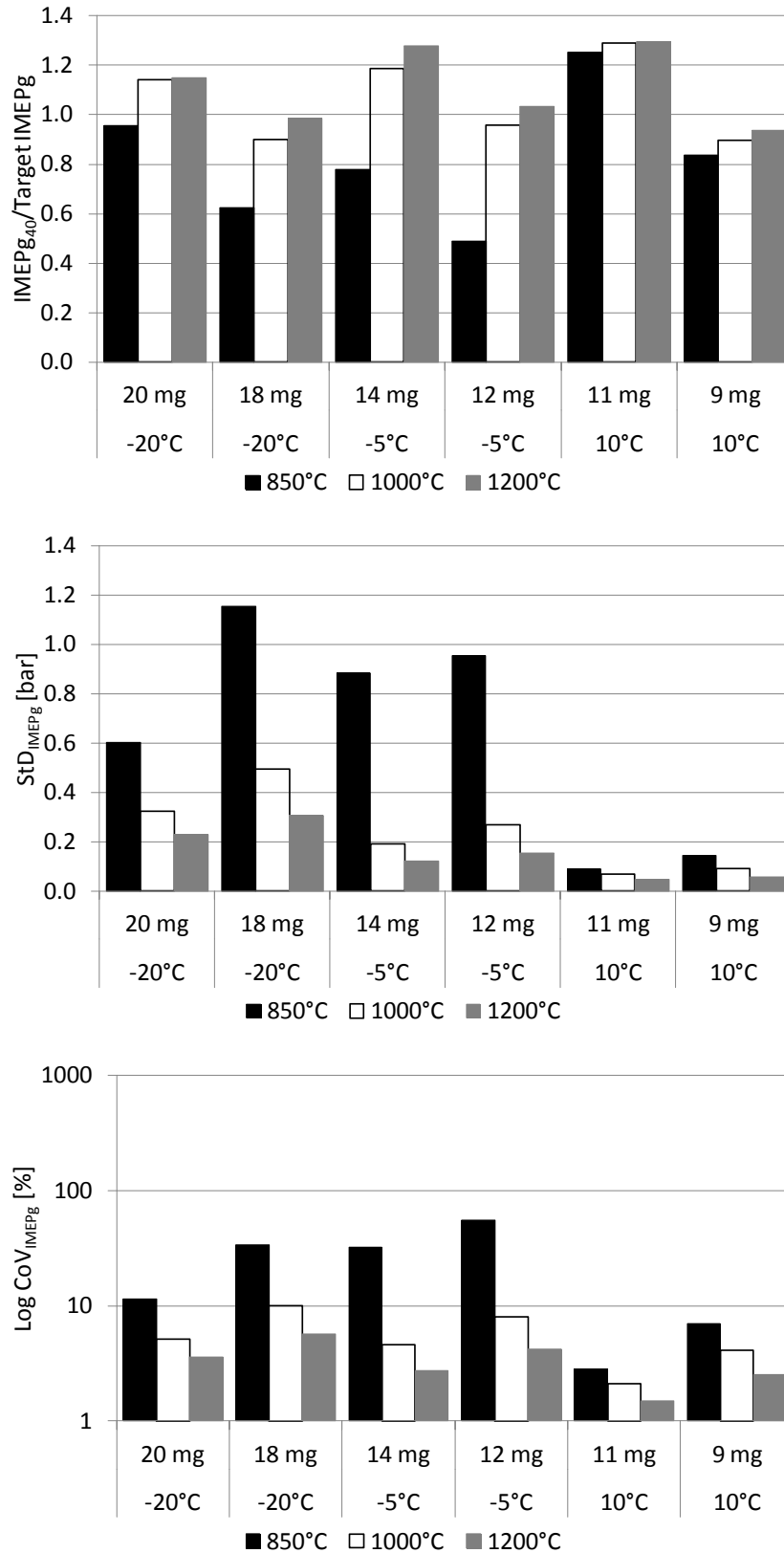
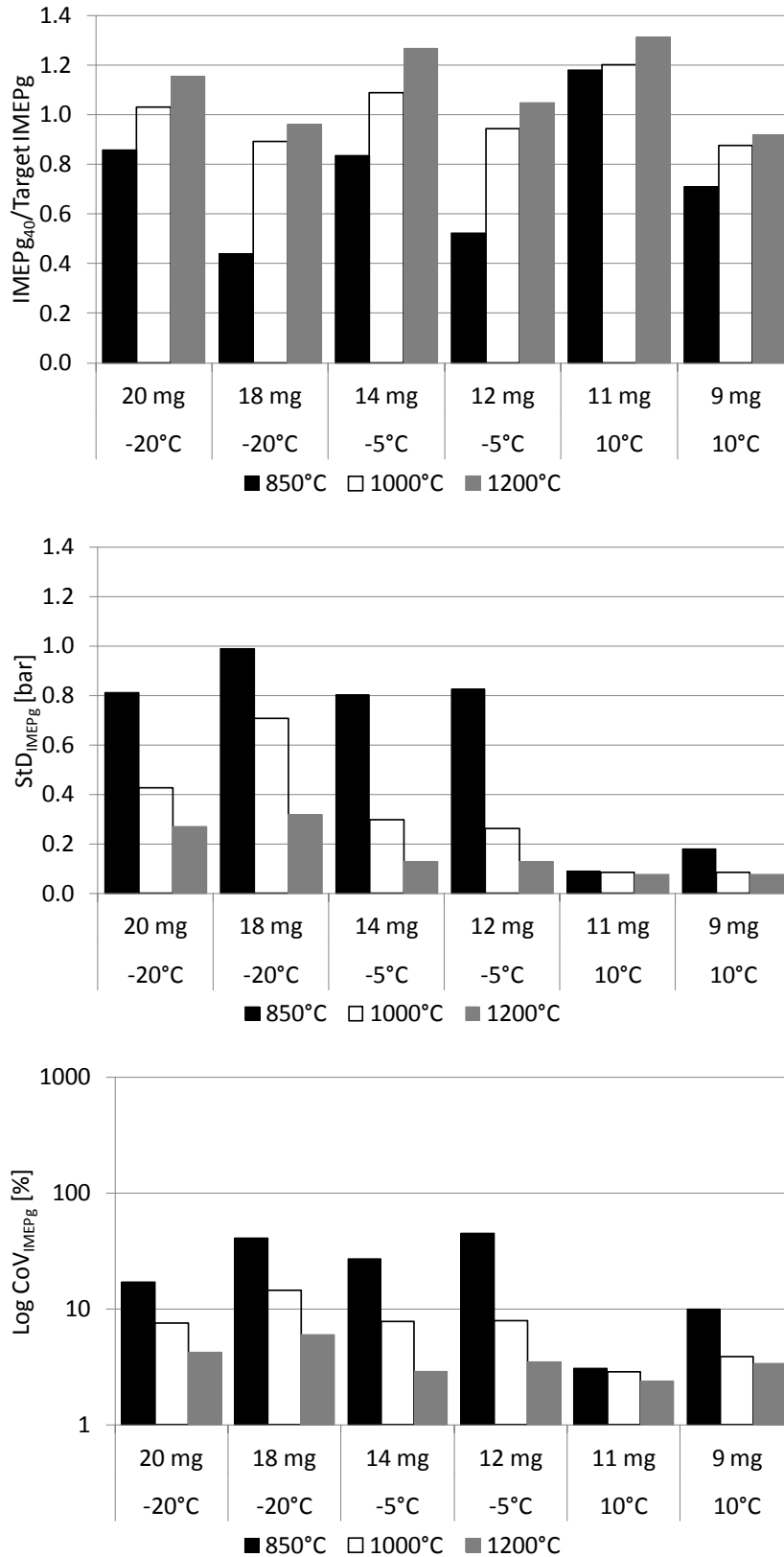


Figure 6-23. IMEP<sub>g</sub>, StD<sub>IMEPg</sub> and CoV<sub>IMEPg</sub> dependency on fuelling level and glow plug temperature at different soak temperatures for a triple-pilot strategy. Conditions: SOI<sub>Main</sub> = -8 °ATDC, 6 °CA separation, 1000 rev/min, 400 bar rail pressure



**Figure 6-24 IMEP<sub>g</sub>, StD<sub>IMEPg</sub> and CoV<sub>IMEPg</sub> dependency on fuelling level and glow plug temperature at different soak temperatures for a quad-pilot strategy. Conditions: SOI<sub>Main</sub> = -8 °ATDC, 6 °CA separation, 1000 rev/min, 400 bar rail pressure**

Figures

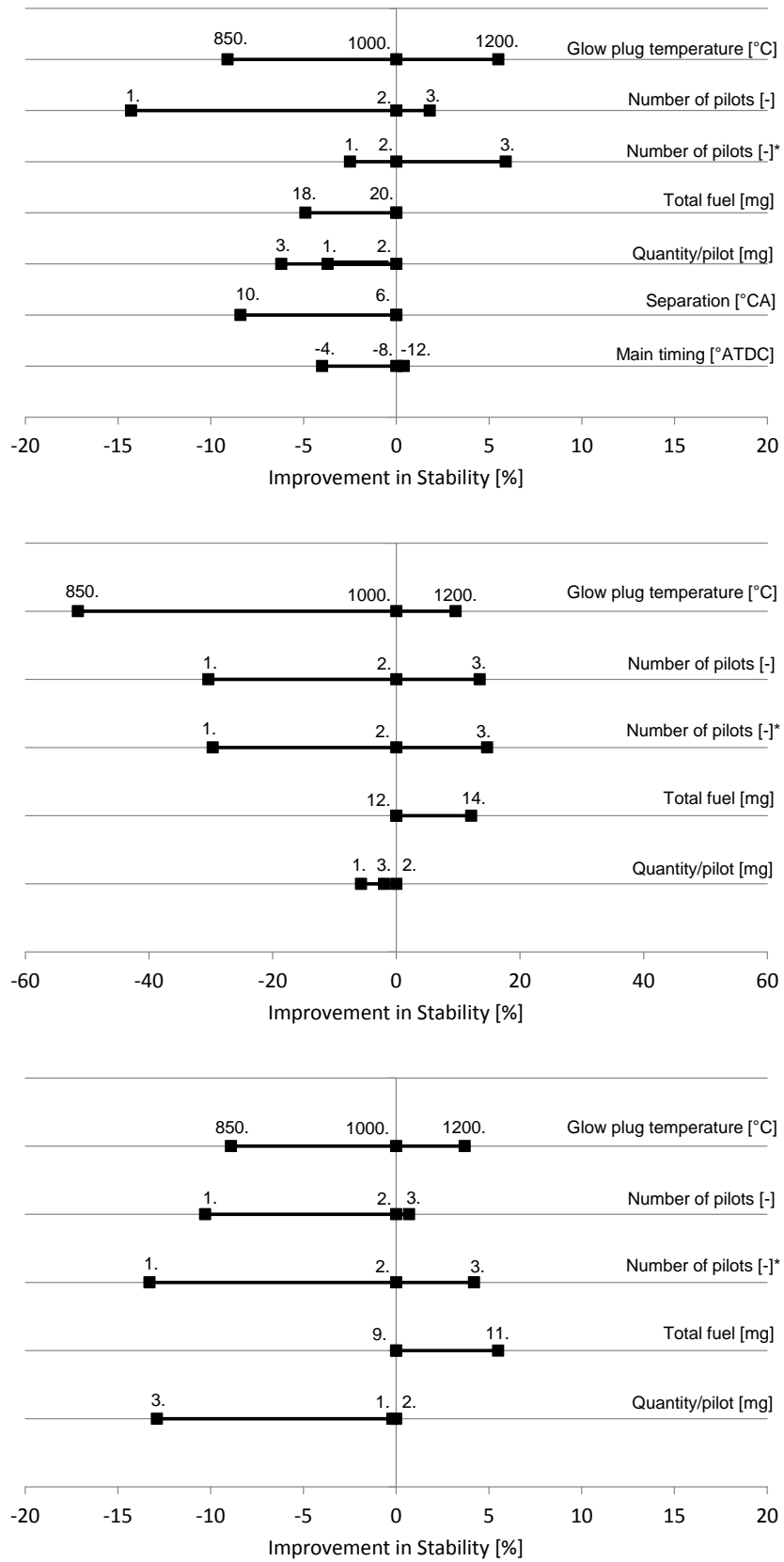


Figure 6-25. Stability response to parameter changes at various soak temperatures (top) -20°C (middle) -5°C and (bottom) 10°C. \*uses ceramic glow plug set at 1000°C

Figures

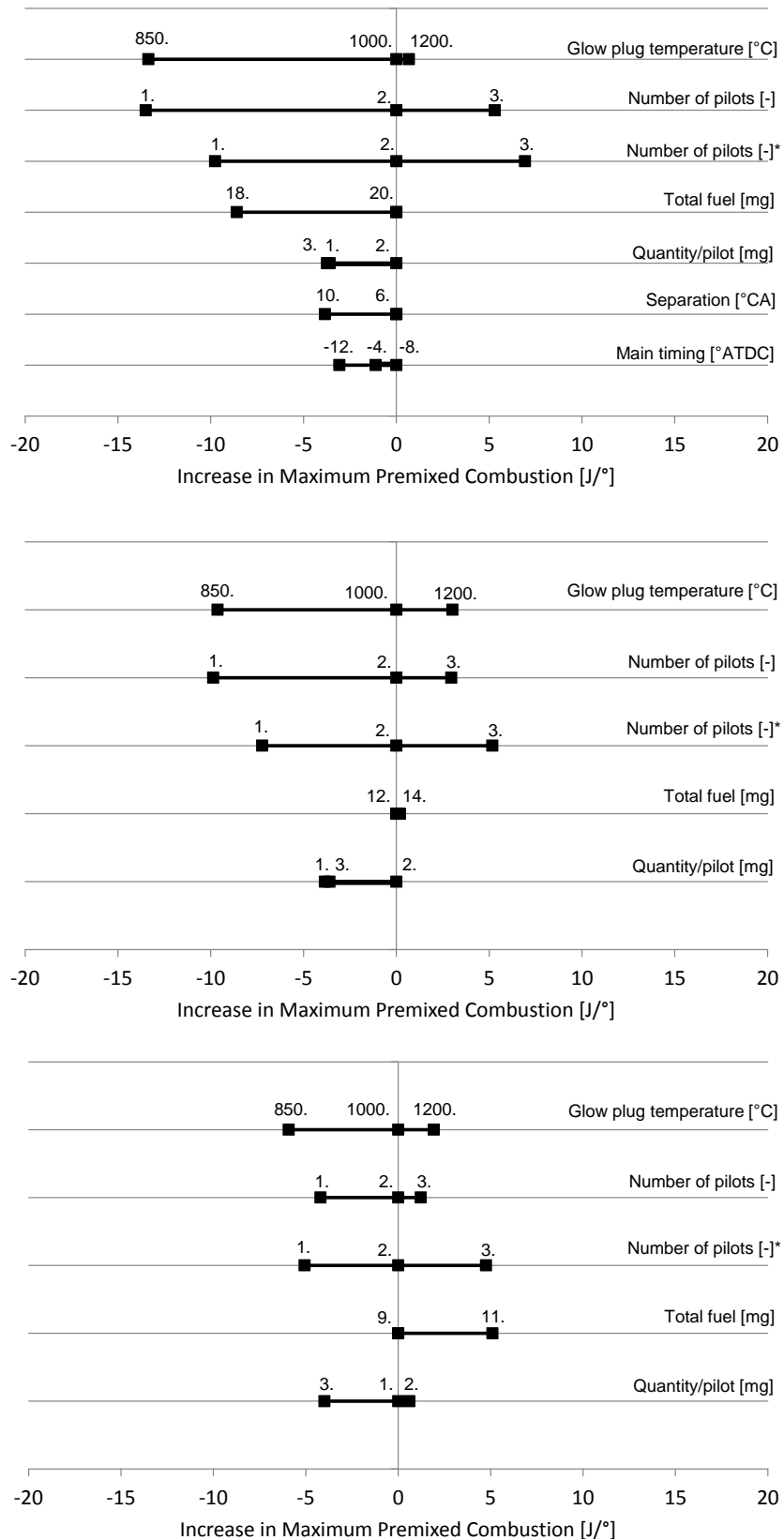


Figure 6-26. Maximum premixed combustion response to parameter changes at various soak temperatures (top) -20°C (middle) -5°C and (bottom) 10°C. \*uses ceramic glow plug set at 1000°C

Figures

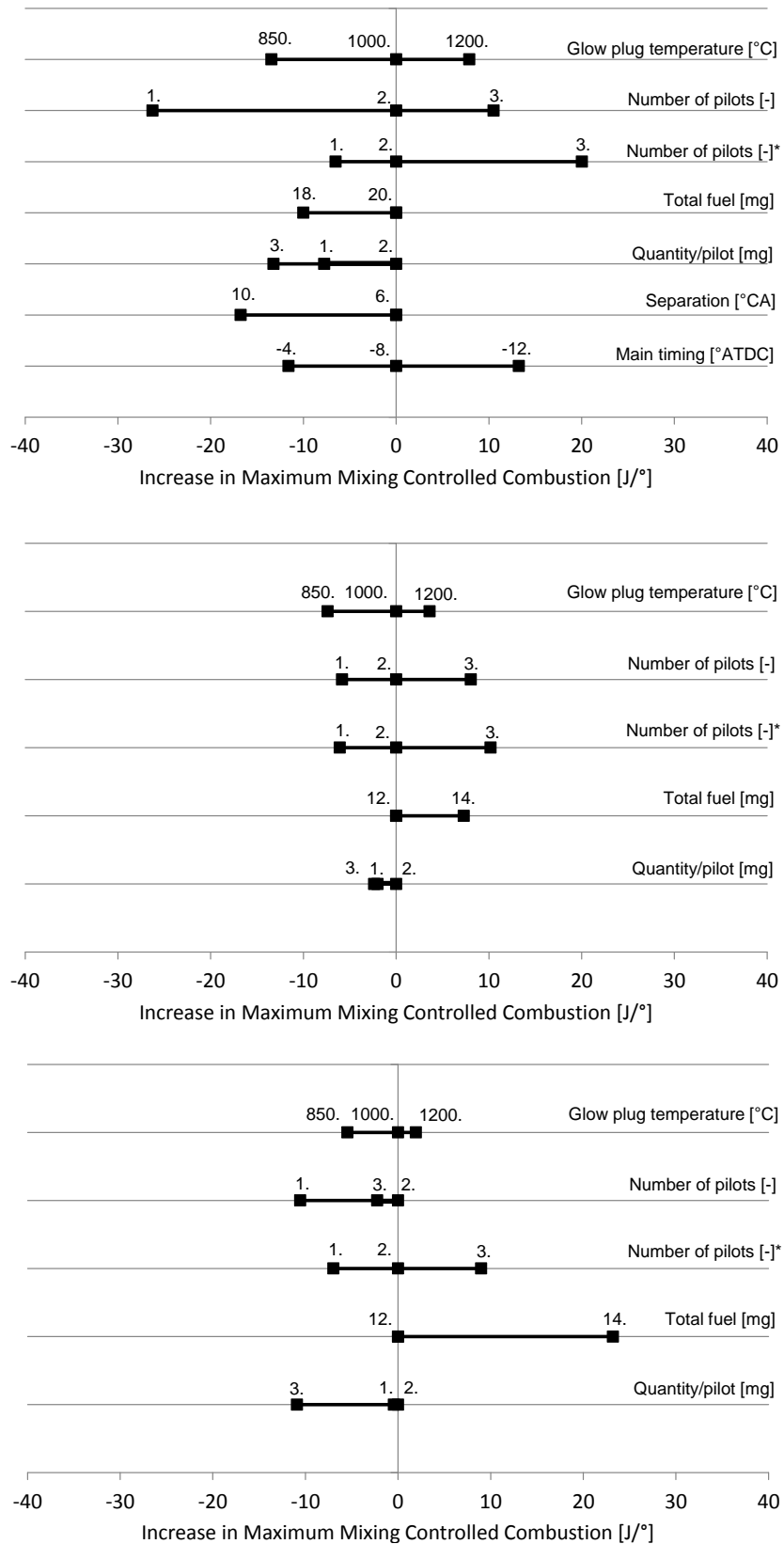


Figure 6-27. Maximum mixing controlled combustion response to parameter changes at various soak temperatures (top) -20°C (middle) -5°C and (bottom) 10°C. \*uses ceramic glow plug set at 1000°C